

CRANFIELD UNIVERSITY

Mousallam Mohammad Almoussalam

IN VITRO FUNCTIONALITY AND TOXICITY OF DACARBAZINE
DELIVERY NANOSYSTEM FOR MELANOMA

School of Energy, Environment and Agrifood

PhD Thesis

Academic Year: 2013 - 2017

Supervisor: Professor Ibtisam E. Tothill,
Dr Sophie Rocks and Dr Huijun Zhu

February 2018

CRANFIELD UNIVERSITY

SCHOOL OF ENERGY, ENVIRONMENT AND AGRIFOOD

PhD Thesis

Academic Year: 2013 – 2017

Mousallam Mohammad Almoussalam

IN VITRO FUNCTIONALITY AND TOXICITY DACARBAZINE
DELIVERY NANOSYSTEM FOR MELANOMA

Supervisor: Professor Ibtisam E. Tothill,
Dr Sophie Rocks and Dr Huijun Zhu

© Cranfield University, 2017. All rights reserved. No part of this publication may be reproduced without the written permission of the copyright owner.

ABSTRACT

Dacarbazine (Dac) is a chemotherapeutic for melanoma. Its poor solubility, short half-life, and side effects limit its therapeutic use. Nanoparticles used as drug delivery systems (DDS) improve drug pharmacological properties, target site concentration, and stability. This study aimed to improve the therapeutic efficiency and decrease the systemic toxicity of Dacarbazine using nanostructured lipid carriers (NLC) for topical administration.

Different NLC compositions were synthesised using a laboratory-based high shear dispersion (HSD) method, and applying varying processes parameters. The preparations were optimized to achieve the desired NLC characteristics (average size 155 ± 2 nm, polydispersity index (PDI) 0.1 ± 0.05 and zeta potential -43.7 ± 0.6) assessed using hydrodynamic light scattering (DLS), zetasizer and transmission electron microscopy (TEM). The optimized NLC (NLC/PI) were then used to encapsulate Dacarbazine. The resultant NLC/PI-Dac was characterized (average size 190 ± 10 nm, PDI 0.2 ± 0.03 and zeta potential -43.5 ± 1.2) and crystallinity determined using X-Ray Diffraction (XRD). The pharmacological properties of NLC/PI-Dac were then investigated and the percentage of encapsulation efficiency and drug loading capacity were determined to be $98.5\pm 0.2\%$ and $23.4\pm 0.2\%$, respectively.

The *in vitro* toxicity of NLC/PI-Dac was assessed using a melanoma cell line (A375). The *in vitro* drug release profile of NLC-Dac showed a biphasic pattern; 50% released over 2 hours and remainder within 30 hours. No toxicity was measured for the different NLC/PI concentrations after 24, 48 and 72 hours treatment, but there was an increase in toxicity of Dacarbazine after NLC/PI encapsulation (NLC/PI-Dac) at all concentrations and all-time points.

NLC/PI and NLC/PI-Dac were stable in size, PDI and zeta potential when stored at 4°C for 3 months and the developed process was transferable to industrial-scale synthesis using the Micro Jet Reactor technique. NLCs were shown to be a suitable drug delivery system for Dacarbazine, achieving a desirable drug loading, encapsulation efficiency and drug release profile.

Keywords: Precirol ATO-5, nanostructured lipid carriers, Dacarbazine, Micro Jet Reactor, Melanoma.

ACKNOWLEDGEMENTS

I would like to thank the support and assistance of my supervisors, Professor Sam Tothill, Dr Sophie Rocks and Dr Huijun Zhu, for all of their help and advice throughout my study at Cranfield University.

This research was financially assisted by the forensics laboratories of interior ministry of Saudi Arabia and under supervision of Saudi Cultural Bureau. I am truly grateful to all staff for making this possible.

Special thanks to my Mum and Dad for advice, pray and encouragement. I really appreciate everything you have done for me. It is a good opportunity to express my gratitude to my wife Mrs Ahoud Alhedian and the rest of my family, friends and colleagues.

TABLE OF CONTENTS

ABSTRTRACT	ii
ACKNOWLEDGEMENTS	iii
TABLE OF CONTENTS	iv
LIST OF FIGURES	ix
LIST OF TABLES	xiii
ABBREVIATIONS	xvii
1. BACKGROUND AND LITERATURE REVIEW	2
1.1. Introduction.....	2
1.2. Skin tumours	4
1.2.1 Melanoma	5
1.2.1. 1 Type of melanoma	9
1.2.1. 2 Treatment of melanoma by chemical drug (dacarbazine).....	10
1.3. Nanomaterials	12
1.3.1 Definition and classification of nanomaterials	12
1.3.2 Nanomaterials in medicine	15
1.3.3 Nanomaterials in drug delivery "Nanocarriers"	17
1.3.4 Toxicity of nanocarriers.....	20
1.4. Lipid-based nanostructured lipid carriers	23
1.5. NLC for topical drug delivery system	28
1.6.1 NLC structures.....	29
1.6.2 NLC formulation and preparation	30
1.6.3 NLC Physical parameters	38
1.6. NLC for anti-tumour drug delivery (dacarbazine).....	39

1.7.	Gap analysis	44
1.8.	Aim and objectives	48
2.	MATERIALS AND METHODS	52
2.1	Introduction.....	52
2.2	Materials	52
2.3	Methods for preparation.....	54
2.3.1	Laboratory-based synthesis of NLCs and NLC-DAC.....	54
2.3.2	Industry-based synthesis of NLC/PI.....	57
2.4	Measurement of physiochemical properties	58
2.4.1	Introduction	58
2.4.2	Dynamic Light Scattering (DLS)	58
2.4.3	Nanoparticles tracking analysis (NTA).....	60
2.4.4	Zeta potential	61
2.4.5	Transmission Electron Microscopy (TEM).....	62
2.4.6	Stability at storage conditions.....	63
2.4.7	Lyophilisation.....	63
2.4.8	Powder X-Ray diffraction (PXRD).....	64
2.5	Measurement of pharmacological effect.....	66
2.5.1	Introduction	66
2.5.2	Drug loading capacity (DL) and encapsulation efficiency (EE)	66
2.5.3	Drug release profile	67
2.6	Methods for NLCs and NLC/PI-Dac toxicity assessment in A375 cells.....	68
2.6.1	Introduction	68
2.6.2	Cell culture	68

2.6.3	phase contrast microscopy for cell imaging	69
2.6.4	Cell counting	71
2.6.5	Morphology of A375	71
2.6.6	Growth rate	72
2.6.7	A375 doubling time	73
2.6.8	MTT assay	73
2.7	Statistical analysis	75
3.	NANOSTRUCTURED LIPID CARRIERS SYNTHESIS CHARACTERISTIC AND OPTIMIZATION	77
3.1	Introduction.....	77
3.2	Preliminary preparation of NLC using evaporation-solidification methods	77
3.3	Optimization of NLC laboratory-based synthesis by using HSD.....	86
3.3.1	NLC/SI	86
3.3.2	NLC/GM.....	90
3.3.3	NLC/PI	94
3.4	Factors influence on NLC properties during the preparation	97
3.4.1	Solid lipid type	98
3.4.2	Time and speed optimization of HSD	100
3.5	Stability of NLC/SI, NLC/GM and NLC/PI.....	104
3.6	NLC/PI 1% preparation assessment.....	105
3.7	Characterization of chemophysical properties of NLC/PI 1%	106
3.7.1	Particles size measurements by DLS.....	106
3.7.2	Nanoparticles tracking analysis (NTA)	107
3.7.3	The morphology study of NLC by TEM.....	108
3.7.4	NLC stability	108

3.8	NLC/PI 1% synthesis and optimization using MicroJet Reactor (MJR)	109
3.9	Discussion	112
3.9.1	NLC formulae	112
3.9.2	Critical steps of NLC synthesis at laboratory-based	113
3.9.3	Critical steps of NLC synthesis at industry-based	115
3.9.4	Comparison between HSD and MJR	116
3.10	Summary	117
4. SYNTHESIS AND THE CHARACTERISATION OF NANOSTRUCTURED LIPID CARRIERS-DACARBAZINE		119
4.1	Introduction	119
4.2	Preparation and physiochemical characteristic of NLC/PI 1%-Dac	119
4.3	NLC/PI 1% carrier pre and post Dac (50mg) encapsulated	124
4.3.1	Particle size, dispersity and zeta potential	124
4.3.2	Morphology	125
4.3.3	Crystallinity	126
4.4	Drug release profile of NLC/PI 1%-Dac 50	128
4.5	Stability of NLC/PI 1%-Dac 50	129
4.6	In vitro cytotoxicity assessment of NLCs and NLC/PI-Dac	130
4.6.1	Growth rate and doubling time of A375 cells	130
4.6.2	Morphology of A375 cells	133
4.6.3	Viability assessment for A375 cells post NLCs treatment	134
4.7	Treatment of A375 cells with Dac with and without NLC/PI encapsulation ...	136
4.8	Discussion	140
4.8.1	Nanostructured lipid carriers encapsulated dacarbazine	140
4.8.2	Cytotoxicity assessment	142

4.8.3	Summary.....	144
5.	GENERAL DISCUSSION, CONCLUSIONS AND FURTHER WORK.....	146
5.1	Summary.....	146
5.2	General discussion	146
5.3	Conclusion	149
5.4	Uncertainties and limitations	150
5.5	Further work	151
	REFERENCES	153
i.	Appendix A collaboration work	177
	Characterization of silica nanoparticles	177
ii.	Appendix B HSD specification sheet	187
iii.	Appendix C silica particles specification sheet	200
iv.	Appendix D Publications and Awards.....	200
A.	Publications	200
B.	Awards	221

LIST OF FIGURES

Figure 1.1: Schematic skin structure shows the melanocyte at the bottom of epidermis.	4
Figure 1.2: Estimated incidence, mortality & prevalence for both sexes	6
Figure 1.3: Image of skin melanoma with approximately 2.5 cm by 1.5 cm.....	7
Figure 1.4: A radial growth phase in the most common type of melanoma superficial spreading melanoma.	9
Figure 1.5: Dacarbazine chemical structure, Systematic (IUPAC) name 5-(3,3-Dimethyl-1-triazenyl) imidazole-4-carboxamide.	10
Figure 1.6: Nanomaterials with a variety of morphologies.....	13
Figure 1.7: Classification of nanomaterials (Sjanlal et al., 2001).	15
Figure 1.8: Effect of contrast agent (super paramagnetic iron oxide nanoparticles) on images	16
Figure 1.9: Illustration of different types of nanodrug delivery system.	18
Figure 1.10: Relationship of the functionality and characteristics of nanoparticles.....	19
Figure 1.11: Schematic showing the different type lipid-based carriers that can be used in nanodrug delivery.	24
Figure 1.12: Scheme for NLC structures.	29
Figure 1.13: Chemical structure of Precirol ATO-5, (hexadecanoic acid;octadecanoic acid;propane-1,2,3-triol)	31
Figure 1.14: Chemical structure of Glyceryl behenate (2,3-dihydroxypropyl docosanoate).....	31
Figure 1.15: Chemical structure of Stearylamine (Octadecan-1-amine).	32
Figure 1.16: Schematic showing HSD mechanism	36
Figure 1.17: Strategy for assessing the safety and therapeutic effect of dermal drugs delivery system.	42
Figure 1.18: TEM images for Dacarbazine loaded cubosomes nanocarriers.....	45
Figure 1.19: TEM image of Dac-MPEG- PLA NPs. (Ma et al., 2011).	46

Figure 1.20: Morphology of nanoemulsion-Dac determined by TEM.....	47
Figure 1.21: Schematic outlining the experimental approach of the project.	50
Figure 2.1: High shear disperser machine which used to prepare NLC (T25 digital Ultra-Turrax, IKA, UK).	56
Figure 2.2: Schematic showing MJR processes of two impinging jets	57
Figure 2.3: Optical configurations of the Zetasizer Nano series for dynamic light	59
Figure 2.4: Schematic presentation of the Nanoparticle Tracking Analysis.....	60
Figure 2.5: Layout of optical components in a basic TEM.....	63
Figure 2.6: X-ray diffractogram for (A) Itraconazole-loaded nanostructured lipid carriers; (B) blank nanostructured lipid carriers; (C) itraconazole.....	64
Figure 2.7: X-ray diffraction pattern of native Dac	65
Figure 2.8: Spectrum diagram and calibration curve of Dacarbazine.	66
Figure 2.9: The configuration of a phase contrast microscope	70
Figure 2.10: Phases curve of cells growth shows the period of treatment.....	72
Figure 2.11: Schematic diagram of Formazan salt formation from MTT by Mitochondrial reductase.....	73
Figure 3.1: The smallest particles size distribution obtained for NLC/PI (F1a) as measured by DLS	79
Figure 3.2: The smallest particles size distribution obtained for NLC/GM (F2b) as measured by DLS	79
Figure 3.3: The smallest particles size distribution obtained for NLC/GM (F3a) as measured by DLS	80
Figure 3.4: The smallest particles size distribution obtained for NLC/PI (F4a) as measured by DLS	81
Figure 3.5: The smallest particles size distribution obtained for NLC/SI (F6a) as measured by DLS	81
Figure 3.6: The smallest particles size distribution obtained for NLC/PI (F7a) as measured by DLS	83

Figure 3.7: The smallest particles size distribution obtained for NLC/GM (F8a) as measured by DLS	83
Figure 3.8: The smallest particles size distribution obtained for NLC/SI (F9a) as measured by DLS	84
Figure 3.9: The smallest particles size distribution obtained for NLC/PI (F10a) as measured by DLS	85
Figure 3.10: The smallest particles size distribution obtained for NLC/SI (F12a) as measured by DLS	85
Figure 3.11: Data obtained from DLS for NLC/SI at 1% surfactant.....	88
Figure 3.12: Data obtained from DLS for NLC/GM at 3% surfactant.....	92
Figure 3.13: Particle size of NLC with different solid lipid and surfactant concentration (1%, 2%, 3%) after HSD (15,000 rpm, 30 min).....	98
Figure 3.14: The effect of HSD speed through the time (up to 40 min) on particle size of NLC/PI 1%	105
Figure 3.15: The effect of HSD speed through the time (up to 40 min) on PDI of NLC/PI 1%	106
Figure 3.16: Size distribution of NLC/PI 1% as measured by DLS.....	107
Figure 3.17: The relative intensity of NLC/PI 3% particle by nanoparticles tracking analysis.....	107
Figure 3.18: TEM micrograph showing the morphology of a NLC/PI particle with 1% concentration prepared by HSD (15,000 rpm, 30 min)	108
Figure 3.19: Particle size against flow rate and temperature as measured by DLS after MJR preparation	111
Figure 3.20: Polydispersity index against flow rate and temperature as measured by DLS after MJR preparation	112
Figure 4.1: A standard curve for mean absorbance of Dac concentrations in acetone solution measured by UV spectrometry at wavelengths 330 nm	121
Figure 4.2: DLS recorded size distribution and the polydispersity index (PDI) for NLC/PI 1% (left) and NLC/PI 1%-Dac 50 (right)	124
Figure 4.3: The analysis obtained from Zetasizer for NLC/PI 1% (left) and NLC/PI 1%-Dac 50 mg (right).....	125

Figure 4.4: TEM micrographs of NLC/PI 1% (a) and NLC/PI 1% -Dac 50 (b) Dacarbazine (Dac).	126
Figure 4.5: XRD trace of (a) Dac, (b) NLC/PI 1% and (c) NLC/PI 1%-Dac	127
Figure 4.6: In vitro drug release profile for the drug Dac from particles NLC/PI 1% for formula NLC/PI 1%-Dac	129
Figure 4.7: The optical density of A375 cells seeded with different concentrations at different time point	131
Figure 4.8: Morphology study for A375 cells (3×10^3 cells/ml) observed by light microscopy ($\times 20$) after 24 hours' incubation.....	133
Figure 4.9: Mean cell line viability (as measured using MTT assay, n=3) when exposed to NLC/PI 1%	134
Figure 4.10: Mean cell line viability (as measured using MTT assay, n=3) when exposed to NLC/SI 1%	135
Figure 4.11: Mean cell line viability (as measured using MTT assay, n=3) when exposed to NLC/GM 1%	136
Figure 4.12: The effect of Dac pre and post NLC/PI 1% encapsulated on the viability of A375 cells after 24hours treatment as measured using MTT assay	137
Figure 4.13: The effect of Dac pre and post NLC/PI 1% encapsulated on the viability of A375 cells after 48hours treatment as measured by MTT assay.....	138
Figure 4.14: The effect of Dac pre and post NLC/PI 1% encapsulated on the viability of A375 cells after 72hours treatment as measured using MTT assay	139
Figure 5.1: Schematic for Dac mechanism of action post NLC encapsulated.	149

LIST OF TABLES

Table 1.1: Unpredictable of cellular injuries may occur post nanoparticles treatment. .	22
Table 1. 2: Common techniques used to measure nanoparticles properties as a carrier for drug delivery system.	23
Table 1.3: Examples of solid lipid nanoparticles (SLN) nanodrug delivery for oral and topical administrations.	26
Table 1.4: Examples of drugs applied nanostructured lipid carriers (NLC) nanodrug delivery for topical administrations.	28
Table 1.5: Different methods were used to prepare nanostructured lipid carrier (NLC).	37
Table 1.6: Advantages for anti-tumour drugs post NLC loading as nanodrug delivery system.	43
Table 2.1: Cell lines, media and supplements.	53
Table 2.2: Cell-based and molecular biology assay reagents.	54
Table 2.3: The formula components of NLC preparations.	55
Table 2.4: Zeta potential value guidelines and stability evaluation.	61
Table 2.5: MTT plan for A375 cells treated by different type and concentrations of NLCs.	74
Table 2.6: MTT plan for A375 cells treated by different concentrations of NLC/PI carrier before and after encapsulated Dac and Dac.	75
Table 3.1: Formula components of NLCs preparations by evaporation-solidification methods.	78
Table 3.2: The particle size and polydispersity index (PDI) data obtained from DLS for different NLC preparation, different stirring time at 400 rpm, mean \pm SD (n = 5).	78
Table 3.3: The particle size and polydispersity index (PDI) data obtained from DLS for different NLC preparation, different stirring time at 200 rpm, mean \pm SD (n = 5).	80
Table 3.4: The formula components of NLC.	82
Table 3.5: The particle size and polydispersity index (PDI) data obtained from DLS for different NLC preparation, different stirring time at 400 rpm, mean \pm SD (n = 5).	82

Table 3.6: The particle size and polydispersity index (PDI) data obtained from DLS for different NLC preparation, different stirring time at 200 rpm, mean \pm SD (n = 5).....	84
Table 3.7: The formula components of NLC/SI preparations by high sheer dispersion.	86
Table 3.8: The particle size and polydispersity index (PDI) data obtained from NLC/SI prepared with different surfactant concentration by high sheer dispersion (HSD) with varying speed and time, mean \pm SD (n = 5).....	87
Table 3.9: Table 3.9: One-way ANOVA results to investigate the above hypothesis. ..	88
Table 3.10: One-way ANOVA results to investigate the above hypothesis.	89
Table 3.11: The formula components of NLC/GM preparations by high sheer dispersion.	90
Table 3.12: The particle size and polydispersity index (PDI) data obtained from NLC/GM prepared with different surfactant concentration by high sheer dispersion (HSD) with varying speed and time, mean \pm SD (n = 5).....	91
Table 3.13: One-way ANOVA results to investigate the above hypothesis.	92
Table 3.14: One-way ANOVA results to investigate the above hypothesis.	93
Table 3.15: The formula components of NLC/PI preparations by high sheer dispersion.	94
Table 3.16: The particle size and polydispersity index (PDI) data obtained from NLC/PI prepared with different surfactant concentration by high sheer dispersion (HSD).....	95
Table 3.17: One-way ANOVA results to investigate the above hypothesis.	96
Table 3.18: One-way ANOVA results to investigate the above hypothesis.	96
Table 3.19: One-way ANOVA results to investigate the above hypothesis.	98
Table 3.20: The results of LSD analysis for particle size according of different solid lipid of different NLC prepared by HSD.	99
Table 3.21: One-way ANOVA results to investigate the above hypothesis.	99
Table 3.22: The results of LSD analysis for PDI according of different solid lipid of different NLC prepared by HSD, where *** shows $P \leq 0.01$	100
Table 3.23: One-way ANOVA results to investigate the above hypothesis.	101
Table 3.24: The results of LSD analysis for nanoparticle size according of different time of different NLC prepared by HSD	101

Table 3.25: One-way ANOVA results to investigate the above hypothesis.	102
Table 3.26: The results of LSD analysis for PDI according of different time of different NLC prepared by HSD.....	102
Table 3.27: Means and standard deviations for nanoparticles size according to speed variable and T-test results for independent samples test to investigate for any differences between means.....	103
Table 3.28: Means and standard deviations for PDI according to speed variable and T-test results for independent samples test to investigate for any differences between means.	104
Table 3.29: Particle size, PDI and zeta potential after one-week preparation of NLC/PI formula synthesized by HSD at 15,000 rpm and 30 min.	104
Table 3.30: The effect of storage of NLC/PI with 1% surfactant at 4°C on average particle size, PDI and zeta potential over a period of 6 months, formula synthesized by HSD at 15,000 rpm and 30 min.....	109
Table 3.31: The formula components of NLC/PI preparations by MicroJet Reactor. .	110
Table 3.32: Particle size and PDI of NLC/PI 1% obtained after MJR preparation with varying flow rate and temperature	110
Table 3.33: The differences between HSD (15,000 rpm and 30 min) and MJR method (70 °C and flow rate 75 ml/sec) during the preparation of in NLC/PI 1%.	116
Table 4.1: The formula components of NLC/PI 1%-Dac preparations formed using high shear dispersion at 15,000 rpm for 30 min.....	120
Table 4.2: Particle size, PDI and zeta potential for NLC/PI 1%-Dac formula synthesized by high shear dispersion at 15,000 rpm and 30 min	120
Table 4.3: The absorbance and equivalent amount of un-entrapped Dac in NLC/PI 1%-Dac formula with different concentration of Dac prepared by high shear dispersion at 15,000 rpm and 30 min	122
Table 4.4: The results obtained from the calculation for the percentage of encapsulation efficiency and the percentage of drug loading capacity obtained from the equation 1 and 2 for NLC/PI 1%-Dac formula with different concentration of Dac.....	123
Table 4.5: Physical properties of particle size, PDI and zeta potential for NLC/PI and NLC/PI-Dac 24 hours post preparation by high shear dispersion at 15,000 rpm and 30 minutes	125

Table 4.6: Physical properties of particle size, polydispersity index (PI) and zeta potential for NLC/PI-Dac 50 post preparation by high sheer dispersion at 15,000 rpm and 30 min	130
Table 4.7: The doubling time of different concentrations of A375 cells in culture, mean \pm SD (n = 3).....	132
Table 5.1: The result of NCL physical properties post Dac encapsulation from different attempts.	147
Table 5.2: Biophysical measurments of Dac post encapsulated in different nanoparticles.	148

ABBREVIATIONS

- ALM: Acral lentiginous melanoma
ATP: Adenosine triphosphate
C60: New form of carbon
DDS: Drug delivery system
DLS: Dynamic light scattering
DSC: Differential scanning calorimetry
FBS: Foetal bovine serum
FCM: Flow cytometry
GB: Glyceryl behenate
HLA-DR antigen: is Human leukocyte antigen – antigen D related
HPLC: High-performance liquid chromatography
HSD: High sheer dispersion
IM: Isopropyl myristate
IPM: Isopropyl myristate
ISO: International standardization organization
LDC: Lipid drug conjugates
LDH: Lactate dehydrogenase assays
LMM: Lentigo maligna melanoma
MAPKs: Mitogen activated protein kinase
MCTs: Medium-chain triglycerides
MRI: Magnetic resonance imaging
MTT: 3-(4,5-dimethylthiazol-2-yl)-2,5-diphenyltetrazolium bromide
NLC/GM: Nanostructured lipid carrier using solid lipid Glyceryl behenate
NLC/PI: Nanostructured lipid carrier using solid lipid Precirol ATO-5
NLC/PI-Dac: Dacarbazine encapsulated NLC with solid lipid Precirol ATO-5
NLC/SI: Nanostructured lipid carrier using solid lipid Stearylamine
NLC: Nanostructured lipid carrier
NLC-Dac: Dacarbazine encapsulated nanostructured lipid carrier
NM: Nodular melanoma
NTA: Nanoparticle tracking analysis
PDI: Polydispersity index
SA: Stearylamine

SEM: Scanning electron microscopy

SLN: Solid lipid nanoparticles

SLT: Soybean lecithin

SSM: Superficial spreading melanoma

TEM: Transmission electron microscopy

TEM: Transmission electron microscopy

TPGS: D-alpha-tocopherol polyethylene glycol succinate

UV: Ultra violet

UV-Vis: Ultraviolet-visible spectrophotometry

W/O: Water in oil

W/O/W: Water in oil in water

CHAPTER ONE

BACKGROUND AND LITERATURE REVIEW

1. BACKGROUND AND LITERATURE REVIEW

1.1. INTRODUCTION

The application of nanotechnology has been explored into diverse fields, particularly into industrial applications, in energy and medicine. It is a new concern where the unique phenomena over nanomaterial (materials in nanoscale <1000 nanometres) custom perform stand exploited within novel applications. However, the phenomena also mean that there remain a deficiency concerning the knowledge about these novel materials. Nanomedicine refers to the science, which apply nanotechnology into the medical field. In nanomedicine studies, nanoscale materials are used to enhance drugs properties. The research in this field aims at developing nanomaterials in imitation of obtaining the required efficacy or reduce the undesirable effects of current medicines. Different strategies are used such as drug delivery, this method is recognized namely as "drug delivery nanosystem". In drug delivery nanosystems, nanocarriers (synthesised using nanomaterials) were introduced as an effective parameter among the therapeutics properties of the drug such as pharmacokinetics and bioavailability. The main advantages of drug delivery nanosystems includes (Paolino et al., 2006):

1. The possibility to control plasma drug levels in a therapeutic window range,
2. The opportunity to eliminate or reduce harmful side effects from systemic route,
3. The feasibility of variable routes of administration for example oral administration, inhalation and dermal application.

Skin tumour melanoma is considered as the most common type of skin cancer which has high mortality incident. It can be surgically removed in early stage of the disease, while metastasized melanoma causes the death of more than 86% of patients within five years (Tas et al., 2012). Metastasized melanoma, the disease can spread to lymph nodes and other sites. Dacarbazine (Dac) is the drug of choice for melanoma patients. However, Dac has unacceptable side effects with sever patient complains. There is an opportunity to improve the chemical treatment for skin tumour melanoma by Dac using drug delivery nanosystem. The utilization of drug delivery nanosystem has some advantages over the traditional technique in that delivery of the drug can be specific to

the diseased site and also fewer drugs administrations and improved patient compliance. Nanocarriers may provide an effective drug delivery system for Dac in that, it can enhance the solubility of poorly water-soluble drug, increase the drug half-life, progress pharmacokinetics and bioavailability, as well as improve the drug metabolism. Nanocarriers can carry the melanoma drug Dac to the disease site specifically for example, using topical drug nanosystem and, consequently, significantly improve treatment efficacy.

This thesis illustrates the forms of nanocarriers as the nanostructured lipid carrier (NLC), which can be used for topical drug delivery nanosystem. NLC have many advantages in topical drug delivery nanosystem, moreover, recent research shows the importance of nanostructured lipid particles NLC as a carrier for cancer chemotherapy among drug delivery system for topical application (Sanad, 2010; Selvamuthukumar and Velmurugan, 2012 and Jaiswal et al., 2016). Like others nanocarriers, NLC must be adjusted regarding its physicochemical characteristic and unpredictable toxicity effect, and it is very important to be evaluated before using them in drug delivery. However, despite these potential advantages from nanocarriers, the complexity of their functionalization and the outcome, they require attentive engineering, reproducible method of synthesis, characteristics analysis and toxicity assessment. This is needed in order to achieve a reliable nanocarrier with the intended physicochemical properties, biological and pharmacological performance. The safety and efficacy of nanocarriers can be influenced by slight variations in different parameters during their synthesis and hence, the need to conduct *in vitro* and *in vivo* study to analyse their performance. The research conducted in this thesis investigated first silica particles and their properties in relation to their application in treatment for topical application (Appendix A Collaboration Work). Then, these procedures established the methods for nanostructured lipid carrier NLC characterization and cell toxicity assessment.

In this chapter, the background to the research project conducted in this thesis to develop novel nanocarriers for melanoma disease treatment will be given. This will include the challenges of working in this new and novel field of nanomedicine.

1.2. SKIN TUMOURS

The skin is a very important organ for human being as it has the largest surface interacting with the outside environment and is a barrier, protecting the inside parts of the human body. The human skin is composed of three layers and each of them performing specific functions (Figure 1.1). The deepest layer of the skin is the subcutis (Hypodermis) that consists of a network of collagen and fat cells. The subcutis layer helps preserve the body's heat and protects the body from injury. The middle layer of the skin, the dermis, gives the skin flexibility and strength. The dermis contains blood vessels, lymph vessels, hair follicles, sweat glands, collagen bundles, fibroblasts and nerves. The outer layer of the skin is the epidermis which consists of stratum corneum, keratinocytes, and basal layer as major components (Cichorek et al., 2013). Stratum corneum consists of fully mature keratinocytes which contain fibrous proteins (keratins).

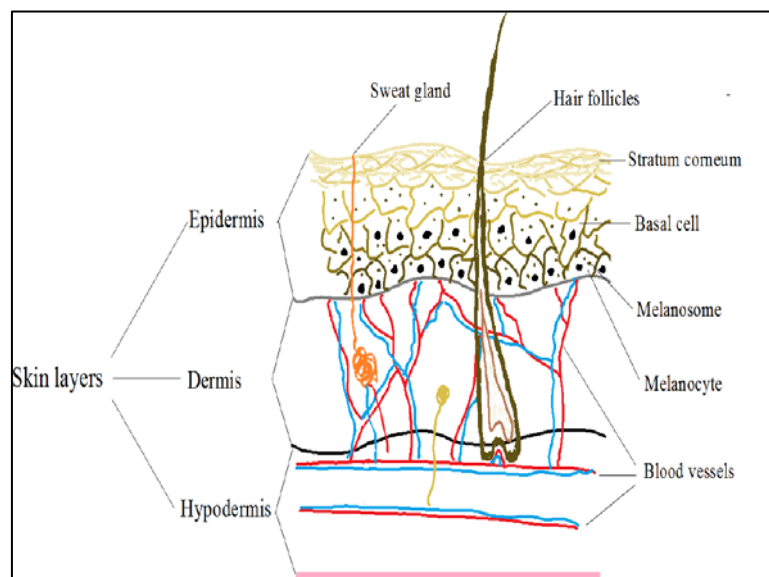


Figure 1.1: Schematic skin structure shows the melanocyte at the bottom of epidermis.

Stratum corneum is the major barrier for the penetration of substances into the skin because of its heterogeneous composition and packed organization of corneocytes and the intracellular lipid matrix. Keratinocytes (squamous cells) contain living

keratinocytes which mature and form the stratum corneum. The basal layer contains basal cells which continually divide to form new keratinocytes to replace the old ones that are shed from the skin's surface. The epidermis also contains merkel cells, langerhans cells and melanocytes which produce melanin skin pigmentation. The symptoms such as redness, swelling, burning and itching are common signs shared within many skin disorders such as eczema, psoriasis, vitiligo and skin cancer. There are three common skin tumours classified by the type of cells that become malignant (Horner et al., 2009). Basal cell carcinomas are the most common form of skin cancer (Woodward et al., 2003). This cancer occurs in the epidermis, in places that have often been exposed to the sun such as the face (Neale et al., 2007). Squamous skin cancer initiates in squamous cells and it is typically found in places that are not often exposed to the sun but are suitable for bacteria growth, for example the feet and the armpit (Leiter and Garbe, 2008). Squamous cell carcinoma is not as dangerous as much but may spread to other parts of the body if not treated. It grows over around months and appears on the skin a thickened, red, scaly spot and ulcerate bleeding. The third type of skin cancer is melanoma. Despite being less common than the other two forms; melanoma is much more lethal if it is not diagnosed at early stage (Eikenberry et al., 2009).

1.2.1 Melanoma

Melanoma is a cancer of the cells that produce the pigment melanin that colours the skin in hair and eyes (Scherer and Kumar, 2010). The occurrence of melanoma has risen at an alarming rate over recent years. Melanoma incidence rates have been increasing for at least 30 years and it is the most common of all cancers (Linos et al., 2009). Melanoma is the most serious type of skin cancers and it is associated with one of the highest mortality rates (Dai et al., 2005). The world health organization (WHO) reported that "the global incidence of melanoma continues to increase, and 132,000 melanoma skin cancers occur globally each year" (source WHO <http://www.who.int/uv/faq/skincancer/en/index1.html> accessed on 23.04.2017).

In the United State of America, there is an estimation from skin cancer that there will be 87,110 new cases of melanoma in 2017 (source Skin cancer foundation

<http://www.skincancer.org/skin-cancer-information/skin-cancer-facts> accessed on 03.07.2017). The incidence of melanoma has increased dramatically in numbers of cases over the past few decades "15 times in the last 40 years in USA".

In addition, a similar increase in the incidence rate of melanoma has been seen in United Kingdom and this is a more rapid increase than for any other cancer (source AIM at Melanoma <https://www.aimatmelanoma.org/about-melanoma/melanoma-stats-facts-and-figures/> accessed on 12.10.2017). In 2012, the European cancer research has estimated the incidence, mortality and prevalence for malignant melanoma of skin. Switzerland has the highest incidence rate and the Norway has the highest mortality rate of melanoma (Figure 1.2).

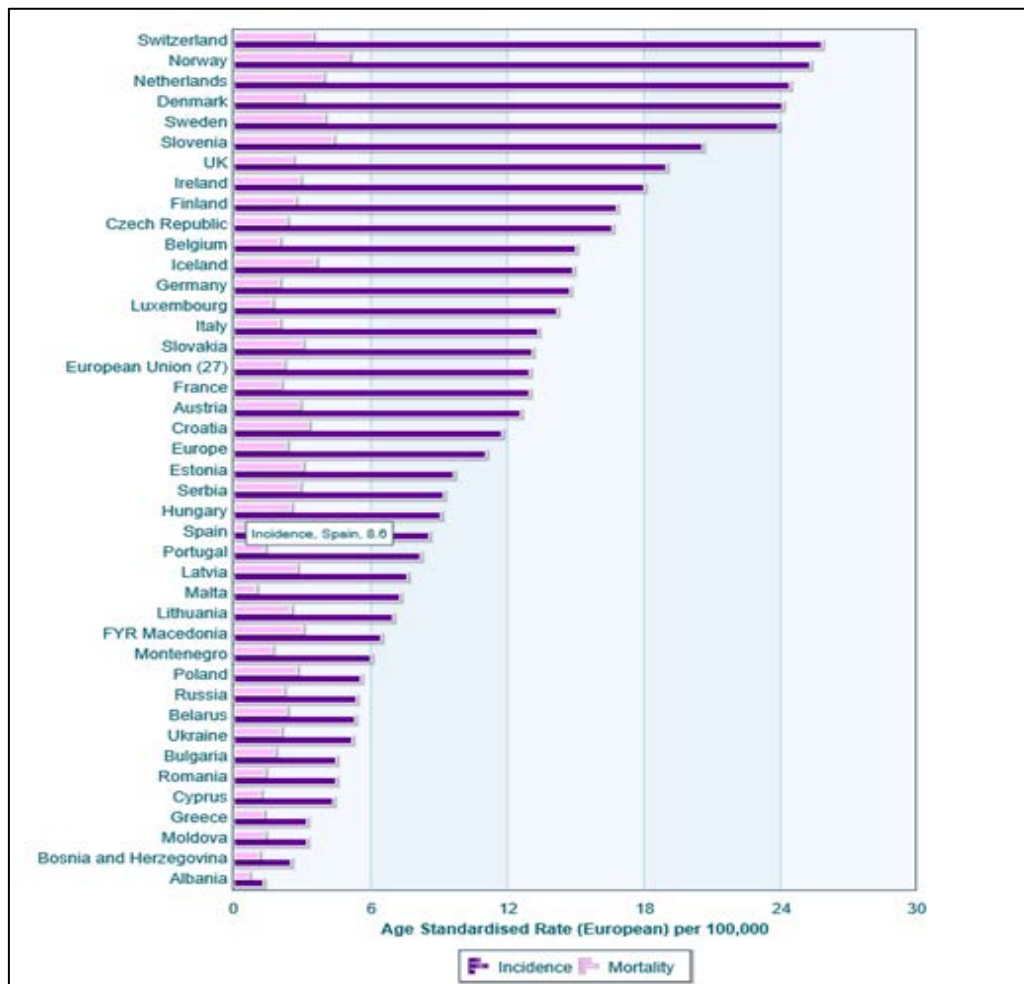


Figure 1.2: Estimated incidence, mortality & prevalence for both sexes (source: EUCAN <http://eco.iarc.fr/EUCAN/Cancer.aspx?Cancer=20> accessed on 07.10.2017).

Although reasons for this increase is not clear, a variety of factors including inheritance of gene mutation, ageing and environmental risk such as increase exposure to ultraviolet light, have all been considered to have influence on the progression of the diseases (D'Orazio et al., 2013). There are a few symptoms that can be used to identify melanomas, for example changes in skin colour, non-healing sores, painful spots and red lumps bleeding (Figure 1.3). The cancerous growth develops when unrepaired DNA damages the skin cells triggers mutations (genetic defects) that lead the skin cells to multiply rapidly and form malignant tumours. These tumours originate in the pigment-producing melanocytes in the basal layer of the epidermis. The primary cause of melanoma is ultraviolet light (UV) exposure in those with low levels of skin pigment (Kanavy and Gerstenblith, 2011 and Stewart et al., 2014). The UV light may be from either the sun or from tanning devices. About 25% incidence of the disease develop from moles (Kanavy and Gerstenblith, 2011). Those with many moles, a history of affected family members, and who have poor immune function is at greater risk (Stewart and Wild, 2014).



Figure 1.3: Image of skin melanoma with approximately 2.5 cm by 1.5 cm (source: National Cancer Institute <http://visualsonline.cancer.gov/details.cfm?imageid=2184> accessed on 27.09.2016).

A number of rare genetic defects such as xeroderma pigmentosum also has increased risk and incidence of the disease (Azoury and Lange, 2014). Melanoma begins in melanocytes which are responsible for producing the skin pigmentation. Most melanocytes occur in the skin and other parts of the body that contain melanocytes. For example, in the eye tissue the melanocytes may proliferate, causing uveal tumours (Jovanovic et al., 2013). In the skin, melanocytes reside at the basal layer of the epidermis and are present also in hair follicles (Cichorek et al., 2013). It has been stated that about 12% of melanoma tumours reside in families with hereditary predisposition, and most familial melanomas bear mutations in the CDKN2A gene encoding the p16INK4 protein and CDK inhibitor (Hansson, 2010). In 2002 Davies et al., reported that approximately 65% of melanomas have mutation of V600E in B-RAF gene, and 25% have mutations of N-RAS. MITF-M (microphthalmia-associated transcription factor) is an essential transcription factor of the melanocyte lineage. It can regulate many other genes during melanoma progression such as genes involved in the regulation of anti-apoptosis, invasion, migration, and metastasis of melanoma. A smaller percentage of hereditary patients have mutations in p14ARF or CDK4 genes.

The voltage-gated ion channels are a different group of ion channels that are selectively permeable to sodium ion, potassium ion, chloride ion and calcium ion. They are respond to changes in the membrane potential. The voltage-gated ion channels have roles in controlling rapid bioelectrical signalling (Bezanilla, 2005). These channels can also contribute significantly to cell mitotic biochemical signalling and cell cycle progression. All these functions are critically important for cancer cell proliferation (Kale et al., 2015). In cancer researches, the increasing evidences demonstrating that voltage-gated ion channels play a major role in cancer cell biology (Rao et al., 2015). The ion channel blockers depolarized the melanoma cell membrane and this mechanism in turn reduce the intracellular driving force. Consequently, the admittance process of chemical drugs such as Dacarbazine (Dac) to melanocyte might be inadequate.

1.2.1. 1 Types of melanoma

In 2008, Mocellin et al., histologically classify melanoma into many types depending on its occurrence. Superficial spreading melanoma (SSM) which makes up about 70% of all melanomas most often occurs in young people. Histologically, SSM is characterized by the presence of a radial growth phase (Figure 1.4).

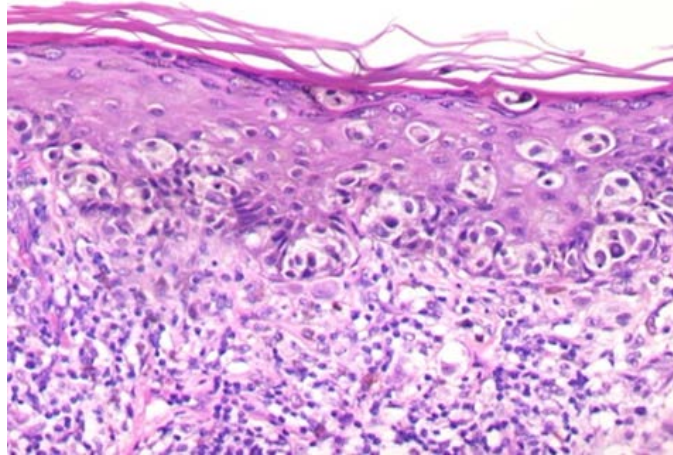


Figure 1.4: A radial growth phase in the most common type of melanoma superficial spreading melanoma (source: Melanoma Molecular Map project <http://www.mmmp.org/MMMP/import.mmmp?page=pathology.mmmp> accessed on 20.09.2016).

Nodular melanoma (NM) which has a vertical growth phase with no radial growth phase and it is the second most frequent histological type of melanoma (10 to 15% of all melanomas in Caucasians). Acral lentiginous melanoma (ALM) which has radial growth phase characterized by a lentiginous proliferation and the vertical growth phase often presents a spindle cell component. ALM is a relatively rare type of melanoma, approximately 5% of all cases, (Park and Cho, 2010). Lentigo maligna melanoma (LMM) it is histologically characterized by a confluent growth of atypical melanocytes along the dermal-epidermal junction frequently extending downwards the cutaneous appendages and it is naturally occurring in older people on sun-exposed areas.

Desmoplastic melanoma (DM) is a rare variant of malignant melanoma (2% to 4% of all melanomas) that occurs mainly on the neck and head of elderly patients. In 2007 Gray-Schopfer et al. demonstrated that LMM and SSM are most frequently associated with intermittent UV exposure.

1.2.1. 2 Treatment of melanoma by chemical drug (dacarbazine)

Usually at early-stage, melanoma is treated by the surgical removal of a very thin melanoma using the biopsy technique. For melanoma at metastasis stage, the treatment options may include radiation therapy, chemotherapy, immunotherapy and targeted therapy (Maverakis et al., 2015). Chemotherapy drug can be given intravenously or in pill form so that it travels throughout body to destroy tumour cells. In melanoma, the most common chemotherapy drug used for metastatic stage is Dacarbazine (Bedikian et al., 2006). Dacarbazine, or 5-(3, 3-dimethyl-1-triazenyl) imidazole-4-carboxamide, is an antineoplastic chemotherapy agent which is light sensitive and is partially soluble in water with pH 3-4 (Figure 1.5). Dacarbazine has a molecular formula $C_6H_{10}N_6O$ with molecular weight 182.187 g/mol and it has chemical names under DTIC; Biocarbazine, Deticene, and DTIC-Dome. It is white to ivory crystalline solid has a melting point 482 to 255° C.

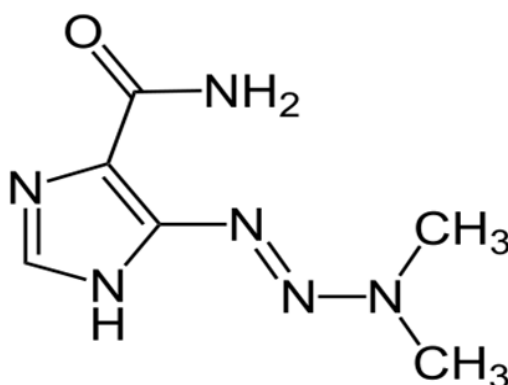


Figure 1.5: Dacarbazine chemical structure, Systematic (IUPAC) name 5-(3,3-Dimethyl-1-triazenyl) imidazole-4-carboxamide. (source: PubCem

<https://pubchem.ncbi.nlm.nih.gov/compound/dacarbazine> accessed on 13.07.2016).

Dac has been used to treat various cancers (Jiang et al., 2014), but it is the US Food and Drug Administration (FDA)-approved chemotherapeutic agent for treating wild-type melanomas, which account for most of skin cancer deaths and dacarbazine continues to be the standard of care for most patients with this disease (Bhatia et al., 2009). Dac is the most active single agent currently used for treating metastatic melanoma (Quirin et al., 2007). Its absorption through oral administration is very low (Gustafson and Page, 2013). It is metabolized in the liver to an alkylating agent (diazomethane) that methylates nucleic acids and inhibits DNA, RNA, and protein synthesis, consequently destroys cancer cells (Al-Badr and Alodhaib, 2016). After injection at 2.6-6.8 mg/body weight, the plasma concentration of the drug is 6 µg/ml, and the half-life of Dac is only 41 minutes in plasma, it is excreted in urine via renal tubular secretion and in about 40% in 6 hours unchanged (source: Parma Knowledge Base <https://www.pharmakb.com/dacarbazine/> accessed on 19.07.2016). A single-dose of 850–1000 mg/m² administered once every three weeks is standard therapy with a positive response rate seen in 13-20% of patients (Eggermont and Kirkwood, 2004; Davar and Kirkwood, 2012). Studies demonstrated that Dac enhances languid apoptotic response (Legha et al., 1989; Legha et al., 1996; Phan et al., 2001; Tsao et al., 2004; Anvekar et al., 2012). In 2011, Engesæter et al., showed the promotion of apoptosis after Dac treatment. The effect of Dac may only last for 3- 6 months as the melanoma cells develop resistance to drug induced-apoptosis by increased activity of DNA repair enzymes such as O6-alkylguanine-DNA alkyltransferase (AGAT) and aberrant survival pathways during progression (Soengas and Lowe, 2003).

The only available formulation for clinical use is delivered through intravenous injection (I.V.). The trade names available of dacarbazine are DTIC-Dome, DTIC, DIC and imidazole carboxamide. There are some common side effects for patient taking Dac such as irritation at the needle site during the infusion, local pain, burning sensation, numbness or tingling in the hands or feet, flu symptoms with fever. Moreover, the patient may temporarily have decreasing in white and red blood cells and platelets (source: Cemo Care <http://chemocare.com/chemotherapy/drug-info/dacarbazine.aspx> accessed on 14.07.2016). Like other chemotherapeutical agents, Dac also exhibits side effects by killing normally dividing cells. The strong damage for the healthy cells was diagnosed after Dac treatment, therefore, there is an imperative need for a new Dac

topical formulation for melanoma treatment (for example drug delivery nanosystem), which could reduce systemic side effects as well as protecting the drug from light and from fast degradation, and therefore extending the drug half-life *in vivo* while also achieving higher tolerable dose. The new drug delivery system that used nanomaterials as nanomedicine technology for Dac, may enhance these drug activities at tumour site.

This study will investigate the preparation of drug delivery system using nanostructured lipid materials as nanocarrier. This system is intending to improve the therapeutic effect of Dac through topical drug delivery system as well as reducing Dac side effect and melanoma`s patient complains.

1.3. NANOMATERIALS

With the emerging of nanotechnology, many nanotechnology research centres have been established worldwide. These centres focused their research activities manly on novel discoveries in this new and innovative technology. In many countries, nanotechnology like other new science is strongly supported. For example, National Nanotechnology Initiative in the United States, The National Centre in China, The London Centre of Nanotechnology in the United Kingdom and The King Abdullah Institute for Nanotechnology in Saudi Arabia. These nanotechnology centres, and others in the world, research and investigate the unique utilization of nanomaterials according to the global community needs. Presently, there are many applications of nanomaterials that are used to assist humans, for instance as nano-electronics, nano-engineering and nanomedicine.

1.3.1 Definition and classification of nanomaterials

The research in the field of nanomaterials discoveries, properties characterisation and application, has risen significantly at the end of last century. The major expectation has been in improving human life in transport, telecommunication, food and medicine. There are a range of different definitions for the term “nanomaterials”, but these are generally primarily based on size. The International Standardization Organization (ISO)

has defined nanomaterials as that “a nano-object which has one or more external dimensions in the nanoscale 1-100 nano meter (nm)” (Oberdorster, 2004). This definition can also include nanostructured substances as hold interior constructions or surface structures of the nanoscale (ISO/TS 27687:2008, ISO/TS 80004-1:2010). In case of one particle that has <100 nm in size with a surrounding interfacial layer the term called nanoparticle.

Materials in nanoscale have started to emerge as products that have supportive uses in human life. Unusual properties of particles can be revealed at the nanoscale and these include physical, chemical, biological and toxicological properties (Yakobson et al., 1997; Wang et al., 2005; Chauhan et al., 2011; Fang et al., 2011). Nowadays, nanomaterials have applications in the field of nanotechnology, and display different physicochemical characteristics from normal chemicals for example silica nanoparticles, nanolipids, gold nanoparticles and carbon nanotubes. The selection of any nanomaterials in products is based on their properties and applications suitability. For instance, in electronic devices, nanoparticles have extra dynamic expectations over electronics which are currents applied. While in the clinical application, much less toxic and effective nanoparticles are used.

The structure of the materials at the nanoscale often have unique optical, electronic, or mechanical properties. Nanomaterials have different structure and shapes, it executes appear in single, fused, agglomerated or aggregated forms with spherical, tubular and irregular shapes (Figure 1.6).

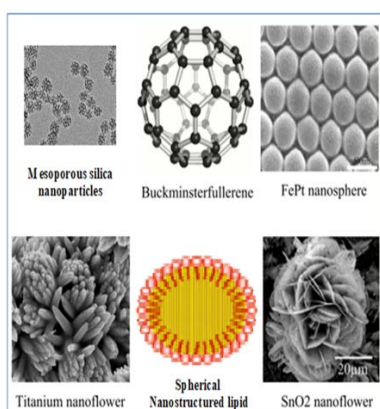


Figure 1.6: Nanomaterials with a variety of morphologies (source: Prof Sheama Farheen Savanur: <http://www.slideshare.net> accessed on 30.04.2015).

These nanomaterials structures are generally observed directly using imaging techniques such as scanning electron microscope (SEM), transmission electron microscopy (TEM), scanning tunnelling microscope (STM), or atomic force microscope (AFM), which are principal characterization tools. Nanostructured materials have distinctive structures such as nanocrystalline forms and they might be understood as the interfacial state. The crystal structure is an important property of nanomaterials, which can influence the behaviour of the materials, and thus also modulate potential toxic effects. In 2000, Gleiter published, "one of the very basic results of the physics and chemistry of solids is the insight that most properties of solids depend on the chemical composition, the arrangement of the atoms and the size of a solid in one, two or three dimensions".

Nanomaterials can be differentiated according to their chemical configuration and crystallite shapes. For example, silica nanomaterials have pores with diameters less than 100 nm and they are known as mesoporous silica nanoparticles. Nanostructured lipid carriers have lipid materials in their structure at the nanoscale level. Nanomaterials may be labelled differently depending on the cause of the study and or the area of application. For example, nanomaterials can be categorized by means of their physical, chemical or mechanical properties (Aitken et al., 2006). In 2011, Sajanlal *et al.* demonstrated that nanomaterials can also be characterized depending on the shape of their structure (i.e. plates, networks and nanocubes) or the number of surfaces zero, one, two or three dimensions and each dimension represented with the non-nanoscale size. For example, the nanostructured lipid carriers (NLC) has spherical structure and silica (SiNP) has particle form and both have zero dimension (Figure 1.7).

These nanomaterials have been implemented into medical research and the use of nanomaterials are included within the "nanomedicine" field. One of the greatest active research areas of the nanomaterials is nanomedicine. Nanomedicine involves the engineering of functional systems at the nanoscale to be applied for developing targeted nanomaterials for medicine use.

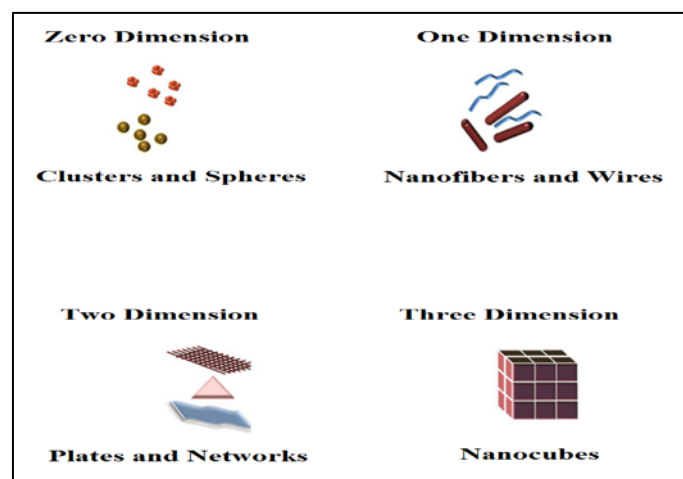


Figure 1.7: Classification of nanomaterials (Sjanlal et al., 2001).

1.3.2 Nanomaterials in medicine

Nanomedicine is the science that use nanotechnology for biomedical purposes to improve the prevention, diagnosis and treatment of diseases (Prego et al., 2005; Wagner et al., 2006). Nanomedicine is the rising beyond medicinal science where nanomaterials derived out of nanotechnology are employed to deliver promising and novel approaches for patient services. They are used globally in conformity concerning enhancing healthcare services and lives of patients. Recently, in the nanomedicine field diverse innovations are taking place due to the nanomaterials application and their unprecedented accomplishment and performance. New and promising drugs candidates have been formulated for medicinal research. This is because nanomedicine works where disease processes find their origin at the organellar, cellular, and molecular level. The research is concentrated on nanoscale materials that can fill full the expectation and be able to stand to challenging conditions such as for diagnostic, pharmaceutical and medicine applications. Previous articles have demonstrated the definitions of nanomedicine based on their applications within healthcare. These applications were classified into:

1) Biomaterials, self-assembling nanoscale materials that improve the mechanical properties and the biocompatibility concerning biomaterials for therapeutic implants. Thus, molecular materials composed partially or completely of biological molecules (such as DNA, RNA, proteins, antibodies, viruses, and cells) known as

bionanomaterials. The bionanomaterials products may have potential applications for example of fibres, sensors and energy generating.

2) Drugs and therapy, nanoscale materials used in the treatment of diseases that according to their shape have special clinical outcomes, for example drugs based on dendrimers or fullerenes.

3) *In vivo* diagnosis, nanoscale materials contrast agents that present enhanced contrast and good bio distribution, mainly for magnetic resonance imaging (MIR) and ultrasound for instance super paramagnetic iron oxide nanoparticles (Figure 1.8).

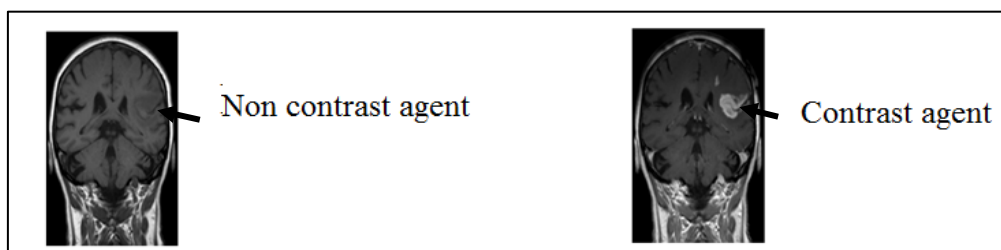


Figure 1.8: Effect of contrast agent (super paramagnetic iron oxide nanoparticles) on images: Defect of the blood–brain barrier after stroke shown in MRI. left image without, right image with contrast agent (Source Hellerhoff:

<https://www.pinterest.com/pin/516999232206177736/> accessed on 13.03.2010).

4) Drug delivery, nanoscale materials were established to improve the bioavailability and pharmacokinetics of medicine for example metal nanoparticles, silica nanoparticles and lipid-based nanoparticles. Consequently, they are combined with drugs to enhance their efficiency and efficacy, and known as nanocarriers, while the system used for carrying out the drug will be classified as drug delivery nanosystem. Although the definition recognizes nanoparticles as having dimensions less than 100 nm, particularly, in the uses of drug delivery relatively large nanoparticles, more than 100 nm, may be needed for loading an enough drug onto the particles.

In the field of nanomedicine in the drug delivery research, there are already a few number of products have come to be recognised as first generation nanomedicines. For

example, Abraxane anticancer drug encapsulated, Doxil in liposomes nanoscale, and Cimzia an antibody (Malam et al., 2009 and Ma and Mumper, 2013).

1.3.3 Nanomaterials in drug delivery "Nanocarriers"

In the past, conventional drug delivery system was used in different routes such as oral ingestion or intravascular injection. It was known to provide an immediate release of drug without perfect controlling and cannot maintain effective concentration at the target site for longer time. The major limitations of the conventional drug delivery systems include the poor drug loading capacity, possible toxicity of the materials used, dose dumping and higher manufacturing costs (Martinho et al., 2011). In addition, it cannot perform ideal controlled-drug release in some cases. Nowadays with the emerging of nanotechnology, drug delivery system has been improved by using nanoscale materials which are known as "nanocarriers". These molecules are principally based on unique assemblies of synthetic or natural nanoparticles media to form drug delivery systems. Engineered nanoparticles are an important tool to realize a drug delivery system. Nanoparticles are attractive for medical purposes due to their important and unique features, such as their surface to mass ratio which is much larger than that of other particles, their quantum properties and their ability to adsorb and carry other compounds.

The drug delivery system by using nanoparticles have been developed to introduce a therapeutic substance into the target site in the body and improve its efficacy by controlling the rate, time and place of release. Among the researchers, the interests in drug delivery nanosystems to provide multiple drug delivery solutions were increased in recent years. This kind of systems must be intending to enhance drug bioavailability, site targeting, minimal immune response, controlled release kinetic and ease of administration. Consequently, enhanced convenience, reduced dosage frequency, shorter hospitalizations, improved patient compliance and lesser healthcare costs.

An ideal drug delivery nanosystem should be able to carry an enough drug to pass through physiological barriers and reach targeted diseased site at a right time and to release the drug at a desired rate (Freitas, 2006). For chemical drug delivery such as dacarbazine, the drug delivery nanosystem may significantly reduce drug resistance and

accomplished a therapeutic effect at target site. It may enhance the intracellular concentrations of drugs by easily bypass via receptor-mediated endocytosis (Cho et al. 2008). These essential achievements from drug delivery nanosystem are depending on the nanocarrier properties. The design of a drug delivery nanosystem needs to consider nanocarriers, which have high stability, good vehicle capacity, higher encapsulation efficiency, degradation of drug carriers in the body and practicability of incorporation of both hydrophilic and hydrophobic substances (Gelperina et al., 2005). The potential success of these nanocarriers in drug delivery nanosystem depend on their properties through the preparation, route of administration and metabolism.

The nanodrug delivery systems are designed to carry drugs including, but not limited to, drug carrier conjugates, dendrimers, quantum dots and nanoparticles (Figure 1.9).

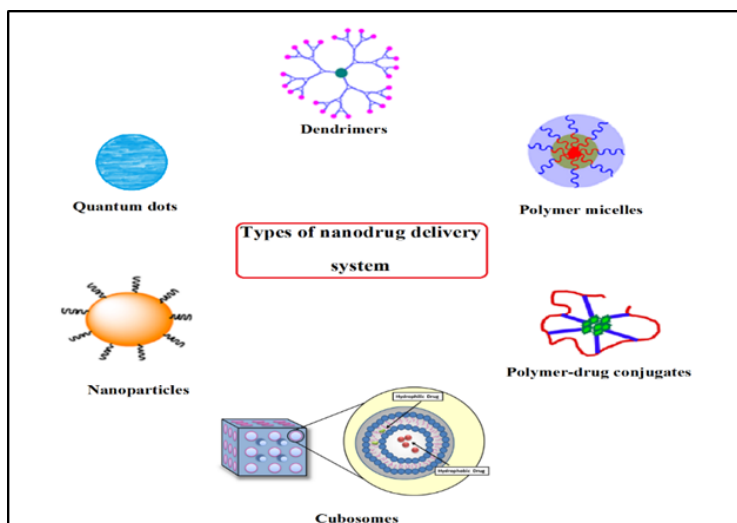


Figure 1.9: Illustration of different types of nanodrug delivery system (Sharma et al., 2015).

Recently, there has been an increase in the number of nanoparticles that have been identified as fit for use in nanodrug delivery systems as they allow for access into the cell and various cellular compartments including the nucleus. In 2003, Chourasia and Jain demonstrated that nanoparticles in a drug delivery system can be adjusted to produce the drug concentrations required at the target organ to preserve a therapeutic

effect for as long as necessary. The main advantages of using nanoparticles in drug delivery systems include the possibility to control plasma drug levels in a therapeutic window range, the opportunity to eliminate or reduce harmful side effects from systemic route and feasibility of variable routes of administration, for example oral administration, dermal application and inhalation (Paolino et al., 2006).

The preparation of nanodrug delivery particles is based on the assembly of synthetic and/or natural components such as metal ions, polymers and lipids. Physiochemical properties, drug loading capacity, targeting, drug release and, the safety of the nanoparticles itself are important parameters to be considered for use in nanodrug delivery (Sonam et al., 2013; Mirza and Siddiqui, 2014). In 2007, Han et al., highlighted that the shape and size of gold nanoparticles play an essential role in formation of DNA delivery vectors. In 2010, Kumari et al., demonstrated the impact of nano-encapsulation of different disease related drugs on properties nanoparticles. The issues related to the adverse health impacts and toxicity of these nanoparticles as nanocarriers in nanodrug delivery system is one of the main concerns in development of nanomedicines (Nerlich et al., 2007). Preparation, classification, characterization and functionalization of nanoparticles remain a challenge and the understanding of the biological effects including toxicity is far from complete (Shaw et al., 2008). Several models have been established to demonstrate and model the characteristics and functionality of nanoparticles (Craig et al., 2010). Several approaches can be used to measure the response of cells and to characterise nanoparticles (Figure 1.10). Previously, research and development of multifunctional nanoparticles have led to these being used as drug delivery systems, exploiting the unique behaviour of nanoparticles to enable efficient drug delivery.

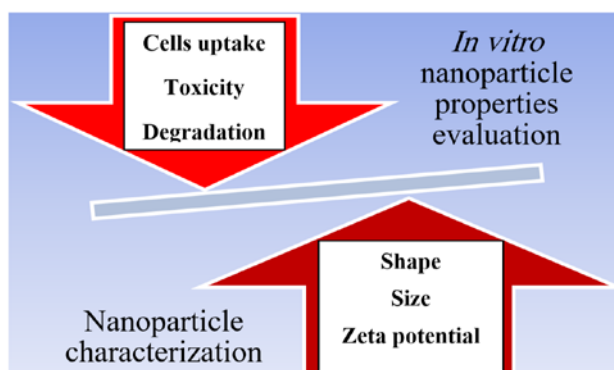


Figure 1.10: Relationship of the functionality and characteristics of nanoparticles. The reactivity and toxicity of nanoparticles with biological systems are determined by their physiochemical features including size, shape, zeta potential and surface chemistry.

1.3.4 Toxicity of nanocarriers

In medical applications of nanomaterials such as imaging diagnosis and systemic drug delivery, understanding the relationship between the physiochemical properties of nanomaterials and their pharmacological, physiological and toxicological effects is very important to accomplish the desired therapeutic result. One of the greatest challenges facing the toxicology community is to recognize the toxic effects of nanomaterials on living organisms and the environment. Therefore, nanotoxicology science emerged as a new branch of toxicology to study the adverse health effects may cause from nanomaterials. Nanotoxicology term refers to the science, which identifies the hazardous and undesirable effects of nanomaterials (Donaldson et al., 2004). It is the response to a rising unregulated use of nanomaterials in many health and industrial applications. The existing information about nanomaterials and their possible toxic effect in human is still insufficient and under researched (Zhu et al., 2012). For example, nanocarriers for drug delivery, the manipulation and application of engineered nanoparticles uses has become the subject of argument, regarding its toxicological effects. Nanoparticles can potentially disrupt cellular processes and cause disease. They can directly, or by their metabolites, cause toxic effects to various types of cells including, but not limited to, gastrointestinal epithelium (Ingrid and Frank, 2013), endothelial cells (Garcia-Garcia et al., 2005), pulmonary epithelium (Gurr et al., 2005), platelets (Nemmar. et al., 2002), red blood cells (Rothen-Rutishauser et al., 2006) and nerve cells (Yang et al., 2013).

The size of nanoparticles, surface area, composition and structure which have the most important role in the new formulations, may alter the toxic level of these materials (Gatoo et al., 2014). These parameters can influence the cellular uptake and subcellular localization as well as may catalyse the production of reactive oxygen species (ROS). The major mechanisms for cell toxicity of the nanoparticles is through the generation of oxidative responses by formation of free radicals. These free radicals have been known as hazards to biological systems, the process mainly through DNA damage.

Particle size and surface area play a greatest role in interaction of nanoparticles with biological system. Due to their small size, nanoparticles can penetrate physiological barriers. Furthermore, they can enter the circulatory and lymphatic systems of the body reaching most tissues and organs. The internalization location of a nanoparticle depends on its size, for instance, particles with sizes ranging between 2 - 10 μm may stay in large cytoplasmic vacuoles whereas smaller nanoparticles (<100 nm) may be found in organelles such as mitochondria. Very small nanoparticles with a diameter of <1 nm such as C60 molecules (a spherical fullerene molecule with the formula C60) can penetrate cells through different mechanisms other than phagocytosis, such as via ion channels or via pores in the cell membrane (Porter et al., 2006). Although, both genes and protein macromolecules are the most frequently affected by nanoparticles with significant roles in cellular toxic such as oxidative stress, other cellular injuries may occur due to unuseful nanoparticles (Table 1.1).

The nanoparticles can disrupt mitochondrial architecture (Bagchi et al., 2012). Thus, the large particle size of nanoparticles can improve the cell toxicity. Gurr et al, in 2005 demonstrated the toxicity post the aggregation, increasing the particles size of nanoparticles will reduce its toxicity. Reducing the particle size leads to an increasing in surface area relative to volume, which causes a dose dependent to induce in oxidation abilities of these nanoparticles much higher than larger particles with the same mass dose. Nanoparticles with higher surface area also has an inducing oxidation effect, sever cellular inflammation and DNA injury, leads to cells damage (Janrao et al., 2005). To decide on which nanoparticles or nanocarriers to use for drug delivery, it is crucial to investigate their properties and link to nanotoxicity. In addition, it is a mandatory to study the cellular toxic assessments of any nanocarriers before their use in drug delivery. De and Borm in 2008, concluded that "A conceptual understanding of biological responses to nanomaterials is needed to develop and apply safe nanomaterials in drug delivery in the future". Furthermore, a close collaboration between those working in drug delivery and particle toxicology is necessary for the exchange of concepts, methods and know-how to move this issue ahead".

Table 1.1: Unpredictable of cellular injuries may occur post nanoparticles treatment.

Nanoparticles effects	Cellular injuries outcomes	References
Oxidative stress	Protein, DNA, Membrane Damage	Manke et al., 2013
Mitochondrial disorder	Energy Failure, Apoptosis	Pathak et al., 2015
Nuclear Uptake and DNA attack	Mutagenesis and Carcinogenesis	Duan et al., 2013
Altered Cell Cycle Regulation	Proliferation, Cell Cycle Arrest	Falagan-Lotsch et al., 2016
Generation of antigens	Autoimmunity disorder	Maldonado et al., 2015

In this study, some important measurements were used in order to understand the role of nanoparticles, nanocarriers for drug delivery nanosystems in organism. They measured size, surface charge, nanoparticles shape and structure/crystallinity of molecules by different methods to assess at which concentration a substance is useful or harmful (Table 1.2).

These measurements allow for a better understanding of how to control toxic substances. Nanocarriers for drug delivery system included but not limited to silica nanoparticles (SiNP) and nanostructured lipid carrier (NLC). They are the most suitable drug delivery nanosystems for administration via topical and systemic route (Asadujjaman and Mishuk, 2013; Purohit 2016). SiNP, has been described as easily functionalized drug carriers, while NLC, has been employed in encapsulation of chemical drug to provide sustained release and successfully for targeted use of drug.

Table 1. 2: Common techniques used to measure nanoparticles properties as a carrier for drug delivery system.

Type	Properties	Common techniques
Morphology	Size	DLS, NTA and TEM
	Size distribution	DLS
	Structure	SEM, TEM
	Stability	DLS
	Zeta potential	Zetasizer
	Crystallinity	DSC
Others	Drug loading	UV-Vis
	In vitro release	HPLC, UV-Vis
	<i>In vitro</i> toxicity	MTT

1.4. LIPID-BASED NANOSTRUCTURED LIPID CARRIERS

The design of bioactive molecules into inert and non-toxic carriers conjugated with site-specific ligands for in vivo delivery establishes a promising approach to improving their therapeutic index and decreasing their side effects. In the last years, extraordinary efforts have been made toward developing bioavailability and efficacy of drugs and pharmaceuticals by improving drug delivery system in nanomedicine researches. Among the different types of nanoparticles for drug delivery, lipid-based nanoparticles have been favoured as they have more biocompatibility compared with polymers based particles. The physical structure of lipid-based nanoparticles mainly defined by its phospholipids composition, which determines the chemo-physical features such as size, shape, crystallinity and charge (Ahmad and Gadgeel, 2016). The application of lipid-based drug delivery still has many research challenges to overcome some of the limitations like the solubility and stability of poor water-soluble drugs. The delivery system uses the lipid as a carrier in order to protect the drug from degradation (Jain et al., 2014).

There are several different lipid-based formulations that can be used for drug delivery, for example liposomes, nanoemulsion solid lipid nanoparticles and nanostructured lipid particles (Figure 1.11).

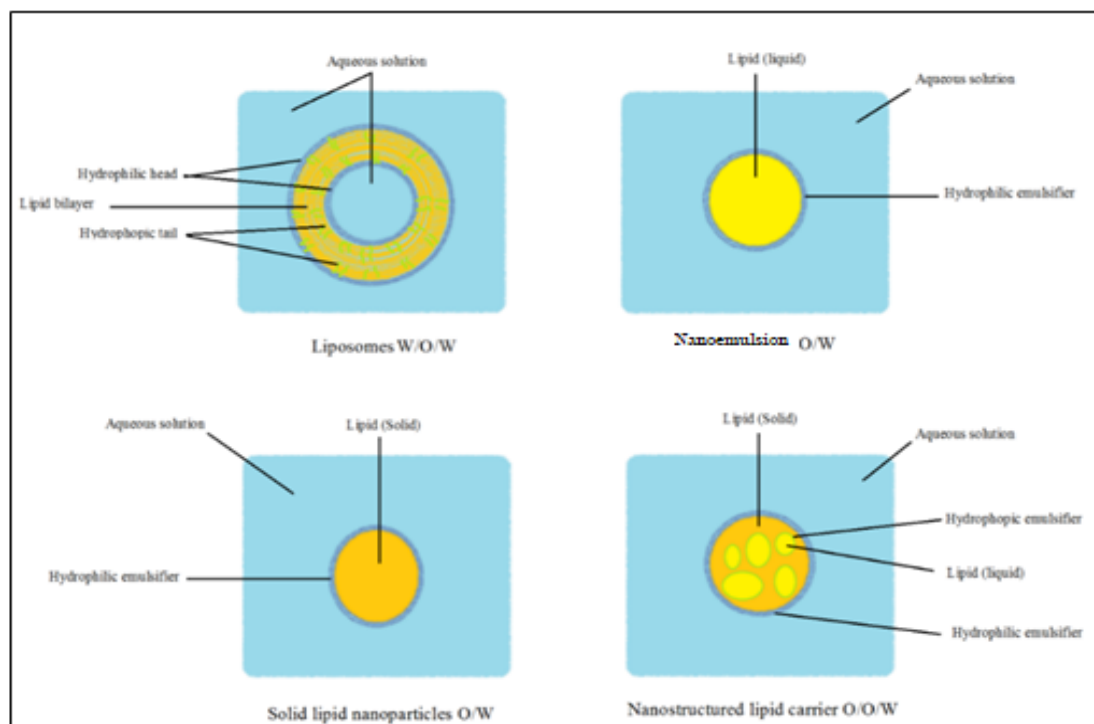


Figure 1.11: Schematic showing the different type lipid-based carriers that can be used in nanodrug delivery.

In comparison with other nanodrug delivery systems, lipid-based nanodrug delivery systems are distinctive (Allen and Cullis, 2004) in their:

- (a) Flexibility and good characterization of lipid excipients;
- (b) Formulation versatility;
- (c) Reduced plasma level variability;
- (d) Improved oral bioavailability and
- (e) Higher penetration for topical treatment.

Lipid-based systems can overcome the limitations of polymer nanoparticles in drug delivery system, for instance in safety and cost issues (Mukherjee et al., 2009).

A number of recent studies demonstrated that lipid-based nanodrug delivery systems are biocompatible and are more biodegradable than other carriers (Patidar et al., 2010; Mahapatro and Singh, 2011). Lipid-based nanodrug delivery systems have demonstrated sustained drug release and protection of loaded drugs from chemical degradation (Attama et al., 2012). In addition, the lipid-based nanodrug delivery systems have pharmacological properties which allow for site specific and controlled drug delivery, leading to reduced side effects (Shrestha et al., 2014). Among the types of lipid-based formulations, lipid-based nanoparticles are new colloidal drug carrier systems that have received recognition for stability, good vehicle capacity and practicability of incorporation of both hydrophilic and hydrophobic substances (Gelperina et al., 2005).

Lipid-based nanoparticles used for nanodrug delivery systems are formulations consisting of different lipid excipients (inactive substance formulated with active ingredient) and other additives. As these are made from physiological lipids, they are likely to exhibit reduced acute and chronic toxicity, for example, when compared with polymeric nanoparticles (Ghorab et al., 2004). In 2009, Puri et al., demonstrated that “lipid-based nanoparticles bear the advantage of being the least toxic for *in vivo* applications”. In pharmaceutical factories, lipid-based nanoparticles can be sterilized easily and there are simple methods that can be used to prepare them (Ekambaram et al., 2012). Such processes are also simple to scale up to large scale production (Saroj et al., 2012). Solid lipid nanoparticles (SLNs) and nanostructured lipid carriers (NLCs) are two main types of lipid-based nanoparticles. SLN is the first generation of lipid-based nanoparticles introduced in the 1990s as an alternative to traditional lipid-based nanodrug delivery such as liposomes. It can be produced from a broad selection of solid lipid materials such as glycerides and fatty acids. These materials are lipid particle matrix being solid at room and body temperatures and dispersed at 0.1% - 30% (w/w) in an aqueous medium. For instance, in dermal application, SLN formulas have 70-99% water content which can lead to a variety of stability states within the final topical product. They are stabilized in colloid systems by physiologically-compatible surfactants at levels between 0.5% - 5% (w/w).

These lipid-based nanoparticles drug delivery systems have been used for cosmetic and pharmaceutical activities (Bonifacio et al., 2014). Table 1.3, shows some of drugs used SLN as lipid-based nanodrug delivery.

Table 1.3: Examples of solid lipid nanoparticles (SLN) nanodrug delivery for oral and topical administrations.

Drug	Route of Administration	Advantages	References
5-Fluorouracil	Oral	Prolonged release in simulated colonic medium	Yassin et al., 2010
Baclofen	Oral	Significantly higher drug concentrations	Priano et al., 2011
Cyclosporin A	Topical	Controlled release	Sawant et al., 2008
Doxorubicin	Oral	Enhanced apoptotic death	Kang et al., 2010
Benzyl nicotinate	Topical	Increased oxygenation in the skin	Krzic et al., 2001

The mean particle size of SLNs have been reported between 40 nm to 1000 nm and they have several potential applications in drug delivery due to their distinctive size dependent properties (Mukherjee et al., 2009). Even though they have numerous advantages such as controlled and targeted drug delivery and improved stability of incorporated drug, there are some limitations to their use such as the drug being expelled from the particles during storage. This expulsion of drug was thought to occur due to the extremely ordered crystalline lipid matrix that leaves very little space for drug molecules (Kumar et al., 2012). This is more likely to occur as the lipid structure of the particles can be changed partially to crystallized in a higher energy modification e.g. with heating/cooling. The crystallized structure can then transform to the low energy

form during storage that can lead to the decrease in the number of imperfections in the crystal lattice. To overcome these limitations and the drawbacks associated with SLN, nanostructure lipid carriers (NLC) were introduced.

When using NLC as a drug delivery system, it is important to evaluate the toxic effects of the nanosize particles. The toxicity of NLC is a scientific subject of concern due to the improved reactivity of it as nanoparticles. The small size of NLC provides easy penetration into the body and high risk may occur. The impact of NLC as a dermal drug delivery system is still under investigation. The interaction of NLC with the skin cells is dependent on the particles size, chemical composition, surface structure, solubility and shape (Tofani et al., 2010). Furthermore, the effect of NLC on drug release, cellular uptake, cytotoxicity and effects on tumour growth should be studied and defined.

In vitro NLC characteristics may be affected by the surroundings and the presence of biological molecules. Recent studies have demonstrated that different toxicological studies show varying conclusions about the same nanoparticles because of undefined characterization both during synthesis and during operational use (Izak-Nau et al., 2013). Therefore, the NLC properties and toxicity parameters need to be evaluated both in the culture medium as well as in the delivery solution. Topically, cell culture medium contains amino acids, salts, glucose and vitamins plus antibiotics, L-glutamine and foetal bovine serum (FBS). FBS is essential for the maintenance and growth of cells and it is the liquid fraction of clotted blood from foetal calves that is depleted of cells, fibrin and clotting factors. FBS contains a large number of nutritional and protein factors essential for cell growth. Once NLC are in contact with biological fluids, for instance FBS, changes may occur to their surface or their structure which alter their function. This study will assess the impact of the presence of NLC in cell culture media. In 2013, How et al., demonstrated the effect of NLC aggregation on cell toxicity using different oil in formulation and the study concluded, the correlation between NLC physical properties and its safety as carrier.

1.5. NLC for topical drug delivery system

In 2012, Andalib et al., stated "Nanostructured lipid carriers (NLC) are the second generation of SLN and have a solid matrix at room temperature. They are demonstrated that NLC are "a mixture of solid and liquid lipids or oils form the colloidal carrier system that leads to an imperfect matrix structure with high ability for loading water soluble drugs". NLC are produced using blends of solid lipids mixed with liquid lipids preferably in a ratio of 70:30 up to a ratio of 99.9:0.1. In comparison with SLN, NLC have highly unordered lipid structures that can provide surface to host drug (Selvamuthukumar and Velmurugan, 2012). NLC include a greater amount of lipids compared to SLN which significantly reduces the water content in the final formulation. For that reason, NLC have been used for drug delivery through different routes including oral, intravenous injection and topical. Among them, topical applications of NLC are preferred because they exhibit distinct features, such as the small size of NLC that ensures a close contact to the stratum corneum and can increase drug penetration into the skin. Many drugs have been successfully incorporated into NLC for topical administration (Table 1.4).

Table 1.4: Examples of drugs applied nanostructured lipid carriers (NLC) nanodrug delivery for topical administrations.

Drugs	Advantages	References
Ascorbylpalmitate	high performance topical delivery	Teeranachaideekul et al., 2007
Tripterine	enhance drug penetration	Chen et al., 2012
Terbinafine	reduction of fungal burden in the infected area	Gaba et al., 2015
Aceclofenac	superior the anti-inflammatory activity compared to the marketed product	Patel et al., 2012
Miconazole Nitrate	faster relief from fungal infection	Sanap et al., 2013

1.5.1 NLC structures

The NLC has solid lipid and liquid lipid in its construction while SLN has only solid lipid (Figure 1.12). SLN has highly organized crystalline lipid matrices that lead to drug expulsion (Jawahar et al., 2013). To address this disadvantage, NLC have been designed with a controlled nanostructure to have enough space to accommodate drugs. NLC mixtures have a lower melting point as compared to the pure solid lipid yet they are still solid at room and body temperatures (Müller et al., 2000). By optimization of the process of synthesis, the overall solid content of NLC could reach to 95%. Structurally, NLC has different types and each of them has specific properties.

There are three different structure of NLC, and each structure represent the correlation between the solid lipid and the liquid lipid in the NLC formulation. In the first structure of NLC (Figure 1.12: I), there is an imperfect solid lipid matrix structure with low liquid lipid that offers space for molecules and amorphous clusters of drug. In the second NLC structure (Figure 1.12: II), the liquid lipid particles during the production process are cooled from the molten state to room temperature to crystallize and form solid particles that precipitate out as high liquid lipids. In third structure of NLC (Figure 1.12: III), lipids are mixed in a way that prevents them from crystallizing and ensure solid lipid in liquid lipid matrix in an amorphous state.

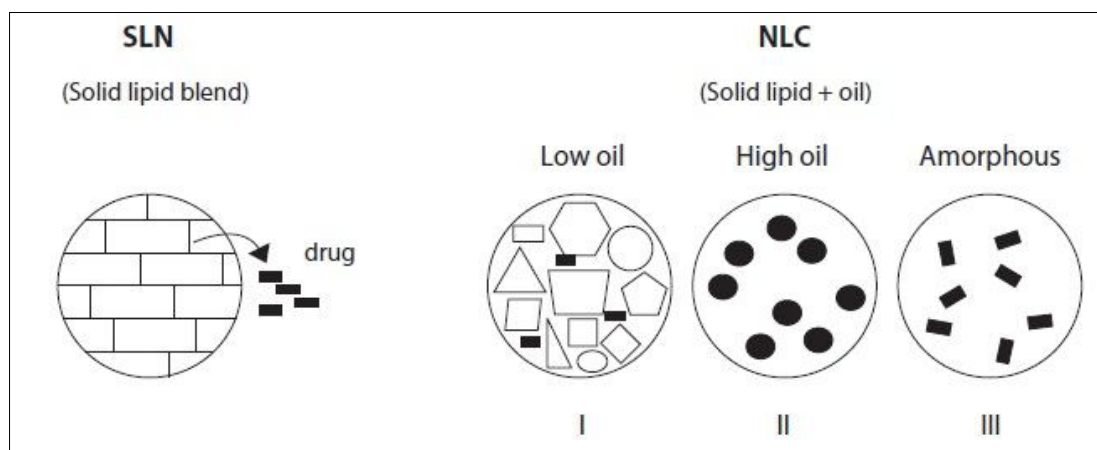


Figure 1.12: Scheme for NLC structures (Kumar et al., 2012).

During the preparation of NLC containing a drug (NLC-Drug), the drug is conjugated with a solid lipid and forms a water insoluble lipid conjugate. This conjugation occurs using covalent bonds (Müller et al., 2000).

1.5.2 NLC formulation and preparation

The NLC consist from solid lipid, liquid lipid, surfactant and other additives depends on the preparation method. It has been reported that the attributes of NLC are related to the composition of the solid and liquid lipid (Wiechers and Souto, 2010; Beloqui et al., 2013 and Shete et al., 2013). The excipients of nanostructured lipid carriers such as liquid lipid, solid lipid, surfactants and emulsifiers are selected considering their regulatory status. The solid lipid used in the NLC formula is a long chain lipid such as beeswax, apifil, dynasan, sterylamine, glyceryl behenate and precinol ATO-5 and the liquid lipid used in the NLC formula is normally a medium or short chain lipid for instance olive oil, palm oil, castor oil, isopropyl myristate and medium-chain triglycerides. Both solid lipid and liquid lipid are well tolerated and generally recognized as safe (Rizwanullah et al., 2016). The coefficient of oil/oil in NLC is important as this form its structure in the colloidal system and may affect their properties.

The NLC delivery system also needs a hydrophilic emulsifier agent such as Tween 80, Plaronic F68, Phospholipon 90G or Kolliphor® P 188. In some NLC formulas the hydrophobic emulsifier is added to a lipid mixture such as soybean lecithin (SI) or d- α -tocopherol polyethylene glycol succinate (TPGS). These agents can enhance the homogeneity of lipid phase as well as improve the NLC properties. The combination of emulsifiers might stop particle agglomeration more efficiently. Some NLC formulas also add organic solvents to the lipid phase while distilled water is used as the aqueous phase in all NLC formulas. The selection of the matrix materials is dependent on many factors, for instance: (1) size of nanoparticles; (2) inherent properties of the drug such as aqueous solubility and stability; (3) degree of biodegradability, biocompatibility and toxicity; (4) surface characteristics such as charge and permeability; (5) drug release profile; and (6) antigenicity of the final product.

In 2012, Chen et al., concluded that NLC are promising for use as a nanodrug delivery system for the topical anti-melanoma drug tripterine. This research studied the skin permeation for three different solid lipids. This study used those components in the formulation of NLC preparation and the solid lipids used are:

Precirol ATO-5

Precirol ATO-5 is a solid lipid (also known as glyceryl palmitostearate) which has a melting point of 56 °C with a molecular weight of 632.99514 g/mol and formula C₃₇H₇₆O₇. It has binding properties with three functional groups able to undergo covalent bonding with other molecules (Figure 1.13).

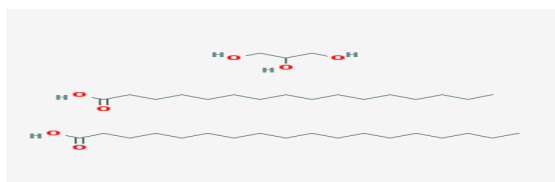


Figure 1.13: Chemical structure of Precirol ATO-5, (hexadecanoic acid;octadecanoic acid;propane-1,2,3-triol; **source:** <https://pubchem.ncbi.nlm.nih.gov/compound/114690#section=Top>).

Glyceryl behenate

Glyceryl behenate is a solid lipid also known as behenin. It has a high melting point (61 °C) and has been exploited for use in modified release dosage forms. It has a 414.6621 g/mol molecular weight and its molecular formula is C₂₅H₅₀O₄ with one functional group able to be undergoing covalent bonding with other molecules (Figure 1.14).



Figure 1.14: Chemical structure of Glyceryl behenate (2,3-dihydroxypropyl docosanoate; **source:** [https://pubchem.ncbi.nlm.nih.gov/compound/Glyceryl behenate#section=Top](https://pubchem.ncbi.nlm.nih.gov/compound/Glyceryl%20behenate#section=Top)).

Stearylamine

Stearylamine is a solid lipid also known as octadecylamine. It has white flakes with characteristic odour and melting point of 52.9 °C. It has a 269.50896 g/mol molecular weight and its molecular formula is C₁₈H₃₉N with one functional group able to undergo covalent bonding with other molecules (Figure 1.15).



Figure 1.15: Chemical structure of Stearylamine (Octadecan-1-amine; source: <https://pubchem.ncbi.nlm.nih.gov/compound/octadecylamine#section=Top>).

NLC have been prepared using different methods and biodegradable solid and liquid lipid materials. There are many systems for the synthesis of NLC, the commonly methods used were:

- **High pressure homogenization technique (HPH)**, it has emerged as the most reliable and powerful technique for preparation of lipid nanoparticles since the nineties. This technique has several advantages such as appropriate for large-scale production, no organic solvent, good product stability, high loading of drugs, however specific high pressure and temperature conditions were considered challenges about its application. The HPH technique has two general processes, hot homogenization and cold homogenization. In first step of HPH technique, the pharmaceutical compound is dissolved in the melted lipid, in both processes. High pressure (100–2000 bar) moves the fluid in the narrow gap in homogenizer (Ekambaram et al., 2012).

In hot homogenization, homogenization occurs at temperatures higher than melting point of lipid. Drug loaded lipid melt is dissolved in hot aqueous surfactants phase by using mixing device leads to the formation of pre-emulsion. The high temperatures of homogenization reduced viscosity and particle size becomes smaller (Poonia et al.,

2012). In most cases, 3–5 homogenization cycles are sufficient to have appropriate particle size 50-100 nm and increasing the homogenization pressure or number of homogenization cycles often leads to an increase in particle size (Müller et al., 2000). The disadvantages of hot homogenization technique including temperature-dependent degradation of the drug, the drug penetrates the aqueous phase during homogenization and several modifications during the crystallization step of the nanoemulsion (Silva et al., 2011).

In cold homogenization, the primary step is like the hot homogenization technique and it includes dispersion of the drug into the lipid melt, then the drug-loaded lipid melt is solidified quickly cooled by liquid nitrogen or dry ice. This process leads to formation of nanoparticles which are dispersible in a cold surfactant phase that form a pre-emulsion. The intra forces are playing their role to break lipid microparticles directly into the nanoparticles. This process of cold homogenization reduces thermal exposure of the product but does not stop it completely because of the melting of the lipid-drug mixture in the primary step (Müller et al., 2000). Although, cold homogenization technique has emerged to overcome the disadvantages of hot homogenization technique, it has a complex equipment required and high pressure homogenization possible leads to degradation of the components.

- **Emulsification-solvent diffusion technique**, the method based on the emulsification of an organic solution of a solid lipid in an aqueous emulsifier solution. In the method procedure, the lipid dissolve in a water saturated by organic solvent and this organic solution initially emulsified with a solvent saturated by aqueous solution containing emulsifier to form a pre-emulsion. Then, lipid nanoparticles precipitate by rapidly adding water into the initial pre-emulsion to extract the solvent into continuous phase and to produce lipid nanoparticles nanodispersion. This nanodispersion washed by ultrafiltration to remove residual solvent and lyophilized (Trotta et al., 2003). This method cannot be used to prepare the nanosuspensions of drugs with poor solubility in both organic and aqueous media.
- **Emulsification-solvent evaporation technique (ESE)**, in the procedure of this technique, firstly lipophilic material dissolved in an appropriate volume of organic

solvent by magnetic stirring. Then lipid containing organic phase is dispersed in an appropriate volume of aqueous solution using a high-speed homogenizer to form a coarse pre-emulsion. Finally, the resulting coarse pre-emulsion is immediately passed through a high-pressure homogenizer at an operating pressure to obtain nanodispersion, which kept on the magnetic stirrer overnight in a fume hood to evaporate the organic solvent. This step formed nanodispersion by precipitation of lipid material in aqueous medium. The lipid and drug agglomerates can be filtered through a sintered glass filter to obtain nanoparticles with small size, monodisperse and have high encapsulation efficiency (Jaiswal et al., 2004).

- **Microemulsion based technique**, microemulsion must be formed at a temperature above the melting point of the lipid to produce a microemulsion with the lipid solid at room temperature (Heydenreich et al., 2003). it consists of a lipophilic phase, surfactant, in most cases a co-surfactant, and water. In method procedure, lipid is melted first, then a mixture of surfactant, co-surfactant and water is heated to the same temperature as the lipid phase then added to the lipid melt under mild stirring. Once compounds are mixed in an accurate ratio, microemulsion system is produced. Later, this microemulsion dispersed in a cold aqueous medium (4 °C) under mild mechanical mixing to precipitate the lipid phase and forming fine particles (Anurak et al., 2011).
- **Double emulsion based technique**, the double emulsions are complex system, it is also termed “emulsions of emulsions”, in which the droplets of the dispersed phase contain one or more types of smaller dispersed droplets themselves. It is commonly used for the encapsulation of hydrophilic molecules. In this method there are two step of emulsification procedure. In the first step, a primary water in oil emulsion is obtained by dispersing the aqueous solution of the hydrophilic drug molecule into organic phase then use vortex machine for mixing, and simultaneous homogenized by using a high speed stirrer. Then the second step, syringed the primary w/o emulsion into an aqueous solution to obtain w/o/w multiple emulsions by high pressure homogenization. Additional stirring under decrease pressure, leads to extract and evaporate of organic solvent with subsequent solidifying of the nanospheres.

- **Rapid expansion of supercritical solution (RESS)**, it is one of the two common routes for particle formation in supercritical fluids (any substance at a temperature and pressure above its critical point). RESS technique has a suitable alternative to produce nanoparticles of heat sensitive materials. The process of RESS technique consists of two steps. Firstly, an extraction, in which the supercritical fluid is saturated with the substrates of interest. This extraction is followed by a sudden depressurization in a nozzle, which forms a large decrease in the temperature and the solvent power of the fluid, consequently causing the precipitation of the solute (Satvati et al., 2011). Lipid nanoparticles can be prepared by RESS carbon dioxide solutions and carbon dioxide (99.99 %) was good choice of solvent for this method (Gosselin et al., 2003). The primary limitation of RESS technique is that the extraction must be operated at the high pressure (1,000 - 5,000 psia) and the result is higher capital and operating costs.
- **High speed homogenization technique (HSH)**, This technique is most widely used since the required equipment exists in many laboratories. There are two commonly methods of sonication. A bath or probe tip ultrasonic are employed in laboratories, a bath sonicator for large volumes of diluted lipid dispersions, while the probe tip sonicator is more suitable for high energy in a small volume dispersion. The particles size and size distribution are affected by the composition and concentration of lipids, time and power of sonication and the temperature during the homogenization (Xie et al., 2011). The most formidable problem associated with this technique is broader particle size distribution of several micrometers. This, upon storage, may give signs of physical instability, like particle growth and particle aggregation.
- **High shear dispersion technique (HSD)**, This homogenisation technique used a high speed rotational instrument (3000 – 25,000 rpm) in laboratory dispersion tasks under sample preparation methods as used in medical research. This system is ideal for batch homogenizing of cell tissues and emulsifying suspended solids using rotor-stator generator. Due to the simplicity and less demand in expensive facilities, high shear dispersion has been increasingly employed in the recent years. Typically, HSD transports one phase gas, liquid or solid into a main continuous liquid phase which would usually be immiscible. It is rotor-stator systems composed of coaxial

intermeshing rings with radial openings. When the fluid goes into the centre of HSD, it is accelerated and decelerated multiple times, leading to high tangential forces (Figure 1.16). The pre-emulsion is transported through the radial openings of the rotor systems.

Then it mixes with the liquid in the gap between the rotor and the stator. The forces of HSD and turbulent flow situations generate which result in a disruption of droplets. This mechanism will be continuous until the emulsion reaches the saturation state.

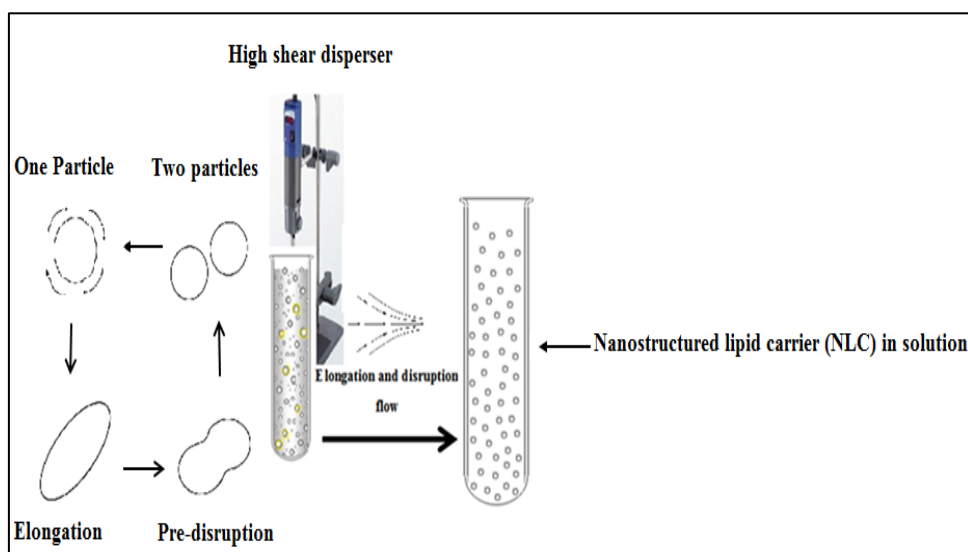


Figure 1.16: Schematic showing HSD mechanism, it can create elongation and disruption flow that separate one particle into two new particles with continuous mechanism until the emulsion reach the saturation state.

All the above methods of NLC synthesis and others are still under investigation. Although, each of NLC synthesis method has advantages, there are some limitations which may be tackled to obtain NLC with good properties (Table 1.5).

The selection from the preparation methods of NLC depends on the purpose of the NLC used, NLC formulation and the method properties. As such there is no one standard method set for the preparation of nanostructured lipid carriers (NLC). Moreover, some studies used more than one method to prepare NLC in order to improve the particles properties and avoid methods limitation.

Table 1.5: Different methods were used to prepare nanostructured lipid carrier (NLC).

Method	Advantages	Disadvantages	References
Hot and Cold homogenization	<ul style="list-style-type: none"> • Suitable technology on large scale • Good reproducibility • Organic solvent free method 	<ul style="list-style-type: none"> • Complex equipment required • High temperature process in hot homogenization • High energy input and possible degradation of the components caused by high pressure homogenization 	Al Haj et al., 2008 Ekambaram et al., 2012
Emulsion formation solvent-diffusion or evaporation	<ul style="list-style-type: none"> • Allows incorporation of thermosensitive drugs • Reduces mean particle size and narrow size distribution 	<ul style="list-style-type: none"> • Concentration of final formulation is required • Possible organic solvent residues in the final formulation 	Gasco 1999
Microemulsion based	<ul style="list-style-type: none"> • Decreases mean particle size and narrow size distribution • No energy consuming method • Easy to scale up 	<ul style="list-style-type: none"> • High concentration of surfactants and co-surfactants • Concentration of final formulation is required 	Sinha et al., 2009
Double emulsion	<ul style="list-style-type: none"> • Allows incorporation of hydrophilic drugs 	<ul style="list-style-type: none"> • Concentration of final formulation is required • Large particle size obtained 	Singhal et al., 2011
Rapid expansion of supercritical solution	<ul style="list-style-type: none"> • Good for heat sensitive components • Good reproducibility 	<ul style="list-style-type: none"> • High energy input • operating costs 	Gosselin et al., 2003
High speed homogenization "Ultrasonication"	<ul style="list-style-type: none"> • No complex equipment is required • Easy to handle • High concentration of surfactants and are not required • Organic solvent free method 	<ul style="list-style-type: none"> • High energy input • Polydisperse distributions • Possible metal contamination • Concentration of final formulation is required 	Ekambaram et al., 2012
High sheer dispersion	<ul style="list-style-type: none"> • Good reproducibility • Particle size controlling 	<ul style="list-style-type: none"> • High energy input • Possible organic solvent residues in the final formulation • Concentration of final formulation is required 	Patel et al., 2012

1.5.3 NLC Physical properties

The physiochemical characterization of NLC including particle size, size distribution and stability are very important criteria to achieve the quality control of NLC. The particle size is essential parameter for NLC in delivery system because as it decreases, the surface area properties increase as a function of total volume. The particle size index of NLC will affect its drug delivery efficiency (Bahari and Hamishehkar al., 2016). Recently, a study has demonstrated that NLC with particle sizes less than 200 nm could be promising transdermal delivery carriers (Guo et al., 2015). In 2013, Rahman al., demonstrated that the particle size and polydispersity index (PDI) are critical properties of NLC that influence the distribution of nanoparticles. Zeta potential is an important parameter indicating the stability of NLC (Thakkar et al., 2014). It represents the level of repulsion between adjacent particles in solution. The stability of NLC can be improved by modifying the preparation of NLC and controlling the zeta potential. The NLC properties such as size, PDI, drug loading capacity, encapsulation efficiency and stability may vary between each manufacturing formula. This variation in properties may depend on critical factors such as formula components and manufacturing methods. For example, the percentage of oil in lipid should be adjusted to form NLC (Müller et al., 2000).

The surfactant type also has a potential effect on NLC properties such as size and PDI (Mitrea and Meghea et al., 2014). Different concentrations of surfactant in the NLC formula need to be optimised to achieve the desired properties (Agrawal et al., 2010). The impact of these characteristics needs to be evaluated for their effect on risk issues such as cytotoxicity. The different forms of NLC may be obtained by modifying various process parameters such as system contents (for instance solid/liquid lipid type) and formulation parameters (such as ratio of drug to lipid, emulsifier to lipid and emulsifier to co-emulsifier). Consequently, these characteristics can be evaluated by analysing the physical properties of NLC such as size, zeta potential, polydispersity index and entrapment efficiency. Moreover, other factors should also be investigated including morphology and lamellarity, melting behaviour and the crystallinity of NLC.

1.6. NLC for anti-tumour drug delivery (dacarbazine)

Topical treatment is safe and is the preferred method of drug delivery for treating skin diseases since the therapeutic agents goes directly to target side avoiding the first pass and systemic metabolism, therefore ensuring optimal local drug level. The metabolism of drug can occur at different sites of the body dependent on the route of drug administration. For example, in the case of drug delivery through an oral route, the gastro intestinal tract and first pass metabolism of the liver may affect the degradation and toxicity of therapeutic agents. The risk of systemic side effects of drug administration through conventional routes for treating skin diseases have been addressed previously (Schäfer-Korting et al., 2007).

Nevertheless, conventional dermal drug application has enabled therapeutic drugs to reach different levels of the skin such as epidermis and dermis. Several problems have been reported with traditional topical preparations including poor biodistribution, lack of selectivity and low uptake due to the barrier function of the *stratum corneum*. Many research groups are interested in applying lipid nanocarriers to dermal applications. Typical advantages for topical drug delivery using lipid nanocarriers are controlled release, drug targeting, negligible skin irritation and protection of active compounds. A topical application of a drug delivery system appears more attractive as specific carrier systems have the ability to penetrate skin layers to a desired stratum. The epidermal layer of the skin is rich in lipids that allow lipid carriers such as NLC to attach for lipid exchange and penetration. Moreover, the epidermis can tolerate lipid nanoparticles which enhance the targeting properties of drug delivery systems (Üner and Yener, 2007). Consequently, they have the potential to improve treatment efficiency and reduce the systemic toxicity of drugs.

Dermal delivery systems have received general acceptance in cosmetic and pharmaceutical skin products (Pardeike et al., 2009). Both the benefits and risks of a drug delivery system depends essentially on the capability of such carriers to pass through the skin barrier and the types of the tissue and organ it can reach. Therefore, the interaction of lipid nanocarriers with both *in vivo* and *in vitro* skin models is an attractive area of researchers (Schneider et al., 2009). Müller et al., in 2002, observed an

increased skin hydration due to the occlusive properties of lipid nanocarriers. Furthermore, lipid nanocarriers are able to enhance the chemical stability of compounds that are sensitive to light, oxidation and hydrolysis. NLC represent the latest generation of drug delivery system for topical application and they are composed of physiological and biodegradable lipids that show enhancement in treatment efficiency.

NLC are known as 'nano-safe carriers' because they are made of complete biodegradable lipid components and naturally biocompatible materials. Moreover, NLC has properties that are beneficial for dermal delivery of therapeutic and cosmetic active agents; for example: (1) decreases the occlusive factor (Teeranachaideekul et al., 2007); (2) enhances ultra violet blocking activity (Song et al., 2005); (3) increases skin penetration (Zhai et al., 2001); (4) enhances chemical stability (Jenning et al., 2001); and (5) protects the skin from dehydration (Puglia and Bonina, 2012). NLC for dermal drug delivery has previously been evaluated in a number of studies with respect to the skin interaction and the impact on drug penetration. For example, some non-steroidal anti-inflammatory drugs have improved bioavailability (four times greater) in dermal drug delivery than in oral administration (Bhaskar et al., 2009). Regarding the duration of drug effectiveness, dermal drug delivery systems were demonstrated to have an increased duration of anaesthesia (Pathak and Nagarsenker, 2009). In 2002, Müller et al., demonstrated that lipid nanocarriers were more stable on gel formulation and they can protect drugs against degradation. The development and the implementation for NLC as dermal drugs delivery for treating tumour are on-going activities and the final products of engineered dermal drugs delivery system require a thorough safety evaluation.

For topical anticancer therapy, drugs should penetrate the *stratum corneum* to reach the tumour cells. Usually, there are three different routes of skin penetration:

(1) through the *stratum corneum* between the *corneocytes* (intercellular route); (2) through these cells and the intervening lipids (intracellular route); and (3) through the skin appendages, such as hair follicles and sweat glands (Moser et al., 2001). Molecules with an oil/water partition have adequate solubility in water and oil. In addition, molecules with a molecular weight lower than 0.6 kDa may penetrate the skin (lipid membranes) easier than larger molecules (Barry 2001; Hadgraft and Lane, 2005 and Schafer-Korting et al., 2007). Therefore, topical drug administration is restricted to hydrophobic and high-molecular weight drugs. However, anticancer drugs generally cannot easily penetrate the *stratum corneum* since they are hydrophilic; have low oil/water partition coefficients, high molecular weights and ionic characters (Souza et al., 2011).

Current topical treatments for skin cancer including 5-fluorouracil, diclofenac and imiquimod are approved by the FDA only to treat non-melanoma skin cancers, because they are inefficient in reaching the deep layers of skin (such as melanocyte) and have a relatively long treatment regime. These drawbacks give emphasis to the requirement for alternative methods or techniques to improve the skin penetration of anti-neoplastic drugs.

Drug penetration through the *stratum corneum* can be described with Ficks second law:

$$(J= D_m .C_v. P/L)$$

where (J) is the flux of a drug through the skin and it can be controlled by (1) the diffusion coefficient of the drug in the *stratum corneum* (D_m); (2) the concentration of the drug in the vehicle (C_v); (3) the partition coefficient between the formulation and the *stratum corneum* (P); permeability and (L); (4) the membrane thickness (Williams and Barry, 2004). Therefore, the anticancer drug flux can be enhanced by increasing its concentrations using specific materials for instance nanolipid carriers.

NLC appear to be promising systems because they often increase anticancer drug penetration through the skin in addition to other advantages such as improving stability of compounds that are sensitive to light, oxidation and hydrolysis. For example, Topotecan is an anticancer drug that can be hydrolysed *in vivo* but when it incorporated

with nanolipid carriers the chemical constancy of drug molecules changes (Souza et al., 2011). In 2014, Fan et al., used nanostructured lipid carrier (NLC) to load the Phenylethyl Resorcinol (PR), the study demonstrated that " the incorporation of PR into NLC could give greater chemical stability, particularly photo-stability, during storage under natural light exposure as compared to that of free PR".

Generally, the effectiveness of chemotherapeutic agents for treating skin cancer can be improved if certain NLC-drug delivery systems are applied topically. The factors that have to be considered in development of strategies for topical application of NLC-drugs are illustrated in Figure 1.17.

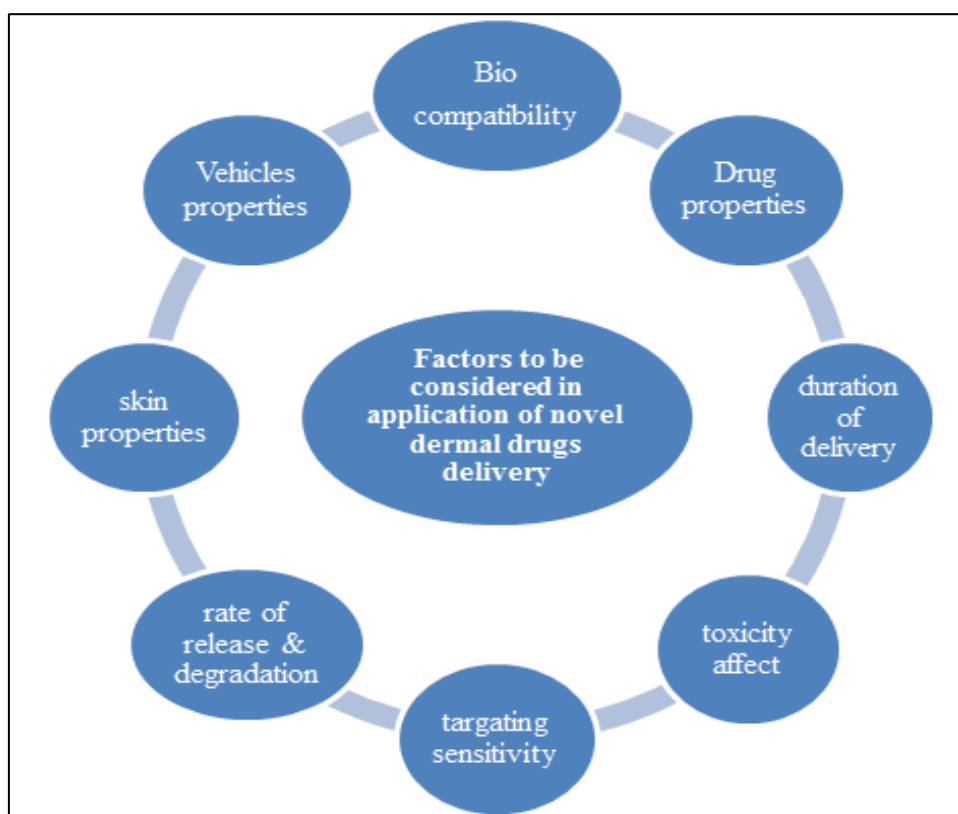


Figure 1.17: Strategy for assessing the safety and therapeutic effect of dermal drugs delivery system.

Many biocompatible and biodegradable lipids such as triglycerides, solid fats and lipid acids are easy to obtain and are used to prepare NLC (Mehnert and Mäder, 2001). Moreover, NLC formulations use emulsifiers approved by pharmaceutical regulatory bureaus, such as lecithin, Kolliphor® P 188 and polysorbate 80 (Smith, 1986). NLC can increase the solubility of most of the hydrophobic tumour drugs in aqueous solution (Kumbhar and Pokharkar, 2013). The encapsulation of anti-tumour drugs is one of strategies to overcome drug resistance, NLC could be address this need (Selvamuthukumar and Velmurugan, 2012). In 2016, Rizwanullah et al., demonstrated that surface modification of NLC can be used to overcome drug resistance in cancer chemotherapy, increasing site specific targeting for better efficacy and reduced dose related toxicity. Recently, researchers have identified that NLC has advantages as an anti-tumour drug delivery system (Table 1.6).

The use of NLC as a carrier for anti-tumour drug Dacarbazine (Dac) will be studied in this thesis.

Table 1.6: Advantages for anti-tumour drugs post NLC loading as nanodrug delivery system.

Drugs	Advantageous after NLC encapsulated	References
Zerumbone	sustained-release characteristics and high cytotoxicity in a human T-cell acute lymphocytic leukaemia cell line	Rahman et al., 2013
Tributylin	promising alternative to intravenous administration	Silva et al., 2015
Transferrin	enhanced the active targeting ability of the carriers to NCI-H460 cells	Shao et al., 2015
Docetaxel	<i>in vivo</i> pharmacokinetic study indicated markedly increased	Fang et al., 2015
Berberine	<i>In vivo</i> studies also showed higher antitumor efficacy	Wang et al., 2015

1.7. Gap analysis

The work elucidated in this thesis is focussed on the use of lipid-based nanoparticles as carriers for chemotherapy drug delivery in nanomedicine. In nanomedicine technology, therapeutic experiments primarily based on lipid nanoparticles such as nanostructured lipid carrier (NLC) particularly in colloidal state have been shown to be promising in providing better drug delivery solutions (Üner and Yener, 2007). The drug delivery system of NLC nanoparticles has become an area of special interest for researchers, however, Lipid-based of NLC nanoparticles for drug delivery systems consist of an abundance, amorphous foundations of different lipid excipients (i.e., an inactive substance formulated with active ingredient) and other substances. Each formulation of nanostructured lipid carrier (NLC) has had different structural and functional characteristics which can be manipulated by the controlling contents of the system. During the last years, the number of studies describing NLC nanoparticles formulations has dramatically increased (Beloqui et al., 2016). An increasing in NLC utilization is due to its diverse formulation process and improved knowledge of the underlying mechanisms of NLC transportation via different routes of administration.

Researchers have previously tried to create a novel delivery system for Dacarbazine (Dac) to overcome its limitations and side effects. In 2009, Bei et al., examined the combined influence of three-level, three-factor variables on the preparation of Dac (a water-soluble drug) loaded cubosomes, the TEM structure of cubosomes is shown in Figure 1.18.

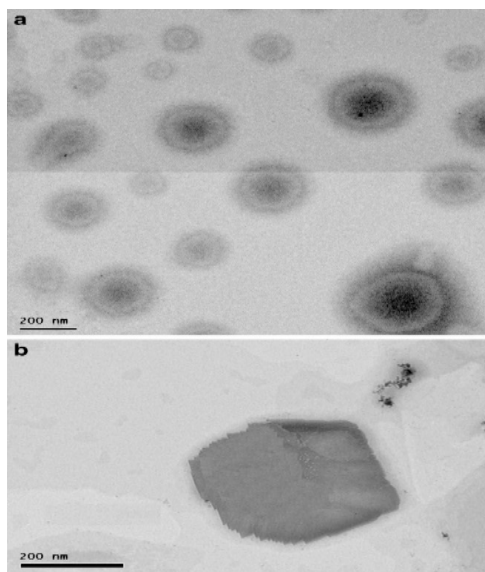


Figure 1.18: TEM images for Dacarbazine loaded cubosomes nanocarriers: (a) population of cubosomes. (b) Single cubosomes to better view the cubic structure (Bei et al., 2009).

Cubosomes were made from 100 mg of monoolein, 107 mg of polymer, and 2 mg of drug and had an average diameter of 104.7 nm and an encapsulation efficiency of 6.9%. The physicochemical properties of dacarbazine-loaded cubosomes were studied (Bei et al., 2009). Differential scanning calorimetry (DSC) and X-ray Powder Diffraction (XRD) analysis suggested that the 0.06 or 0.28% w/w of drug loaded inside the cubosomes was in the amorphous state. These physicochemical characteristics would affect the nano-formulation shelf-life, efficacy, and safety. The study investigated the combined influence of process parameters (independent variables) such as homogenization speed, duration, and temperature during the preparation of dacarbazine-loaded cubosomes. The optimal process parameters (homogenization speed ~24,000 rpm, duration = 5.5 min, and temperature = 76°C) led to the production of cubosomes with 85.6 nm in size and 16.7% in encapsulation efficiency.

In 2011 Ma et al., prepared Dac loaded or blank methoxy poly (ethylene glycol)-poly (lactide) (MPEG-PLA) nanoparticles (NPs), by modified water/oil/water (w/o/w) double emulsion-solvent evaporation method through an ultrasonic processor without any additional additives (Figure 1.19).

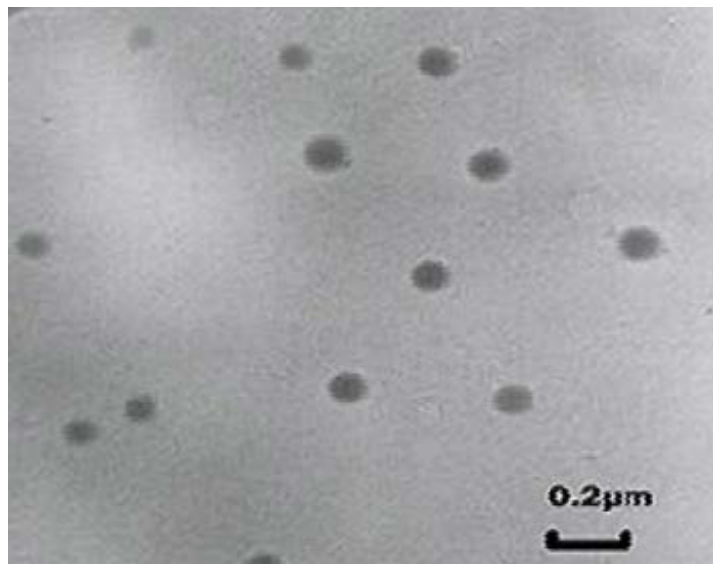


Figure 1.19: TEM image of Dac-MPEG-PLA NPs. (Ma et al., 2011).

The results showed that the haemolytic test and cytotoxicity test of blank MPEG-PLA NPs demonstrated that the obtained drug delivery system is safe and intact to handle and Dac could induce more apoptosis of melanoma cells after Dac-delivery system. The particle size distribution, morphology, drug loading, drug release profile and anticancer activity *in vitro* about methoxy poly (ethylene glycol)-poly (lactide) (MPEG-PLA) nanoparticles, were studied in detail. The small sized nanoparticles with a particle size of 144.2 ± 7.8 nm in diameter and drug encapsulation efficiency of $70.1 \pm 2.3\%$ were easy to disperse in water and suitable for vascular administration.

In 2011, Kakumanu et al., prepared nano-emulsion as a carrier for Dac as nanodrug delivery system (Figure 1.20).

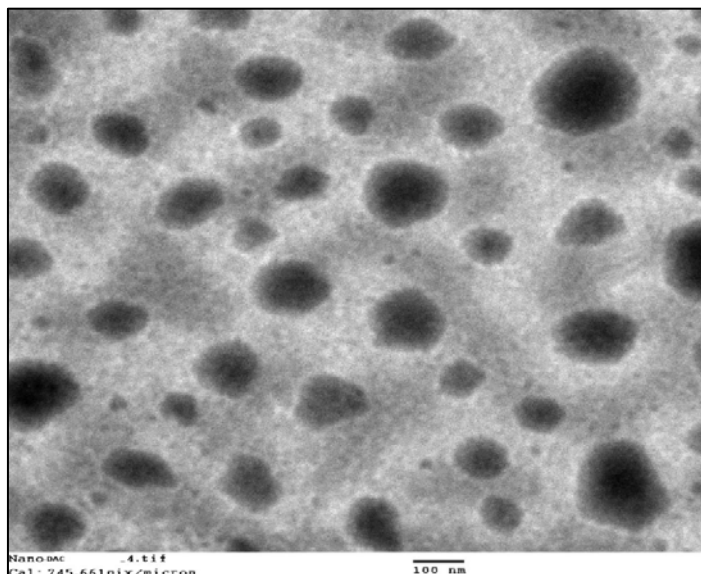


Figure 1.20: Morphology of nanoemulsion-Dac determined by TEM (Kakumanu et al., 2011).

The study tested whether there was an increased efficacy of Dac as a nanoemulsion on reducing tumour size in an epidermoid carcinoma xenograft mouse model. "The mice were untreated or treated with a suspension of Dac (0.1 mg/kg), a nanoemulsion of Dac (0.1 mg/kg), or Nano-Control (same composition as the suspension and nanoemulsion but no Dac), every 2 days by either intramuscular injection (IM) or topical application. After 40 days, the final tumour size of mice receiving the nanoemulsion of Dac IM ($0.83 \pm 0.55 \text{ mm}^3$) was significantly reduced compared to the suspension of Dac IM ($4.75 \pm 0.49 \text{ mm}^3$), Nano-Control IM ($7.63 \pm 0.91 \text{ mm}^3$), and untreated ($10.46 \pm 0.06 \text{ mm}^3$). The final tumour size of mice receiving the nanoemulsion of Dac topically ($3.33 \pm 0.63 \text{ mm}^3$) was also significantly reduced compared to the suspension of Dac topically ($7.64 \pm 0.68 \text{ mm}^3$)".

These formulations have shown unsatisfactory drug encapsulation efficiency and drug loading. In addition, the methods for their preparation may not be suitable for scaling up

to industrial manufacture production requirements. In this regard, NLC has emerged as an auspicious alternative for Dac as nanodrug delivery system to treat the skin disease “melanoma”. The core of this research is the use of nanostructures in medicine as drug delivery for melanoma chemotherapeutic drug (Dacarbazine). The research and experiments of this study systemically reviews the project on the application of NLC nanoparticles as a carrier, and the previous studies used nanoparticles as a carrier for Dacarbazine (Dac).

The development of novel therapeutic drugs alone is not adequate to ensure progress in drug therapy. Poor water solubility and stability of drug molecules, such as tumour drugs, is a common problem. Consequently, there is an appeal to provide a drug carrier system to diminish impediments associated with tumour drugs such as, Dacarbazine (5-(3,3-Dimethyl-1-triazenyl). The carrier in a drug delivery system (DDS) should have appropriate properties such as: a sufficient drug loading capacity, specificity of drug "tumor" targeting, controlled release, and reduced drug toxicity. The carrier in DDS should also provide homeostasis among the incorporated drug. Moreover, feasibility of DDS production, including scaling up with reasonable overall costs, should be possible.

1.8. Aim and objectives

The literature review presented above show that some research problems around NLC as a drug delivery system have been identified. These include different methods of preparations (i.e. no standard method used) and different lipid materials applied (i.e. no standard formula). In the pharmaceutical industry, the effect of NLC as drug excipients in different applications, including the topical route, are still under debate amongst researchers. Thus, it has not been possible to identify published reports on the use of NLC as a carrier for therapeutic agents. NLC can be considered as a good candidate vehicle that could encapsulate a therapeutic agent for topical tumour treatment. Therefore, the principal aim of this research is to establish modelling the functionality of NLC as a drug delivery system for a therapeutic agent such as Dacarbazine (Dac) that can be used for the treatment of Melanoma. The objectives of this project can be summarized in the following:

- 1- Development of a standardised laboratory-based preparation of NLC particles that have optimal properties for use as a carrier for drug delivery system, modifying the NLC formula and the NLC preparation method.
- 2- Development and characterisation of the encapsulation of a chemotherapeutic drug (Dacarbazine) within NLC particles. Investigate the effect of formula modification on physical properties (size, disparity and stability) and delivery system (drug loading capacity and encapsulation efficiency) using different therapeutic agent concentrations.
- 3- Assessment of the particle structure and cellular toxicity of NLC particles and therapeutic drug pre and post encapsulation in relevant environments (e.g. *in vitro* using tumour skin cells)
- 4- Provide recommendations for an industry-based preparation method (large scale) and development of NLC particles that have optimal properties for use as a carrier for drug delivery system by defining the effect of modifying the NLC formula and preparation method on its properties.

The research approach is shown in Figure 1.21.

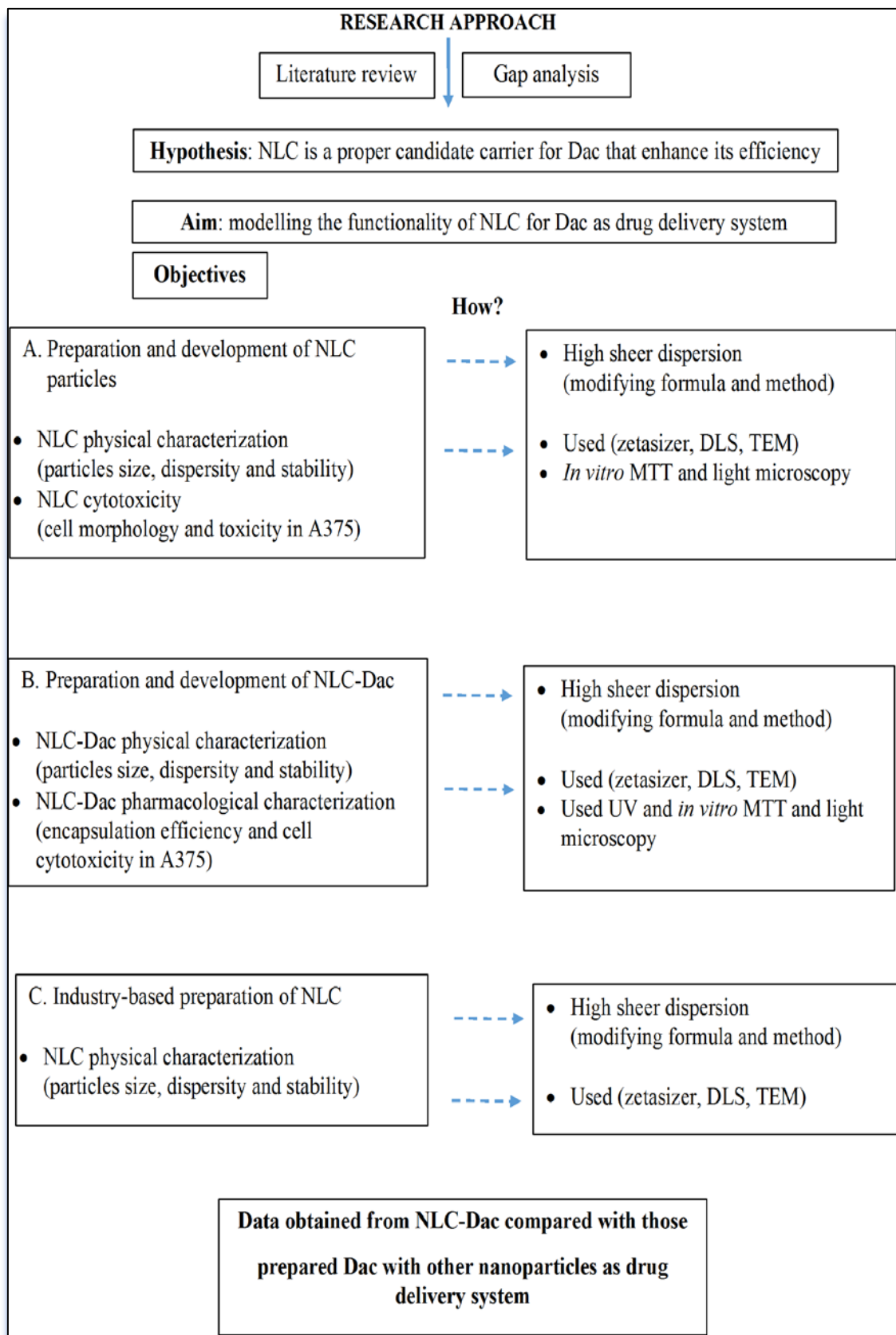


Figure 1.21: Schematic outlining the experimental approach of the project.

CHAPTER TWO
MATERIALS AND METHODS

2. MATERIALS AND METHODS

2.1 Introduction

This chapter lists the purity and sources of the materials used within the experiments presented in this thesis and summarize the methods applied to prepare nanoparticles, encapsulate the active agents, and characterize the resultant particles and to assess the toxicity of the different end points.

2.2 Materials

The materials used within the experiments (both cell assessments and nanoparticle preparations) were purchased from different suppliers; these are listed here under the different experimental headings for ease.

For nanostructured lipid preparations, glyceryl behenate (product No: 1295709) was purchased from Sigma Aldrich Ltd (Dorset, UK). Stearylamine, D- α -tocopheryl polyethylene glycol succinate (TPGS), isopropyl myristate (IPM; 98% purity), acetone 99.9%, ethanol 99.98% and Kolliphor® P 188 were obtained from Sigma Aldrich Ltd (Dorset, UK). Precirol ATO-5® (glycerol distearate) and medium-chain triglycerides (Labrafac™ Lipophile WL1349) were purchased from Gattefossé (Cédex, France). D- α -Soybean lecithin (SL) was obtained from Cuisine Innovation (Dijon, France). See appendix B2 for all material specification sheets.

For nanostructured lipid measurements, glass cuvettes, phosphotungstic acid (PTA 0.02; g/ml) were purchased from Sigma Aldrich Ltd catalogue number 79690. In the establishment of nanoparticles measurements, the experiments used silica nanoparticles SiNP 20 from Sigma Aldrich Ltd (Dorset, UK), catalogue number 420875 and SiNP 200 from Postnova Analytics Ltd (Malvern Hills Science Park, UK) catalogue number Z-PS-SIL-GFP-0,2.

The therapeutic drug selected for encapsulated by NLC is dacarbazine (Dac) and it was purchased from Sigma Aldrich (Gillingham, Dorset, UK).

For *in vitro* cell bio viability assessments, a human malignant melanoma A375 cell line was obtained from Sigma Aldrich Ltd (Dorset, UK). Nunclon® flasks (75 and 25 cm²)

and Nunclon® TC Microwell 96-flat bottom well plates and 6-well plates were purchased from Fisher Scientific Ltd (Loughborough, UK). For cell counts, cell counting chamber slides were purchased from Gibco® (Paisley, UK).

The information regarding the materials used for the cell-based experiments, including the media and the supplements used for cell growth are listed in Table 2.1.

Table 2.1: Cell lines, media and supplements.

Materials	Supplier	Catalogue Number
DMEM/F-12 Medium	Gibco®	31330-038
Fetal Bovine Serum	Sigma Aldrich Ltd	F2442-500ML
Penicillin/Streptomycin 100UI/ml	Gibco®	15070-063
Phosphate Buffered Saline	Sigma Aldrich Ltd	P4417-100TAB
Trypsin-EDTA 0.05%	Gibco®	25300-054
Trypsin Neutralizer Solution	Gibco®	R-002-100

The materials used for the cell-based assays, such as cell viability, apoptotic cell death and fluorescent staining, as well as those used for molecular biology experiments, are presented in Table 2.2.

Table 2.2: Cell-based and molecular biology assay reagents.

Materials	Supplier	Catalogue Number
MTT reagent (3-(4,5dimethylthiazol-2-yl)-2,5diphenyltetrazolium bromide)	Sigma Aldrich Ltd	M2128-500MG
Trypan Blue stain solution 0.4%	Gibco®	21051-024
Dimethyl Sulfoxide (DMSO; 99.9% purity)	Sigma Aldrich Ltd	D5879-500ML
Hydrogen peroxide 30 % (w/w) in H ₂ O	Sigma Aldrich Ltd	H1009-100ML
Annexin V/FITC conjugate	Gibco®	APOAF-50TST
Propidium Iodide fluorescent stain	Sigma Aldrich Ltd	P4170-10MG

2.3 Methods for preparation

2.3.1 Laboratory-based synthesis of NLCs and NLC-DAC

Several methods were applied to prepare NLC and each of them has its characteristics (see Section 1.6.2). Generally, in the laboratory-based method, a simple evaporation technique was used to eliminate the organic solvent in the NLC solution (Naseri et al., 2015). This method involves dissolving the lipophilic material in aqueous phase by using an organic solvent. Upon evaporation of the solvent, NLC dispersion is formed in emulsion. In the next step, the organic solvent can be removed from the emulsion by evaporation under stirrer – heating technique. For further particles homogenizations and size adapting, high shear dispersion (HSD) is useful. This mixing technique used a high speed rotational instrument (3000 – 25,000 rpm) for emulsifying suspended solids lipid. The technique passages one phase such as solid lipid into a main mobile liquid phase. The pre-emulsion mixed at high speed to produce a disruption of droplets. This

technique has advantages of low cost, particles size controlling and simple to use in laboratory.

In this study, NLC was prepared using the laboratory-based method by using HSD after solidification of emulsion-evaporation methods in oil/oil/water matrix. Generally, NLC prepared by mixing the oil phase with liquid phase in the present of organic solvent. Evaporation method used in this study to dissolve the lipophilic material in aqueous phase by using an organic solvent. Upon evaporation of the solvent, NLC dispersion is formed in emulsion and the organic solvent removed from the emulsion by evaporation under stirring technique. The fridge (2°C) was used to stabilize the NLC and keep the solution temperature for 2 hours. Up to the solidification step, the study followed the previous method published by (Chen et al., 2012), using the same formula as stated within the paper and the initial results were reported. Then, HSD was used to optimize the NLC properties, which involves decrease the particle size of NLC and improve the particles dispersity in solution. Practically, three solid lipids with suitable liquid lipid matrices were chosen to prepare NLCs (as shown in Table 2.3).

Table 2.3: The formula components of NLC preparations.

NLC Formulation	Solid lipid			Liquid lipid		Emulsifier		surfactant
	SA (mg)	Gb (mg)	Precirol ATO-5 (mg)	IM (mg)	MCT (mg)	SLT (mg)	TPGS (mg)	Kolliphor ® P 188 w/v %
NLC/PI			180	60		30	30	1-3
NLC/GM		180			60	30	30	1-3
NLC/SI	180			60		30	30	1-3
* SA, stearylamine; Gb, glyceryl behenate lipid; IM, isopropyl myristate; MCT, medium-chain triglycerides; SLT soybean lecithin; TPGS tocopheryl polyethylene glycol succinate.								

The preparation involved oil-in-water emulsion, evaporation and solidification followed by high shear dispersion. The solid lipid, liquid lipid and emulsifiers were mixed with 12.5 mL of organic solvents (equal volume of acetone and ethanol) at temperature 5 °C above their melting point. The emulsion was made by adding the oil phase drop-wise to

an equal volume of aqueous phase, which contained nonionic surfactant kolliphor® P 188 (1–3 % w/v) and was heated at the same temperature. The mixture was stirred for 4 hours at 400 rpm using a magnetic stirrer, and then solidified at 0 °C for 2 hours. Finally, the solution was subjected to high shear dispersion by a mixing step at 10,000–15,000 rpm for up to 40 min using the instrument shown in Figure 2.1.



Figure 2.1: High shear disperser machine which used to prepare NLC (T25 digital Ultra-Turrax, IKA, UK).

The same procedure was used to achieve NLC/PI-Dac, where the amount of 0, 35, 50, 70 mg of Dac was added to the oil phase to prepare three different formula of NLC/PI-Dac. NLC/SI NLC is made of stearylamine (SA) and isopropyl myristate lipids, NLC/GM NLC is made of glyceryl behenate lipid (GB) and medium-chain triglycerides (MCT), NLC/PI NLC is made of precirol ATO-5 and isopropyl myristate (IM) lipids, SL soybean lecithin and TPGS D- α -tocopheryl polyethylene glycol succinate was used in all preparations as emulsifier.

2.3.2 Industry-based synthesis of NLC/PI

As the post laboratory-based technique, the study used the Microjet reactor (MJR) method to prepare NLC at a large scale. MJR is a technique for producing microparticles or nanoparticles of water-soluble and water-insoluble substances. The lipid phase, including solvent, and a liquid phase are mixed as jets that collide with each other in a microjet reactor. The flow rates and temperature thereby cause very rapid microparticles or nanoparticles to be formed (Türelı, 2015). The high energy dissipation from the jets promotes nanoparticle formation in large scale (Figure 2.2). Micro jet reactors (MJR) can be used to form nanoparticles where two streams of chemicals (solvent and a nonsolvent) impinge. Schwertfirm et al, 2008 have previously demonstrated that the flow rate and temperature of the reactor has an effect on the properties of the particles. To prepare NLC by the microjet reactor, the formula of NLC/PI 1% was selected as the best carrier properties obtained from the laboratory-based synthesis.

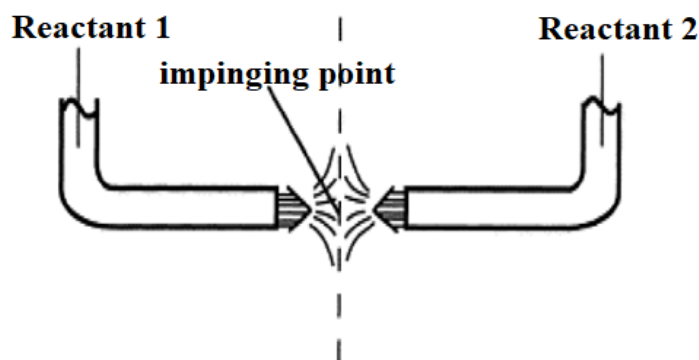


Figure 2.2 : Schematic showing MJR processes of two impinging jets (Türelı, 2015).

The effect of MJR flow rate (50, 75, 100 ml/sec) at different reactor temperatures (at 60, 65, 70 °C) on the properties of the formula of NLC/PI 1% was also measured. Initially, Precirol ATO-5 as solid lipid, isopropyl myristate as liquid lipid, soybean lecithin and D- α -tocopheryl polyethylene glycol succinate as emulsifiers were mixed with 125 mL of organic solvents (equal volumes of acetone and ethanol) at a temperature which was set at 5 °C above their melting point (65 °C). Then, the NLC was made by pumping the

oil phase to an equal volume of aqueous phase, which contained 1 % of nonionic surfactant Kolliphor® P 188.

2.4 Measurement of physiochemical properties

2.4.1 Introduction

Nanodrug carriers use biodegradable and biocompatible lipid materials encapsulated by surfactants and dispersed within colloidal system. The properties of nanostructured lipids that may affect its function as a carrier have to be measured and improved. So, it is important to evaluate NLC properties after each preparation step. This study used different technique to assess the NLCs and NLC-Dac attributes such as average size, dispersity index, particle morphology and zeta potential.

2.4.2 Dynamic Light Scattering (DLS)

In nanoparticles research, it is importance to study the particles size and the particle size distribution (polydispersity index, PDI). Dynamic Light Scattering (DLS) can analyze the particle size by monitoring the Brownian motion (Figure 2.3).

It is the random movement of particles due to the bombardment by the solvent molecules that surround them. Usually DLS is concerned with measurement of particles suspended within a liquid and by using the Stokes-Einstein relationship the intensity fluctuations can be inferred. A typical dynamic light scattering system comprises of six main constituents; (1) a laser provides a light source to illuminate the sample contained in a cell,

(2) most of the laser beam passes through the sample, but some is scattered by the particles within the sample at all angles,

(3) a detector is used to measure the scattered light and the intensity of scattered light must be within a specific range for the detector to successfully measure it,

- (4) an attenuator is used to reduce the intensity of the laser source and hence reduce the intensity of scattering,
- (5) the correlator compares the scattering intensity at successive time intervals to derive the rate at which the intensity is varying,
- (6) this correlator information is then passed to a computer to analyse the data by specific software.

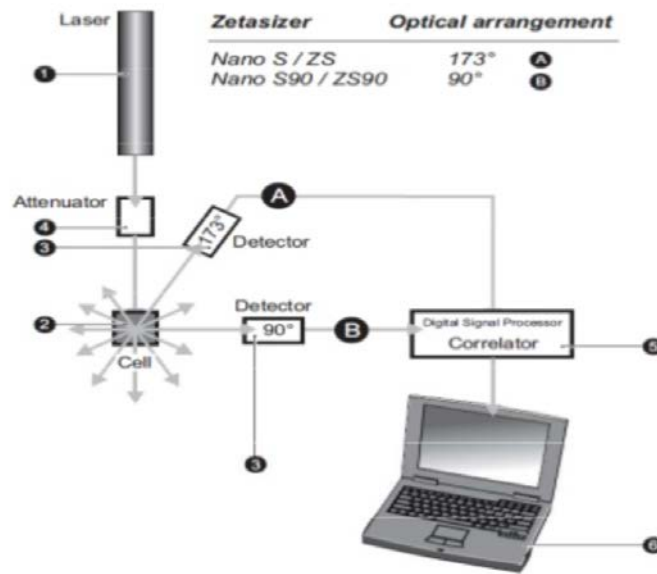


Figure 2.3 : Optical configurations of the Zetasizer Nano series for dynamic light (source: Malvern technical note “Achieving high sensitivity at different scattering angles with different optical configurations”).

This study used DLS to measure the particles size and polydispersity index (PDI) of NLC under certain conditions included temperature (25 °C), fixed angle (90°), refractive index set at 1.590 and samples were suitably diluted with deionized water (Fang et al., 2012; Gomes et al., 2014; Yue et al., 2016). DLS is concerned with the measurement of particles size and dispersity in a suspension. NLCs and NLC-Dac preparations were measured with a Malvern Zetasizer (Zetasizer Nanosizer S; Malvern Instruments Ltd, Worcestershire, UK) as described previously (Irfan et al., 2014). The measurements were obtained at 633 nm with a 4-m He–Ne laser. To give an average value and standard deviation for the particle size and polydispersity index (PDI), three different

batches for each formula from NLC/PI, NLC/GM and NLC/SI were analyzed five times. Prior to the measurement, all the samples were diluted with double-distilled water to a suitable scattering intensity.

2.4.3 Nanoparticles tracking analysis (NTA)

Nanoparticles tracking analysis (NTA) is a newly developed method which combines laser light scattering microscopy and a video imaging system for measuring the particles size between approximately 10-2000 nm. A laser beam is passed through the particles in solution in the path of the beam scatter light that they can be simply visualized via magnification microscope onto which is mounted a video camera (Figure 2.4).

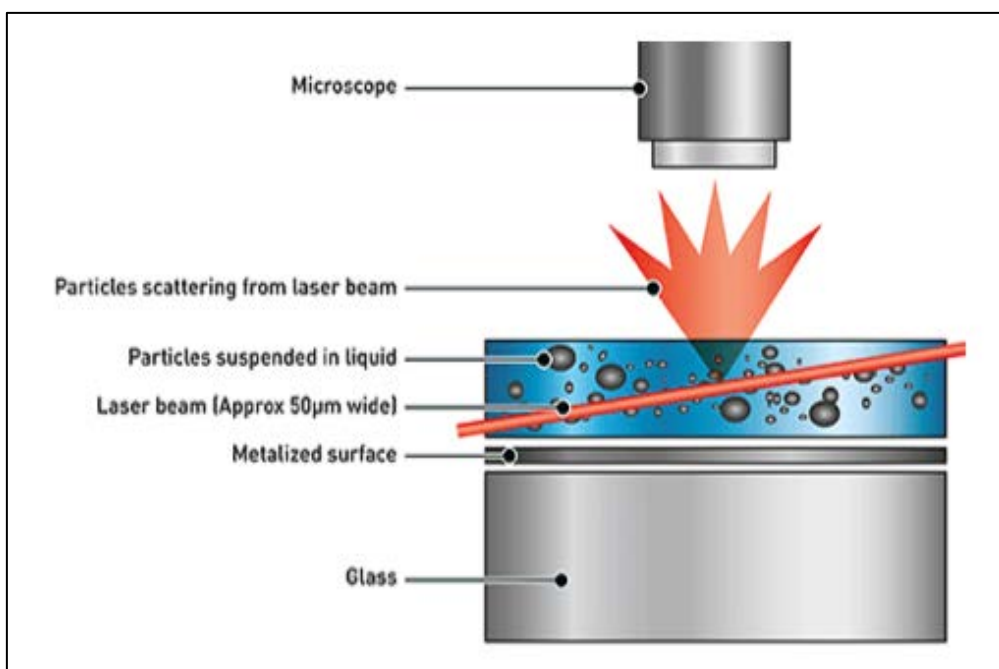


Figure 2.4: Schematic presentation of the Nanoparticle Tracking Analysis (source: Malvern articles "Studying Nanoparticle-Based Drug Delivery and Targeting with Nanoparticle Tracking Analysis").

The NTA technique can access a unique size range and is reflected a more quantitative than DLS. When recording a video, the rate of movements of each individual particle captured on film is related to its size according to a modified Stokes–Einstein relationship. The NTA can identify and track the individual particle in the field

of view which is moving by Brownian motion in liquid. The particle size measurements of NLC/PI were confirmed using NTA.

A stock solution of the sample was diluted with double-distilled water to 200 $\mu\text{g/mL}$. Three ml of the dilute solution was loaded into a 5 ml glass syringe and this was injected to the sample chamber of the laser illumination module of a Malvern Nanosight LM20 (Malvern Instruments Ltd, Worcestershire, UK). The laser was turned on and the focus of the instrument set on a location where nanoparticles were existent. When particle showed, and tracking were optimized, a sequence of automated batch clip experiments was performed to increase the sample size and improve statistical analysis. The temperature during the experiment was held constant at 20 $^{\circ}\text{C}$ and 30 frames/sec.

2.4.4 Zeta potential

Zeta potential is a scientific term for electro-kinetic potential for particles in colloidal system. The potential difference between the dispersion medium fluid and the surface of the dispersed particle is a reflection of the stability of colloidal dispersions. (Table 2.4). The higher zeta potential values on either side reflects the stabilization of the particles in suspension (Gonzalez-Mira et al., 2010)

Table 2.4: Zeta potential value guidelines and stability evaluation.

Zeta potential (mVolt)	Stability behavior of the colloid
From 0 to ± 5	Rapid flocculation
From ± 5 to ± 25	Incipient instability
From ± 25 to ± 45	Moderate stability
From ± 45 to ± 65	Good stability
From ± 65 to ± 100	Excellent stability

Typically, the stability of nanoparticles is reliant on the value of zeta potential, i.e. high value zeta potential suggests a high degree of repulsion between adjacent particles and the dispersion will not flocculate, while low value of zeta potential suggest that there is a high degree of attraction between particles and the dispersion will aggregate and reduce the stability of the suspension (Hanaor 2012). In NLC drug delivery, the stability of NLC particles is a good influence of the quality of delivery system (Wa et al., 2011; Thatipamula et al., 2011; Shinde et al., 2013; Sütő et al., 2016).

The electro-kinetic potential for particles in colloidal system is referred to its zeta potential, indicating the level of repulsion between adjacent particles in solution. The potential difference between the dispersion medium fluid and the surface of the dispersed particle reflects the stability of colloidal dispersions. The zeta potential of each of the three NLC/PI formulas and NLC/PI-Dac were prepared as previously stated for NTA (200 µg/ml dilution in double-distilled water) and then the solutions were injected into Malvern Instrument 3000 HSa Zetasizer (Malvern Instruments Ltd, Worcestershire, UK). They were analyzed with 5 cycles of measurements to measure the average zeta potential taken for each sample and the results were recorded.

2.4.5 Transmission Electron Microscopy (TEM)

The transmission electron microscope (TEM) functions on the same basic principles as the light microscope but uses electrons instead of light (Figure 2.5). What can be observed with a light microscope is limited by the wavelength of light so TEMs use electrons as light source. In that case their much lower wavelength creates it potential to get a resolution a thousand times better than with a light microscope. Objects to the order of a few angstroms (10^{-10} m) can then be seen. For structural investigation and particles morphology of NLC, TEM presented a useful image (Saupe et al., 2006; Lin et al., 2007; Silva et al., 2009).

The structure and morphology of the NLCs were studied by TEM. NLC preparations were diluted with double-distilled water (50 µg/ml dilution in double-distilled water). A droplet of each sample was applied to a copper grid coated with carbon film and air-dried. The grid was then stained with 0.02 g/mL phosphotungstic acid (PTA) solution

and dried under room temperature (25 °C). The particles were examined using TEM (CM20, Philips) at an operating voltage of 200 kV. Later, TEM technique was also used with same conditions to analyze the structure of NLC/PI-Dac comparing with NLC/PI (NLC with and without drug).

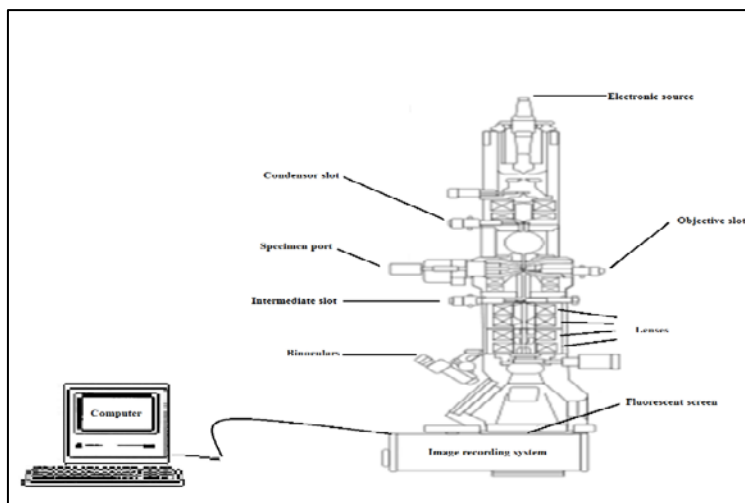


Figure 2.5: Layout of optical components in a basic TEM (Williams and Carter al., 1996).

2.4.6 Stability at storage conditions

The stabilities of each NLC formation (NLC/PI, NLC/GM and NLC/SI) were determined over a period of storage at 2-4 °C for 6 months of each formation. The changes in particle size, polydispersity and zeta potential were investigated using the same conditions as described above.

2.4.7 Lyophilisation

The samples were applied to lyophilization process by using the freeze-dried method. NLC/PI and NLC/PI-DAC were freeze-dried to obtain dried product and then subjected to XRD analysis. Initially, 3% (w/v) concentration of Silica fumed was added to both samples (NLC/PI and NLC/PI-Dac) as cryoprotectants. Then, they were fast frozen under -45°C in a deep-freezer for overnight. Next day, they were moved into the Edwards Modulyo K4 Freeze Dryer (Thermo Electron Corporation, UK). The operating conditions were, temperature of -25 °C and pressure of 0.001

bar. After 24 h, the NLC/PI and NLC/PI-Dac powders were collected and analyzed using an X-Ray Diffractometer.

2.4.8 Powder X-Ray diffraction (PXRD)

The technique of X-ray diffraction (XRD) use a scattering of X-rays produces an interference effect to the atoms of a crystal and gives information of the identity of a crystalline substance. The crystalline fields in the powder are dissimilar and the three-dimensional structure of crystalline materials is defined by steady displacement, repeating of planes for atoms. The X-ray beam interacts with these planes of atoms and produced different atom diffracted. This diffraction is depending on atom crystal lattice and arranged. The X-ray diffraction can measure the distances between the planes of the atoms by applying Bragg's Law. The measurement produced from a typical X-ray scan delivers a unique "fingerprint" of the molecule (Warren al., 1969).

The XRD of NLC have been shown to have different patterns due to the NLC components such as the solid lipid and surfactant. The XRD analyses can also demonstrated the variance between NLC pre and post drug encapsulated. In 2014 Lim et al., found that the XRD showed that the drug itraconazole was encapsulated in the lipid matrix and present in the amorphous form see Figure 2.6.

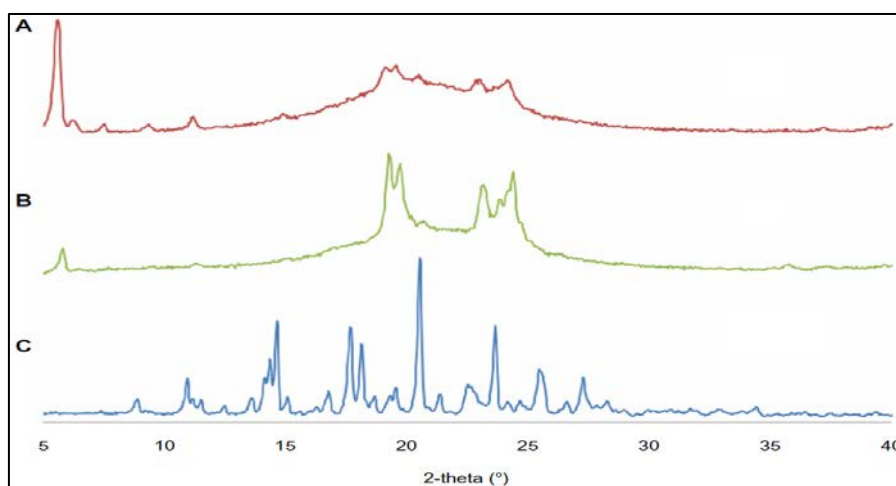


Figure 2.6: X-ray diffractogram for (A) Itraconazole-loaded nanostructured lipid carriers; (B) blank nanostructured lipid carriers; (C) itraconazole.

In this research, the XRD analysis will use to study the crystalline lattice of NLC pre and post Dacarbazine (Dac). In 1979, Freeman and Hutchinson, published the three-dimensional X-ray data and the crystal structure of Dac. It has been reported as monoclinic crystal system (crystal of unequal lengths) with space group $P2_1/m$. Monoclinic crystal exist with $a = 14.042$, $b = 10.661$ and $c = 11.914$ axis. The crystal lattice of Dac exist with \AA , $\beta = 91.49$ and 2 molecules per asymmetric unit (Figure 2.7).

PXRD is used to study structural characteristics and to identify powders. In this study, X-ray diffractometer (Bruker-AXS D5005, Siemens, UK) was used to determine the crystalline structure of Dac (white powder), NLC/PI (white powder) and NLC/PI-Dac (yellowish powder). The samples were pressed into a slit (dimensions $2 \times 2 \times 1 \text{mm}$) and PXRD pattern was measured with a voltage of 40 kV and a current of 30 mA. The radiation source is ^{64}Cu and the range of scan used was $10\text{--}90^\circ$ of the diffraction angle 2θ for 1 h 6 min.

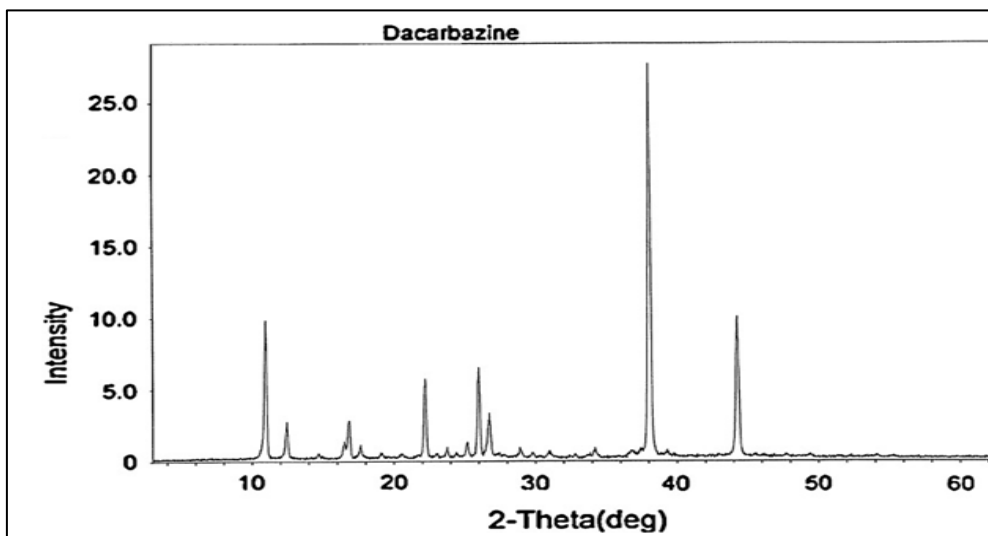


Figure 2.7: X-ray diffraction pattern of native Dac (Bei et al., 2010).

2.5 Measurement of pharmacological effect

2.5.1 Introduction

More methods were used to assess NLC/PI-Dac as drug delivery system to describe its properties. The parameters such as drug loading capacity, encapsulation efficiency and drug release profile were used to improve the NLC/PI-Dac formulations. The next sections discuss the principles of each of these methods.

2.5.2 Drug loading capacity (DL) and encapsulation efficiency (EE)

Ultra violet spectrophotometry (UVs) is a quantitative analysis of the material reflection and deals with light beam's intensity as a function of wavelength and of its colour. The absorbance of a species in the solution is directly proportional to its concentration. UV spectrophotometry has been used in previous studies to measure Dac concentration at 330 nm wavelength (Bei et al., 2010 and Kumar et al., 2016). Initially, a standard curve is created based upon different concentrations of Dac and the regression equation is obtained ($y = dx + b$), where d is the slope of the line and b is the y intercept (Figure 2.8).

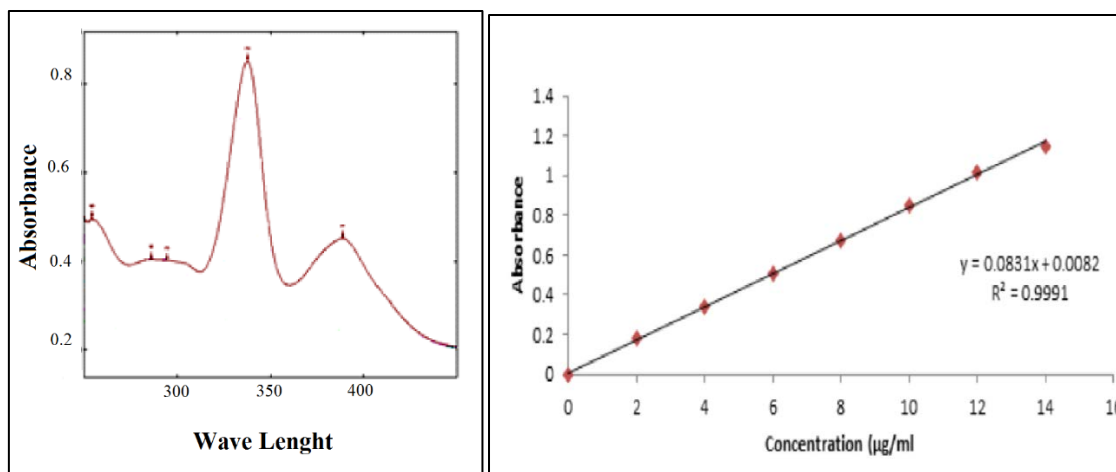


Figure 2.8: Spectrum diagram and calibration curve of Dacarbazine (Kumar et al., 2016).

Many studies demonstrated that UV spectrophotometry can be used to measure the concentration of the drug encapsulated in NLC that is used for drug delivery, by centrifuging the suspension of NLC with specific conditions such as speed and temperature. The centrifugation process causes the NLC to precipitate and the drug is released from NLC (Sanad et al., 2010; Xia and Wu, 2011 and Gaba et al., 2015).

Dac fluoresces can be measured under UV at 330 nm wavelength (Bei, et al. 2010). Dac was therefore dissolved in acetone at concentrations of 0-80 µg/mL and analyzed using a UV spectrometer (Double Beam UV-VIS, UV-2100 Shimadzu, Japan) to provide a fluorescence reading versus concentration in order to plot the standard curve. The concentration of Dac within NLC/PI-Dac was determined by centrifuging NLC/PI-Dac at 12,500 rpm, 4°C for 45 min (Fresco17 Micro-centrifuges, Thermo scientific, UK) to obtain a supernatant. The free drug in the supernatant was then measured using UV spectrometer and the concentration was calculated according to the regression equation for the Dac standard curve.

The encapsulation efficiency (EE) and drug loading (DLC) percentage were derived from the following equations:

$$EE \% = \left(\frac{W_1 - W_2}{W_1} \right) 100 \dots\dots\dots \text{Equation (1)}$$

$$DLC \% = \left(\frac{W_1 - W_2}{W_3} \right) 100 \dots\dots\dots \text{Equation (2)}$$

Where W_1 is the amount of drug added in the NLC/PI, W_2 amount of un-entrapped drug and W_3 amount of the lipids added.

2.5.3 Drug release profile

The release of Dac from NLC/PI-Dac over a period of time was studied by diluting NLC/PI-Dac stock solution. NLC/PI-Dac was diluted to 10 % with PBS (pH = 7.4) and incubated at 37 °C in a capped centrifugation tube. At intervals of 0-30 h, the solutions (6 samples) were centrifuged at 12500 rpm, 4°C for 45 min (Fresco17 Microcentrifuges, Thermo scientific, UK). The concentration of Dac in the supernatant was calculated according to the regression equation of the Dac standard

curve (following the method described in Section 2.3.1). The drug released from NLC/PI was expressed as the percentage of total amount of drug in the solution.

2.6 Methods for NLCs and NLC/PI-Dac toxicity assessment in A375 cells

2.6.1 Introduction

The cell line A375 derived from a 54-year-old female with malignant melanoma was used for toxicity analysis using MTT assay. The viability of cells was counted to assess the effect of NLCs on cell line A375 at different concentrations for up to three days. A blank control was formed of NLC/PI without Dac encapsulation. A positive control was used and comprised of hydrogen peroxide (0.3 g/ml in deionized water). Initially, the toxic effects of NLC/PI, NLC/GM, and NLC/SI (formula shown in Table 3.1) were assessed in A375 cells. Later, the effect of Dac on cell line A375 was analyzed before and after encapsulation in NLC/PI.

Cells are the vital environment to evaluate the bioactivity for the drug delivery system. Studies have shown *in vitro* effect of different drug delivery systems using several cells. For skin tumor research, A375 cells have been used previously to assess NLC particles as a carrier in nanodrug delivery system (Brown et al., 2014; Rigon et al., 2015), but these are different than those developed in this work.

2.6.2 Cell culture

A375 cells are a human amelanotic melanoma cell line which have been applied to a variety of research in cell biology. Melanoma cells are categorized according to the differentiation phases evaluated by morphology, expression of cell-surface marker antigens and pigmentation (Koziel, 1995). A375 cells belong to undifferentiated class due to lack of gp100 antigen and expression of HLA-DR antigen. The cells themselves have clearly epithelioid and slippery shapes with lack of pigmentation. The human melanoma cell line A375 endogenously expresses mutation in B-RAF at V600E that leads to the establishment activation of the cellular proliferation.

In this work, A375 melanoma cells were suspended in the medium of the cells containing Foetal Bovine Serum (FBS; 0.15 g/ml) and penicillin-streptomycin (0.01 g/ml) in 500 ml of Dulbecco's Modified Eagle's (DMEM/F-12). The cells were seeded at a density of 5×10^4 cells/cm² in flasks (Nunclon® 25 cm²) and incubated at 37°C under a humidified atmosphere with 5% CO₂ and 95% air. The cells were passaged every 3 days at sub-confluent cultures (80-90% confluency) using 0.25 g/mL trypsin-EDTA to detach them from the surface of flasks.

The media-cell solution was centrifuged at 1200 rpm using a bench top centrifuge (Thermo-Scientific centrifuges-UK) and the cell pellets were collected and re-suspended in DMEM/F-12 media at 10^4 cells/cm² using flasks (Nunclon® 75 cm²).

2.6.3 Phase contrast microscopy for cell imaging

Phase contrast is a type of light microscopy using an optical contrast technique for making unstained phase samples visible and enhances contrasts of transparent and colorless samples by influencing the optical path of light. A large spectrum of living biological specimens are practically transparent when observed in the optical microscope, while phase contrast microscopy can examine the living cells in their natural state without being killed, fixed and stained. This is useful because cellular processes can be viewed in real time. The technique of phase contrast microscopy, which converts phase shifts in light passing through a transparent specimen to brightness changes in the image, phase changes themselves are invisible, but become visible when shown as brightness variations (Figure 2.9). The first application of phase contrast microscopy technique was by the Dutch physicist Frits Zernike (1888-1966). The phase contrast microscope uses the concept, which the light passing through a transparent part of the specimens travels slower and therefore is shifted compared to the uninfluenced light. The difference in phase can be amplified to half a wavelength by a transparent phase-plate in the microscope, consequently causing a difference in brightness making the transparent sample shine out in contrast to its surroundings. The annulus aperture is placed in the front focal plane of the condenser and confines the angle of the any penetrating light waves. The phase plate lies in the back focal plane of the objective and has a phase ring made from

specific material that dims the light passing through it. Then, changes its phase by $\lambda/4$, when λ represents the light's wavelength. The ring-shaped light that passes the condenser annulus is focused on the specimen by the condenser. Portions of the ring-shaped light are diffracted by optically dense structures of the specimen such as plasma membranes and organelles.

Cell morphology was examined before and after treatment with silica nanoparticles (SiNP) and nanostructured lipid carrier (NLC) 25-100 $\mu\text{g}/\text{ml}$ in medium with 10% FBS (CM-10%) and 0% FBS (CM) at 24 hours. Phase contrast cell images were taken at 20X magnification using Leica DFC 295.

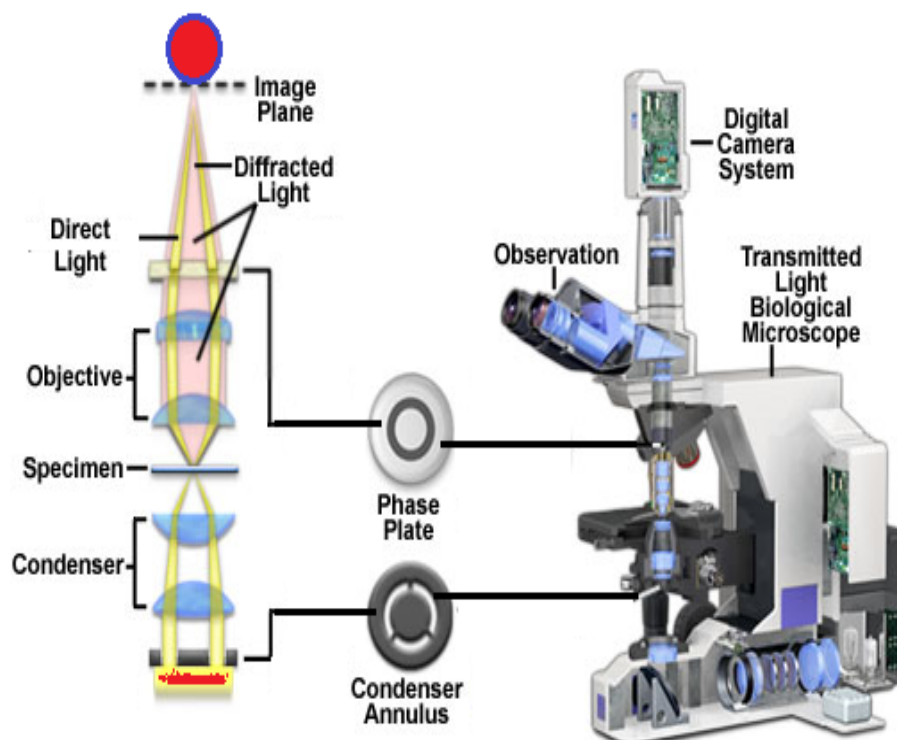


Figure 2.9: The configuration of a phase contrast microscope, a phase contrast microscope amplifies the slight difference in the refractive index which causes the edges of cells to be highlighted (source <https://cellularphysiology.wikispaces.com/Phase+Contrast+Microscopy> accessed on 21/06/2016).

2.6.4 Cell counting

A375 cells were detached from the growth surface area of the flask (Nunclon® 75 cm²) by using 0.25 g/mL of trypsin. Firstly, 5 mL of trypsin added to the flask then the cells were incubated at 37°C under a humidified atmosphere with 5% CO₂ and 95% air for three minutes. Once detached, the cells were centrifuged and re-suspended in the medium of the cells containing Fetal Bovine Serum (FBS; 0.15 g/ml) and penicillin -streptomycin (0.01 g/ml) in 500 mL of Dulbecco's Modified Eagle's (DMEM/F-12). Trypan Blue was used to differentiate between live and dead cells. An aliquot of 25 µg Trypan Blue was mixed with an equal amount of cell solution in an Eppendorf tube and then added on to a Chamber slide®, which was analyzed using an automated cell counter (Invitrogen Countess®). The number of cells per mL and the number of live cells were recorded.

2.6.5 Morphology of A375

Typically, light microscopy can provide information on cell morphology changes in response to treatment. The effect of NLCs in A375 cells was qualitatively assessed by imaging using light microscopy (Leica DM IL LED system). A375 cells from the flask (Nunclon® 75 cm²) were harvested and seeded in 6-well plates at a density of 10⁴ cells/cm². The cells were incubated at 37°C under humidified atmosphere with 5% CO₂ and 95% air. The media was removed after 24hours and replaced with media containing different type of NLC (NLC/PI, NLC/GM and NLC/SI) at 100 µg/ml concentration. Post 24hr incubation, the cells morphology was examined under light microscopy and the images were recorded.

2.6.6 Growth rate

After initially seeding A375 cells, growth starts with a lag phase and proceed to a log phase, where the cells proliferate exponentially (Figure 2.10).

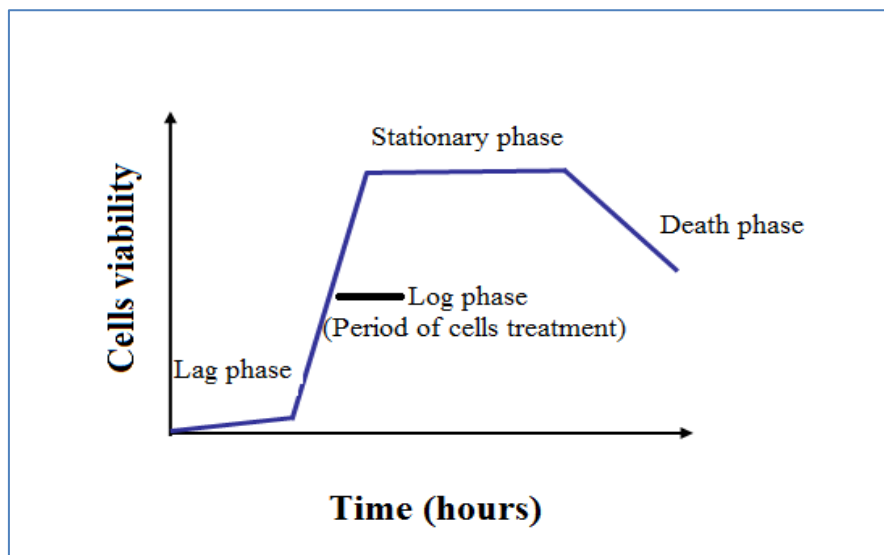


Figure 2.10: Phases curve of cells growth shows the period of treatment.

Then the stationary phase starts where growth rate and death rate are equal. The log phase is also called the exponential growth phase that cells grow rapidly, and the doubling time is often short (period of time required cells for a quantity to double in size). Rapidly growing cells are made competent more easily than cells in other growth phases and the cells in log phase are live, healthy, and actively metabolizing so, it is necessary to brought cells into log phase for treatment. In this study, A375 melanoma cells will be used in log phase and cell viability will assessed after treatment with the drug encapsulated particles.

A375 melanoma cells were suspended in the medium of the cells and seeded in triplicate at 10^4 , 2×10^4 , 3×10^4 and 4×10^4 cells/ cm^2 in 96-well plates. Cell growth was determined by MTT assay (described in Section 3.6.8.) at three time points, namely 24, 48 and 72 hours.

2.6.7 A375 doubling time

Cell population doubling time refers to the period of time required for a quantity of cells to double. The A375 cells were seeded in 96/well plates and incubated at 37°C under humidified atmosphere with 5% CO² and 95% air. At different time points the supernatant was removed and the cells washed using PBS. Then the cells were detached by adding trypsin (0.25 g/ml) and incubated for 3 minutes. The cells were put in Eppendorf tubes and suspended using DMEM/F-12. The media-cell solution was centrifuged at 1200 rpm for 5 min using a bench top centrifuge (Thermo-Scientific centrifuges-UK). Trypan Blue was prepared in Eppendorf for cells counting (50 µl in each). The cell pellets were collected and re-suspended in DMEM/F-12 and equal volumes were add to Trypan Blue and gently mixed. From each mixing sample, 50µl was injected to the chambers of counting slides and analyzed using an automated cell counter (Invitrogen Countess®). The numbers of cells were recorded and calculated using use web site calculator (Roth V. 2006 Doubling Time Computing, Available from: <http://www.doubling-time.com/compute.php>).

2.6.8 MTT assay

MTT assay is a colorimetric test for assessing cell viability when NAD (P) H-dependent cellular oxidoreductase enzymes under defined conditions crystallize 3-(4,5-dimethylthiazol-2-yl)-2,5-diphenyltetrazolium bromide (MTT) to formazan salt (Figure 2. 11).

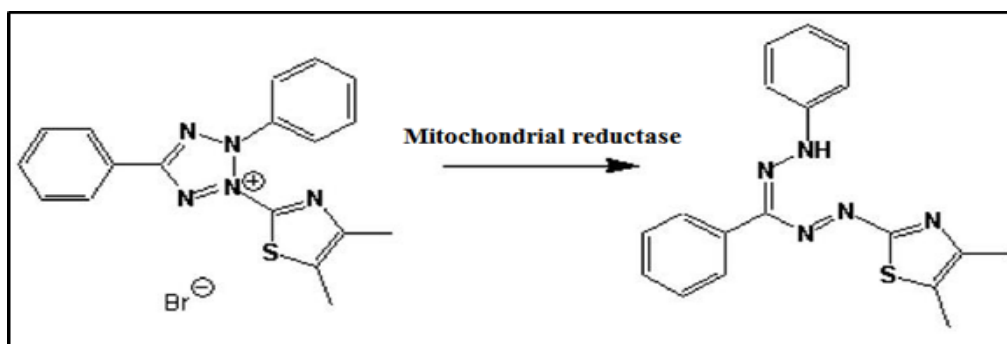


Figure 2.11: Schematic diagram of Formazan salt formation from MTT by Mitochondrial reductase.

In this study, the cell toxicity was assessed by MTT assay, the cell pellets were incubated at 37°C under a humidified atmosphere with 5% CO₂ and 95% air in flasks (Nunclon® 75 cm²) at 10⁴cells/cm². At which point they were detached from the growth surface area by using of trypsin (0.25 g/ml). Once detached, the cells were centrifuged and re-suspended in Dulbecco's Modified Eagle's (DMEM/F-12) containing Foetal Bovine Serum (FBS; 0.15 g/ml) and penicillin -streptomycin (0.01 g/ml) and seeded in three plates of 96-well plates. The cells left for incubation for 24 hours. The media was then removed and replaced with media containing different type of NLC at different concentration (Table 2.5). A positive control of H₂O₂ was used and a blank of media was included. Each plate was marked for a time point and incubated for 24, 48 and 72 hours. The cells were incubated at 37°C under humidified atmosphere with 5% CO₂ and 95% air.

Table 2.5: MTT plan for A375 cells treated by different type and concentrations of NLCs.

Blank (µg/ml)	NLC/PI (µg/ml)			NLC/GM (µg/ml)			NLC/SI (µg/ml)			Control H₂O₂ (µg/ml)
0	50	100	200	50	100	200	50	100	200	50
0	50	100	200	50	100	200	50	100	200	100
0	50	100	200	50	100	200	50	100	200	200

At the time appointed (24, 48 and 72hr), the medium was removed from each 96-well plates and the cells were washed twice with PBS to remove all NLCs for possible interference with absorbance measurements. Then, 100 µl of tetrazolium dye MTT or 3-(4,5-dimethylthiazol-2-yl)-2,5-diphenyltetrazolium bromide solution (1mg/ml) was added to the cells in 96-well plates and incubated for two hours at room temperature 25°C. The plate was covered with aluminum foil to prevent light interaction. After two hours incubation at room temperature an equal volume (100 µl) of dimethyl sulfoxide (DMSO) reagent was added to stop the MTT reaction. The plate was then incubated for a further 20 minutes at room temp (25°C) before the plate was analyzed using a

Thermo Scientific Varioskan platereader (including a spectrometer at a wavelength of 570 nm). Cell viability was expressed as % of control (e.g. cells without particle treatment).

The same procedure of MTT assay was used to analyze the A375 cells toxicity after NLC/PI and NLC/PI-Dac treatment (Table 2.6).

Table 2.6: MTT plan for A375 cells treated by different concentrations of NLC/PI carrier before and after encapsulated Dac and Dac.

Blank (µg/ml)	NLC/PI (µg/ml)			NLC/PI-Dac (µg/ml)			Dac (µg/ml)			Control H₂O₂ (µg/ml)
0	50	100	200	8/50	16/100	32/200	8	16	32	50
0	50	100	200	8/50	16/100	32/200	8	16	32	100
0	50	100	200	8/50	16/100	32/200	9	16	32	200

2.7 Statistical analysis

All experiments were performed at least three times and representative experimental data is presented in each figure. The mean values of three replicates were expressed with standard deviation (shown as mean \pm SD). One-way ANOVA, T-test and Fishers Least Significant Difference (LSD) were performed using Minitab 16 software to determine significance of comparisons. Statistically significant differences (e.g. where $p \leq 0.001$, 0.05 and 0.01) are indicated by asterisks on the figures ($p < 0.01$ shown as ***, $p < 0.05$ shown as ** and $p < 0.1$ shown as *).

CHAPTER THREE

**NANOSTRUCTURED LIPID CARRIERS SYNTHESIS,
CHARACTERISATION AND OPTIMIZATION**

3. NANOSTRUCTURED LIPID CARRIERS SYNTHESIS, CHARACTERISATION AND OPTIMIZATION

3.1 Introduction

Several methods were applied to prepare NLC for use as a nanoparticle carrier for drug delivery (see Section 1.6.2). In this Chapter, the studies focused on the optimization of the NLC synthesis methods. The NLCs were first prepared using a laboratory process with different formulae. Initially the three different types of NLC formulae (NLC/SI, NLC/GM and NLC/PI) were prepared using evaporation-solidification methods (see section 2.3.1). The measurements of NLC properties (particles size and poly dispersity index) were reported for each formulation. Initial results show the necessity to use high shear dispersion (HSD) to improve the NLC properties. Later, HSD and their parameters (speed and time of dispersion) on NLC properties were investigated. The deposition parameters were varied to achieve the optimum properties of NLC for drug delivery (defined in Section 2.3.1). The NLC properties including particle size, polydispersity index (PDI) and the morphology were measured for each sample after preparation and the resultant properties were analyzed to select the most appropriate NLC for use as a carrier. The appropriate formula of NLC was then re-synthesized using an industrial technique, MicroJet Reactor (MJR; discussed in Section 2.3.2) and the effect of flow rate and temperature on particle size and polydispersity of the particles was analyzed. The results and discussions of this work are shown below.

3.2 Preliminary preparation of NLC using evaporation-solidification methods

Three different samples from NLC were prepared, each preparation formulated from lipid phase and aqueous phase. In each formula, each lipid phase has different solid lipid used (Table 3.1). In each formula the solid lipid, liquid lipid and emulsifiers were mixed for evaporation-solidification methods (see section 2.3.1). Then, each sample was measured for particle size and particles homogeneity through the polydispersity index (PDI) by using Dynamic light scattering (DLS).

Table 3.1: Formula components of NLCs preparations by evaporation-solidification methods.

NLC Formulation		Solid lipid			Liquid lipid		Emulsifier		Surfactant
		SA (mg)	Gb (mg)	Precirol ATO-5 (mg)	IM (mg)	MCT (mg)	SLT (mg)	TPGS (mg)	Kolliphor® P 188 w/v %
1	NLC/PI			180	60		30	30	1
2	NLC/GM		180			60	30	30	1
3	NLC/SI	180			60		30	30	1

* SA, stearylamine; Gb, glyceryl behenate lipid; IM, isopropyl myristate; MCT, medium-chain triglycerides; SLT soybean lecithin; TPGS tocopheryl polyethylene glycol succinate.

After the preparation of the NLC as shown in Table 3.1, the NLC particles were characterised using DLS. The NLC results showed that the particles size were larger than 900 nm (Table 3.2), the preparations were repeated using different stirring time (4, 2 and 1 hours) at stirring speed of 400 rpm.

Table 3.2: The particle size and polydispersity index (PDI) data obtained from DLS for different NLC preparation, different stirring time at 400 rpm, mean \pm SD (n = 5).

Formula	NLC Type	Stirring time (hours)	Particle size (nm)	PDI
F 1a	NLC/PI	4	924 \pm 26*	0.75 \pm 0.03
F 1b	NLC/PI	2	1306 \pm 27	0.91 \pm 0.07
F 1c	NLC/PI	1	1562 \pm 49	0.80 \pm 0.05
F 2a	NLC/GM	4	994 \pm 17	0.63 \pm 0.02
F 2b	NLC/GM	2	880 \pm 81*	0.73 \pm 0.06
F 2c	NLC/GM	1	1131 \pm 19	0.69 \pm 0.03
F 3a	NLC/SI	4	1275 \pm 65*	0.87 \pm 0.01
F 3b	NLC/SI	2	1506 \pm 12	0.65 \pm 0.02
F 3c	NLC/SI	1	1722 \pm 13	0.87 \pm 0.07

Note: (F1) NLC/PI formula is made of precirol ATO-5 and isopropyl myristate (IPM) lipids, (F2) NLC/GM NLC is made of glyceryl behenate lipid (GB) and medium-chain triglycerides (MCT) and (F3) NLC/SI is made of stearylamine (SA) and isopropyl myristate lipids.

*indicated the smallest particles size distribution obtained and Figures 3.1, 3.2 and 3.3, showed its DLS results.

For the formulation of NLC/PI (F1a)

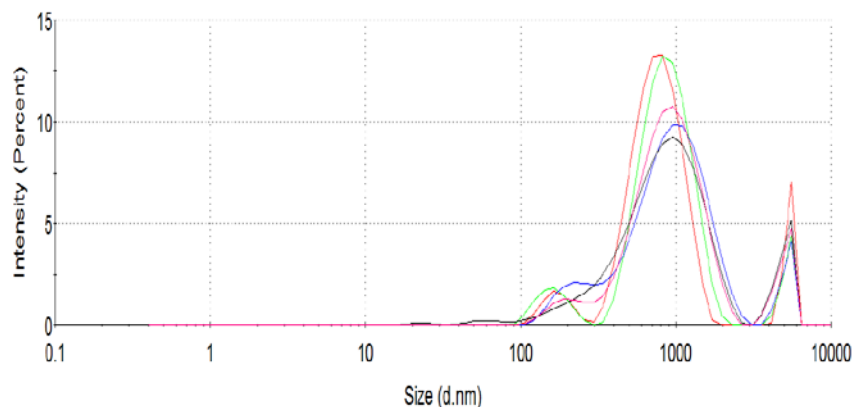


Figure 3.1: The smallest particles size distribution obtained for NLC/PI (F1a) as measured by DLS, the average size was 924 nm \pm 26 and PDI was 0.75 \pm 0.03. Each colour represent sample, mean \pm SD (n=5).

For the formulation of NLC/GM (F2b)

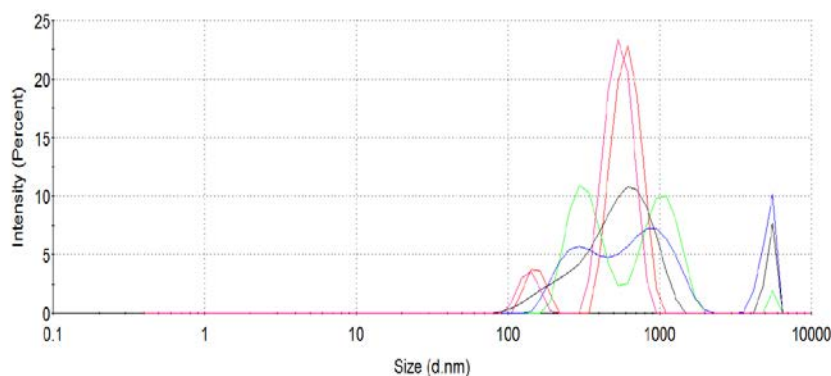


Figure 3.2: The smallest particles size distribution obtained for NLC/GM (F2b) as measured by DLS, the average size was 880 nm \pm 81 and PDI was 0.73 \pm 0.06. Each colour represent sample, mean \pm SD (n=5).

For the formulation of NLC/GM (F3a)

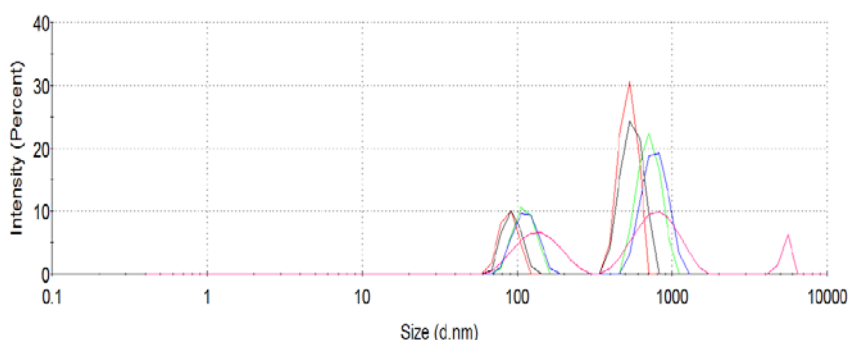


Figure 3.3: The smallest particles size distribution obtained for NLC/GM (F3a) as measured by DLS, the average size was 1275 nm \pm 65 and PDI was 0.87 \pm 0.01. Each colour represent sample, mean \pm SD (n=5).

The results also showed that 2-4 hours stirring time gave the smallest particle size. The NLC preparations were repeated using different stirring time (4, 2 and 1 hours) at 200 rpm in order to improve the NLC properties and reduce their particle size. The results show that the smallest NLC particles size obtained was 951 nm (Table 3.3).

Table 3.3: The particle size and polydispersity index (PDI) data obtained from DLS for different NLC preparation, different stirring time at 200 rpm, mean \pm SD (n = 5).

Formula	NLC Type	Stirring time (hours)	Particle size (nm)	PDI
F 4a	NLC/PI	4	951 \pm 139*	0.83 \pm 0.02
F 4b	NLC/PI	2	1642 \pm 27	0.99 \pm 0.04
F 4c	NLC/PI	1	1858 \pm 91	1 \pm 0.07
F 5a	NLC/GM	4	-	-
F 5b	NLC/GM	2	-	-
F 5c	NLC/GM	1	-	-
F 6a	NLC/SI	4	3465 \pm 87*	0.85 \pm 0.02
F 6b	NLC/SI	2	4366 \pm 61	0.6 \pm 0.05
F 6c	NLC/SI	1	4608 \pm 11	0.7 \pm 0.02

Note: at this stage (F5) NLC/GM did not prepare due to the cost of solid lipid glyceryl behenate lipid (GB) and the study want to assess the effect of stirring time and speed on NLC/PI and NLC/SI first.

*indicated the smallest particles size distribution obtained and Figures 3.4 and, 3.5 shows its DLS results.

For the formulation of NLC/PI (F4a)

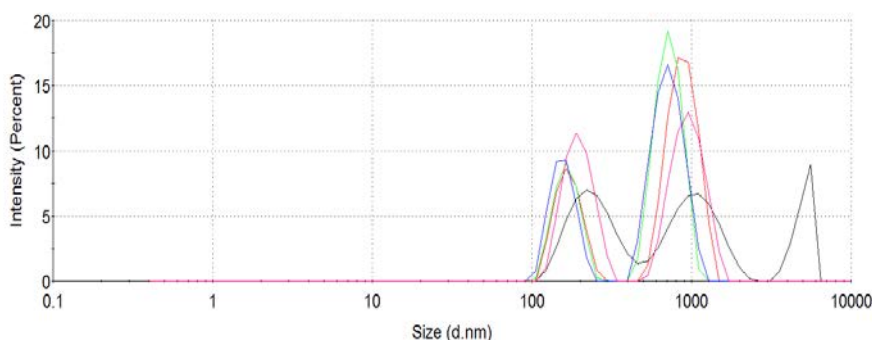


Figure 3.4: The smallest particles size distribution obtained for NLC/PI (F4a) as measured by DLS, the average size was 951 nm \pm 139 and PDI was 0.83 \pm 0.02. Each colour represent sample, mean \pm SD (n=5).

For the formulation of NLC/SI (F6a)

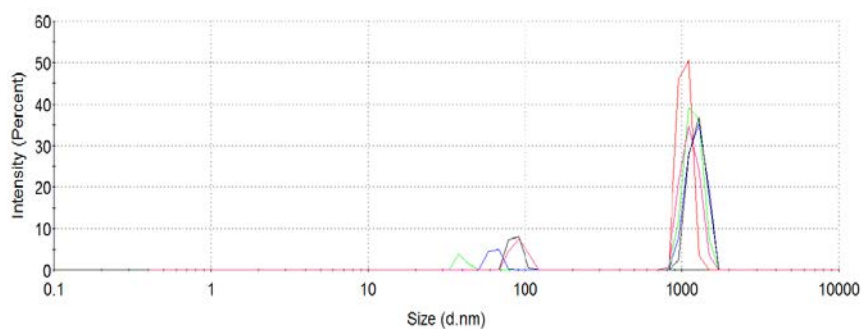


Figure 3.5: The smallest particles size distribution obtained for NLC/SI (F6a) as measured by DLS, the average size was 3465 nm \pm 87 and PDI was 0.85 \pm 0.02. Each colour represent sample, mean \pm SD (n=5).

These results show that using longer stirring time (4 hours) gives the smallest particle size but the speed of the stirring (200 rpm and 400 rpm) in these experiments did not have major effect on reducing the particle size.

The previous preparations did not obtain the target particles size ($\leq 200\text{nm}$) and the PDI indicated high values and all resultants were in polydispersity. Therefore, the NLC preparations were repeated to study the effect of surfactant concentrations on the particles size by using kolliphor® P 188 at 3 % w/v (Table 3.4).

Table 3.4: The formula components of NLC.

NLC Formulation		Solid lipid			Liquid lipid		Emulsifier		Surfactant
		SA (mg)	Gb (mg)	Precirol ATO-5 (mg)	IM (mg)	MCT (mg)	SLT (mg)	TPGS (mg)	Kolliphor® P 188 w/v %
1	NLC/PI			180	60		30	30	3
2	NLC/GM		180			60	30	30	3
3	NLC/SI	180			60		30	30	3

* SA, stearylamine; Gb, glyceryl behenate lipid; IM, isopropyl myristate; MCT, medium-chain triglycerides; SLT soybean lecithin; TPGS tocopheryl polyethylene glycol succinate. (the formulations listed above will be use in Table 3.5 and Table 3.6)

The effect of different stirring time (4, 2 and 1 hours) at 400 rpm on size distribution with surfactant (3% w/v) is shown in Table 3.5.

Table 3.5: The particle size and polydispersity index (PDI) data obtained from DLS for different NLC preparation, different stirring time at 400 rpm, mean \pm SD (n = 5).

Formula	NLC Type	Stirring time (hours)	Particle size (nm)	PDI
F 7a	NLC/PI	4	920 \pm 18*	0.53 \pm 0.08
F 7b	NLC/PI	2	1334 \pm 31	0.72 \pm 0.03
F 7c	NLC/PI	1	1608 \pm 37	0.82 \pm 0.05
F 8a	NLC/GM	4	988 \pm 57*	0.49 \pm 0.04
F 8b	NLC/GM	2	957 \pm 12	0.65 \pm 0.02
F 8c	NLC/GM	1	1131 \pm 19	0.69 \pm 0.07
F 9a	NLC/SI	4	1014 \pm 26*	0.33 \pm 0.09
F 9b	NLC/SI	2	1506 \pm 12	0.65 \pm 0.02
F 9c	NLC/SI	1	1722 \pm 53	0.87 \pm 0.07

Note: (F7) NLC/PI formula is made of precirol ATO-5 and isopropyl myristate (IPM) lipids, (F8) NLC/GM NLC is made of glyceryl behenate lipid (GB) and medium-chain triglycerides (MCT) and (F9) NLC/SI is made of stearylamine (SA) and isopropyl myristate lipids.

*indicated the smallest particles size distribution obtained and Figures 3.6, 3.7 and 3.8 shows its DLS results.

For the formulation of NLC/SI (F7a)

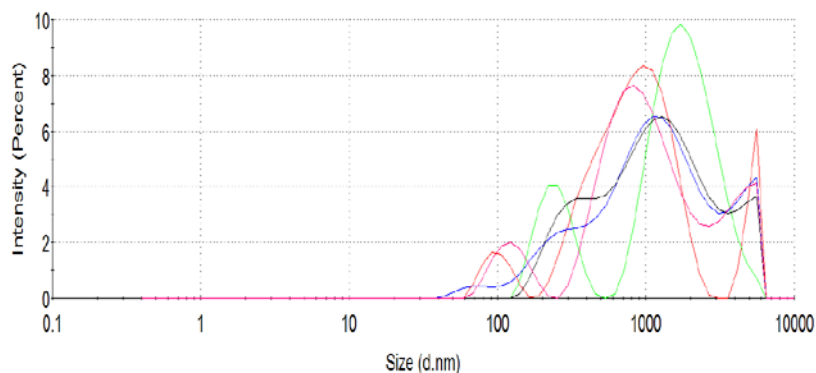


Figure 3.6: The smallest particles size distribution obtained for NLC/PI (F7a) as measured by DLS, the average size was 920 nm \pm 18 and PDI was 0.53 \pm 0.08. Each colour represent sample, mean \pm SD (n=5).

For the formulation of NLC/SI (F8a)

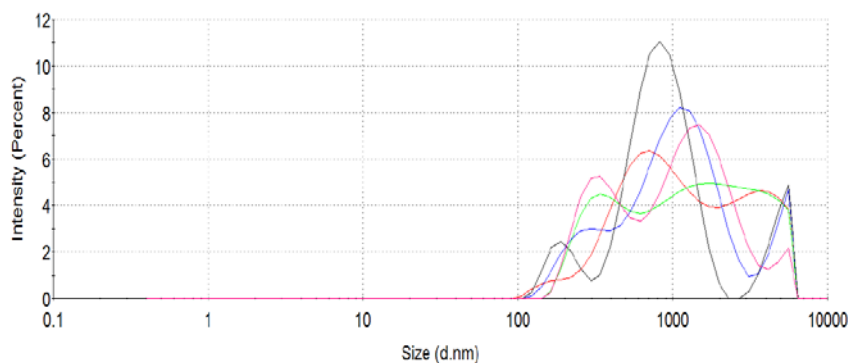


Figure 3.7: The smallest particles size distribution obtained for NLC/GM (F8a) as measured by DLS, the average size was 988 nm \pm 57 and PDI was 0.49 \pm 0.04. Each colour represent sample, mean \pm SD (n=5).

For the formulation of NLC/SI (F9a)

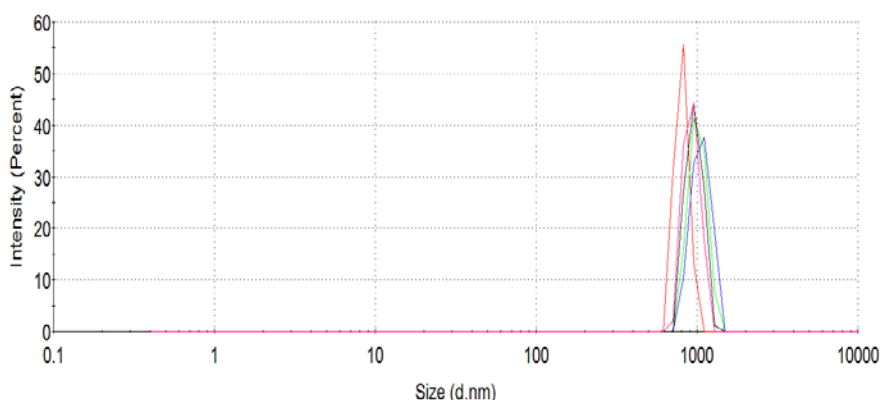


Figure 3.8: The smallest particles size distribution obtained for NLC/SI (F9a) as measured by DLS, the average size was 1014 m ±26 and PDI was 0.33±0.09. Each colour represent sample, mean ± SD (n=5).

The NLC preparations were repeated using different stirring time (4, 2 and 1 hours) at 200 rpm in order to examine the effect on the NLC properties. The results show an increasing in NLC particles size due to low stirring speed (Table 3.6).

Table 3.6: The particle size and polydispersity index (PDI) data obtained from DLS for different NLC preparation, different stirring time at 200 rpm, mean ± SD (n = 5).

Formula	NLC Type	Stirring time (hours)	Particle size (nm)	PDI
F 10a	NLC/PI	4	1581±155*	0.94±0.05
F 10b	NLC/PI	2	1718±94	0.72±0.03
F 10c	NLC/PI	1	1794±116	0.82±0.09
F 11a	NLC/GM	-	-	-
F 11b	NLC/GM	-	-	-
F 11c	NLC/GM	-	-	-
F 12a	NLC/SI	4	6680±623*	0.35±0.09
F 12b	NLC/SI	2	8104±159	0.65±0.09
F 12c	NLC/SI	1	8956±113	0.87±0.07

Note: at this stage (F11) NLC/GM did not prepare due to the high cost of solid lipid glyceryl behenate lipid (GB), see (Appendix B2), and the study want to assess the effect of stirring time and speed on NLC/PI and NLC/SI first.

*indicated the smallest particles size distribution obtained and Figures 3.9 and 3.10 shows its DLS results.

For the formulation of NLC/SI (F10a)

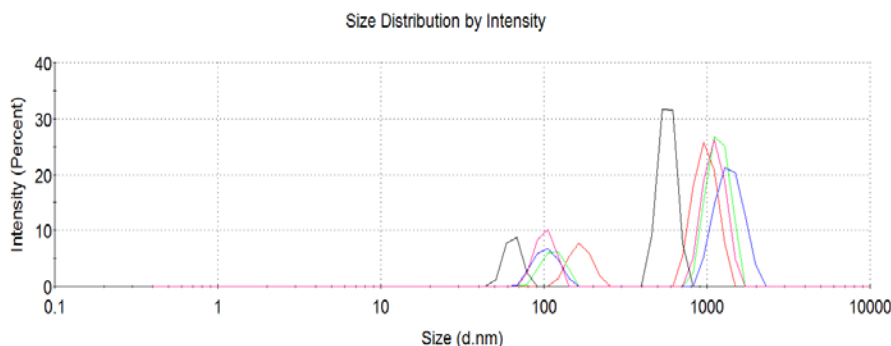


Figure 3.9: The smallest particles size distribution obtained for NLC/PI (F10a) as measured by DLS, the average size was 1581 nm \pm 155 and PDI was 0.94 \pm 0.05. Each colour represent sample, mean \pm SD (n=5).

For the formulation of NLC/SI (F12a)

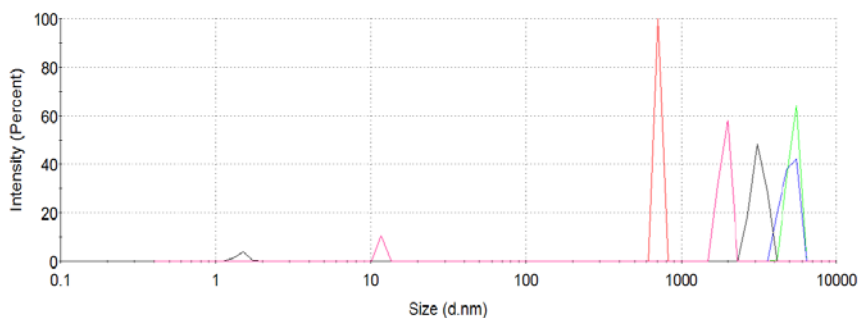


Figure 3.10: The smallest particles size distribution obtained for NLC/SI (F12a) as measured by DLS, the average size was 6680 nm \pm 623 and PDI was 0.35 \pm 0.09. Each colour represent sample, mean \pm SD (n=5).

From the above experiments, the use of higher stirring speed (400 rpm) and longer stirring time (2-4 hours) showed the smallest particle size. However, the surfactant effect was not clear here.

3.3 Optimization of NLC laboratory-based synthesis by using high sheer dispersion (HSD)

In order to obtain a nanolipid carrier with the desired characteristics identified as nanoparticle size (< 200 nm), polydispersity index (≤ 2), the components and synthesis parameters were optimized in laboratory based synthesis. A total of 27 samples were prepared in order to enable the optimization of the lipid matrix, surfactant concentration and the HSD parameters of time and speed. The formula components and procedures for NLC/SI, NLC/GM and NLC/PI preparations are described in Section 2.3.1. The final volume for each solution after evaporation of organic solvent was 12.5 ml and the synthesis required eight hours for completion of the whole procedure.

Once the sample was prepared, the measurements of particle size and the heterogeneity of the particle size in a mixture (dispersity) were studied using DLS.

3.3.1 NLC/SI

NLC/SI were formed using the preparations listed below with differing concentrations of Kolliphor P 188 surfactant (Table 3.7). For each preparation, HSD was used to produce the NLC/SI particles. The homogenization procedure was applied in two different speed (10000 and 15000 rpm). For each speed, HSD was used for different times (10, 20, 30 and 40 minutes).

Table 3.7: The formula components of NLC/SI preparations by high sheer dispersion.

NLC Formulation	Solid lipid	Liquid lipid	Emulsifier		Surfactant
	Stearylamine (mg)	isopropyl myristate (mg)	Soybean lecithin (mg)	D- α -tocopheryl polyethylene glycol succinate (mg)	Kolliphor® P 188 (g/ml)
NLC/SI	180	60	30	30	1%
NLC/SI	180	60	30	30	2%
NLC/SI	180	60	30	30	3%

For each preparation, the resultant particles were analysed for particle size and PDI for the different parameters (speed and time) of HSD (see Table 3.8).

Table 3.8: The particle size and polydispersity index (PDI) data obtained from NLC/SI prepared with different surfactant concentration by high sheer dispersion (HSD) with varying speed and time, mean \pm SD (n = 5).

Surfactant Concentration	Speed (X ³) Rpm	Time (minute)	Particle size (nm)	PDI
NLC/SI 1%	0	0	1295 \pm 9	0.9 \pm 0.02
NLC/SI 1%	10	10	1204 \pm 27	0.9 \pm 0.1
NLC/SI 1%	10	20	583 \pm 9	0.6 \pm 0.05
NLC/SI 1%	10	30	565 \pm 11	0.6 \pm 0.02
NLC/SI 1%	10	40	512 \pm 9	0.6 \pm 0.09
NLC/SI 1%	15	10	1200 \pm 13	0.9 \pm 0.01
NLC/SI 1%	15	20	581 \pm 7	0.7 \pm 0.1
NLC/SI 1%	15	30	510 \pm 10*	0.5 \pm 0.05
NLC/SI 1%	15	40	608 \pm 11	0.6 \pm 0.02
NLC/SI 2%	0	0	1310 \pm 4	0.9 \pm 0.01
NLC/SI 2%	10	10	1309 \pm 9	0.8 \pm 0.09
NLC/SI 2%	10	20	570 \pm 10	0.7 \pm 0.09
NLC/SI 2%	10	30	530 \pm 6	0.5 \pm 0.08
NLC/SI 2%	10	40	592 \pm 11	0.6 \pm 0.04
NLC/SI 2%	15	10	1050 \pm 10	0.8 \pm 0.09
NLC/SI 2%	15	20	594 \pm 11	0.6 \pm 0.07
NLC/SI 2%	15	30	545 \pm 5	0.5 \pm 0.03
NLC/SI 2%	15	40	612 \pm 9	0.5 \pm 0.07
NLC/SI 3%	0	0	1310 \pm 9	0.9 \pm 0.07
NLC/SI 3%	10	10	1300 \pm 14	0.8 \pm 0.08
NLC/SI 3%	10	20	523 \pm 10	0.7 \pm 0.05
NLC/SI 3%	10	30	530 \pm 7	0.5 \pm 0.04
NLC/SI 3%	10	40	585 \pm 10	0.5 \pm 0.04
NLC/SI 3%	15	10	1300 \pm 10	0.8 \pm 0.09
NLC/SI 3%	15	20	617 \pm 6	0.5 \pm 0.01
NLC/SI 3%	15	30	560 \pm 9	0.5 \pm 0.03
NLC/SI 3%	15	40	674 \pm 9	0.6 \pm 0.05

*indicated the smallest particles size distribution obtained and Figure 3.11, showed its DLS results.

For the formulation of NLC/SI (HSD: speed 15000 and time 30 minute)

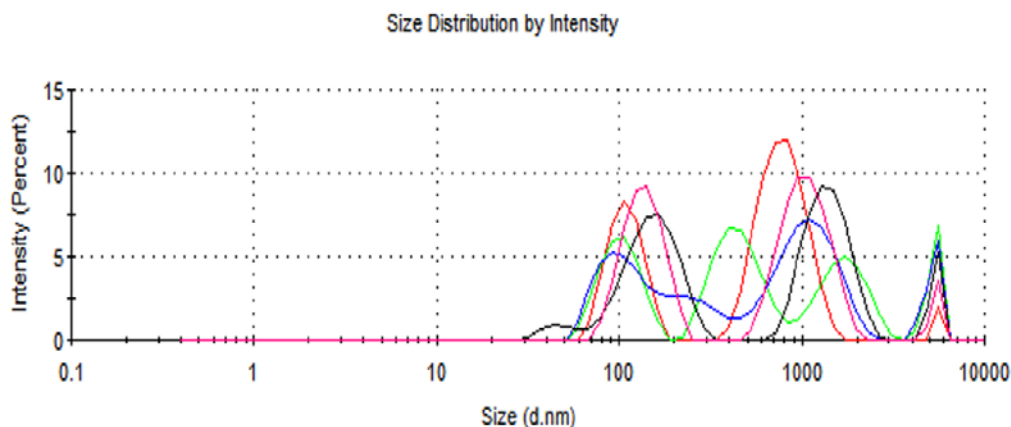


Figure 3.11: Data obtained from DLS for NLC/SI at 1% surfactant showed a typical size 510±10 nanoparticles with PDI 0.5±0.05, Each colour represent sample, mean ± SD (n=5).

The above results show, the amount of surfactant was increased in the NLC/SI manufacture for each time and speed. One-way ANOVA statistical analysis (Table 3.9) was used to answer the study hypothesis:

"There is no statistically significant mean different in nanoparticles size according to different surfactant concentrations (1%, 2% and 3%) in the NLC/SI at an **alpha** level 0.01, 0.05 and 0.1"

Table 3.9: One-way ANOVA results to investigate the above hypothesis.

	Concentration	Mean±SD	F TEST	
			F	P- VALUE
Nanoparticles size	1%	722±281	0.02	0.97
	2%	725±274		
	3%	736±279		

From Table 3.9, the data indicate that there were no statistically significant differences in nanoparticles size mean for surfactant concentrations (1%, 2% and 3%) in the NLC/SI at an **alpha** level 0.01, 0.05 and 0.1.

For the polydispersity index (PDI), One-way ANOVA statistical analysis (Table 3.10) was used to answer the study hypothesis:

"There is no statistically significant mean different PDI according to different surfactant concentrations (1%, 2% and 3%) in the NLC/SI at an **alpha** level 0.01, 0.05 and 0.1"

Table 3.10: One-way ANOVA results to investigate the above hypothesis.

	Concentration	Mean±SD	F TEST	
			F	P-VALUE
PDI	1%	0.67±14	2.56	0.18
	2%	0.62±12		
	3%	0.61±12		

From Table 3.10, the results show that there were no statistically significant differences in PDI mean for surfactant concentrations (1%, 2% and 3%) in the NLC/SI at 0.01, 0.05 and 0.1. In addition, the above results show the effect of time and speed of HSD in all three different surfactant concentrations (1%, 2% and 3%). As the duration of HSD increased (up to 30 minutes), the nanoparticle size decreased, later, the statistical analysis will use to study the effect of speed and time on particles size and PDI in all samples (see section 3.4.3).

The particles size obtained from these preparations were larger than desired (more than 200 nm in all samples), and polydispersity index indicated low homogeneity ($PDI \geq 3$), the results showed that as the HSD time increased (for 10,000 and 15,000 rpm) the particle size decreased and there was improvement in PDI after 20 minutes. The particle size decreased from over approximately 1000 nm to 500 nm as the HSD time increased between 10 and 20 minutes. However, when the HSD time was prolonged up to 30 minutes. The solution reached saturation and the particle size decreased slightly. The NLC/SI particle size increased when HSD duration increased to 40 minutes. For this type of nanolipid particles (i.e. NLC/SI), the improvement of the HSD method by increasing speed and time did not achieve the optimal properties for the carrier (size and

homogeneity). Moreover, the solutions of all samples of NLC/SI prepared were unstable and the particles re-aggregated after 24 hours. Therefore, NLC/SI was excluded as a potential carrier and the study was repeated with another type of NLC that contains a different solid lipid.

3.3.2 NLC/GM

NLC/GM was prepared using the preparations listed below with differing concentrations of Kolliphor P 188 surfactant (Table 3.11). For each preparation, HSD was used to produce the NLC/GM particles. The homogenization procedure was applied in two different speed (10000 and 15000 rpm). For each speed, HSD were used at different time (10, 20, 30 and 40 minutes) (Table 3.11).

Table 3.11: The formula components of NLC/GM preparations by high sheer dispersion.

NLC Formulation	Solid lipid	Liquid lipid	Emulsifier		Surfactant
	Glyceryl behenate (mg)	Medium-chain triglycerides (mg)	Soybean lecithin (mg)	D- α -tocopheryl polyethylene glycol succinate (mg)	Kolliphor® P 188 (g/ml)
NLC/GM	180	60	30	30	1%
NLC/GM	180	60	30	30	2%
NLC/GM	180	60	30	30	3%

* SA, stearylamine; Gb, glyceryl behenate lipid; IM, isopropyl myristate; MCT, medium-chain triglycerides; SLT soybean lecithin; TPGS tocopheryl polyethylene glycol succinate.

For each surfactant concentration formula (1%, 2% and 3%), the study used DLS to measure particle size and the PDI at different speeds and times of HSD (see Table 3.12).

Table 3.12: The particle size and polydispersity index (PDI) data obtained from NLC/GM prepared with different surfactant concentration by high sheer dispersion (HSD) with varying speed and time, mean \pm SD (n = 5).

Surfactant Concentration	Speed (X³) Rpm	Time (minute)	Particle size (nm)	PDI
NLC/GM 1%	0	0	934 \pm 11	0.9 \pm 0.3
NLC/GM 1%	10	10	904 \pm 17	0.8 \pm 0.1
NLC/GM 1%	10	20	400 \pm 4	0.5 \pm 0.08
NLC/GM 1%	10	30	265 \pm 9	0.5 \pm 0.05
NLC/GM 1%	10	40	311 \pm 12	0.5 \pm 0.05
NLC/GM 1%	15	10	900 \pm 10	0.7 \pm 0.1
NLC/GM 1%	15	20	304 \pm 11	0.5 \pm 0.05
NLC/GM 1%	15	30	245 \pm 2	0.5 \pm 0.05
NLC/GM 1%	15	40	337 \pm 8	0.5 \pm 0.06
NLC/GM 2%	0	0	938 \pm 8	0.9 \pm 0.2
NLC/GM 2%	10	10	901 \pm 10	0.7 \pm 0.1
NLC/GM 2%	10	20	377 \pm 7	0.5 \pm 0.04
NLC/GM 2%	10	30	310 \pm 5	0.5 \pm 0.02
NLC/GM 2%	10	40	376 \pm 11	0.5 \pm 0.04
NLC/GM 2%	15	10	872 \pm 15	0.7 \pm 0.1
NLC/GM 2%	15	20	322 \pm 6	0.6 \pm 0.07
NLC/GM 2%	15	30	300 \pm 5	0.5 \pm 0.02
NLC/GM 2%	15	40	396 \pm 2	0.6 \pm 0.02
NLC/GM 3%	0	0	943 \pm 9	0.9 \pm 0.04
NLC/GM 3%	10	10	907 \pm 13	0.7 \pm 0.08
NLC/GM 3%	10	20	424 \pm 9	0.6 \pm 0.04
NLC/GM 3%	10	30	335 \pm 4	0.6 \pm 0.04
NLC/GM 3%	10	40	380 \pm 12	0.6 \pm 0.02
NLC/GM 3%	15	10	929 \pm 19	0.7 \pm 0.06
NLC/GM 3%	15	20	461 \pm 10	0.5 \pm 0.03
NLC/GM 3%	15	30	590 \pm 3	0.3 \pm 0.02*
NLC/GM 3%	15	40	447 \pm 5	0.5 \pm 0.04

*indicated the proper dispersity index obtained and Figure 3.12 showed its DLS result.

For the formulation of NLC/GM (HSD: speed 15000 and time 30 minute)

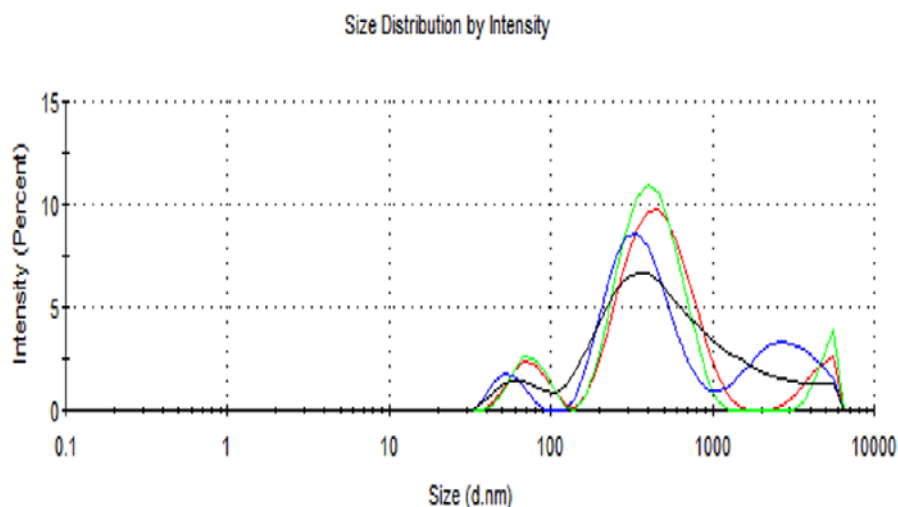


Figure 3.12: Data obtained from DLS for NLC/GM at 3% surfactant showed a typical size 590 ± 3 nanoparticles with PDI 0.3 ± 0.02 , Each colour represent sample, mean \pm SD (n=4).

It can be observed from Table 3.12, that the amount of surfactant was increased in the NLC/GM manufacture for each time and speed. One-way ANOVA statistical analysis (Table 3.13) was used to answer the study hypothesis:

"There is no statistically significant mean different nanoparticles size according to different surfactant concentrations (1%, 2% and 3%) in the NLC/GM at an **alpha** level 0.01, 0.05 and 0.1"

Table 3.13: One-way ANOVA results to investigate the above hypothesis.

	Concentration	Mean \pm SD	F TEST	
			F	P- VALUE
Nanoparticles size	1%	458 \pm 263	0.248	1.409
	2%	481 \pm 239		
	3%	549 \pm 254		

From Table 3.13, the results show that there were no statistically significant differences in nanoparticles size mean for surfactant concentrations (1%, 2% and 3%) in the NLC/GMI at 0.01, 0.05 and 0.1

For the polydispersity index (PDI), One-way ANOVA statistical analysis (Table 3.14) was used to answer the study hypothesis:

"There is no statistically significant mean different PDI according to different surfactant concentrations (1%, 2% and 3%) in the NLC/GM at an **alpha** level 0.01, 0.05 and 0.1"

Table 3.14: One-way ANOVA results to investigate the above hypothesis.

	Concentration	Mean±SD	F TEST	
			F	P- VALUE
PDI	1%	0.56±.11	0.808	.213
	2%	0.57±.08		
	3%	0.57±.09		

From Table 3.14, the results showed that there were no statistically significant differences in PDI mean for surfactant concentrations (1%, 2% and 3%) in the NLC/GM at 0.01, 0.05 and 0.1. In addition, the above results showed the effect of time and speed (10000 and 15000 rpm) of HSD for all three different surfactant concentrations (1%, 2% and 3%). As the HSD time increases up to 30 minutes, the nanoparticle size decreased, (later, the statistical analysis will use to study the effect of speed and time on particles size and PDI in all samples (see section 3.4.3).

Moreover, the particle size was larger than desired (more than 200 nm in all samples) and the polydispersity index indicated low homogeneity ($PDI \geq 3$), the results showed the effect of time of HSD (at 10,000 and 15000 rpm) was to decrease the particle size and improve PDI after 10, 20 and 30 minutes (but not significantly). The particle size decreased from over 900 nm to 300 nm approximately with increased time. The smallest mean particle size of NLC/GM was obtained after 30 minutes homogenization of 1 % concentration of surfactant at either 10,000 or 15,000 rpm HSD (265 and 245 nm, respectively). When compared to the desired NLC characteristics (Section 1.6.3), this

was not adequate as the size was required to be below 200 nm, and the particle homogeneity was low (PDI were 0.5 ± 0.05 for both of them). Unfortunately, the particle size of NLC/GM increased as the HSD time increased up to 40 minutes. As, for this type of nanolipid particles (NLC/GM), the increased HSD speed and time were not sufficient to achieve the desired carrier properties (i.e. size and homogeneity) it was decided that this formulation should be excluded. Moreover, the NLC/GM suspensions were unstable and the particles re-aggregated after 72 hours.

3.3.3 NLC/PI

For NLC/PI, the result showed the effect of speed and time of HSD process on nanoparticle size and PDI for different concentrations of surfactant (Table 3.15). For each preparation, HSD was used to produce the NLC/PI particles. The homogenization procedure was applied in two different speed (10000 and 15000 rpm). For each speed, HSD were used at different time (10, 20, 30 and 40 minutes).

Table 3.15: The formula components of NLC/PI preparations by high shear dispersion.

NLC Formulation	Solid lipid	Liquid lipid	Emulsifier		Surfactant
	Precirol ATO-5 (mg)	isopropyl myristate (mg)	Soybean lecithin (mg)	D- α -tocopheryl polyethylene glycol succinate (mg)	Kolliphor® P 188 (g/ml)
NLC/PI	180	60	30	30	1%
NLC/PI	180	60	30	30	2%
NLC/PI	180	60	30	30	3%

For each surfactant concentration formula (1%, 2% and 3%), the study used DLS to measure particle size and the PDI at different speeds and times of HSD (see Table 3.16).

Table 3.16: The particle size and polydispersity index (PDI) data obtained from NLC/PI prepared with different surfactant concentration by high sheer dispersion (HSD) with varying speed and time, mean \pm SD (n = 5). The highlighted rows show the NLC particles with small size.

Surfactant Concentration	Speed (X ³) rpm	Time (minute)	Particle size (nm)	PDI
NLC/PI 1%	0	0	914 \pm 10	0.9 \pm 0.04
NLC/PI 1%	10	10	909 \pm 13	0.8 \pm 0.01
NLC/PI 1%	10	20	472 \pm 9	0.5 \pm 0.01
NLC/PI 1%	10	30	205 \pm 10	0.3 \pm 0.02
NLC/PI 1%	10	40	245 \pm 9	0.3 \pm 0.01
NLC/PI 1%	15	10	756 \pm 11	0.6 \pm 0.04
NLC/PI 1%	15	20	221 \pm 12	0.2 \pm 0.01
NLC/PI 1%	15	30	155\pm2**	0.1\pm0.05
NLC/PI 1%	15	40	245 \pm 5	0.3 \pm 0.06
NLC/PI 2%	0	0	963 \pm 9	0.9 \pm 0.05
NLC/PI 2%	10	10	952 \pm 17	0.8 \pm 0.03
NLC/PI 2%	10	20	322 \pm 9	0.3 \pm 0.02
NLC/PI 2%	10	30	240 \pm 9	0.2 \pm 0.01
NLC/PI 2%	10	40	331 \pm 4	0.3 \pm 0.01
NLC/PI 2%	15	10	767 \pm 13	0.7 \pm 0.01
NLC/PI 2%	15	20	308 \pm 6	0.3 \pm 0.02
NLC/PI 2%	15	30	175\pm3**	0.2\pm0.01
NLC/PI 2%	15	40	285 \pm 3	0.3 \pm 0.04
NLC/PI 3%	0	0	1009 \pm 4	0.9 \pm 0.03
NLC/PI 3%	10	10	1007 \pm 21	0.7 \pm 0.05
NLC/PI 3%	10	20	461 \pm 10	0.3 \pm 0.03
NLC/PI 3%	10	30	273 \pm 10	0.2 \pm 0.01
NLC/PI 3%	10	40	310 \pm 8	0.3 \pm 0.03
NLC/PI 3%	15	10	1001 \pm 15	0.6 \pm 0.08
NLC/PI 3%	15	20	323 \pm 9	0.3 \pm 0.02
NLC/PI 3%	15	30	195\pm7**	0.2\pm0.04
NLC/PI 3%	15	40	260 \pm 10	0.3 \pm 0.04

** Indicated the proper particles size and dispersity index value from NLC/PI between different surfactant concentrations and different HSD speed/time.

The above table showed that, the amount of surfactant was increased in the NLC/PI manufacture for each time and speed. One-way ANOVA statistical analysis (Table 3.17) was used to answer the study hypothesis:

"There is no statistically significant mean different nanoparticles size according to different surfactant concentrations (1%, 2% and 3%) in the NLC/PI at an **alpha** level 0.01, 0.05 and 0.1"

Table 3.17: One-way ANOVA results to investigate the above hypothesis.

	Concentration	Mean±SD	F TEST	
			F	P-VALUE
Nanoparticles size	1%	401±270	0.79	0.45
	2%	422±264		
	3%	478±315		

From Table 3.17, the results showed that there were no statistically significant differences in nanoparticles size mean for surfactant concentrations (1%,2%,3%) in the NLC/PI at an **alpha** level 0.01, 0.05 and 0.1.

For the polydispersity index (PDI), one-way ANOVA statistical analysis (Table 3.18) was used to answer the study hypothesis:

"There is no statistically significant mean different PDI according to different surfactant concentrations (1%, 2% and 3%) in the NLC/PI at an **alpha** level 0.01, 0.05 and 0.1"

Table 3.18: One-way ANOVA results to investigate the above hypothesis.

	Concentration	Mean±SD	F TEST	
			F	P-VALUE
PDI	1%	0.38±0.21	0.200	.810
	2%	0.38±0.21		
	3%	0.37±0.17		

From Table 3.18 the results showed that there were no statistically significant differences in PDI mean for surfactant concentrations (1%, 2% and 3%) in the NLC/PI at 0.01, 0.05 and 0.1. Furthermore, the above results show that there was an effect of time and speed of HSD in all three different surfactant concentrations (1%, 2% and 3%). As the HSD time increased up to 30 minutes, the nanoparticle size decreased and PDI improved. Later, the statistical analysis will use to study the effect of speed and time on particles size and PDI in all samples (see section 3.4.3).

The results showed that the increased HSD time from 10,000 to 15,000 rpm decreased the nanoparticle size and improved PDI after 10, 20 and 30 minutes. The particle size decreased from over 900 nm to less than 200 nm. The smallest NLC/PI particle size (mean 155 nm \pm 2) was obtained after 30 minutes homogenization of the 1 % concentration of surfactant at 15,000 rpm. When compared to the desired NLC characterizations (in Section 1.6.3), the size achieved was adequate, and the suspension was homogeneous (PDI 0.1 \pm 0.05). As the HSD time increased to 40 minutes, the mean particle size of NLC/PI also increased suggesting that 30 minutes was the maximum HSD time for the manufacturing process.

It was possible using this type of NLC nanolipid particles to achieve the desirable carrier properties (size and homogeneity). The stability of NLC/PI in solution was measured and the results are shown in Section 4.5.

3.4 Factors influencing NLC properties during their preparation

The previous results achieved in Section 3.3 were further analysed to evaluate the effect of each different parameter used during the NLC synthesis. The results demonstrated the influence of the type of solid lipid, the surfactant concentration, HSD time and speed on the particle size and PDI of the resultant NLC.

3.4.1 Solid lipid type

From the previous results obtained for NLC/SI, NLC/GM and NLC/PI (Tables; 3.8, 3.12 and 3.16), the nanoparticle size and PDI for all samples were analysed (Figure 3.13).

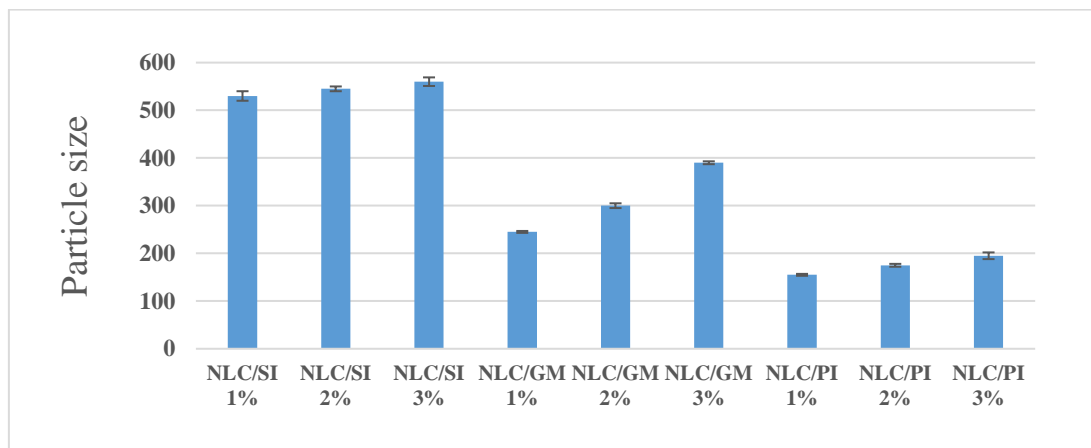


Figure 3.13: Particle size of NLC with different solid lipid and surfactant concentration (1%, 2%, 3%) after HSD (15,000 rpm, 30 min), Bars represent mean \pm SD (n = 5).

One-way ANOVA statistical analysis (Table 3.19) was used to investigate the effect of solid lipid type on nanoparticles size for all NLCs samples and to answer the study hypothesis:

"There were statistically significant differences in nanoparticle size between different lipid type using HSD method at 0.01, 0.05 and 0.1"

Table 3.19: One-way ANOVA results to investigate the above hypothesis.

	NCL	Mean \pm SD	F TEST	
			F	P-VALUE
Nanoparticles size	NLC/SI	728 \pm 276	39.086***	0
	NLC/GM	496 \pm 253		
	NLC/PI	434 \pm 283		

*** The F test is significant at an **alpha** level 0.01

From Table 3.19, it was noted that there were statistically significant differences in nanoparticles size mean for lipid type using HSD method, $p \leq 0.01$ between NLC/PI and NLC/SI and $p \leq 0.1$ between NLC/PI and NLC/GM. To investigate which type of lipids there were differences, it was used Least Significant Difference (LSD) test and Table 3.20 show the results achieved.

Table 3.20: The results of LSD analysis for particle size according of different solid lipid of different NLC prepared by HSD , where * and * shows $P \leq 0.1$ and $P \leq 0.01$ respectively.**

	NCL	SI	GM	PI
Difference in	SI	0	231***	294***
the mean	GM		0	62*
nanoparticle	PI			0
size (nm)				

* The mean difference is significant at an **alpha** level 0.1

*** The mean difference is significant at an **alpha** level 0.01

From Table 3.20, the results show that the mean difference was statistically significant difference for nanoparticles size and for all types of lipid favouring NLC/PI.

For study of the effect of solid lipid type on the polydispersity index (PDI) for all NLCs samples a One-way ANOVA test (Table 3.21) was used to analysis the hypostasis:

"There were statistically significant differences in PDI between different lipid type using HSD method at 0.01, 0.05 and 0.1"

Table 3.21: One-way ANOVA results to investigate the above hypothesis.

	NCL	Mean±SD	F TEST	
			F	P-VALUE
PDI	SI	0.6±0.13		
	GM	0.5±0.09	94.800***	0
	PI	0.3±0.20		

*** The F test is significant at an **alpha** level 0.01

Table 3.21, show that there were statistically significant differences in PDI for the different types of lipid using HSD method at $p \leq 0.01$.

Fishers Least Significant Difference (LSD) test was used to investigate which type of lipids were most favourable (Table 3.22).

Table 3.22: The results of LSD analysis for PDI according of different solid lipid of different NLC prepared by HSD, where * shows $P \leq 0.01$.**

	NCL	SI	GM	PI
Difference in the mean PDI	SI	0	0.6***	0.25***
	GM		0	0.19***
	PI			0

The data in the above table show that the mean difference was statistically significant difference for PDI and for all types of lipid favouring NLC/PI.

3.4.2 The concentration of the surfactant

For each NLC solution, the smallest particle size was obtained using the lowest surfactant concentration (Figure 3.13). For each NLCs (NLC/SI, NLC/GM and NLC/PI), the statistical analysis shows no statistically significant differences in nanoparticle size and PDI when surfactant concentration increased from 1% to 2% and 3% (see Tables 3.9, 3.10, 3.13, 3.14, 3.17 and 3.18). In addition, out of the three formulations, the NLC/PI with 1% surfactant produced the smallest mean nanoparticle size with HSD conditions of 15,000 rpm at 30 minutes.

3.4.3 Time and speed optimization of HSD

For study of the effect of high shear dispersion time (10, 20, 30 and 40 minutes) on the particles size of NLC for all samples preparations, a One-way ANOVA test (Table 3.23) was used to analysis the hypothesis:

"There were statistically significant differences in particles size between different time (10, 20, 30 and 40 minutes) of HSD at an **alpha** level 0.01, 0.05 and 0.1"

Table 3.23: One-way ANOVA results to investigate the above hypothesis.

	Time	Mean±SD	F TEST	
			F	P-VALUE
Nanoparticles size	10	898±104	550***	0
	20	351±90		
	30	207±40		
	40	279±33		

*** The F test is significant at an **alpha** level 0.01

The results on the above table showed that there were statistically significant differences within the mean nanoparticle size distribution for HSD time (10, 20, 30, 40 mint) and $p \leq 0.01$.

A Fishers LSD test was used to investigate which times were favourable (Table 3.24).

Table 3.24: The results of LSD analysis for nanoparticle size according of different time of different NLC prepared by HSD, where * showed $P \leq 0.01$.**

	Time	10	20	30	40
Difference in the mean nanoparticle Size (nm)	10	0	547***	691***	619***
	20		0	144***	71***
	30			0	72***
	40				0

The results from Table 3.24, showed there were statistically significant differences in nanoparticle size with the optimal conditions identified as being 30 minutes.

For study of the effect of HSD time (10, 20, 30 and 40 minutes) on the PDI of NLC for all samples preparations, a One-way ANOVA test (Table 3.25) was used to analysis the hypostasis:

"There were statistically significant differences in PDI between different time (10, 20, 30 and 40 minutes) of HSD at an **alpha** level 0.01, 0.05 and 0.1"

Table 3.25: One-way ANOVA results to investigate the above hypothesis.

	Time	Mean±SD	F TEST	
			F	P-VALUE
PDI	10	0.7+0.08	310***	0
	20	0.3±0.09		
	30	0.2±0.05		
	40	0.3±0.00		

*** The F test is significant at an **alpha** level 0.01

The results on the above table showed that there were statistically significant differences within the mean PDI for HSD time (10, 20, 30 and 40 mint) and $p \leq 0.01$.

A Fishers LSD test showed that there were statistically significant differences in PDI (Table 3.26).

Table 3.26: The results of LSD analysis for PDI according of different time of different NLC prepared by HSD, where * showed $P \leq 0.01$.**

	Time	10	20	30	40
Difference in the mean PDI	10	0	0.4***	0.5***	0.4***
	20		0	0.1***	0.01
	30			0	0.1***
	40				0

The results show, there were statistically significant differences in PDI with the optimal conditions identified as being 30 minutes.

After the study of the effect of HSD time (10, 20, 30 and 40 minute) on mean particles size distribution of NLCs and mean polydispersity index, the above statistical analysis results showed, there is statistically significant differences suggested 30 mint duration for HSD.

For study of the effect of HSD speed on nanoparticles size of NLCs, an independent Samples T-test was used to investigate the differences in nanoparticle size for all NLC types, different concentration of surfactant and time of HSD at 10,000 and 15,000 rpm (Table 3.27).

Table 3.27: Means and standard deviations for nanoparticles size according to speed variable and T-test results for independent samples test to investigate for any differences between means.

	Speed (rpm)	Mean±SD	T	p-value
Nanoparticles size	10,000	477±289	1.68*	0.096
	15,000	390±272		

* The t test is significant at an **alpha** level 0. 1

From Table 3.27, the results showed that there were statistically significant differences in nanoparticles size mean for speed of HSD (10,000 or 15,000 rpm) preferring speed 15,000 rpm ($P \leq 0.1$).

For study of the effect of HSD speed on PDI of NLCs, an independent Samples T-test was used (Table 3.28) to investigate the differences in PDI for all NLC types, different concentration of surfactant and time of HSD at 10,000 and 15,000 rpm.

Table 3.28: Means and standard deviations for PDI according to speed variable and T-test results for independent samples test to investigate for any differences between means.

	Speed	Mean±SD	T	p-value
Different PDI	10000	0.4±0.21	2.052**	0.042
	15000	0.3±0.1		

* The t test is significant at an **alpha** level 0. 05

Table 2.28, showed that there were statistically significant differences in PDI mean for speed of HSD (10,000, 15,000 rpm) preferring speed 15,000 rpm ($P \leq 0.05$).

3.5 Stability of NLC/SI, NLC/GM and NLC/PI

Testing the zeta potential of a particle measures the effective electric charge on the nanoparticle surface, which is related to nanoparticle stability or aggregation in suspension (see Section 2.4.4). The re-aggregation and precipitation of nano lipid particles were observed in solutions of NLC/SI and NLC/GM for all surfactant concentrations over one week (15,000 rpm, 30 min). This instability was not observed in the NLC/PI formulations for all surfactant concentrations (15,000 rpm, 30 min). The stability of the three NLC/PI formulations (1%, 2% and 3%) were assessed by zeta potential measurement one week after preparation. NLC/PI 1% solution was found to be more stable than other concentrations and was recorded as -43.4mV (Table 3.29).

Table 3.29: Particle size, PDI and zeta potential after one-week preparation of NLC/PI formula synthesized by HSD at 15,000 rpm and 30 min, mean ± SD (n = 5).

Surfactant concentration	Particle size (nm)	PDI	Zeta potential (mV)
NLC/PI 1%	156±8	0.1±0.06	-43.4±0.2
NLC/PI 2%	173±3	0.2±0.07	-35.1±0.4
NLC/PI 3%	191±2	0.2±0.01	-31.8±0.2

3.6 NLC/PI 1% preparation assessment

The particle size and PDI of NLC/PI 1% using HSD speeds of 10,000 and 15,000 rpm were studied at different HSD times. As the HSD speed increased (from 10,000 to 15,000 rpm) the particle size decreased, therefore it can be expected that when the time increases the particle size will decrease linearly above 30 minutes.

Unfortunately, as next plot demonstrates, the particle size started to increase at 40 minutes for both speeds (Figure 3.14).

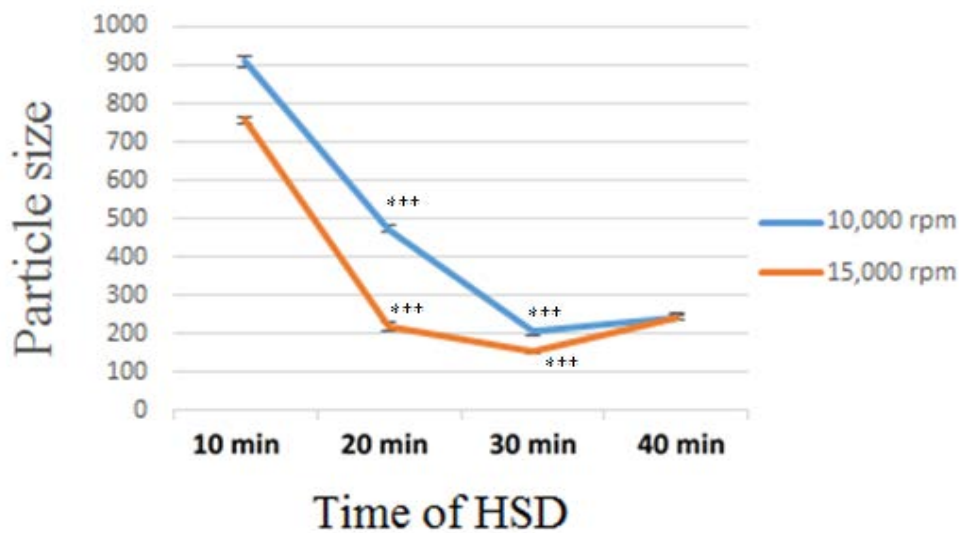


Figure 3.14: The effect of HSD speed through the time (up to 40 min) on particle size of NLC/PI 1%, showing mean \pm SD ($n = 5$), $P \leq 0.01$ when compared to time = 10 minutes.

When the PDI results were considered, the PDI was shown to decrease with increased HSD speed (from 10,000 to 15,000 rpm), up to 30 minutes duration. The particles were monodispersed in suspension. PDI also starts to increase at 40 minutes for both speeds (Figure 3.15)

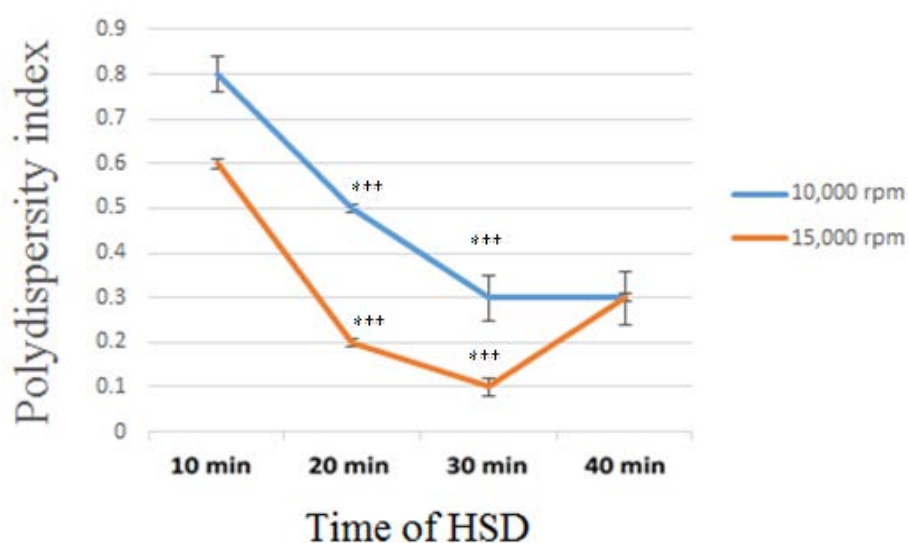


Figure 3.15: The effect of HSD speed through the time (up to 40 min) on PDI of NLC/PI 1%, showing mean \pm SD (n = 5), $P \leq 0.01$ when compared to time = 10 minutes.

The NLC/PI with 1% surfactant concentration formula prepared by HSD (15,000 rpm, 30 min) has the smallest mean particle size (155 nm) and PDI (0.1), therefore it was chosen as the optimal nanostructured lipid carrier to be used in this work. The NLC/PI particles with 1% concentration will therefore be further characterised in the next section.

3.7 Characterization of chemophysical properties of NLC/PI 1%

3.7.1 Particles size measurements by DLS

The optimal NLC/PI particles with 1% surfactant concentration prepared by HSD (15,000 rpm, 30 min) were characterised for particle size and PDI using DLS. The result showed that the mean particle size was 155 ± 2 nm and the polydispersity index was 0.1 (Figure 3.16).

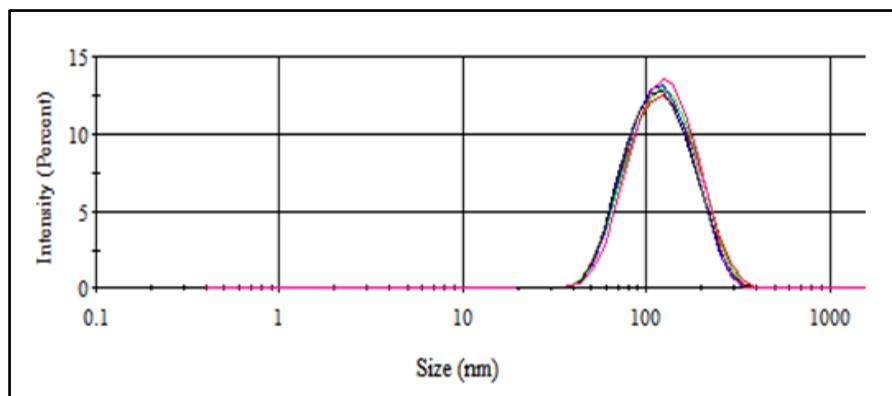


Figure 3.16: Size distribution of NLC/PI 1% as measured by DLS, the average size was 155 nm \pm 2 and PDI was 0.1 \pm 0.05. Each colour represent sample, mean \pm SD (n=5).

3.7.2 Nanoparticles tracking analysis (NTA)

Nanoparticle tracking analysis was performed to complement the result obtained from DLS for NLC/PI particles with 3% surfactant concentration prepared by HSD (15,000 rpm, 40 min) for comparison. The NTA trace shows that the size distribution of particles was 215 nm and this result is compatible with DLS measurement (Figure 3.17).

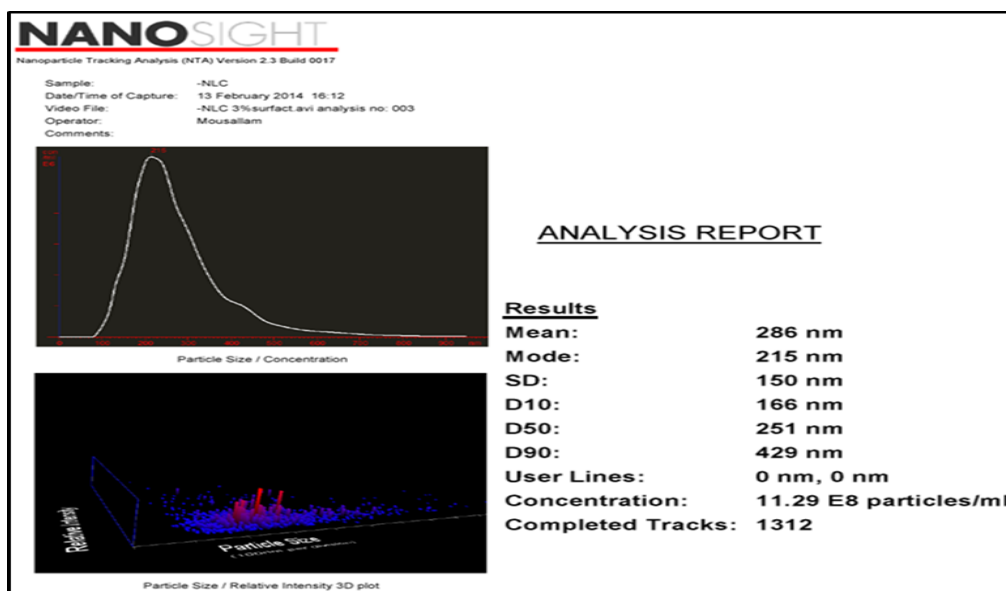


Figure 3.17: The relative intensity of NLC/PI 3% particle by nanoparticles tracking analysis, red light represent intensity for particles, highest value at 215 \pm 150 nm, (mean \pm SD n=1312).

3.7.3 The morphology study of NLC by TEM

The sample of NLC/PI particles with 1% concentration prepared by HSD (15,000 rpm, 30 min) was examined using TEM. The micrograph shows the structure of the particle of NLC/PI, and it indicated that the particle is spherical with a uniform structure for all of the particles observed in the samples (Figure 3.18).

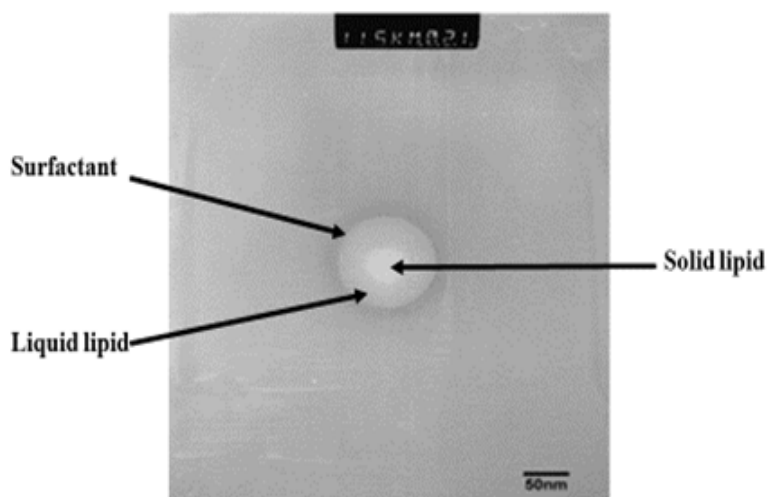


Figure 3.18: TEM micrograph showing the morphology of a NLC/PI particle with 1% concentration prepared by HSD (15,000 rpm, 30 min), (CM20, Philips).

The solid lipid is seen as a white cloud in the centre of particle and the liquid lipid matrix surrounding the core (solid lipid) is shown as grey on the micrograph. The surfactant forms an outer layer (seen as a dark shell) preventing dissolution in aqueous media.

3.7.4 NLC stability

The long-term stability of NLC/PI particles with 1% concentration prepared by HSD (15,000 rpm, 30 min) was tested after storage at 4°C in a sealed glass vial as described in Section 3.4.6. The particle size, PDI and zeta potential were measured using DLS and a Zetaseizer at different time points over a period of 180 days, with tests repeated 5 times (Table 3.30).

One-way ANOVA analysis used to investigate the differences of mean nanoparticle size, PDI and zeta potential mean at different times (1, 7, 30, 90 and 180 days) for NLC/PI 1%. The results show there were no statistically significant differences in mean nanoparticle size, PDI and zeta potential at the different times. The particles stay monodispersed in suspension with the mean particles size < 160 nm and the NLC/PI 1% sample stays stable over the time period (zeta potential above 40 mV).

Table 3.30: The effect of storage of NLC/PI with 1% surfactant at 4°C on average particle size, PDI and zeta potential over a period of 6 months, formula synthesized by HSD at 15,000 rpm and 30 min, mean \pm SD (n = 5).

Time (day)	Particle size (nm)	PDI	Zeta potential (mV)
1	155 \pm 2	0.1 \pm 0.05	-43.7 \pm 0.6
7	156 \pm 8	0.1 \pm 0.03	-40.4 \pm 0.9
30	155 \pm 3	0.1 \pm 0.02	-42.8 \pm 0.2
90	158 \pm 7	0.1 \pm 0.06	-41.9 \pm 0.9
180	156 \pm 7	0.1 \pm 0.05	-42.1 \pm 0.5

The work in these experiments showed that NLC nanoparticles with the appropriate properties were successfully achieved and therefore these will be used in future work.

3.8 NLC/PI 1% synthesis and optimization using MicroJet Reactor (MJR)

For industry-scale preparation of pharmaceuticals a method able to produce large quantities of formulations will be needed. Therefore, MicroJet reactor was investigated here for this purpose. MJR is a quick production technique capable of a high output. MJR was used to prepare NLC/PI with 1% surfactant formula (Table 3.31). Both lipid phase and hydrous phase (surfactant in distilled water) were pumped simultaneously into MJR reactor (see Section 2.3.2).

Table 3.31: The formula components of NLC/PI preparations by MicroJet Reactor.

NLC Formulation	Solid lipid	Liquid lipid	Emulsifier		Surfactant
	Precirol ATO-5 (mg)	isopropyl myristate (mg)	Soybean lecithin (mg)	D- α -tocopheryl polyethylene glycol succinate (mg)	Kolliphor® P 188 (g/ml)
NLC/PI	1800	600	300	300	1%

The flow rate and the temperature of the reactor were adjusted to improve the particle size and particle dispersity. Different batches were prepared and tested. After each preparation, the samples were measured by DLS and the particle size and PDI were recorded (Table 3.32).

Table 3.32: Particle size and PDI of NLC/PI 1% obtained after MJR preparation with varying flow rate and temperature, mean \pm SD (n = 5).

Flow rate (ml/sec)	Temp. °C	Particle size (nm)	PDI
50	65	291 \pm 4	0.1 \pm 0.9
50	70	174 \pm 2	0.1 \pm 0.3
50	75	219 \pm 11	0.1 \pm 0.9
75	65	192 \pm 3	0.2 \pm 0.7
75	70	150 \pm 3	0.2 \pm 0.1
75	75	208 \pm 7	0.2 \pm 0.6
100	65	284 \pm 1	0.4 \pm 0.2
100	70	238 \pm 10	0.2 \pm 0.1
100	75	309 \pm 5	0.3 \pm 0.2

The result showed that the smallest particle size of NLC/PI with 1% surfactant made using MJR was achieved at temperature of 70 °C and flow rate of 75 ml/sec (150 nm). While, the lowest PDI (0.1) was obtained using 50 ml/sec flow rates, at this flow rate the smallest particle size was 174 nm and obtained at 70 °C.

The effect of increasing the reactor temperature on particle size was plotted to show the temperature effect profile (Figure 3.19).

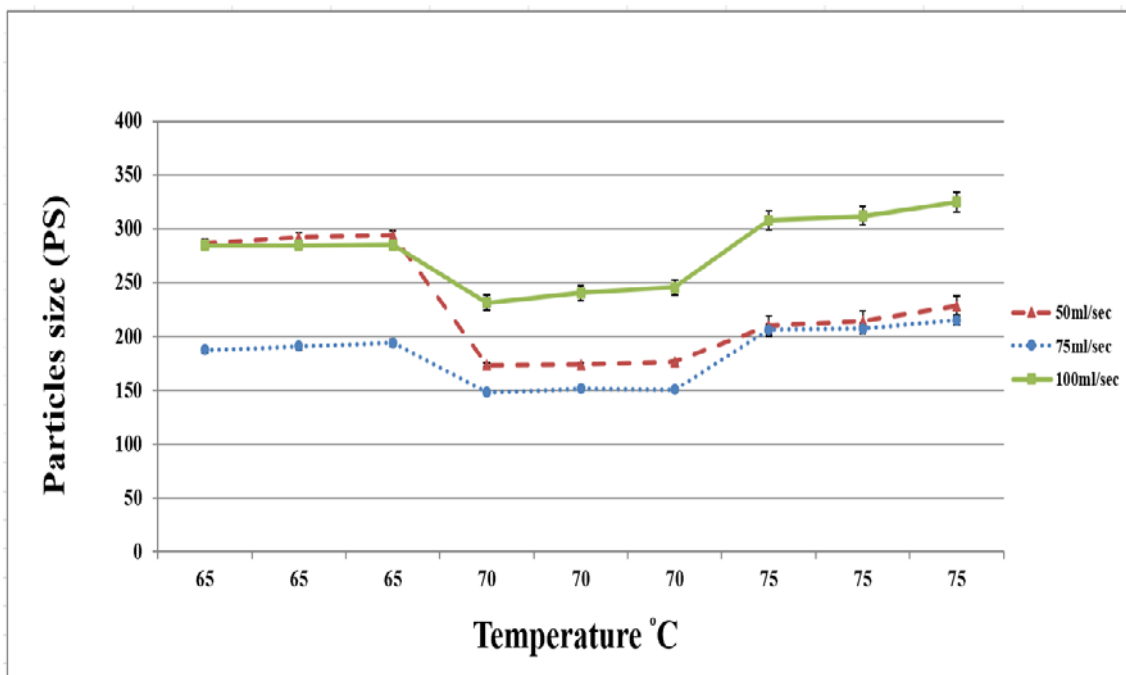


Figure 3.19: Particle size against flow rate and temperature as measured by DLS after MJR preparation, showing the ideal particle size at 75 ml/sec and 70 °C, Error bars mean \pm SD (n=5). Please note that the studies were replicated three times at the different temperature points.

The result showed that increasing the reactor temperature from 65 °C to 70 °C resulted in a decrease in particle size. Conversely, the particle size started to increase when the reactor was heated above 75 °C.

When PDI was measured for the same samples, the result showed that increasing reactor temperature from 65 °C to 70 °C resulted in a decrease in PDI. Conversely, PDI was increased when the reactor heated above 75 °C (Figure 3.20).

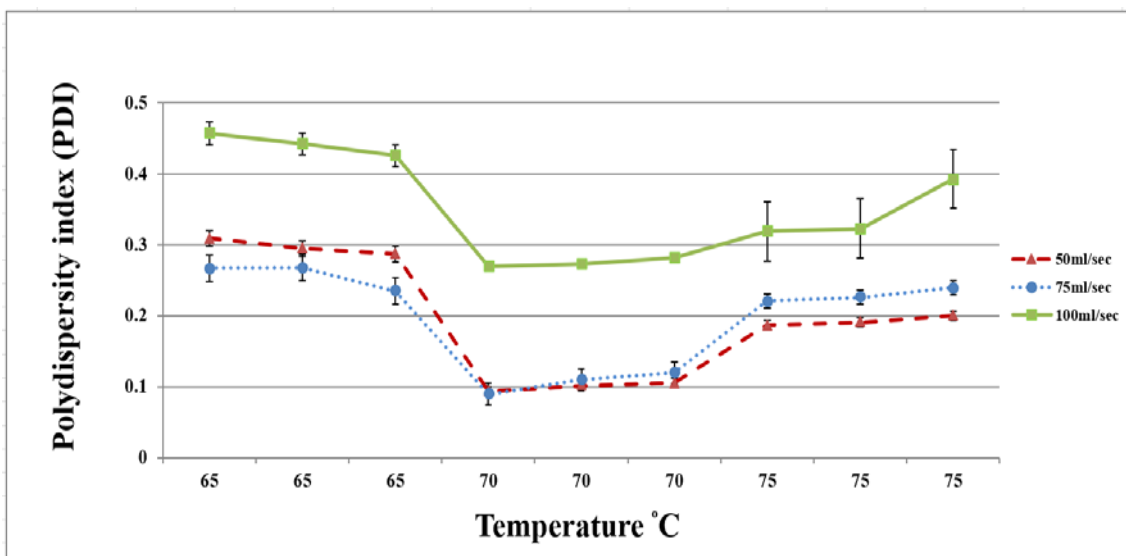


Figure 3.20: Polydispersity index against flow rate and temperature as measured by DLS after MJR preparation, showing the ideal PDI at 50 and 75 ml/sec flow rate with temperature at 70 °C, Error bars mean \pm SD (n=5), Please note that the studies were replicated three times at the different temperature points.

3.9 Discussion

For drug delivery systems, the smallest particle sizes are attractive for their potential to improve performance of pharmaceuticals (Cavalli et al., 1993). In addition, a uniform particle suspension (monodisperse) is required to avoid aggregation of particles and therefore the PDI should be as small as possible (Lyklema, 2005). In this study, there were different factors that affected NLC properties and could impact the function as a carrier in drug delivery system. These factors rely on formulae components, method of the preparation and the procedure.

3.9.1 NLC formulae

There are a large variety of NLC compositions and potential delivery system designs. This study considered the NLC preparations and components from previously published reports (Chen et al., 2012). Three different types of solid lipids (stearylamine, glyceryl behenate and precirol ATO-5) were used to prepare different nanostructured lipid carriers, namely NLC/SI, NLC/GM and NLC/PI, respectively. For each formula, the

different types of solid lipid were used and combined with suitable liquid lipids and surfactants (see Tables 4.2, 4.4 and 4.6 for details) and were investigated for particle size and PDI. The results showed that NLC/SI and NLC/GM have high re-aggregation rate during the homogenization which led to an increased particle size and polydispersity index. This is likely to be due to NLC/SI and NLC/GM not having enough long solid lipid chains in their structure. NLC/SI uses stearylamine as the solid lipid which is an eighteen-carbon long chain (see Section 1.6.2 and Figure 1.17), while NLC/GM has glyceryl behenate which is a twenty-five-carbon long chain (see Section 1.6.2 and Figure 1.16). Recently, a study has demonstrated that a long chain solid lipid tends to decrease the aggregation of particles (Nimtrakul et al., 2016). The current study found that the solid lipid precirrol ATO-5, which has thirty-seven-carbon long chain (see Section 1.6.2 and Figure 1.15), was more suitable to form the required NLC with the properties required for nanomedicines formulation. These results, confirmed the conclusion of Yang et al., (2014), that the oil type can affect the aggregation stability of nanostructured lipid carriers.

The surfactant acts to promote the formation of the NLC uniform structure and to increase their stability in a colloidal suspension (Taratula et al., 2013). Previous studies have demonstrated the effect of surfactant concentrations on NLC preparation and stability (Teeranachaidekul et al., 2007; Han et al., 2008). The results achieved in this work have confirmed those previous reports which suggested that lower concentrations of surfactant can produce stable NLCs (Table 3.29). Lower concentrations of surfactants are also desirable when considering the potential toxicity of the NLC preparation, and therefore the optimum NLC/PI preparation (1% surfactant, HSD conditions) has been selected for further study.

3.9.2 Critical steps of NLC synthesis at laboratory-based

In this study, NLC was prepared using a laboratory-based process using high sheer dispersion (HSD) after solidification of emulsion-evaporation method in oil/oil/water matrix. The most commonly used method for NLC synthesis involves oil-in-water emulsion, homogenization and solidification, which allow NLC to disperse in an aqueous phase and the inner oil phase to solidify (Puglia et al., 2008; Gonzalez-Mira et

al., 2010 and Lim et al., 2014). Generally, NLC are prepared by mixing the oil phase with liquid phase in the presence of organic solvent. This organic solvent may contribute to enhance the toxic effect of the final solution of NLC. The evaporation method used in this study has previously been identified as the appropriate technique to eliminate organic solvents in NLC suspensions (Naseri et al., 2015). This method can dissolve the lipophilic material in aqueous phase by using an organic solvent. Upon evaporation of the solvent, NLC dispersion is formed in an emulsion. In the next step, the organic solvent can be removed from the emulsion by evaporation using a stirrer – heating technique.

Cold temperature at 2°C was used to stabilize the NLC and to store the suspension for over 2 hours. Up to the solidification step, the study followed the previous method published by Chen et al., (2012), using the same formula as stated. When the resultant solution was examined using DLS, it was not possible to detect particles in the nano-size (i.e. all of the particle sizes recorded were over 1 µm). As a result, the method was adapted by adding the HSD method to encourage nanosize particles to form. This solution was also tested using DLS and showed the presence of smaller particles (less than 1 µm) within the optimal nano size range which validated the HSD method.

For this particular study, a modification was made compared to previously published methods as HSD was used after lipid solidification to achieve the required particle sizes for NLC drug delivery. The deposition parameters were then varied to achieve the optimum properties of NLC for drug delivery (defined in Section 4.3). It is known that the particle size of the NLC can be controlled by the speed and time of HSD (Hou et al., 2003). The large particle size obtained by HSD without prior solidification suggests that particles are formed during the solidification step (Müller et al., 2002). The revised method used in this study uses a process of solidification at low temperatures prior to HSD. Initial studies indicated that particles of a size of 400 nm were obtained using this method. It is suggested that HSD can disrupt the agglomerates of the particles, formed possibly due to hydrophobic interaction, and stabilizes the particles by thoroughly remixing them with surfactant thereby encouraging the formation of smaller particle sizes.

Increasing the speed and time of HSD up to 15000 rpm and 30 minutes, respectively, resulted in a lower mean particle size and PDI (up to 155 ± 2 particle size and 0.1 ± 0.05 PDI for NLC/PI) indicating that sufficient dispersion energy was achieved to disrupt the particle aggregates and distribute them throughout the suspension. Whilst it could be suggested that further increases of the HSD speed and time would result in a further reduction of particle size, the results (Figure 4.2) showed that if the HSD time was increased over 30 minutes, there was a resultant increase in the measured particle size. This may be due to an increase in re-aggregation of particles due to high inter-particle interaction force between small particles (Paunov et al., 1993). The particles made using NLC/PI with 1% surfactant were imaged using TEM and the micrographs showed spherical particles with a corona of surfactant (Figure 4.6).

3.9.3 Critical steps of NLC synthesis at industry-based

The NLC properties including particle size, PDI and the morphology were measured for each sample after laboratory-based preparation. The resultant properties were analysed to select the most appropriate NLC for use as a carrier. The appropriate formula of NLC (NLC/PI 1%) selected to re-synthesize using an industry-relevant technique, MJR (discussed in Section 2.3.2). In the MJR method, the effect of flow rate and temperature on particle size and polydispersity of NLC/PI was analysed. Previously it has been reported that NLC preparation should occur at temperatures above the melting point of the solid lipid (Kullavadee et al., 2012). The melting point for the lipid used in the NLC/PI formula (Precirol) is 60°C . The results reported in this chapter showed that an increase in the preparation temperature from 65°C to 70°C led to decrease in mean particle size (from 192 ± 3 to 150 ± 3 nm) at flow rate 75 (ml/sec). The particle size increased when the preparation temperature increased to 75°C . The smallest particle size for NLC/PI 1% MJR preparation was obtained at 70°C and using a flow rate of 75 ml/sec (Figure 4.8). Recent studies have demonstrated the effect of flow rate on particle preparation. In 2015, Türeli et al. showed that the high-energy dissipation from the flow rate promotes the formation of nanoparticles. Moreover, it was evident that PDI can be affected by the flow rate and this result confirmed those previously reported (Türeli et al., 2015).

3.9.4 Comparison between HSD and MJR

The laboratory-based NLC manufacture, whilst labour intensive, allows for method development without significant waste of materials. Industry-based manufacturing techniques such as MJR allows for commercial quantities of NLC to be produced at a much quicker rate and are such less labour intensive, however there is a greater loss of materials if the manufacturing process fails. The HSD method and associated experiments shown above allowed for the optimisation of the lipid formulae prior to the MJR manufacture to reduce materials wastage.

There are some differences between HDS and MJR methods in preparation and the resultant NLC/PI with 1% surfactant particle properties (Table 3.33).

Table 3.33: The differences between HSD (15,000 rpm and 30 min) and MJR method (70 °C and flow rate 75 ml/sec) during the preparation of in NLC/PI 1%.

Method	Materials	Time	Reproducibility	Particle size	PDI
HSD	Small (in Milligram)	Long (in Hours)	reproducible	155±2	0.1±0.05
MJR	Large (in Gram)	Short (in Minutes)	reproducible	150±3	0.2±0.1

For laboratory-based preparations, a small amount of material (mgs) was used but the process needed a relatively long time (up to 8 hours) to produce a small amount of NLC/PI suspension (12.5 ml). Whilst the MJR process has much shorter (5 minutes), it needed a large amount of material (grams) to synthesize a large amount of NLC/PI suspension (1000 ml). However, the NLC/PI 1% formula was successfully treated to produce the desired particle sizes and PDIs using both HSD and MJR.

3.10 Summary

The above results have identified that the smallest particle size and greatest homogeneity are achieved using NLC/PI with 1% surfactant using HSD parameters of 15,000 rpm for 30 minutes. This result has been published in article journal ("Development of nanostructured lipid carrier for dacarbazine delivery", see Appendix B). The laboratory-based technique was used to identify the formula that had the optimal particle size and homogeneity, which was selected for a large-scale preparation using an industry-based technique. This large-scale preparation used MJR method which was the first preparation of NLC by this technique.

In addition, this NLC/PI 1% formulation was selected to be used as a drug delivery system for Dacarbazine (Dac), a drug used to treat melanoma.

CHAPTER FOUR

**SYNTHESIS AND CHARACTERISATION OF
NANOSTRUCTURED LIPID CARRIERS-DACARBAZINE**

4. SYNTHESIS AND CHARACTERISATION OF NANOSTRUCTURED LIPID CARRIERS-DACARBAZINE

4.1 Introduction

Dacarbazine (Dac) is a cytotoxic drug used in the treatment of various cancers, including melanoma. This chapter considers the encapsulation of Dac in a nanostructured lipid carrier (NLC) to test whether there is an increased efficacy of NLC-Dac in abnormal cells. The previous chapter (Chapter 3) showed the achievement of the study to synthesize NLC and optimize the properties in laboratory-based preparation. The optimal formula obtained NLC/PI with 1% surfactant was selected and prepared as a delivery system for Dac. This chapter shows, the method of NLC-DAC preparation then the characteristics of NLC with and without DAC. The physicochemical studies involve the use of NLC/PI 1% as an encapsulation media for Dac, describes the properties of NLC/PI 1%-Dac for three different Dac concentrations and investigates the encapsulation efficiency and drug loading capacity.

Later, this chapter shows the pharmacological studies of NLC with and without DAC that involves, the toxic effects of the varying concentrations of the different types of NLC (e.g. NLC/PI, NLC/SI and NLC/GM) on A375 cells at three-time points (24, 48 and 72 hours). The cytotoxicity of Dac on A375 cells, pre and post encapsulation, is also presented. The cell viability was assessed using both light microscopy and MTT assay after treating A375 cells with Dac, NLC/PI 1% and NLC/PI 1%-Dac at different concentrations and at different time intervals (24, 48 and 72 hours).

4.2 Preparation and physicochemical characteristic of NLC/PI 1%-Dac

The synthesis of NLC/PI 1% by HSD method was followed, and the particles were used to encapsulate Dac, NLC/PI 1%-Dac (see Section 2.3.1). This method was validated and published under the title: Development of nanostructured lipid carrier for dacarbazine delivery (Almousallam et al., 2015). Three samples with different formulations of NLC/PI 1%-Dac were prepared containing different concentrations of Dac to study the encapsulation efficiency and the drug loading capacity in order to evaluate NLC drug delivery system (Table 4.1).

Table 4.1: The formula components of NLC/PI 1%-Dac preparations formed using high shear dispersion at 15,000 rpm for 30 min.

NLC/PI 1%-Dac Formulation	Solid lipid	Liquid lipid	Emulsifier		Surfactant	Drug
	Precirol ATO-5 (mg)	isopropyl myristate (mg)	Soybean lecithin (mg)	D- α -tocopheryl polyethylene glycol succinate (mg)	Kolliphor® P 188 (g/ml)	Dac (mg)
NLC/PI 1%-Dac 35	180	60	30	30	1%	35
NLC/PI 1%-Dac 50	180	60	30	30	1%	50
NLC/PI 1%-Dac 70	180	60	30	30	1%	70

Each NLC/PI 1%-Dac preparation was assessed for particle size, dispersity and stability after 24 hours of preparation (Table 4.2).

Table 4.2: Particle size, PDI and zeta potential for NLC/PI 1%-Dac formula synthesized by high shear dispersion at 15,000 rpm and 30 min, mean \pm SD (n = 5).

Formulation of NLC/PI 1%-Dac (mg)	Particle size (nm)	PDI	Zeta potential (mV)
NLC/PI 1%-Dac 35	181 \pm 9	0.2 \pm 0.07	-38.9 \pm 0.8
NLC/PI 1%-Dac 50	190 \pm 10	0.2 \pm 0.03	-43.5 \pm 1.2
NLC/PI 1%-Dac 70	185 \pm 3	0.2 \pm 0.09	-35.8 \pm 0.4

The results show that the carriers were maintained after Dac encapsulation and the relative particle size was between 181 nm to 190 nm measured using dynamic light scattering DLS at 100 μ g/ml particles concentration. The increasing of NLC particles size after Dac encapsulations from 155 nm (see section 4.5) to larger than 180 nm,

indicated the drug of Dac resize the NLC carriers. The poly dispersity index indicated the aggregation in the particles, as the value is more it shows a polydisperse system and if it is closer to zero it denotes the monodisperse system. The polydisperse system have greater tendency to aggregation than monodisperse system. In this study, the measurements of the polydispersity index showed that the particles distribution in solutions were monodisperse in all three resultants of NLC/PI 1%-DAC using DLS. The information about the particle stability in solution was obtained by Zeta Potential (ZP) analysis of particles at 100 µg/ml. The result showed that all particles exhibited a negative charge zeta potential (Table 4.2), and the particles in solution were moderately stable (Zeta potential > -35 mV).

The encapsulation efficiency and drug loading capacity of the three resultants NLC/PI 1%-Dac was measured. Initially, a calibration curve was produced by absorbance of known concentrations of Dac at 330 nm wavelength using UV spectrophotometry (Double Beam UV–VIS, UV-2100 Shimadzu, Japan; Figure 4.1). This standard curve was used to determine the amount of free Dac within a solution.

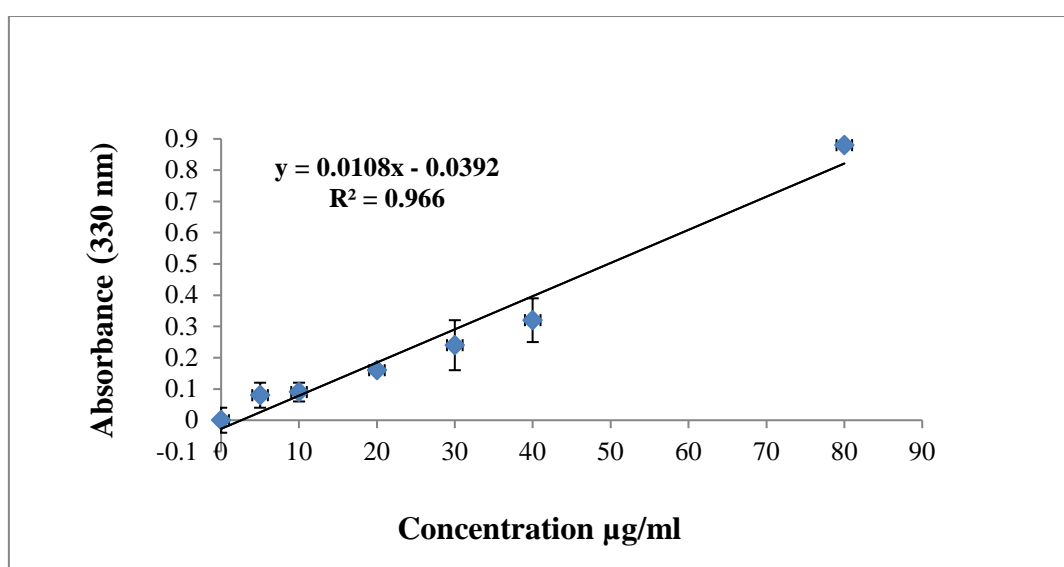


Figure 4.1: A standard curve for mean absorbance of Dac concentrations in acetone solution measured by UV spectrometry at wavelengths 330 nm, Bars represent mean \pm SD (n = 3).

The encapsulated samples were tested after 24 hours incubation at 4 °C. Briefly, 1 ml samples were withdrawn from each NLC/PI-Dac preparation, centrifuged at 12,500 rpm at 4°C for 45 minutes to obtain a supernatant (un-entrapped Dac). After the centrifugation, 500 µl of supernatant was added to 1 ml acetone and measured using UV spectrometry. The result showed a different level of absorbance for Dac for each of the NLC/PI-Dac formula at 330 nm measured using UV spectrometry. The UV absorbance of the drug was then compared to the standard curve (Figure 4.1) and the equation from the standard curve was used to determine the amount of un-entrapped Dac (Table 4.3).

Table 4.3: The absorbance and equivalent amount of un-entrapped Dac in NLC/PI 1%-Dac formula with different concentration of Dac prepared by high sheer dispersion at 15,000 rpm and 30 min, mean ± SD (n = 3).

Formulation of NLC/PI 1%-Dac (mg)	UV absorbance at 330 (nm)	Equivalent amount of Dac (mg)	Total amount of un-entrapped Dac (mg)
NLC/PI 1%-Dac 35	0.27±0.2	0.03±0.2	1.5±0.2
NLC/PI 1%-Dac 50	0.12±0.5	0.15±0.5	0.75±0.5
NLC/PI 1%-Dac 70	0.36±0.7	0.04±0.7	2.0±0.7

The percentage of encapsulation efficiency (EE) and drug loading capacity (DLC) were calculated. The encapsulation efficiency is the ratio of encapsulated drug to the total amount (see Equation 1), while the drug loading capacity is the ratio of encapsulated drug to the total amount of carrier system (see Equation 2).

$$EE \% = \left(\frac{W_1 - W_2}{W_1} \right) 100 \dots\dots\dots \text{Equation (1)}$$

$$DLC \% = \left(\frac{W_1 - W_2}{W_3} \right) 100 \dots\dots\dots \text{Equation (2)}$$

Where W_1 is the amount of drug added in the NLC/PI 1% formula, W_2 amount of un-entrapped drug and W_3 amount of the lipids added in NLC/PI formula.

The results obtained from un-entrapped Dac (Table 4.3) were used to calculate the percentage of encapsulation efficiency and the percentage of drug loading capacity (W_2 in equations = un-entrapped Dac). The result showed that the percentage of encapsulation efficiency and the percentage of drug loading capacity were increased when the amount of Dac in the NLC/PI 1%-Dac formula was increased from 35 mg to 50 mg (Table 4.4).

Table 4.4: The results obtained from the calculation for the percentage of encapsulation efficiency and the percentage of drug loading capacity obtained from the equation 1 and 2 for NLC/PI 1%-Dac formula with different concentration of Dac, mean \pm SD (n = 3).

Formulation of NLC/PI 1%-Dac (mg)	Encapsulation efficiency (%)	Drug loading capacity (%)
NLC/PI 1%-Dac 35	95.7 \pm 0.4	15.9 \pm 0.4
NLC/PI 1%-Dac 50	98.5 \pm 0.2	23.4 \pm 0.2
NLC/PI 1%-Dac 70	97.1 \pm 0.8	32.3 \pm 0.8

When the amount of Dac in NLC/PI 1%-Dac was increased from 50 mg to 70 mg, the drug loading increased but the encapsulation efficiency decreased. This decrease in encapsulation efficiency suggests that the carrier NLC/PI 1% has achieved saturation level. The highest percentage of encapsulation efficiency (98.5%) was obtained from NLC/PI 1%-Dac 50 with 23.4% drug loading capacity and this formula was selected for further study (see next sections).

4.3 NLC/PI 1% carrier pre and post Dac (50 mg) encapsulated

Changes to the structure of the NLC/PI 1 % carrier post drug encapsulation were investigated and the variation between NLC/PI 1% and NLC/PI 1%-Dac 50 mg was determined. The next sections will show these comparisons.

4.3.1 Particle size, dispersity and zeta potential

The NLC/PI 1% carrier (without drug) and NLC/PI 1%-Dac (carrier with drug) were characterized for particle size and PDI using DLS at 100 µg/ml. The results showed that the NLC/PI 1% carrier increases in diameter after Dac is encapsulated (measured increase from 155 nm to 190 nm). Also, DLS showed good homogeneity of NLC/PI 1% and NLC/PI 1% -Dac with $PDI \leq 0.2$ (Figure 4.2).

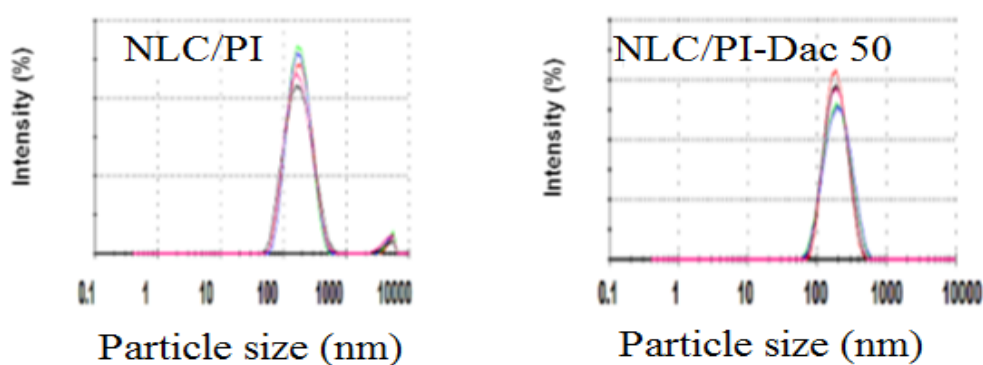


Figure 4.2: DLS recorded size distribution and the polydispersity index (PDI), 155 nm ± 10 with PDI 0.1 ± 0.05 and 190 nm ± 10 with PDI 0.2 ± 0.03 for NLC/PI 1% (left) and NLC/PI 1%-Dac 50 (right) respectively, each color represent sample, mean \pm SD (n=5).

The stability of particles in of NLC/PI 1% and NLC/PI 1% -Dac 50 solutions after 24 hours were also assessed by determining the zeta potential at 100 µg/ml using a Zetasizer (Figure 4.3).

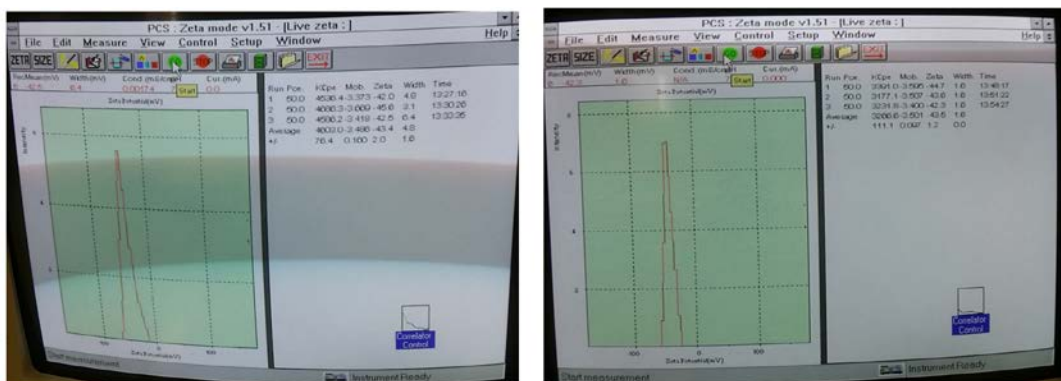


Figure 4.3: The analysis obtained from Zetasizer (Malvern Instrument 3000 Has Zetasizer), the results for zeta potential of NLC/PI 1% (left) and NLC/PI 1%-Dac 50 mg were (right) -43.4 ± 2.0 and -43.5 ± 1.2 respectively.

The results showed the particles in NLC/PI 1% and NLC/PI 1% -Dac (50 mg) were stable in solutions and they have a zeta potential > -40 mV and Table 4.5, shows the summary of the properties of the evaluation for both preparation.

Table 4.5: Physical properties of particle size, PDI and zeta potential for NLC/PI and NLC/PI-Dac 24 hours post preparation by high shear dispersion at 15,000 rpm and 30 minutes, each value represents the mean \pm SD (n = 5).

Samples	Particle size (nm)	PDI	Zeta potential (mV)
NLC/PI 1%	155 \pm 10	0.1 \pm 0.05	-43.4 \pm 2.0
NLC/PI 1%-Dac 50mg	190 \pm 10	0.2 \pm 0.01	-43.5 \pm 1.2

4.3.2 Morphology

The structure of NLC/PI 1% particles was investigated before and after the drug (Dac) encapsulation using TEM (Figure 4.4).

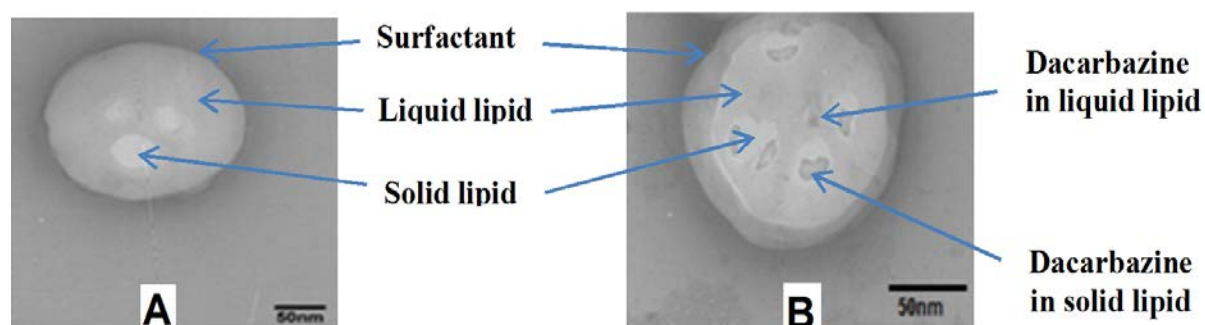


Figure 4.4: TEM micrographs of NLC/PI 1% (a) and NLC/PI 1% -Dac 50 (b), The arrows indicate the encompass materials of carrier; surfactant Kolliphor® P 188, solid lipid Precirol ATO-5®, liquid lipid isopropyl myristate and the drug encapsulated Dacarbazine (Dac).

Both NLC/PI 1% and NLC/PI 1% -Dac particles were spherical in shape and slightly different in size as observed. The particle diameters measured using TEM (NLC/PI 139 nm and NLC/PI-Dac 167 nm) were consistent with the results obtained by DLS measurement. The NLC/PI 1% particles appeared to have a distinct boundary between each particle and NLC/PI-Dac was larger than the carrier on its own. Both the NLC/PI 1% and the NLC/PI 1% -Dac (50 mg) particle appeared to be covered by a dark layer, indicative of the presence of some surfactant and remains of media (Figure 4.4). Under the dark surfactant layer inside the particles, the liquid lipid matrix is shown as a grey area containing several solid lipid core structures seen as white masses. Inside the core structures within the NLC/PI 1% -Dac particles a dark area can be seen which suggests that this is where the drug is encapsulated (Figure 4.4 B). Dark areas were also seen outside of the core structures within the particles, suggesting that there is a wide distribution of the drug inside the lipid matrix.

4.3.3 Crystallinity

X-ray diffraction (XRD) analysis was performed to characterize the crystallinity of Dac, NLC/PI 1% and NLC/PI 1% -Dac (50 mg). The crystal structure and quality of a sample can be determined by comparing its XRD pattern with that of reference crystalline substances in a database (see Section 2.4.8). The traces show the XRD patterns for (a) Dac, (b) NLC/PI 1% and (c) NLC/PI 1% -Dac (Figure 4.5).

From Figure 4.5, the diffraction peaks at 2 theta values of 17.1, 19.3 and 23.2° in NLC/PI-Dac are found in patterns of NLC/PI (see Figure 2.6 for NLC diffractogram). The Dac sample (a) shows two broad peaks (38.4 and 44.7°) which can be correlated with NLC/PI-Dac (38.5 and 44.7°). The patterns of the samples (a, c) show the alteration in pure Dac post NLC encapsulation suggesting that there is a change in the structure. The relative intensity of the diffraction peaks at 2 theta value of 38.5° appear to decrease in the NLC/PI 1%-Dac (50 mg) sample compared with pure Dac, suggesting that Dac loading prevents the formation of solid lipid crystals to certain extent and this will lead to reduce of the crystallinity.

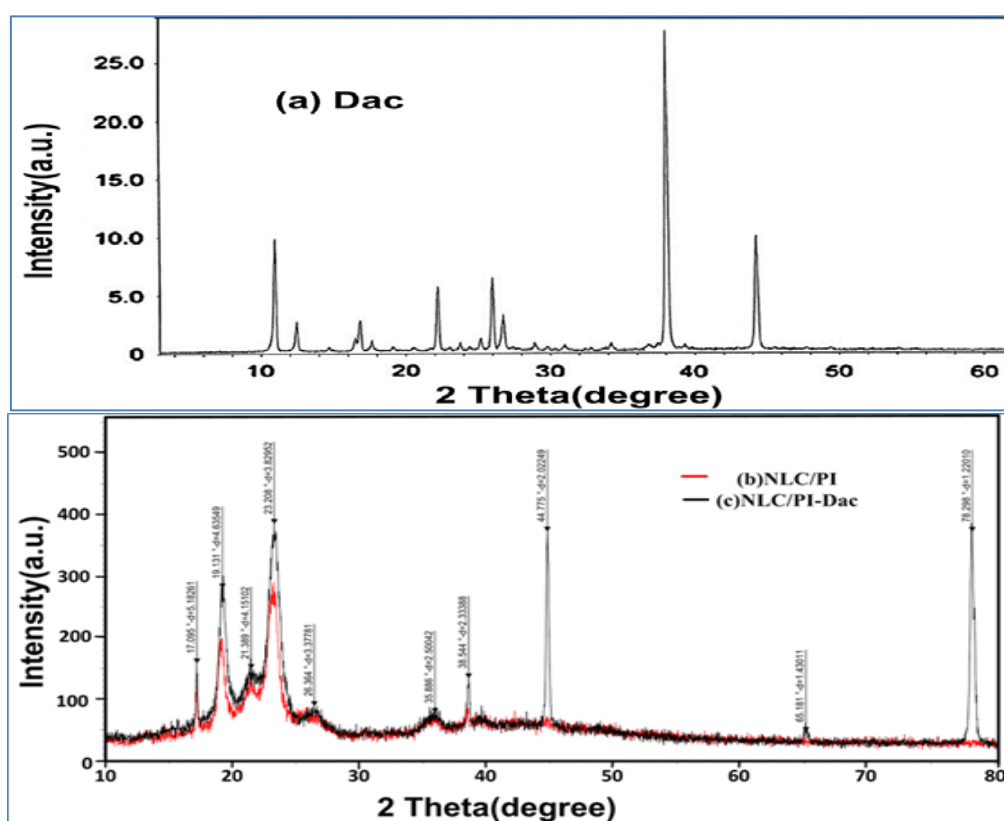


Figure 4.5: XRD trace of (a) Dac (Freeman and Hutchinson, 1979), (b) NLC/PI 1% and (c) NLC/PI 1%-Dac. (a) Dac exhibits a characteristic peaks at 2 Theta values of 11.3, 22.2, 26.1, 38.4 and 44.7° while NLC/PI 1% exhibits characteristic peaks at 2 Theta values of 17.1, 19.3, 23.2, 38.5, 44.7 and 78.29°.

From the XRD data the average crystallite size is calculated using the Scherrer Formula:

$$D = \frac{0.9\lambda}{d \cos \theta}$$

where D is the average crystallite size (diameter), $\lambda = 0.15406$ nm, d is the full-width at half maximum (FWHM, rad), and θ is the Bragg angle ($^{\circ}$). Using the equation, and considering the peak at 2 theta value of the estimated crystallite sizes of (b) NLC/PI 1% and (c) NLC/PI 1% -Dac (50 mg) are about 22.3 ± 0.5 , 44.87 ± 1.1 nm, respectively.

The Dac peaks are not visible in the NLC/PI 1%-Dac trace and this is likely to be due to the low amount of Dac compared to the NLC/PI 1% (15 %). The long-range structure (at the lower degree levels) shows a shift between the NLC/PI 1% and NLC/PI 1%-Dac traces. This is likely to be due to inter-chain changes (e.g. the spaces between the lipid chains). The short-range structure (at the higher degree levels – where $d < 2\text{\AA}$) are completely removed when Dac is added to the system. This suggests that there is significant intra-chain (e.g. within the lipid crystal) changes as a result of Dac being added to the system. These peaks are high intensity and therefore, there would have been significant changes in the structure to result in their removal.

4.4 Drug release profile of NLC/PI 1%-Dac 50

In the formula NLC/PI 1%-Dac 50, the release of the drug Dac *in vitro* was tested by measuring the amount of un-entrapped Dac that was discharged from the particles NLC/PI. The NLC/PI 1%-Dac 50 preparation was diluted to 10% v/v in PBS (pH = 7.4) and incubated at 37 $^{\circ}$ C in multiple vials. At predetermined intervals, individual samples were centrifuged at 12,500 rpm, 4 $^{\circ}$ C for 45 minutes (see Section 2.5.3.). The un-entrapped Dac concentration calculated from the measured absorption at 330 nm wavelength measured by UV spectrometry and calculated from the equivalent known concentration values (see Section 4.3). The release of Dac was determined and expressed as percentage of total loaded amount of the drug. The results showed that approximately 50 % of the drug was released from the particles in the first 2 hours, followed by a sustainable release of the remaining drug for up to 30 hours (Figure

4.6). The release of the drug Dac from the particles NLC/PI 1% appeared to follow a biphasic pattern.

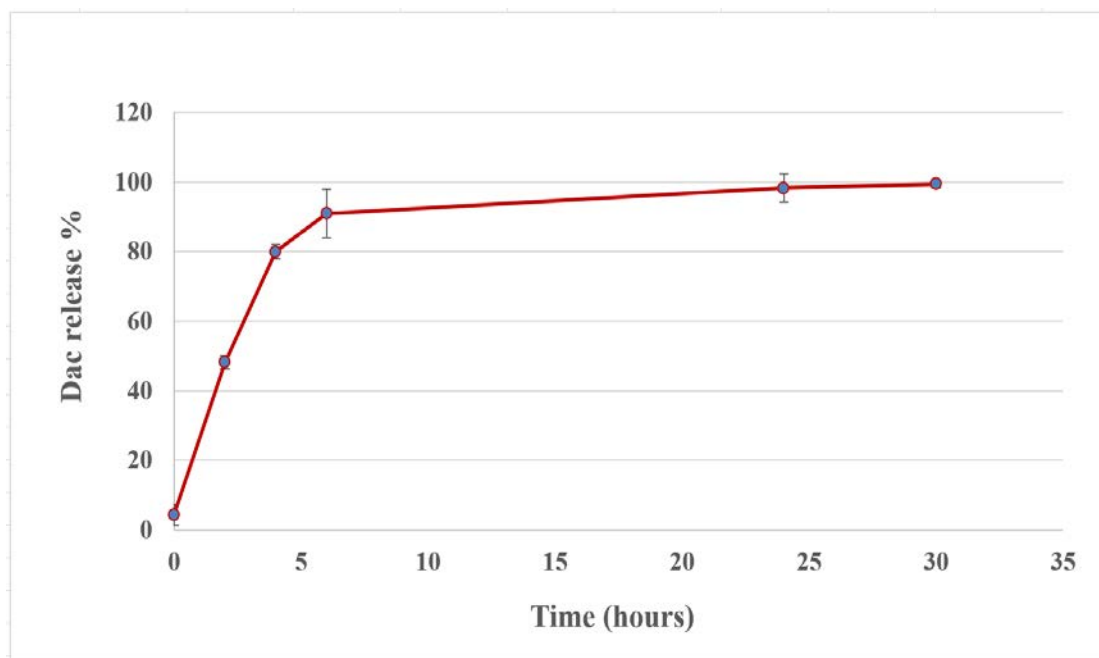


Figure 4.6: In vitro drug release profile for the drug Dac from particles NLC/PI 1% for formula NLC/PI 1%-Dac. Bars represent mean \pm SD (n = 3).

4.5 Stability of NLC/PI 1%-Dac 50

The NLC/PI-Dac 50 preparation achieved an encapsulation efficiency of 98.5 % of the drug as determined using the UV detection and encapsulation efficiency measurements (see Section 4.3). Samples were prepared and stored in sealed amber coloured glass vials in the dark at 4 °C for up to three months for stability assessment. The particles were then characterised for particle size, aggregation and zeta potential (Table 4.6).

Table 4.6: Physical properties of particle size, polydispersity index (PI) and zeta potential for NLC/PI-Dac 50 post preparation by high sheer dispersion at 15,000 rpm and 30 min, each value represents the mean \pm SD (n = 5).

Time (day)	Particle size (nm)	PDI	Zeta potential (mV)
1	190 \pm 4	0.1 \pm 0.07	-40.7 \pm 0.3
7	189 \pm 9	0.2 \pm 0.05	-43.7 \pm 0.5
30	197 \pm 5	0.2 \pm 0.02	-39.7 \pm 0.8
90	204 \pm 3	0.2 \pm 0.09	-36.1 \pm 0.2

The results show that the physical properties of the NLC/PI-Dac, namely the particle size, PDI and the zeta potential, were stable for up to 3 months (not statistically significantly different at $p \leq 0.05$ using T-test). The results in Table 4.6, show little change in the physical properties of the particles over the time of storage.

4.6 *In vitro* cytotoxicity assessment of NLCs and NLC/PI-Dac

An effective nanostructured lipid carrier (NLC) loaded with a chemotherapeutic agent should be able to demonstrate a cytotoxic effect *in vitro* that is more cytopathic than the unloaded drug (see Section 1.9). After having determined the optimal conditions for preparation of the lipid carrier with the desired characteristics (shown in Chapter 3), experiments were carried out using A375 cell lines in culture media in order to assess:

- i) The cytotoxicity of NLC: Demonstrating the effect of NLC (NLC/PI 1%, NLC/GM 1%, and NLC/SI 1%) on A375 cells; and
- ii) The cytotoxic effect of Dacarbazine (Dac) both pre- and post-encapsulation.

4.6.1 Growth rate and doubling time of A375 cells

A cytotoxic effect is best demonstrated in rapidly dividing cells. The concentration of the cell population is essential to interpret the growth kinetics. Initially it was required for the purposes of the experiment to determine a A375 cell concentration with the

shortest doubling time so that this concentration could then be selected to evaluate the effect of the various NLC concentrations and of Dac, both encapsulated and un-encapsulated.

A population of A375 was propagated to the optical density of 0.8 at 570 nm determined using Thermo Scientific Varioskan plate reader (see Section 2.6.6), to observe the growth of cells during the log phase when the cells are dividing rapidly. This is the point when it is expected that the cells are more vulnerable to the treatment. The cell population was measured by means of an automated cell counter. Four different concentrations of A375 cells (1,000, 2,000, 3,000 and 4,000 cells/ml) were seeded and growth was measured using the MTT assay (described in Section 2.6.8). The growth rate was measured by recording the optical density at 570 nm and the growth of A375 cells was used to calculate the doubling time at 24, 48 and 72 hours. The experimental procedure is further described in Section 2.6.6.

It was possible to identify the log phase of A375 cell growth within the experiment's time intervals of 24, 48 and 72 hours (Figure 4.7). The growth of A375 cells was used to calculate the doubling time at 24, 48 and 72 hours.

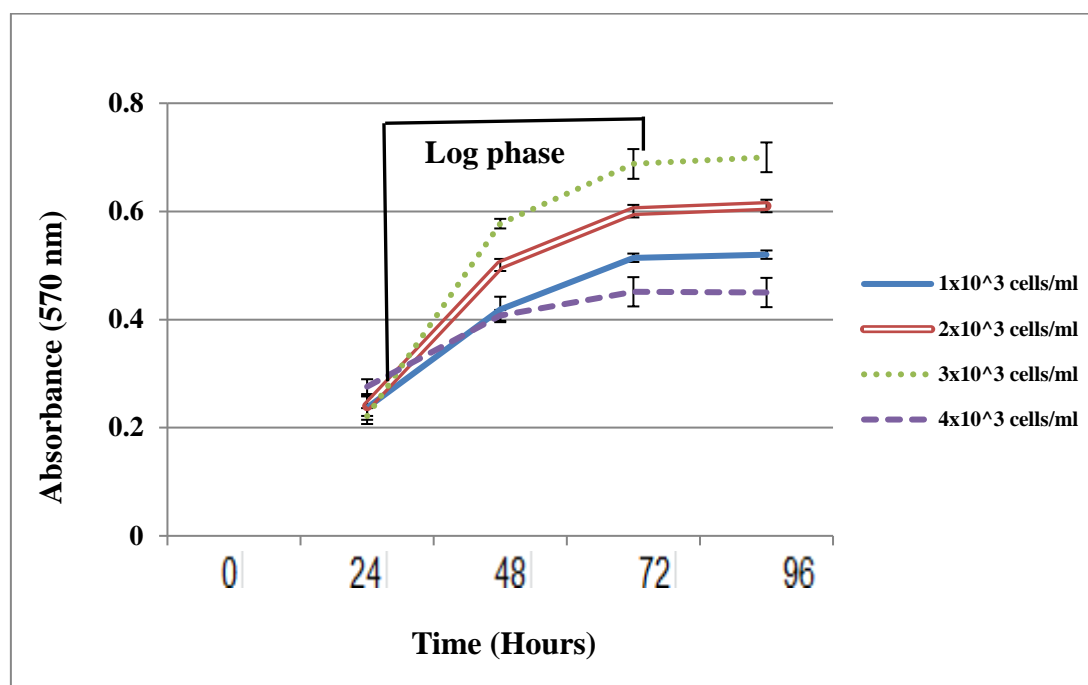


Figure 4.7: The optical density of A375 cells seeded with different concentrations at different time point. The individual points indicate mean \pm SD (n = 3).

The doubling time is further confirmed in Table 4.7, and shows that the shortest doubling time occurred with a cell density of 3×10^3 cells/ml. This density was therefore selected for subsequent experiments of A375 cells.

Table 4.7: The doubling time of different concentrations of A375 cells in culture, mean \pm SD (n = 3).

Cell density (cells/ml)	Doubling time		
	24 (Hours)	48 (Hours)	72 (Hours)
1×10^3	10.94	27.50	46.47
2×10^3	6.11	20.82	43.31
3×10^3	5.03	15.38	32.67
4×10^3	14.20	31.75	49.11

From the above results, the cell density for the A375 cells for the remaining experiments was determined to be 3×10^3 cells/ml. The assessment of the three potential NLC carriers (NLC/SI 1%, NLC/GM 1% and NLC/PI 1%) and the drug of Dac with and without NLC/PI 1% carrier were done at 24, 48 and 72 hours (see next sections).

In order to establish the best methods for the cytotoxicity assessment for the NLC particles developed in this work, commercially available silica nanoparticles (SiNP20 and SiNP200) from Sigma Aldrich, were first used and studied for their effect on A375 melanoma cells. This work has been listed in Appendix A. By conducting this work we were able to study the effect of these commercial particles on the A375 cell line and device the appropriate procedures to test the NLC particles developed in this thesis (please see Appendix A).

4.6.2 Morphology of A375 cells

The morphological features of A375 cells after 24 hours treated with the different types of NLC (NLC/PI 1%, NLC/SI 1% and NLC/GM 1%) were studied using light microscopy (Leica DM IL LED system; Figure 4.8).

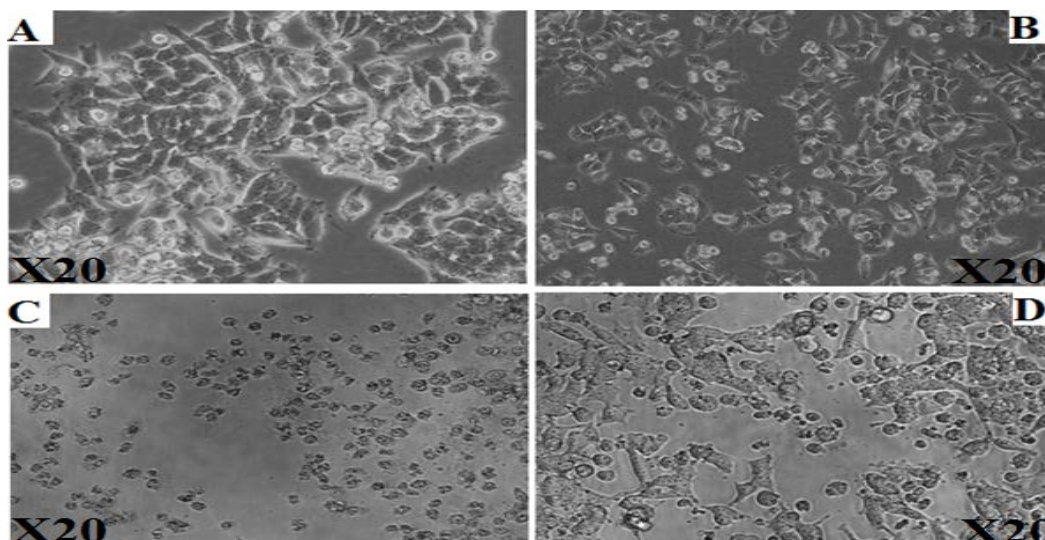


Figure 4.8: Morphology study for A375 cells (3×10^3 cells/ml) observed by light microscopy ($\times 20$) after 24 hours' incubation, A: cells without treatment; B: cells treated by 100 $\mu\text{g/ml}$ NLC/PI 1%; C: cells treated by 100 $\mu\text{g/ml}$ NLC/SI 1%; and D: cells treated by 100 $\mu\text{g/ml}$ NLC/GM 1%.

A375 cells after seeding without treatment (Figure 4.8A) were seen to be nearly confluent with each other and had sharp ends in contact at 24 hours. The cells after treatment with NLC/PI 1% (100 $\mu\text{g/ml}$), at the same time showed preservation of their contact to each other without morphological change (Figure 4.8B). At 24 hours, the effect on the cells treated with 100 $\mu\text{g/ml}$ NLC/SI 1% shows that the A375 cells appear to be shrinking and demonstrate what appear to be cytopathic changes (Figure 4.8C). The A375 cells exposed to NLC/GM 1% demonstrated changes to their morphology post treatment with 100 $\mu\text{g/ml}$ at 24 hours, with alteration in terminals and cell shrinkage (Figure 4.8D).

The effect of NLC can be seen in Figures 4.8C and D, as compared to Figures 4.8A and B where the cells do not show a clear cytopathic effect. In Figures 4.8C and D (cells treated with NLC/SI 1% and NLC/GM 1%, respectively), the results show the cell

distortion and a cytopathic effect demonstrating a high level of cellular toxicity from these types of NLC. In Figure 4.8B (cells treated by NLC/PI 1%), the results show that the cells have some changes but they are still relatively intact in structure without significant cytopathic changes suggesting that there is cytotoxicity, but it is at an acceptable level of cellular effect from this type of NLC.

4.6.3 Viability assessment for A375 cells post NLCs treatment

A toxicity assessment is necessary to evaluate the product for a health risk assessment. This involves two steps, hazard identification and dose response. The quantitative relationship between exposure (or dose) and extent of toxic response can be established. The MTT assay was used to evaluate the cell viability after treatment with the carriers (NLC/PI 1%, NLC/GM 1% and NLC/SI 1%). The cells were treated with NLC/PI 1% (50, 100 and 200 µg/ml) for 24, 48 and 72 hours. A positive control was included in the experiment where cells were exposed to H₂O₂ at a concentration of 100 µg/ml (Figure 4.9).

The results show that when A375 cells were exposed to NLC/PI 1% there was no statistically significant toxic response at 50, 100 and 200 µg/ml for 24, 48 and 72 hours when compared to untreated cells and the positive control (H₂O₂, 100 µg/ml). These results indicate that NLC/PI 1% as carrier can be used safely for encapsulation.

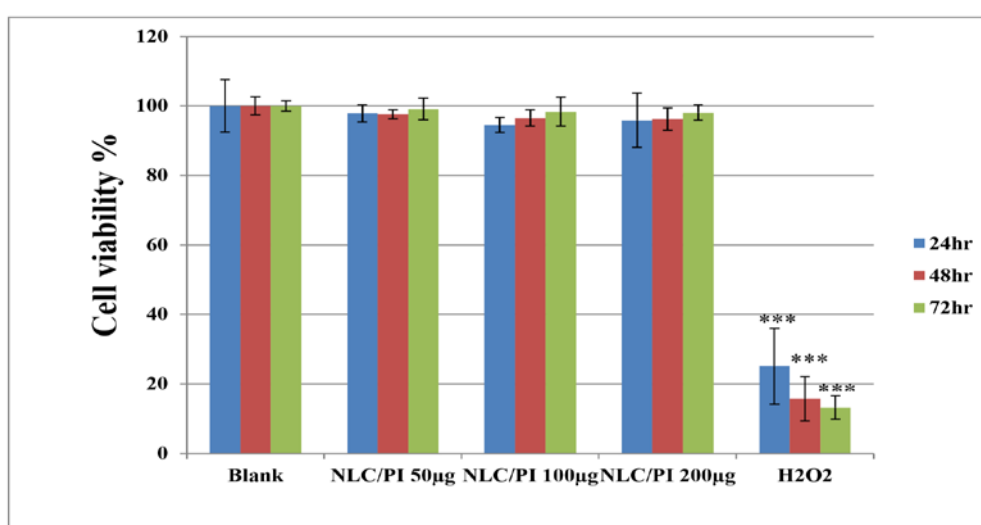


Figure 4.9: Mean cell line viability (as measured using MTT assay, n=3) when exposed to NLC/PI 1%. The error bar indicates the SD, where * shows $P \leq 0.01$.**

The A375 cells were then treated with NLC/SI 1% (50, 100 and 200 $\mu\text{g}/\text{ml}$) for 24, 48 and 72 hours. A positive control was included in the experiment where cells were exposed to H_2O_2 at a concentration of 100 $\mu\text{g}/\text{ml}$ (Figure 4.10).

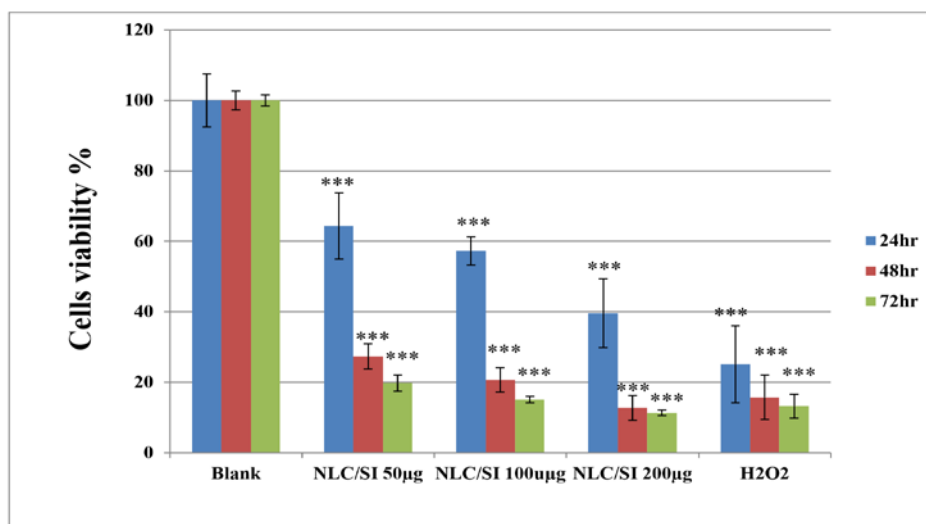


Figure 4.10: Mean cell line viability (as measured using MTT assay, n=3) when exposed to NLC/SI 1%. The error bar indicates the SD, where * shows $P \leq 0.01$.**

Figure 4.10, shows that the A375 cell line, when treated with NLC/SI 1%, demonstrated toxic effects on the cells at 50, 100 and 200 $\mu\text{g}/\text{ml}$ for 24, 48 and 72 hours. The results obtained from the above figure suggest that NLC/SI 1% cannot be used safely for encapsulation as a carrier. At 100 $\mu\text{g}/\text{ml}$ of NLC/SI 1% after 24 hours the cell viability was 58% which indicates a cytopathic effect and this result supports the light microscopy images (Figure 4.8C) which were performed at the same time and concentration.

Cells were treated by NLC/GM 1% (50, 100 and 200 $\mu\text{g}/\text{ml}$) for 24, 48 and 72 hours. A positive control was included in the experiment where cells were exposed to H_2O_2 at a concentration of 100 μg (Figure 4.11).

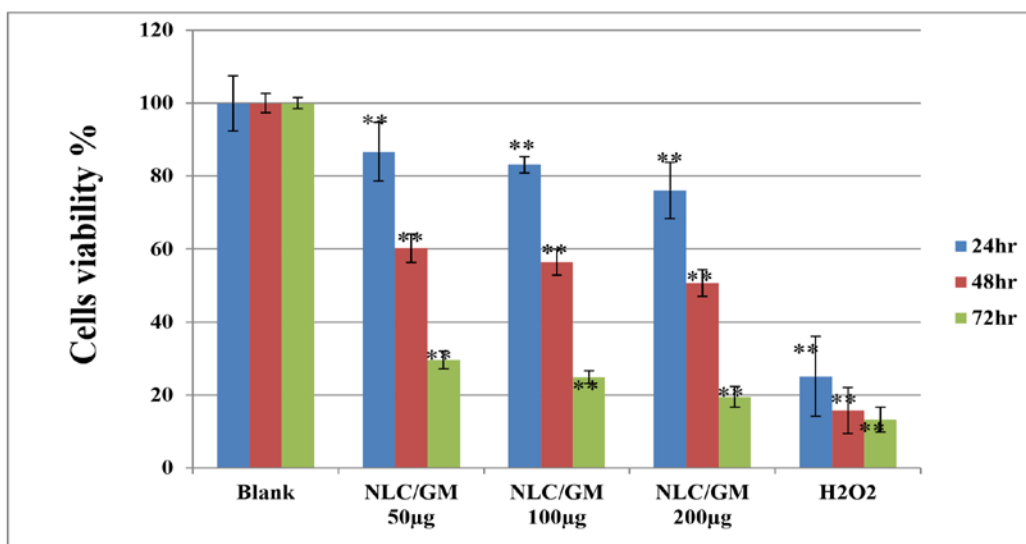


Figure 4.11: Mean cell line viability (as measured using MTT assay, n=3) when exposed to NLC/GM 1%. The error bar indicates the SD, where ** and * shows $P \leq 0.05$ and $P \leq 0.01$.**

Figure 4.11, shows that NLC/GM 1% treatment has a toxic effect on A375 cells when exposed at concentrations of 50, 100 and 200 µg/ml for 24, 48 and 72 hours. These results suggest that NLC/GM 1% cannot be used for encapsulation. At 100 µg/ml of NLC/GM 1% after 24 hours the cell bioavailability shows 83% which indicates some cytopathic effect and this result correlates with light microscope image (Figure 4.8D) which was performed at the same time and concentration.

From these observations, the results confirm that, separate to the non-optimal size of the carriers demonstrated in Section 4.2, the NLC/SI 1% and NLC/GM 1% carriers prepared by the HSD method cannot be used for Dac encapsulation. However, NLC/PI has been identified as a potential carrier for Dac as a drug delivery system.

4.7 Treatment of A375 cells with Dac with and without NLC/PI encapsulation

The MTT cell viability assay showed normal growth of the A375 cells when treated with the carrier NLC/PI 1% (50, 100 and 200 µg/ml; Figure 4.8). This section shows the effect of Dac pre and post NLC/PI 1% encapsulation on A375 cells by using MTT assay at 24, 48 and 72 hours.

4.7.1 24 hours treatment

A375 Cells were treated by different concentrations of Dac and NLC/PI 1%-Dac (Figure 4.12). The results show that cell viability decreases with increased drug concentration, from 49% to 41% and then 36% for 8, 16 and 32 $\mu\text{g/ml}$, respectively and there was no statistical significant difference between them.

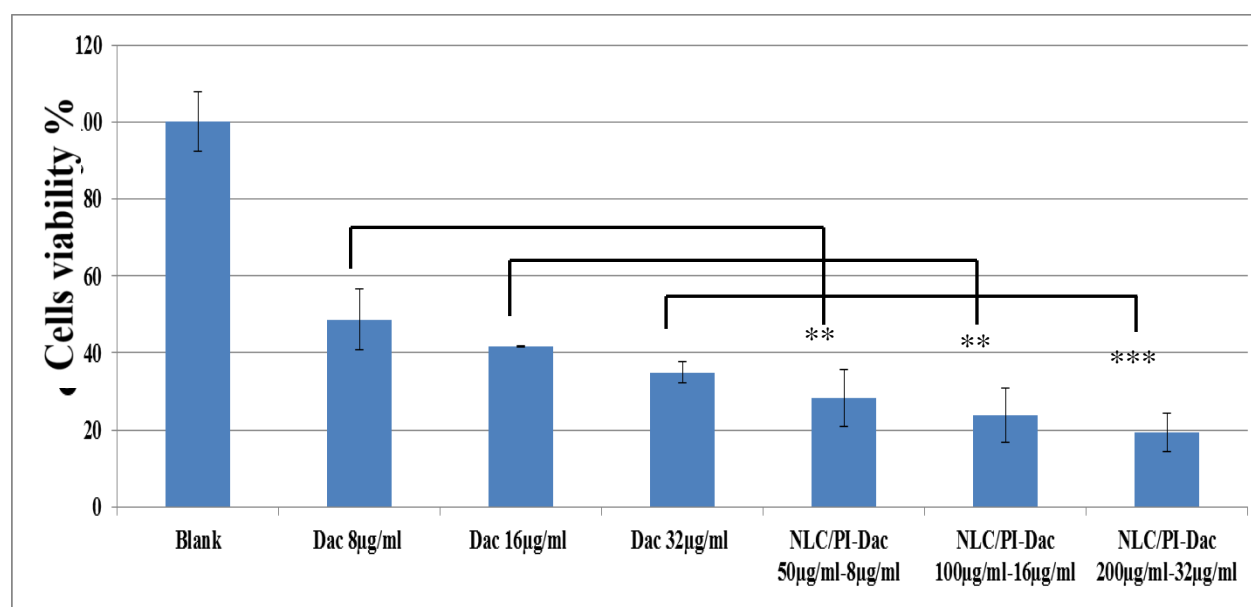


Figure 4.12: The effect of Dac pre and post NLC/PI 1% encapsulated on the viability of A375 cells after 24hours treatment as measured using MTT assay. The bars show mean (n=3) and the error bar indicates the SD, were and *** shows $P \leq 0.05$ and $P \leq 0.01$.**

The encapsulated carrier showed a greater toxic effect compared to the un-encapsulated drug itself; cell viability decreased to 20% with 32 $\mu\text{g/ml}$ drug concentration encapsulated in NLC/PI 1% at 200 $\mu\text{g/ml}$. The results show there was no statistical significant difference in cell viability between all three concentrations of NLC/PI 1%-Dac but there was a statistically significant difference between the encapsulated and un-encapsulated drug.

4.7.2 48 hours treatment

The experiment was repeated after 48 hours exposure to Dac (with and without encapsulation). The cell viability decreased as the drug concentration increased from 40% to 38% and 34% for 8, 16 and 32 $\mu\text{g/ml}$ respectively and there was no significant difference between them (Figure 4.13). After encapsulation, the decrease was more markedly reduced than with un-encapsulated drug itself and the cell viability decreased from 35% (un-encapsulated DAC) to 5% at 32 $\mu\text{g/ml}$ Dac encapsulated in 200 $\mu\text{g/ml}$ NLC/PI 1% and there was no statistical significant difference in cell viability between all three concentrations of NLC/PI 1%-Dac.

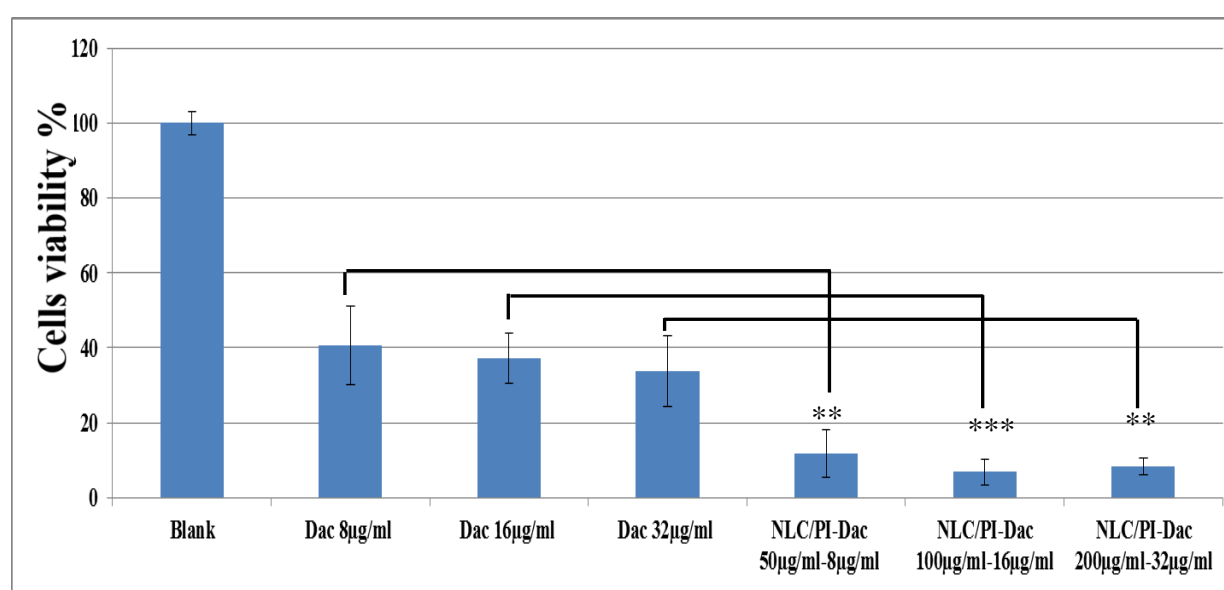


Figure 4.13: The effect of Dac pre and post NLC/PI 1% encapsulated on the viability of A375 cells after 48hours treatment as measured by MTT assay. The bars show mean (n=3) and the error bar indicates the SD, were ** and *** shows $P \leq 0.05$ and $P \leq 0.01$.

When the results measured at 48 hours are compared to those measured at 24 hours, the cell viability was 25% less after encapsulation.

4.7.3 72 hours treatment

The experiment was repeated after 72 hours exposure to Dac (with and without encapsulation). With the cells exposed to Dac, the cell viability decreased with the increasing drug concentration from 49% to 37% and 34% for 8, 16 and 32 $\mu\text{g/ml}$ respectively and there was no significant difference between them (Figure 4.14). After encapsulation, the decrease in viability was more marked than with the drug itself and the cell viability decreased to 5% with 32 $\mu\text{g/ml}$ Dac encapsulated in 200 $\mu\text{g/ml}$ NLC/PI 1%. The results show there was no statistical significant difference in cell viability between all three concentrations of NLC/PI 1%-Dac

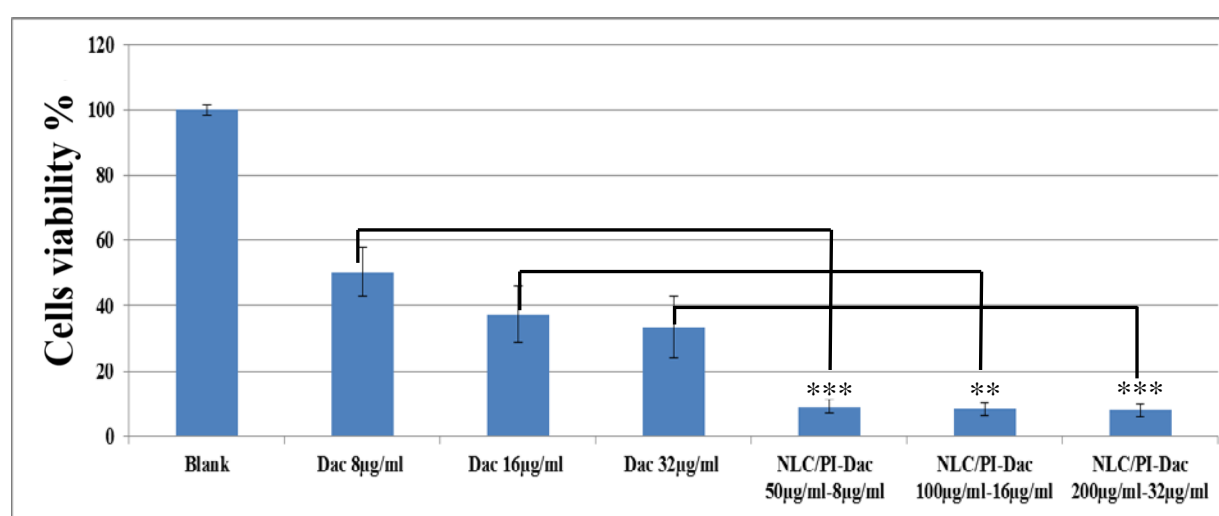


Figure 4.14: The effect of Dac pre and post NLC/PI 1% encapsulated on the viability of A375 cells after 72hours treatment as measured using MTT assay. The bars show the mean (n=3) and the error bar indicate the SD, where *** shows $P \leq 0.01$.

There was no significant difference in cell viability and drug action after encapsulation between measurements taken at 48 and 72 hours. This is most likely due to the cell growth kinetics having reached asymptotic stage, where the increasing drug concentration may not have any further cytotoxic effect. Again, a statistically significant decrease in cell viability was seen with the encapsulation of the drug.

The results shown in this work indicate a very successful outcome in selecting the appropriate NLC formulation and the correct encapsulation method used for Dac

loading as well as the optimal testing procedures chosen to test the viability of the synthesised particles.

4.8 Discussion

4.8.1 Nanostructured lipid carriers encapsulated dacarbazine

The NLC that has the optimal properties such particle size and polydispersity index was selected to encapsulate the melanoma therapeutic drug Dac. The formula was NLC/PI 1%, and it was re-synthesized with Dac to prepare a system for nanodrug delivery in order to enhance its efficacy. The encapsulation efficiency of the carrier in nanodrug delivery can be calculated by the ratio of the concentration of the entrapped drug to its initial concentration. In order to determine the successful encapsulation of the drug within the nanoparticle, the encapsulation efficiency is an important property for the drug carrier and an efficient encapsulation process avoids direct biological interactions occurring with the drug. In addition, it can prevent the drug's potential unwanted toxicity at other sites, for example the effect of Dac on normal tissue. In 2012, Delmas et al. stated that engineering nanostructured particles that can efficiently encapsulate drugs at high concentrations is a major challenge in nanomedicine. Other nanodrug delivery systems have been previously used to encapsulate Dac (see Section 1.7 for examples).

The highest encapsulation efficiency percentage in the literature was obtained with MPEG-PLA (methoxy poly (ethylene glycol)-poly (lactide)) nanoparticles and was $70.1\pm 2.3\%$ (Ma et al., 2011). In this study, NLC/PI 1%-Dac was used to encapsulate three different concentrations of Dac (see Table 4.4). The results showed that the highest encapsulation efficiency was measured for NLC/PI 1%-Dac 50 ($98.5\pm 0.2\%$; see Table 4.3). This result is similar to the results of previous studies which have stated that an advantage of using NLC in nanodrug delivery as a carrier was due to their high encapsulation efficiency (Tamjidi et al., 2013; Patel et al., 2015; Purohit et al., 2016), however it is the first time that this type of NLC/PI 1% has been demonstrated for Dac.

The drug loading capacity can be calculated by the ratio of encapsulated drug to the total amount of the lipid in formula. This is known as one of the advantages of using NLC for encapsulation (Iqbal et al., 2012). The highest reported drug loading capacity obtained from nanoparticles encapsulating Dac in the literature was with Dacarbazine-loaded cubosomes 28% (Bei et al., 2010). In this current study, the highest recorded drug loading capacity was seen with NLC/PI 1%-Dac 70 and was $32.3 \pm 0.8\%$ (see Table 4.4), which is higher than that previously reported, suggesting that the NLC/PI carrier is able to encapsulate more Dac than the cubosomes. This increased encapsulation may be due to the spherical particle shape of NLC. The spherical shape has been considered to be the basis of features such as a high loading capacity and controlled drug release due to smaller lipid–water interfaces and longer diffusion pathways (Saupe et al., 2006).

The different NLC/PI 1% particles were characterized, and comparisons drawn between NLC/PI 1% and NLC/PI 1%-Dac 50. The results showed that there was a predictable increase in particle size for NLC/PI 1% post Dac encapsulation and this was expected due to the increased material within the lipid core (see Figure 4.4). The drug (Dac) did not affect the homogeneity or the stability of NLC/PI 1% in solution after encapsulation measured by PDI and zeta potential (see Table 4.5). The results shown in this study suggest that Dac, when encapsulated in NLC/PI 1%-Dac, is located within the particle in a drug-enriched core and Dac largely stays associated with the solid lipid. Due to the liquid lipid in the outer layers of NLC, the carrier will absorb lipophilic drugs easily (Zur Mühlen et al., 1996). Consequently, if the drug is loaded in a high enough concentration, release of the drug from the lipid matrix will either occur by diffusion or matrix erosion (Hu et al., 2005). Previous studies have suggested that NLCs containing drugs display a biphasic drug release pattern (i.e. an initial burst release of drug followed by a sustained release of the drug at a constant rate) due to their different lipid structures (Khan et al., 2015). The NLC lipid structure contain solid lipids in their core and liquid lipid in the outer shell (see NLC structure in Figure 4.4). The drug release profile of NLC/PI 1%-Dac measured in this study also showed this pattern of release (see Figure 4.6). In the first phase, Dac could be released from the outer layer of the NLC/PI 1% through a short diffusion path, whilst in the second phase Dac could be released in a sustained manner from the deeper liquid lipid phase and solid lipid cores through diffusion and erosion mechanisms. A

similar in vitro profile for drug release from NLC/PI containing Precirol ATO 5 has been reported previously (Lim et al., 2014; Song et al., 2014).

In the case of NLC/PI 1%-Dac, although the drug in the outer layer of the NLC (see Figure 4.3) could diffuse into the blood circulation, the drug incorporated inside NLC is likely to remain encapsulated in the carrier long enough to reach the site of action, thereby improving the Dac therapeutic profile and prolonging the therapeutic use of the drug (see Figure 4.6). In addition, previous studies have suggested that lipid nanoparticles (<200 nm in diameter) could form a monolayer on the skin and prevent the evaporation of water from the skin. By forming a transcutaneous hydration gradient, lipid nanoparticles could facilitate drug penetration into the deeper layers of the skin allowing more of the drug to reach the target tissue (Müller et al., 2002). Lipid-based vehicles have been proposed for treating cutaneous melanoma and epidermoid carcinoma through topical drug delivery (Kakumanu et al., 2011 and Lei et al., 2015), indicating that the NLC/PI 1%-Dac developed in this study could also be beneficial for use via a topical route for which early drug release would not potentially lead to severe systemic toxicity. However, the results presented in this chapter suggest that NLCs could have the potential for use in drug delivery via multiple administration routes.

4.8.2 Cytotoxicity assessment

The results in this chapter were collected following an extended period of experimentation used to develop an understanding of the specific cell line behaviors and handling requirements. The presented results are taken from an optimized process whereby a low passage number is used. The optimization process is documented in a conference paper under the title "Cell type- and size-dependent in vitro toxicity of silica particles in human skin cells" (Claudia Moia, Huijun Zhu and Mousallam Almousallam, 2014; see the article in Appendix B).

The preparation and assessment of different NLC properties relevant for use as a carrier for drug delivery have been demonstrated (see Chapter 3). In this chapter, the cytotoxicity was measured for the three NLCs to confirm the selection of NLC/PI as the optimal carrier. The toxicity evaluation used the A375 cell line which is a melanoma cell line. The time interval of the experiments was determined by the log phase

of the A375 cells (described in Section 2.6.6). In the log phase, A375 cells grow more rapidly and are representative of the real-life conditions such as increased cellular intake and metabolism (Hu et al., 2013; Zhang and Wang al., 2015). The results showed that the log phase of A375 was within the interval period of the experiments, from 24 hours to 72 hours (see Section 4.6.1).

The development of a nanostructured lipid particle system is driven by a desire for: (i) targeted drug delivery; (ii) greater drug efficiency; (iii) increasing the availability of the drug at the disease site; and (iv) prevention of harmful side effects (Naseri et al., 2015; Velmurugan and Selvamuthukumar, 2016). The study of the effect of each type of NLC on cells was strongly suggested (Pizzol et al., 2014) and it was determined that these experiments should be performed on the A375 cell line to mimic the potential target within the body. The safety and efficiency of the nanostructured lipid particle system (NLC) was also evaluated. The results presented here demonstrate the viability of A375 cells treated with different NLCs (NLC/SI 1%, NLC/GM 1% and NLC/PI 1%) whose physical properties have been previously determined (see Chapter 3).

The undesirable properties of NLC/SI 1% and NLC/GM 1% such as particle size (over 400 nm) and particle aggregating (PDI > 0.3) were reflected their effect on cells as a carrier. Particle size above 300 nm is undesirable for their transport and is not suitable (Das et al., 2011). In 2015, Ng et al. demonstrated that particle aggregation impedes the targeting efficiency of NLC to cells and tissues. The results of two of these NLCs (NLC/SI 1% and NLC/GM 1%) showed that cell viability significantly decreased ($P \leq 0.05$) when exposed to the NLCs. This result suggests that these carriers have cytotoxic effects and should not be candidates for a nanodrug delivery system. This is an increasing in cytotoxicity maybe due to the increasing tendency of these NLCs (NLC/SI and NLC/GM) to aggregating either coating the lipid membrane of the cell or one absorbed coating cell organelle preventing normal function (see Chapter 3; results of NLC/SI and NLC/GM aggregating and reasons). On other hand, NLC/PI 1% showed good carrier properties (see Section 3.2.3) and no toxic effects on cells viability in the results of this chapter. This indicates that NLC/PI 1% formulation that prepared by HSD method in this study can be used as carrier for encapsulation.

NLCs with and without drug encapsulation (using NLC/PI 1%) were exposed to A375 cells for 24, 48 and 72 hours at NLC/PI 1% concentrations varying from 50 µg to 200 µg/ml and Dac concentrations at 8 to 32 µg/ml with appropriate negative controls. The most promising results were seen with NLC/PI 1%-DAC after 48 and 72 hours where cell viability was statistically significant reduced compared with Dac itself after 48 and 72 hours (Figures 4.12 and 4.13), indicating that the drug release from the encapsulated particles to the cells inhibited further growth of cells and led to degeneration. Additionally, NLC/PI 1% without drug encapsulation showed no cytotoxic activity in comparison to the drug-loaded NLC/PI 1% which had the drug in the core, with the shell releasing the drug into the cells over 30 hours (see Section 4.5, Figure 4.6).

4.8.3 Summary

The results in this chapter show that the optimal particle characteristics identified for NLC/PI 1% were not affected when used for Dac encapsulation, suggesting that NLC/PI 1% is an appropriate carrier for Dac. The encapsulation efficiency and drug loading capacity of NLC/PI 1% were higher than those previously reported in the literature for other carriers, suggesting that this drug delivery system is likely to be more effective. After that, the cellular toxicity associated with the different types of NLCs (NLC/SI 1%, NLC/GM 1% and NLC/PI 1%) and Dac with and without encapsulation will be demonstrated. This will support and validate the selection of NLC/PI as the best nanocarriers for Dac.

CHAPTER FIVE
FINAL DISCUSSION, CONCLUSIONS AND FUTURE
WORK

5. GENERAL DISCUSSION, CONCLUSIONS AND FURTHER WORK

5.1 Summary

In this study, the properties of NLC were optimized by modifying the formula and the method of the preparation (e.g. laboratory-based method: high sheer dispersity). Then the study used the identified optimised formula obtained from NLC preparation to encapsulate Dacarbazine (the chemotherapy drug used in this study). After the synthesis of the drug delivery system of Dacarbazine (Dac) using NLC, the cellular toxicity was assessed using *in vitro* assessments and a melanoma cell line (A375). Finally, the MicroJet Reactor (MJR) was used as industry-based method to prepare large scale NLC.

5.2 Final discussion

The use of NLC as a drug carrier for chemotherapeutic drugs has been increasingly studied over the last five years. The use of drug carrier systems has the ability to overcome the limitations of the anticancer drugs such as poor solubility, toxicity of normal tissue, poor targeting and control, in addition to drug degradation and resistance. Despite the advantages of NLCs, it is essential to understand the implications of the method of preparation and formulae components. This study developed the strategy to improve NLC properties and to optimise the use of NLCs as a drug carrier system for a particular chemotherapeutic drug, Dac. The NLCs properties were developed through modifying the formulation and the preparation methods of NLCs. The study investigated the influence of the solid lipid on NLC properties such as particle size. The high negative charge of the solid lipid (Precirol ATO-5®) tends to form polar covalent bonds with isopropyl myristate (IPM) in the NLC/PI formulae. This helps to explain the stability of the solid lipid in the liquid lipid matrix during the NLC preparation using HSD.

The studies in this thesis have demonstrated that it is possible to control the particle size and improve the PDI of the NLCs using the HSD method. Previous studies have presented the advantages of using NLC for skin applications (see Section 1.5). In

NLC/PI, the formulae use IPM which has been shown to significantly improve the bioavailability of drug in topical preparations (Suh and Jun., 1996).

Several previous attempts have been made to develop drug delivery vehicles for Dac to improve the therapeutic profile of the drug (Bei et al., 2009; Ma et al., 2011 and Kakumanu et al., 2011). However, the developed delivery systems were not stable enough over the study period (Table 7.1). While in this study, the NLC stability was shown to be more stable than previously reported carrier systems (shown in Table 5.1), as Almousallam et al 2015, which is suggested to be due to the ratio between the solid lipid and liquid lipid of the NLC formulae resulting in a low level of repulsion between adjacent particles in solution.

Table 5.1: The comparison of NCL physical properties post Dac encapsulation in this study with previous attempts.

Formula	Particles size nm	PDI	Zeta potential	Stability	References
Dacarbazine-Loaded Cubosomes 10 mg in 65ml	88.4±1.3	0.191	-	-	Bei et al., 2009
MPEG/PLA-Dac 3 mg/ 35ml	144. 2±7.8	<0.3	-32.1±5.4	-	Ma et al., 2011
Nanoemulsion-Dac 100mg	111.7 ± 0.33	0.218 ± 0.002	-8.20 ± 0.07	>75% of Dac release after 6 months storage	Kakumanu et al., 2011
NLC-Dac 50mg	190 ± 10	0.2 ± 0.01	-43.5 ± 1.2	Stable up to 3 months	Almousallam et al., 2015

In addition, previous studies have reported drug loading efficiencies and encapsulation efficiencies for other carriers which were lower than those reported for NLC (Table 5.2, data reported in this thesis identified as “PhD Thesis”). This increased of encapsulation efficiency in NLC due to a spherical shape of particle (see Section 4.7).

Table 5.2: The comparison of NLC biophysical properites of Dac post encapsulated in this study with previous attempts .

Formula	Drug loading capacity	encapsulation efficiency	Brief of efficiency improved	References
Dacarbazine-Loaded Cubosomes	28	16.7%	-	Bei et al., 2010
MPEG/PLA-Dac	15.0±0.3	70.1±2.3%	enhanced antitumor activity	Ma et al., 2011
Nanoemulsion	-	-	significantly reduced in tumor size	Kakumanu et al., 2011
NLC-Dac	23.4±0.2	98.5 %	Decrease cell viability in melanoma cell line	PhD thesis

In the *in vitro* cell assessement, studies showed that NLC encapsulation enhanced the toxicity of Dac and decreased the cell viability in formulae NLC/PI-Dac (see Section 4.6.3) Other studies on other formula have demonstrated that membrane ion channels play an important role in cell proliferation and cell apoptosis (Wonderlin and Strobl al., 1996; Wang al., 2004; Pardo al., 2004) which may be affected by the presence of Dac and prolonged by its encapsulation by NLCs.

Dac is a known alkylating agent and can damage DNA at N7 guanine which will promote cell apoptosis (Figure 5.1).

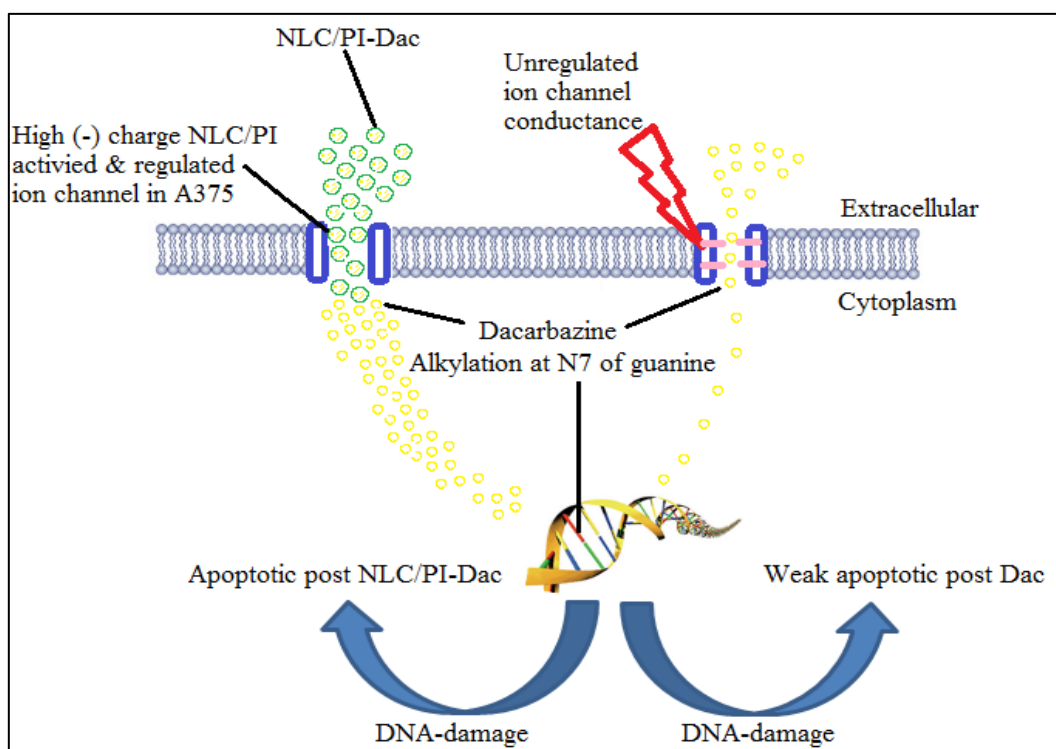


Figure 5.1: Schematic for Dac mechanism of action post NLC encapsulated.

The presence of Dac may enhance a comparatively weak apoptotic response (Legha et al., 1989; Legha et al., 1996; Phan et al., 2001; Tsao et al., 2004). Previous studies have demonstrated that highly negatively charged anionic lipids can regulate the activity of ion channels (Fan and Makielski al., 1997). In this study, NLC/PI-Dac has a negative charge (see the result of zeta potential for NLC/PI and NLC/PI-Dac in Section 4.3.1) which may act to enhance the apoptotic effect by increasing the level of Dac after ion channel regulation.

5.3 Conclusion

In this study, NLC carrier was developed for Dac as nanodrug delivery system. The commonly used method for NLC synthesis has been modified in this work to include an

oil-in-water emulsion, evaporation and solidification followed by HSD to achieve NLC with the identified desirable size. Compared with other approaches for Dac encapsulation with different materials, using NLC/PI proved beneficial in improving the drug encapsulation and loading efficiency, prolonging drug release, storage stability, and simplified synthesis. NLC/PI showed an enhancement in Dac activity (shown as a decrease in cell viability) post NLC/PI encapsulation.

In conclusion, this research suggests that NLC/PI is a new potential candidate for Dac delivery to overcome the limitations of short half-life, and low tolerant dose of the drug.

The originality of the research work in this study are the following findings:

- This study is the first to report the use of encapsulation of a chemotherapeutic drug Dac within NLC particles by defining the effect of modification of the NLC-Dac formula on its physical properties (size, disparity and stability) and its delivery system (drug loading capacity and encapsulation efficiency) using different Dac concentrations.
- The experiments succeeded in showing a high loading capacity of NLC as a carrier for Dac.
- The study enhanced Dac efficiency *in vitro* as a chemotherapeutic agent by using NLC as a carrier.
- This study is the first to report the use MicroJet Reactor (MJR) in industry-based to prepare NLC particles as a carrier for drug delivery system.
- The study has shown that it is possible to manufacture NLC particles with optimised properties using industry-based preparation and development by defining the effect of modification of the NLC formula and preparation method on its properties (size, dispersity and stability) using different solid lipid matrix, different surfactant concentrations.

5.4 Uncertainties and limitations

In this study there are some uncertainties have to consider as:

- Cell line not representative of all body:
- Skin model such as pig skin/artificial skin

- Medical exposure in vivo
- Duration of exposure:
- Clinically representatives
- Media of exposure
- Variability:
- Inter/interspecies
- Human and use
- Genetic variability
- Skin atrophy

The study has some limitations:

- One type of cell line, is it applicable to others
- NLC's techniques
- Limited facilities due to the move of the laboratory to a different building.

5.5 Further work

This study demonstrated the effect of NLCs on melanoma, further measurements need to evaluate NLCs bioactivity, on other cell line such as normal skin cells. Further study will be required to assess the effect of NLC/PI on cell channels and if any alteration on gene expression in melanoma cells. It is important to understand the mechanism of action of NLC/PI-Dac in A375 using molecular biology techniques such as Western blot. Such techniques can measure the level of protein associated with melanoma with and without NLC/PI-Dac treatment. This formula (NLC/PI-Dac) has to prepare in final product for skin for example, gel formulation, and the physical properties of particles need to be re-assess. The drug release profile and the toxicity of NLC/PI-Dac *in vivo* will be required to confirm the *in vitro* results. Skin models is a good way forward to reduce the animal testing that may be required.

Also, there are opportunities to use this method (HSD) to prepare NLC/PI for another cancer agent encapsulated.

REFERENCES

REFERENCES

- Accomasso, L., Rocchietti, E. C., Raimondo, S., Catalano, F., Alberto, G., Giannitti, A., Minieri, V., Turinetti, V., Orlando, L. and Saviozzi, S. (2012), "Fluorescent Silica Nanoparticles Improve Optical Imaging of Stem Cells Allowing Direct Discrimination between Live and Early-Stage Apoptotic Cells", *Small*, vol. 8, no. 20, pp. 3192-3200.
- Agrawal, Y., Petkar, K. C. and Sawant, K. K. (2010), "Development, evaluation and clinical studies of Acitretin loaded nanostructured lipid carriers for topical treatment of psoriasis", *International journal of pharmaceutics*, vol. 401, no. 1–2, pp. 93-102.
- Ahmad, A. and Gadgeel, S. M. (2016), *Lung Cancer and Personalized Medicine: Novel Therapies and Clinical Management*, Springer.
- Aitken, R. J., Chaudhry, M. Q., Boxall, A. B. and Hull, M. (2006), "Manufacture and use of nanomaterials: current status in the UK and global trends", *Occupational medicine (Oxford, England)*, vol. 56, no. 5, pp. 300-306.
- Al-Badr, A. A. and Alodhaib, M. M. (2016), "Chapter Four-Dacarbazine", *Profiles of Drug Substances, Excipients and Related Methodology*, vol. 41, pp. 323-377.
- Al Haj, N. A., Abdullah, R., Ibrahim, S. and Bustamam, A. (2008), "Tamoxifen drug loading solid lipid nanoparticles prepared by hot high pressure homogenization techniques", *American Journal of Pharmacology and Toxicology*, vol. 3, no. 3, pp. 219-224.
- Allen, T. M. and Cullis, P. R. (2004), "Drug delivery systems: entering the mainstream", *Science (New York, N.Y.)*, vol. 303, no. 5665, pp. 1818-1822.
- Almoussallam, M., Moia, C. and Zhu, H. (2015), "Development of nanostructured lipid carrier for dacarbazine delivery", *International Nano Letters*, vol. 5, no. 4, pp. 241-248.
- Almoussalam, M. and Zhu, H. (2016), "Encapsulation of cancer therapeutic agent dacarbazine using nanostructured lipid carrier", *JoVE (Journal of Visualized Experiments)*, , no. 110, pp. e53760-e53760.
- Andalib, S., Varshosaz, J., Hassanzadeh, F. and Sadeghi, H. (2012), "Optimization of LDL targeted nanostructured lipid carriers of 5-FU by a full factorial design", *Advanced biomedical research*, vol. 1, pp. 45-9175.100147. Epub 2012 Aug 28.
- Anurak, L., Chansiri, G., Peankit, D. and Somlak, K. (2011), "Griseofulvin solid lipid nanoparticles based on microemulsion technique", *Advanced Materials Research*, Vol. 197, Trans Tech Publ, pp. 47.
- Anvekar, R., Ascioffa, J., Lopez-Rivera, E., Floros, K., Izadmehr, S., Elkholi, R., Belbin, G., Sikora, A. and Chipuk, J. (2012), "Sensitization to the mitochondrial

pathway of apoptosis augments melanoma tumor cell responses to conventional chemotherapeutic regimens", *Cell death & disease*, vol. 3, no. 11, pp. e420.

- Asadujjaman, M. and Mishuk, A. U. (2013), "Novel approaches in lipid based drug delivery systems", *Journal of Drug Delivery and Therapeutics*, vol. 3, no. 4, pp. 124-130.
- Attama, A. A., Momoh, M. A. and Builders, P. F. (2012), *Lipid nanoparticulate drug delivery systems: a revolution in dosage form design and development*, INTECH Open Access Publisher.
- Azoury, S. C. and Lange, J. R. (2014), "Epidemiology, risk factors, prevention, and early detection of melanoma", *Surgical Clinics of North America*, vol. 94, no. 5, pp. 945-962.
- Bagchi, M., Moriyama, H. and Shahidi, F. (2012), *Bio-nanotechnology: a revolution in food, biomedical and health sciences*, John Wiley & Sons.
- Bahari, L. A. S. and Hamishehkar, H. (2016), "The Impact of Variables on Particle Size of Solid Lipid Nanoparticles and Nanostructured Lipid Carriers; A Comparative Literature Review", *Advanced Pharmaceutical Bulletin*, vol. 6, no. 2, pp. 143.
- Bhatia, S., Tykodi, S. S. and Thompson, J. A. (2009), "Treatment of metastatic melanoma: an overview", *Oncology (Williston Park, N.Y.)*, vol. 23, no. 6, pp. 488-496.
- Balakrishnan, V., Ab Wab, H. A., Razak, K. A. and Shamsuddin, S. (2013), "In vitro evaluation of cytotoxicity of colloidal amorphous silica nanoparticles designed for drug delivery on human cell lines", *Journal of Nanomaterials*, vol. 2013, pp. 4.
- Barry, B. (2001), "Novel mechanisms and devices to enable successful transdermal drug delivery", *European Journal of Pharmaceutical Sciences*, vol. 14, no. 2, pp. 101-114.
- Bedikian, A. Y., Millward, M., Pehamberger, H., Conry, R., Gore, M., Trefzer, U., Pavlick, A. C., DeConti, R., Hersh, E. M., Hersey, P., Kirkwood, J. M., Haluska, F. G. and Oblimersen Melanoma Study Group (2006), "Bcl-2 antisense (oblimersen sodium) plus dacarbazine in patients with advanced melanoma: the Oblimersen Melanoma Study Group", *Journal of clinical oncology : official journal of the American Society of Clinical Oncology*, vol. 24, no. 29, pp. 4738-4745.
- Bei, D., Marszalek, J. and Youan, B. C. (2009), "Formulation of dacarbazine-loaded cubosomes—part II: influence of process parameters", *AAPS PharmSciTech*, vol. 10, no. 3, pp. 1040-1047.

- Bei, D., Zhang, T., Murowchick, J. B. and Youan, B. C. (2010), "Formulation of dacarbazine-loaded cubosomes. Part III. Physicochemical characterization", *AAPS PharmSciTech*, vol. 11, no. 3, pp. 1243-1249.
- Beloqui, A., Solinís, M. Á., Gascón, A. R., del Pozo-Rodríguez, A., des Rieux, A. and Préat, V. (2013), "Mechanism of transport of saquinavir-loaded nanostructured lipid carriers across the intestinal barrier", *Journal of Controlled Release*, vol. 166, no. 2, pp. 115-123.
- Beloqui, A., Solinís, M. Á., Rodríguez-Gascón, A., Almeida, A. J. and Préat, V. (2016), "Nanostructured lipid carriers: promising drug delivery systems for future clinics", *Nanomedicine: Nanotechnology, Biology and Medicine*, vol. 12, no. 1, pp. 143-161.
- Bezanilla, F. (2005), "Voltage-gated ion channels", *IEEE transactions on nanobioscience*, vol. 4, no. 1, pp. 34-48.
- Bharti, C., Nagaich, U., Pal, A. K. and Gulati, N. (2015), "Mesoporous silica nanoparticles in target drug delivery system: A review", *International journal of pharmaceutical investigation*, vol. 5, no. 3, pp. 124-133.
- Bhaskar, K., Anbu, J., Ravichandiran, V., Venkateswarlu, V. and Rao, Y. M. (2009), "Lipid nanoparticles for transdermal delivery of flurbiprofen: formulation, in vitro, ex vivo and in vivo studies", *Lipids Health Dis*, vol. 8, no. 6, pp. 10.1186.
- Biosciences, B. (2000), "Introduction to Flow Cytometry: A learning guide", *Manual Part*, vol. 1.
- Bonifacio, B. V., Silva, P. B., Ramos, M. A., Negri, K. M., Bauab, T. M. and Chorilli, M. (2014), "Nanotechnology-based drug delivery systems and herbal medicines: a review", *International journal of nanomedicine*, vol. 9, pp. 1-15.
- Brown, B. S., Patanam, T., Mobli, K., Celia, C., Zage, P. E., Bean, A. J. and Tasciotti, E. (2014), "Etoposide-loaded immunoliposomes as active targeting agents for GD2-positive malignancies", *Cancer biology & therapy*, vol. 15, no. 7, pp. 851-861.
- Cavalli, R., Caputo, O. and Gasco, M. R. (1993), "Solid lipospheres of doxorubicin and idarubicin", *International journal of pharmaceuticals*, vol. 89, no. 1, pp. R9-R12.
- Chauhan, V. P., Stylianopoulos, T., Boucher, Y. and Jain, R. K. (2011), "Delivery of molecular and nanoscale medicine to tumors: transport barriers and strategies", *Annual review of chemical and biomolecular engineering*, vol. 2, pp. 281-298.
- Chen, Y., Zhou, L., Yuan, L., Zhang, Z., Liu, X. and Wu, Q. (2012), "Formulation, characterization, and evaluation of in vitro skin permeation and in vivo pharmacodynamics of surface-charged tripterine-loaded nanostructured lipid carriers", *Int J Nanomedicine*, vol. 7, pp. 3023-3032.

- Cho, K., Wang, X., Nie, S., Chen, Z. G. and Shin, D. M. (2008), "Therapeutic nanoparticles for drug delivery in cancer", *Clinical cancer research: an official journal of the American Association for Cancer Research*, vol. 14, no. 5, pp. 1310-1316.
- Chourasia, M. and Jain, S. (2003), "Pharmaceutical approaches to colon targeted drug delivery systems", *J Pharm Pharm Sci*, vol. 6, no. 1, pp. 33-66.
- Cichorek, M., Wachulska, M., Stasiewicz, A. and Tyminska, A. (2013), "Skin melanocytes: biology and development", *Postepy Dermatol Alergol*, vol. 30, no. 1, pp. 30-41.
- Craig, G. A., Allen, P. J. and Mason, M. D. (2010), "Synthesis, characterization, and functionalization of gold nanoparticles for cancer imaging", in *Cancer Nanotechnology*, Springer, , pp. 177-193.
- Moia, C. (2015), "In vitro toxicological assessment of amorphous silica particles in relation to their characteristics and mode of action in human skin cells", .
- Dai, D. L., Martinka, M. and Li, G. (2005), "Prognostic significance of activated Akt expression in melanoma: a clinicopathologic study of 292 cases", *Journal of clinical oncology*, vol. 23, no. 7, pp. 1473-1482.
- Das, S. and Chaudhury, A. (2011), "Recent advances in lipid nanoparticle formulations with solid matrix for oral drug delivery", *Aaps Pharmscitech*, vol. 12, no. 1, pp. 62-76.
- Davar, D. and Kirkwood, J. M. (2012), "New therapies in the treatment of melanoma", *Expert opinion on investigational drugs*, vol. 21, no. 11, pp. 1643-1659
- De Jong, W. H. and Borm, P. J. (2008), "Drug delivery and nanoparticles: applications and hazards", *International journal of nanomedicine*, vol. 3, no. 2, pp. 133-149.
- De Villiers, M. M., Aramwit, P. and Kwon, G. S. (2008), *Nanotechnology in drug delivery*, Springer Science & Business Media.
- Delmas, T., Fraichard, A., Bayle, P., Texier, I., Bardet, M., Baudry, J., Bibette, J. and Couffin, A. (2012), "Encapsulation and release behavior from lipid nanoparticles: Model study with nile red fluorophore", *Journal of Colloid Science and Biotechnology*, vol. 1, no. 1, pp. 16-25.
- Desai, M. P., Labhasetwar, V., Walter, E., Levy, R. J. and Amidon, G. L. (1997), "The mechanism of uptake of biodegradable microparticles in Caco-2 cells is size dependent", *Pharmaceutical research*, vol. 14, no. 11, pp. 1568-1573.
- Donaldson, K., Stone, V., Tran, C., Kreyling, W. and Borm, P. J. (2004), "Nanotoxicology", *Occupational and environmental medicine*, vol. 61, no. 9, pp. 727-728.

- D'Orazio, J., Jarrett, S., Amaro-Ortiz, A. and Scott, T. (2013), "UV radiation and the skin", *International journal of molecular sciences*, vol. 14, no. 6, pp. 12222-12248.
- Duan, J., Yu, Y., Li, Y., Yu, Y., Li, Y., Zhou, X., Huang, P. and Sun, Z. (2013), "Toxic effect of silica nanoparticles on endothelial cells through DNA damage response via Chk1-dependent G2/M checkpoint", *PloS one*, vol. 8, no. 4, pp. e62087.
- Eggermont, A. M. and Kirkwood, J. M. (2004), "Re-evaluating the role of dacarbazine in metastatic melanoma: what have we learned in 30 years?", *European journal of cancer*, vol. 40, no. 12, pp. 1825-1836.
- Eikenberry, S., Thalhauser, C. and Kuang, Y. (2009), "Tumor-immune interaction, surgical treatment, and cancer recurrence in a mathematical model of melanoma", *PLoS computational biology*, vol. 5, no. 4, pp. e1000362.
- Ekambaram, P., Sathali, A. A. H. and Priyanka, K. (2012), "Solid lipid nanoparticles: a review", *Scientific reviews and chemical communications*, vol. 2, no. 1.
- Engesæter, B., Engebraaten, O., Flørenes, V. A. and Mælandsmo, G. M. (2012), "Dacarbazine and the agonistic TRAIL receptor-2 antibody lexatumumab induce synergistic anticancer effects in melanoma", *PloS one*, vol. 7, no. 9, pp. e45492.
- Falagan-Lotsch, P., Grzincic, E. M. and Murphy, C. J. (2016), "One low-dose exposure of gold nanoparticles induces long-term changes in human cells", *Proceedings of the National Academy of Sciences of the United States of America*, vol. 113, no. 47, pp. 13318-13323.
- Fan, H., Liu, G., Huang, Y., Li, Y. and Xia, Q. (2014), "Development of a nanostructured lipid carrier formulation for increasing photo-stability and water solubility of Phenylethyl Resorcinol", *Applied Surface Science*, vol. 288, pp. 193-200.
- Fan, Z. and Makielski, J. C. (1997), "Anionic phospholipids activate ATP-sensitive potassium channels", *Journal of Biological Chemistry*, vol. 272, no. 9, pp. 5388-5395.
- Fang, C., Al-Suwayeh, S. and Fang, J. (2013), "Nanostructured lipid carriers (NLCs) for drug delivery and targeting", *Recent patents on nanotechnology*, vol. 7, no. 1, pp. 41-55.
- Fang, G., Tang, B., Chao, Y., Xu, H., Gou, J., Zhang, Y., Xu, H. and Tang, X. (2015), "Cysteine-functionalized nanostructured lipid carriers for oral delivery of docetaxel: a permeability and pharmacokinetic study", *Molecular pharmaceutics*, vol. 12, no. 7, pp. 2384-2395.

- Fang, M., Jin, Y., Bao, W., Gao, H., Xu, M., Wang, D., Wang, X., Yao, P. and Liu, L. (2012), "In vitro characterization and in vivo evaluation of nanostructured lipid curcumin carriers for intragastric administration", *Int J Nanomedicine*, vol. 7, pp. 5395-5404.
- Fang, W. Q., Gong, X. and Yang, H. G. (2011), "On the unusual properties of anatase TiO₂ exposed by highly reactive facets", *The Journal of Physical Chemistry Letters*, vol. 2, no. 7, pp. 725-734.
- Freeman, H. C. and Hutchinson, N. (1979), "The crystal structure of the anti-tumor agent 5-(3, 3-dimethyl-1-triazenyl) imidazole-4-carboxamide (NSC-45388)", *Acta Crystallographica Section B: Structural Crystallography and Crystal Chemistry*, vol. 35, no. 9, pp. 2051-2054.
- Freitas, R. A. (2006), "Pharmacytes: An ideal vehicle for targeted drug delivery", *Journal of Nanoscience and Nanotechnology*, vol. 6, no. 9-1, pp. 2769-2775.
- Gaba, B., Fazil, M., Khan, S., Ali, A., Baboota, S. and Ali, J. (2015), "Nanostructured lipid carrier system for topical delivery of terbinafine hydrochloride", *Bulletin of Faculty of Pharmacy, Cairo University*, vol. 53, no. 2, pp. 147-159.
- Garcia-Garcia, E., Andrieux, K., Gil, S., Kim, H. R., Doan, T. L., Desmaële, D., d'Angelo, J., Taran, F., Georgin, D. and Couvreur, P. (2005), "A methodology to study intracellular distribution of nanoparticles in brain endothelial cells", *International journal of pharmaceutics*, vol. 298, no. 2, pp. 310-314.
- Gasco, M. R., Priano, L. and Zara, G. P. "Chapter 10 - Solid lipid nanoparticles and microemulsions for drug delivery: The CNS", in *Progress in Brain Research*, Elsevier, , pp. 181-192.
- Gatoo, M. A., Naseem, S., Arfat, M. Y., Dar, A. M., Qasim, K. and Zubair, S. (2014), "Physicochemical properties of nanomaterials: implication in associated toxic manifestations", *BioMed research international*, vol. 2014, pp. 498420.
- Gaur, P. K., Mishra, S., Bajpai, M. and Mishra, A. (2014), "Enhanced oral bioavailability of efavirenz by solid lipid nanoparticles: in vitro drug release and pharmacokinetics studies", *BioMed research international*, vol. 2014, pp. 363404.
- Gelperina, S., Kisich, K., Iseman, M. D. and Heifets, L. (2005), "The potential advantages of nanoparticle drug delivery systems in chemotherapy of tuberculosis", *American journal of respiratory and critical care medicine*, vol. 172, no. 12, pp. 1487.
- Gleiter, H. (2000), "Nanostructured materials: basic concepts and microstructure", *Acta materialia*, vol. 48, no. 1, pp. 1-29.
- Gomes, M. J., Martins, S., Ferreira, D., Segundo, M. A. and Reis, S. (2014), "Lipid nanoparticles for topical and transdermal application for alopecia treatment: development, physicochemical characterization, and in vitro release and

- penetration studies", *International journal of nanomedicine*, vol. 9, pp. 1231-1242.
- Ghorab, M. M., Abdel-Salam, H. M. and Abdel-Moaty, M. M. (2004), "Solid lipid nanoparticles-effect of lipid matrix and surfactant on their physical characteristics", *bulletin of pharmaceutical sciences-assiut university*, vol. 27, no. 1, pp. 155-160
- Gonzalez-Mira, E., Egea, M., Garcia, M. and Souto, E. (2010), "Design and ocular tolerance of flurbiprofen loaded ultrasound-engineered NLC", *Colloids and Surfaces B: Biointerfaces*, vol. 81, no. 2, pp. 412-421.
- Gosselin, P., Thibert, R., Preda, M. and McMullen, J. (2003), "Polymorphic properties of micronized carbamazepine produced by RESS", *International journal of pharmaceutics*, vol. 252, no. 1, pp. 225-233.
- Gray-Schopfer, V., Wellbrock, C. and Marais, R. (2007), "Melanoma biology and new targeted therapy", *Nature*, vol. 445, no. 7130, pp. 851-857.
- Guo, T., Zhang, Y., Zhao, J., Zhu, C. and Feng, N. (2015), "Nanostructured lipid carriers for percutaneous administration of alkaloids isolated from *Aconitum sinomontanum*", *Journal of nanobiotechnology*, vol. 13, no. 1, pp. 1.
- Gurr, J., Wang, A. S., Chen, C. and Jan, K. (2005), "Ultrafine titanium dioxide particles in the absence of photoactivation can induce oxidative damage to human bronchial epithelial cells", *Toxicology*, vol. 213, no. 1, pp. 66-73.
- Gustafson, D. L. and Page, R. L. (2013), "Cancer chemotherapy", *Withrow and MacEwen's Small Animal Clinical Oncology*, , pp. 157-179.
- Hadgraft, J. and Lane, M. E. (2005), "Skin permeation: the years of enlightenment", *International journal of pharmaceutics*, vol. 305, no. 1, pp. 2-12.
- Han, F., Li, S., Yin, R., Liu, H. and Xu, L. (2008), "Effect of surfactants on the formation and characterization of a new type of colloidal drug delivery system: nanostructured lipid carriers", *Colloids and Surfaces A: Physicochemical and Engineering Aspects*, vol. 315, no. 1, pp. 210-216.
- Han, G., Ghosh, P. and Rotello, V. M. (2007), "Functionalized gold nanoparticles for drug delivery",.
- Hanaor, D., Michelazzi, M., Leonelli, C. and Sorrell, C. C. (2012), "The effects of carboxylic acids on the aqueous dispersion and electrophoretic deposition of ZrO_2 ", *Journal of the European Ceramic Society*, vol. 32, no. 1, pp. 235-244.
- Hansson, J. (2010), "Familial cutaneous melanoma", in *Diseases of DNA Repair*, Springer, pp. 134-145.

- Helgason, T., Awad, T., Kristbergsson, K., McClements, D. J. and Weiss, J. (2009), "Effect of surfactant surface coverage on formation of solid lipid nanoparticles (SLN)", *Journal of colloid and interface science*, vol. 334, no. 1, pp. 75-81.
- Heydenreich, A., Westmeier, R., Pedersen, N., Poulsen, H. and Kristensen, H. (2003), "Preparation and purification of cationic solid lipid nanospheres—effects on particle size, physical stability and cell toxicity", *International journal of pharmaceutics*, vol. 254, no. 1, pp. 83-87.
- Honary, S. and Zahir, F. (2013), "Effect of zeta potential on the properties of nano-drug delivery systems-a review (Part 2)", *Tropical Journal of Pharmaceutical Research*, vol. 12, no. 2, pp. 265-273.
- Horner, M., Ries, L., Krapcho, M., Neyman, N., Aminou, R., Howlader, N., Altekruse, S., Feuer, E., Huang, L. and Mariotto, A. (2009), *SEER Cancer Statistics Review, 1975-2006*, National Cancer Institute. Bethesda, MD, .
- Hou, D., Xie, C., Huang, K. and Zhu, C. (2003), "The production and characteristics of solid lipid nanoparticles (SLNs)", *Biomaterials*, vol. 24, no. 10, pp. 1781-1785.
- How, C. W., Rasedee, A. and Abbasalipourkabir, R. (2013), "Characterization and cytotoxicity of nanostructured lipid carriers formulated with olive oil, hydrogenated palm oil, and polysorbate 80", *IEEE transactions on nanobioscience*, vol. 12, no. 2, pp. 72-78.
- Hu, F., Jiang, S., Du, Y., Yuan, H., Ye, Y. and Zeng, S. (2005), "Preparation and characterization of stearic acid nanostructured lipid carriers by solvent diffusion method in an aqueous system", *Colloids and Surfaces B: Biointerfaces*, vol. 45, no. 3, pp. 167-173.
- Hu, T., Zhang, C., Tang, Q., Su, Y., Li, B., Chen, L., Zhang, Z., Cai, T. and Zhu, Y. (2013), "Variant G6PD levels promote tumor cell proliferation or apoptosis via the STAT3/5 pathway in the human melanoma xenograft mouse model", *BMC cancer*, vol. 13, no. 1, pp. 1.
- Iqbal, M. A., Md, S., Sahni, J. K., Baboota, S., Dang, S. and Ali, J. (2012), "Nanostructured lipid carriers system: recent advances in drug delivery", *Journal of drug targeting*, vol. 20, no. 10, pp. 813-830.
- Ingrid L. Bergin and Frank A. Witzmann, G. V. (2013), " Nanoparticle toxicity by the gastrointestinal route: evidence and knowledge gaps ", *Journal of Int J Biomed Nanosci Nanotechnol*, vol. 3, no. 10, pp. 1-44.
- Irfan, A., Cauchi, M., Edmands, W., Gooderham, N. J., Njuguna, J. and Zhu, H. (2014), "Assessment of temporal dose-toxicity relationship of fumed silica nanoparticle in human lung A549 cells by conventional cytotoxicity and (1)H-NMR-based extracellular metabonomic assays", *Toxicological sciences : an official journal of the Society of Toxicology*, vol. 138, no. 2, pp. 354-364.

- ISO, (2008), *International Organization for Standardization. Technical Specification ISO/TS 27687:2008(E): Nanotechnologies–Terminology and Definitions for Nano-objects–Nanoparticle, Nanofibre and Nanoplate.*
- Izak-Nau, E., Voetz, M., Eiden, S., Duschl, A. and Puentes, V. F. (2013), "Altered characteristics of silica nanoparticles in bovine and human serum: the importance of nanomaterial characterization prior to its toxicological evaluation", *Particle and fibre toxicology*, vol. 10, no. 1, pp. 56-8977-10-56.
- Jain, S., Jain, V. and Mahajan, S. (2014), "Lipid based vesicular drug delivery systems", *Advances in pharmaceuticals*, vol. 2014.
- Jaiswal, J., Gupta, S. K. and Kreuter, J. (2004), "Preparation of biodegradable cyclosporine nanoparticles by high-pressure emulsification-solvent evaporation process", *Journal of Controlled Release*, vol. 96, no. 1, pp. 169-178.
- Jaiswal, P., Gidwani, B. and Vyas, A. (2016), "Nanostructured lipid carriers and their current application in targeted drug delivery", *Artificial cells, nanomedicine, and biotechnology*, vol. 44, no. 1, pp. 27-40.
- Janrao, K., Gadhve, M., Banerjee, S. and Gaikwad, D. (2014), "Nanoparticle induced nanotoxicity: an overview", *Asian Journal of Biomedical and Pharmaceutical Sciences*, vol. 4, no. 32, pp. 1.
- Jawahar, N., Meyyanathan, S., Reddy, G. and Sood, S. (2013), "Solid lipid nanoparticles for oral delivery of poorly soluble drugs", *ChemInform*, vol. 44, no. 27.
- Jenning, V. and Gohla, S. H. (2001), "Encapsulation of retinoids in solid lipid nanoparticles (SLN)", *Journal of microencapsulation*, vol. 18, no. 2, pp. 149-158.
- Jiang, G., Li, R., Sun, C., Liu, Y. and Zheng, J. (2014), "Dacarbazine combined targeted therapy versus dacarbazine alone in patients with malignant melanoma: A meta-analysis", *PloS one*, vol. 9, no. 12, pp. e111920.
- Jovanovic, P., Mihajlovic, M., Djordjevic-Jocic, J., Vlajkovic, S., Cekic, S. and Stefanovic, V. (2013), "Ocular melanoma: an overview of the current status", *International journal of clinical and experimental pathology*, vol. 6, no. 7, pp. 1230-1244.
- Kakumanu, S., Tagne, J. B., Wilson, T. A. and Nicolosi, R. J. (2011), "A nanoemulsion formulation of dacarbazine reduces tumor size in a xenograft mouse epidermoid carcinoma model compared to dacarbazine suspension", *Nanomedicine: Nanotechnology, Biology and Medicine*, vol. 7, no. 3, pp. 277-283.
- Kale, V. P., Amin, S. G. and Pandey, M. K. (2015), "Targeting ion channels for cancer therapy by repurposing the approved drugs", *Biochimica et Biophysica Acta (BBA)-Biomembranes*, vol. 1848, no. 10, pp. 2747-2755.

- Kanavy, H. E. and Gerstenblith, M. R. (2011), "Ultraviolet radiation and melanoma", *Seminars in cutaneous medicine and surgery*, Vol. 30, WB Saunders, pp. 222.
- Kang, K. W., Chun, M., Kim, O., Subedi, R. K., Ahn, S., Yoon, J. and Choi, H. (2010), "Doxorubicin-loaded solid lipid nanoparticles to overcome multidrug resistance in cancer therapy", *Nanomedicine: Nanotechnology, Biology and Medicine*, vol. 6, no. 2, pp. 210-213.
- Khan, S., Baboota, S., Ali, J., Khan, S., Narang, R. S. and Narang, J. K. (2015), "Nanostructured lipid carriers: An emerging platform for improving oral bioavailability of lipophilic drugs", *International journal of pharmaceutical investigation*, vol. 5, no. 4, pp. 182.
- Khurana, S., Bedi, P. and Jain, N. (2010), "Development of nanostructured lipid carriers (NLC) for controlled delivery of meloxicam", *International Journal of Biomedical Nanoscience and Nanotechnology*, vol. 1, no. 2-4, pp. 247-266.
- Koziel, M. J., Dudley, D., Afdhal, N., Grakoui, A., Rice, C. M., Choo, Q. L., Houghton, M. and Walker, B. D. (1995), "HLA class I-restricted cytotoxic T lymphocytes specific for hepatitis C virus. Identification of multiple epitopes and characterization of patterns of cytokine release", *The Journal of clinical investigation*, vol. 96, no. 5, pp. 2311-2321.
- Krysko, D. V., Berghe, T. V., D'Herde, K. and Vandenabeele, P. (2008), "Apoptosis and necrosis: detection, discrimination and phagocytosis", *Methods*, vol. 44, no. 3, pp. 205-221.
- Kržič, M., Šentjurec, M. and Kristl, J. (2001), "Improved skin oxygenation after benzyl nicotinate application in different carriers as measured by EPR oximetry in vivo", *Journal of Controlled Release*, vol. 70, no. 1, pp. 203-211.
- Kullavadee, K. O., Uracha, R. and Smith, S. M. (2012), "Effect of surfactant on characteristics of solid lipid nanoparticles (SLN)", *Advanced Materials Research*, vol. 364, Trans Tech Publ, pp. 313.
- Kumar, B., Singh, A. K., Prasad, R. K., Singh, C. S. and Dwivedi, V. (2016), "Formulation and Evaluation of an Injectable In-Situ Forming Hydrogel of Dacarbazine as Anticancer Agent", vol. 3, no. 1, pp. 100-108
- Kumar, S., Dilbaghi, N., Saharan, R. and Bhanjana, G. (2012), "Nanotechnology as emerging tool for enhancing solubility of poorly water-soluble drugs", *BioNanoScience*, vol. 2, no. 4, pp. 227-250.
- Kumari, A., Yadav, S. K. and Yadav, S. C. (2010), "Biodegradable polymeric nanoparticles based drug delivery systems", *Colloids and Surfaces B: Biointerfaces*, vol. 75, no. 1, pp. 1-18.
- Kumbhar, D. D. and Pokharkar, V. B. (2013), "Engineering of a nanostructured lipid carrier for the poorly water-soluble drug, bicalutamide: physicochemical

investigations", *Colloids and Surfaces A: Physicochemical and Engineering Aspects*, vol. 416, pp. 32-42.

Kwon, S., Singh, R. K., Perez, R. A., Abou Neel, E. A., Kim, H. and Chrzanowski, W. (2013), "Silica-based mesoporous nanoparticles for controlled drug delivery", *Journal of tissue engineering*, vol. 4, pp. 2041731413503357.

Lee, A. L., Wang, Y., Cheng, H. Y., Pervaiz, S. and Yang, Y. Y. (2009), "The co-delivery of paclitaxel and Herceptin using cationic micellar nanoparticles", *Biomaterials*, vol. 30, no. 5, pp. 919-927.

Lee, S., Meng, X. W., Flatten, K. S., Loegering, D. A. and Kaufmann, S. H. (2013), "Phosphatidylserine exposure during apoptosis reflects bidirectional trafficking between plasma membrane and cytoplasm", *Cell Death & Differentiation*, vol. 20, no. 1, pp. 64-76.

Legha, S. S., Ring, S., Bedikian, A., Plager, C., Eton, O., Buzaid, A. C. and Papadopoulos, N. (1996), "Treatment of metastatic melanoma with combined chemotherapy containing cisplatin, vinblastine and dacarbazine (CVD) and biotherapy using interleukin-2 and interferon-alpha", *Annals of Oncology: Official Journal of the European Society for Medical Oncology / ESMO*, vol. 7, no. 8, pp. 827-835.

Legha, S. S., Ring, S., Papadopoulos, N., Plager, C., Chawla, S. and Benjamin, R. (1989), "A prospective evaluation of a triple-drug regimen containing cisplatin, vinblastine, and dacarbazine (CVD) for metastatic melanoma", *Cancer*, vol. 64, no. 10, pp. 2024-2029.

Leiter, U. and Garbe, C. (2008), "Epidemiology of melanoma and nonmelanoma skin cancer—the role of sunlight", in *Sunlight, vitamin D and skin cancer*, Springer, , pp. 89-103.

Lepple-Wienhues, A., Berweck, S., Böhmig, M., Leo, C., Meyling, B., Garbe, C. and Wiederholt, M. (1996), "K channels and the intracellular calcium signal in human melanoma cell proliferation", *The Journal of membrane biology*, vol. 151, no. 2, pp. 149-157.

Li, B. and Ge, Z. (2012), "Nanostructured lipid carriers improve skin permeation and chemical stability of idebenone", *AAPS PharmSciTech*, vol. 13, no. 1, pp. 276-283.

Liberman, A., Mendez, N., Trogler, W. C. and Kummel, A. C. (2014), "Synthesis and surface functionalization of silica nanoparticles for nanomedicine", *Surface science reports*, vol. 69, no. 2, pp. 132-158.

Lim, W. M., Rajinikanth, P. S., Mallikarjun, C. and Kang, Y. B. (2014), "Formulation and delivery of itraconazole to the brain using a nanolipid carrier system", *International journal of nanomedicine*, vol. 9, pp. 2117-2126.

- Li, X., Chen, Y., Wang, M., Ma, Y., Xia, W. and Gu, H. (2013), "A mesoporous silica nanoparticle – PEI – Fusogenic peptide system for siRNA delivery in cancer therapy", *Biomaterials*, vol. 34, no. 4, pp. 1391-1401.
- Lin, X., Li, X., Zheng, L., Yu, L., Zhang, Q. and Liu, W. (2007), "Preparation and characterization of monocaprato nanostructured lipid carriers", *Colloids and Surfaces A: Physicochemical and Engineering Aspects*, vol. 311, no. 1, pp. 106-111.
- Linos, E., Swetter, S. M., Cockburn, M. G., Colditz, G. A. and Clarke, C. A. (2009), "Increasing burden of melanoma in the United States", *Journal of Investigative Dermatology*, vol. 129, no. 7, pp. 1666-1674.
- Lu, J., Liong, M., Sherman, S., Xia, T., Kovoichich, M., Nel, A. E., Zink, J. I. and Tamanoi, F. (2007), "Mesoporous silica nanoparticles for cancer therapy: energy-dependent cellular uptake and delivery of paclitaxel to cancer cells", *Nanobiotechnology*, vol. 3, no. 2, pp. 89-95.
- Lyklema, J. (2005), *Fundamentals of interface and colloid science: soft colloids*, Academic press.
- Ma, X. D. and Hao, Q. (2011), "Biodegradable methoxy poly (ethylene glycol)-poly (lactide) nanoparticles for controlled delivery of dacarbazine: preparation, characterization and anticancer activity evaluation", *African Journal of Pharmacy and Pharmacology*, vol. 5, no. 11, pp. 1369-1377.
- Ma, P. and Mumper, R. J. (2013), "Paclitaxel Nano-Delivery Systems: A Comprehensive Review", *Journal of nanomedicine & nanotechnology*, vol. 4, no. 2, pp. 1000164.
- Mahapatro, A. and Singh, D. K. (2011), "Biodegradable nanoparticles are excellent vehicle for site directed in-vivo delivery of drugs and vaccines", *Journal of nanobiotechnology*, vol. 9, no. 1, pp. 1.
- Malam, Y., Loizidou, M. and Seifalian, A. M. (2009), "Liposomes and nanoparticles: nanosized vehicles for drug delivery in cancer", *Trends in pharmacological sciences*, vol. 30, no. 11, pp. 592-599.
- Maldonado, R. A., LaMothe, R. A., Ferrari, J. D., Zhang, A. H., Rossi, R. J., Kolte, P. N., Griset, A. P., O'Neil, C., Altreuter, D. H., Browning, E., Johnston, L., Farokhzad, O. C., Langer, R., Scott, D. W., von Andrian, U. H. and Kishimoto, T. K. (2015), "Polymeric synthetic nanoparticles for the induction of antigen-specific immunological tolerance", *Proceedings of the National Academy of Sciences of the United States of America*, vol. 112, no. 2, pp. E156-65.
- Manke, A., Wang, L. and Rojanasakul, Y. (2013), "Mechanisms of nanoparticle-induced oxidative stress and toxicity", *BioMed research international*, vol. 2013, pp. 942916.

- Martin, K. (2007), "The chemistry of silica and its potential health benefits", *The journal of nutrition, health & aging*, vol. 11, no. 2, pp. 94.
- Martinho, N., Damgé, C. and Reis, C. P. (2011), "Recent advances in drug delivery systems", *Journal of biomaterials and nanobiotechnology*, vol. 2, no. 05, pp. 510.
- Maverakis, E., Cornelius, L. A., Bowen, G. M., Phan, T., Patel, F. B., Fitzmaurice, S., He, Y., Burrall, B., Duong, C. and Kloxin, A. M. (2015), "Metastatic melanoma—a review of current and future treatment options", *Acta Dermato-Venereologica*, vol. 95, no. 5, pp. 516-527.
- Mehnert, W. and Mäder, K. (2001), "Solid lipid nanoparticles: production, characterization and applications", *Advanced Drug Delivery Reviews*, vol. 47, no. 2, pp. 165-196.
- Mirza, A. Z. and Siddiqui, F. A. (2014), "Nanomedicine and drug delivery: a mini review", *International Nano Letters*, vol. 4, no. 1, pp. 1-7.
- Mitrea, E., Ott, C. and Meghea, A. (2014), "New Approaches on the Synthesis of Effective Nanostructured Lipid Carriers", *Revista de Chimie*, vol. 65, no. 1, pp. 50-55.
- Mocellin, S. and Rossi, C. R. (2008), "The melanoma molecular map project", *Melanoma research*, vol. 18, no. 3, pp. 163-165.
- Moser, K., Kriwet, K., Naik, A., Kalia, Y. N. and Guy, R. H. (2001), "Passive skin penetration enhancement and its quantification in vitro", *European Journal of Pharmaceutics and Biopharmaceutics*, vol. 52, no. 2, pp. 103-112.
- Mu, Q., Hondow, N. S., Krzemiński, T., Brown, A. P., Jeuken, L. J. C. and Routledge, M. N. (2012), "Mechanism of cellular uptake of genotoxic silica nanoparticles", *Particle and Fibre Toxicology*, vol. 9.
- Mukherjee, S., Ray, S. and Thakur, R. S. (2009), "Solid lipid nanoparticles: a modern formulation approach in drug delivery system", *Indian journal of pharmaceutical sciences*, vol. 71, no. 4, pp. 349-358.
- Müller, R. H., Radtke, M. and Wissing, S. A. (2002), "Solid lipid nanoparticles (SLN) and nanostructured lipid carriers (NLC) in cosmetic and dermatological preparations", *Advanced Drug Delivery Reviews*, vol. 54, pp. S131-S155.
- Müller, R., Souto, E. and Radtke, M. (2000), "PCT application PCT", *EP00/04111*, .
- Napierska, D., Thomassen, L. C., Lison, D., Martens, J. A. and Hoet, P. H. (2010), "The nanosilica hazard: another variable entity", *Particle and fibre toxicology*, vol. 7, no. 1, pp. 39.
- Naseri, N., Valizadeh, H. and Zakeri-Milani, P. (2015), "Solid lipid nanoparticles and nanostructured lipid carriers: structure, preparation and application", *Advanced pharmaceutical bulletin*, vol. 5, no. 3, pp. 305.

- Neale, R. E., Davis, M., Pandeya, N., Whiteman, D. C. and Green, A. C. (2007), "Basal cell carcinoma on the trunk is associated with excessive sun exposure", *Journal of the American Academy of Dermatology*, vol. 56, no. 3, pp. 380-386.
- Nemmar, A., Hoylaerts, M. F., Hoet, P. H., Dinsdale, D., Smith, T., Xu, H., Vermynen, J. and Nemery, B. (2002), "Ultrafine particles affect experimental thrombosis in an in vivo hamster model", *American journal of respiratory and critical care medicine*, vol. 166, no. 7, pp. 998-1004.
- Nerlich, B., Clarke, D. D. and Ulph, F. (2007), "Risks and benefits of nanotechnology: How young adults perceive possible advances in nanomedicine compared with conventional treatments", *Health, Risk & Society*, vol. 9, no. 2, pp. 159-171.
- Ng, W. K., Saiful Yazan, L., Yap, L. H., Wan Nor Hafiza, Wan Abd Ghani, How, C. W. and Abdullah, R. (2015), "Thymoquinone-loaded nanostructured lipid carrier exhibited cytotoxicity towards breast cancer cell lines (MDA-MB-231 and MCF-7) and cervical cancer cell lines (HeLa and SiHa)", *BioMed research international*, vol. 2015.
- Nimtrakul, P., Tiyaboonchai, W. and Lamlerthton, S. (2016), "Effect of types of solid lipids on the physicochemical properties and self-aggregation of amphotericin B loaded nanostructured lipid carriers (NLCs)", *asian journal of pharmaceutical sciences*, vol. 11, no. 1, pp. 172-173.
- Oberdorster, E. (2004), "Manufactured nanomaterials (fullerenes, C60) induce oxidative stress in the brain of juvenile largemouth bass", *Environmental health perspectives*, vol. 112, no. 10, pp. 1058-1062.
- Ohshio, G., Hosotani, R., Imamura, M., Sakahara, H., Ochi, J. and Kubota, N. (1998), "Gastrinoma with multiple liver metastases: effectiveness of dacarbazine (DTIC) therapy", *Journal of Hepato-Biliary-Pancreatic Sciences*, vol. 5, no. 3, pp. 339-343.
- Onoue, S., Yamada, S. and Chan, H. K. (2014), "Nanodrugs: pharmacokinetics and safety", *International journal of nanomedicine*, vol. 9, pp. 1025-1037.
- Orrenius, S., Nicotera, P. and Zhivotovsky, B. (2010), "Cell death mechanisms and their implications in toxicology", *Toxicological Sciences*, vol. 119, no. 1, pp. 3-19.
- Orrenius, S., Zhivotovsky, B. and Nicotera, P. (2003), "Regulation of cell death: the calcium–apoptosis link", *Nature reviews Molecular cell biology*, vol. 4, no. 7, pp. 552-565.
- Overgaard, J., Bentzen, S., Gonzalez, D. G., Hulshof, M., Arcangeli, G., Dahl, O. and Mella, O. (1995), "Randomised trial of hyperthermia as adjuvant to radiotherapy for recurrent or metastatic malignant melanoma", *The Lancet*, vol. 345, no. 8949, pp. 540-543.

- Pal, S. L., Jana, U., Manna, P. K., Mohanta, G. P. and Manavalan, R. (2011), "Nanoparticle: An overview of preparation and characterization (2000-2010).", .
- Panyam, J. and Labhasetwar, V. (2003), "Biodegradable nanoparticles for drug and gene delivery to cells and tissue", *Advanced Drug Delivery Reviews*, vol. 55, no. 3, pp. 329-347.
- Paolino, D., Sinha, P., Fresta, M. and Ferrari, M. (2006), "Drug delivery systems", *Encyclopedia of Medical Devices and Instrumentation*, .
- Pardo, L. A. (2004), "Voltage-gated potassium channels in cell proliferation", *Physiology (Bethesda, Md.)*, vol. 19, pp. 285-292.
- Park, H. S. and Cho, K. H. (2010), "Acral lentiginous melanoma in situ: a diagnostic and management challenge", *Cancers*, vol. 2, no. 2, pp. 642-652.
- Patel, D., Dasgupta, S., Dey, S., Roja Ramani, Y., Ray, S. and Mazumder, B. (2012), "Nanostructured lipid carriers (NLC)-based gel for the topical delivery of aceclofenac: preparation, characterization, and in vivo evaluation", *Scientia pharmaceutica*, vol. 80, no. 3, pp. 749-764.
- Patel, D., Qasgupta, S., Dey, S., Roja Ramani, Y., Ray, S. and Mazumder, B. (2012), "Nanostructured Lipid Carriers (NLC)-Based Gel for Topical Delivery of Aceclofenac: Preparation, Characterization and In Vivo Evaluation", *Scientia pharmaceutica*, vol. 80, no. 3, pp. 749.
- Patel, K., Solanki, N. and Solanki, S. (2015), "Nanostructured lipid carrier—a novel drug delivery", *J.Pharm.Sci.Bioscientific Res.*, vol. 5, pp. 385-392.
- Pathak, P. and Nagarsenker, M. (2009), "Formulation and evaluation of lidocaine lipid nanosystems for dermal delivery", *AAPS PharmSciTech*, vol. 10, no. 3, pp. 985-992.
- Pathak, R. K., Kolishetti, N. and Dhar, S. (2015), "Targeted nanoparticles in mitochondrial medicine", *Wiley Interdisciplinary Reviews: Nanomedicine and Nanobiotechnology*, vol. 7, no. 3, pp. 315-329.
- Patidar, A., Thakur, D. S., Kumar, P. and Verma, J. (2010), "A review on novel lipid based nanocarriers", *International Journal of Pharmacy and Pharmaceutical Sciences*, vol. 2, no. 4, pp. 30-35.
- Pardeike, J., Hommoss, A. and Müller, R. H. (2009), "Lipid nanoparticles (SLN, NLC) in cosmetic and pharmaceutical dermal products", *International journal of pharmaceutics*, vol. 366, no. 1–2, pp. 170-184.
- Paunov, V., Kralchevsky, P., Denkov, N. and Nagayama, K. (1993), "Lateral capillary forces between floating submillimeter particles", *Journal of colloid and interface science*, vol. 157, no. 1, pp. 100-112.

- Phan, G. Q., Attia, P., Steinberg, S. M., White, D. E. and Rosenberg, S. A. (2001), "Factors associated with response to high-dose interleukin-2 in patients with metastatic melanoma", *Journal of clinical oncology : official journal of the American Society of Clinical Oncology*, vol. 19, no. 15, pp. 3477-3482.
- Pizzol, C. D., Filippin-Monteiro, F. B., Restrepo, J. A. S., Pittella, F., Silva, A. H., Alves de Souza, P., Machado de Campos, A. and Creczynski-Pasa, T. B. (2014), "Influence of surfactant and lipid type on the physicochemical properties and biocompatibility of solid lipid nanoparticles", *International journal of environmental research and public health*, vol. 11, no. 8, pp. 8581-8596.
- Poonia, N., Kharb, R., Lather, V. and Pandita, D. (2016), "Nanostructured lipid carriers: versatile oral delivery vehicle", *Future science OA*, vol. 2, no. 3, pp. FSO135.
- Porter, A. E., Muller, K., Skepper, J., Midgley, P. and Welland, M. (2006), "Uptake of C₆₀ by human monocyte macrophages, its localization and implications for toxicity: Studied by high resolution electron microscopy and electron tomography", *Acta Biomaterialia*, vol. 2, no. 4, pp. 409-419.
- Prego, C., Alonso, S., Vila, A., Torres, D., Remunan-Lopez, C. and Alonso, M. (2005), "Nanomedicines for overcoming biological barriers: Nanoparticles as a carrier for intestinal drug absorption", *2nd NanoSpain workshop, Barcelona, Spain*, pp. 14.
- Priano, L., Zara, G. P., El-Assawy, N., Cattaldo, S., Muntoni, E., Milano, E., Serpe, L., Musicanti, C., Pérot, C. and Gasco, M. R. (2011), "Baclofen-loaded solid lipid nanoparticles: preparation, electrophysiological assessment of efficacy, pharmacokinetic and tissue distribution in rats after intraperitoneal administration", *European Journal of Pharmaceutics and Biopharmaceutics*, vol. 79, no. 1, pp. 135-141.
- Puglia, C. and Bonina, F. (2012), "Lipid nanoparticles as novel delivery systems for cosmetics and dermal pharmaceuticals", *Expert Opinion on Drug Delivery*, vol. 9, no. 4, pp. 429-441.
- Puglia, C., Blasi, P., Rizza, L., Schoubben, A., Bonina, F., Rossi, C. and Ricci, M. (2008), "Lipid nanoparticles for prolonged topical delivery: An in vitro and in vivo investigation", *International journal of pharmaceutics*, vol. 357, no. 1-2, pp. 295-304.
- Puri, A., Loomis, K., Smith, B., Lee, J., Yavlovich, A., Heldman, E. and Blumenthal, R. (2009), "Lipid-based nanoparticles as pharmaceutical drug carriers: from concepts to clinic", *Critical Reviews™ in Therapeutic Drug Carrier Systems*, vol. 26, no. 6.
- Purohit, D. K. (2016), "Nano-lipid Carriers for Topical Application: Current Scenario", *Asian Journal of Pharmaceutics (AJP): Free full text articles from Asian J Pharm*, vol. 10, no. 1.

- Quirin, C., Mainka, A., Hesse, A. and Nettelbeck, D. M. (2007), "Combining adenoviral oncolysis with temozolomide improves cell killing of melanoma cells", *International Journal of Cancer*, vol. 121, no. 12, pp. 2801-2807.
- Rahman, M. (2006), "Introduction to flow cytometry", *AbD serotec*,.
- Rahman, H. S., Rasedee, A., How, C. W., Abdul, A. B., Zeenathul, N. A., Othman, H. H., Saeed, M. I. and Yeap, S. K. (2013), "Zerumbone-loaded nanostructured lipid carriers: preparation, characterization, and antileukemic effect", *International journal of nanomedicine*, vol. 8, pp. 2769-2781.
- Rao, V. R., Perez-Neut, M., Kaja, S. and Gentile, S. (2015), "Voltage-gated ion channels in cancer cell proliferation", *Cancers*, vol. 7, no. 2, pp. 849-875.
- Rigon, R. B., Oyafuso, M. H., Fujimura, A. T., Goncalvez, M. L., do Prado, A. H., Gremiao, M. P. and Chorilli, M. (2015), "Nanotechnology-Based Drug Delivery Systems for Melanoma Antitumoral Therapy: A Review", *BioMed research international*, vol. 2015, pp. 841817.
- Rizwanullah, M., Ahmad, J. and Amin, S. (2016), "Nanostructured Lipid Carriers: A Novel Platform for Chemotherapeutics", *Current drug delivery*, vol. 13, no. 1, pp. 4-26.
- Rothen-Rutishauser, B. M., Schürch, S., Haenni, B., Kapp, N. and Gehr, P. (2006), "Interaction of fine particles and nanoparticles with red blood cells visualized with advanced microscopic techniques", *Environmental science & technology*, vol. 40, no. 14, pp. 4353-4359.
- Sajanlal, P. R., Sreeprasad, T. S., Samal, A. K. and Pradeep, T. (2011), "Anisotropic nanomaterials: structure, growth, assembly, and functions", *Nano Reviews & Experiments*, vol. 2.
- Sanad, R. A., AbdelMalak, N. S. and Badawi, A. A. (2010), "Formulation of a novel oxybenzone-loaded nanostructured lipid carriers (NLCs)", *AAPS PharmSciTech*, vol. 11, no. 4, pp. 1684-1694.
- Sanap, G. S. and Mohanta, G. P. (2013), "Design and evaluation of miconazole nitrate loaded nanostructured lipid carriers (NLC) for improving the antifungal therapy", *Journal of Applied Pharmaceutical Science*, vol. 3, no. 1, pp. 46.
- Sarmiento, B., Mazzaglia, D., Bonferoni, M. C., Neto, A. P., do Céu Monteiro, M. and Seabra, V. (2011), "Effect of chitosan coating in overcoming the phagocytosis of insulin loaded solid lipid nanoparticles by mononuclear phagocyte system", *Carbohydrate Polymers*, vol. 84, no. 3, pp. 919-925.
- Saroj, S., Baby, D. A. and Sabitha, M. (2012), "Current trends in lipid based delivery systems and its applications in drug delivery", *Asian Journal of Pharmaceutical and Clinical Research*, vol. 5, no. SUPPL. 3, pp. 4-9.

- Satvati, H. R. and Lotfollahi, M. N. (2011), "Effects of extraction temperature, extraction pressure and nozzle diameter on micronization of cholesterol by RESS process", *Powder Technology*, vol. 210, no. 2, pp. 109-114.
- Saupe, A., Gordon, K. C. and Rades, T. (2006), "Structural investigations on nanoemulsions, solid lipid nanoparticles and nanostructured lipid carriers by cryo-field emission scanning electron microscopy and Raman spectroscopy", *International journal of pharmaceutics*, vol. 314, no. 1, pp. 56-62.
- Sawant, K. K., Varia, J. K. and Dodiya, S. S. (2008), "Cyclosporine a loaded solid lipid nanoparticles: optimization of formulation, process variable and characterization", *Current Drug Delivery*, vol. 5, no. 1, pp. 64-69.
- Schäfer-Korting, M., Mehnert, W. and Korting, H. (2007), "Lipid nanoparticles for improved topical application of drugs for skin diseases", *Advanced Drug Delivery Reviews*, vol. 59, no. 6, pp. 427-443.
- Scherer, D. and Kumar, R. (2010), "Genetics of pigmentation in skin cancer—a review", *Mutation Research/Reviews in Mutation Research*, vol. 705, no. 2, pp. 141-153.
- Schneider, M., Stracke, F., Hansen, S. and Schaefer, U. F. (2009), "Nanoparticles and their interactions with the dermal barrier", *Dermato-endocrinology*, vol. 1, no. 4, pp. 197-206.
- Selvamuthukumar, S. and Velmurugan, R. (2012), "Nanostructured lipid carriers: a potential drug carrier for cancer chemotherapy", *Lipids in health and disease*, vol. 11, no. 1, pp. 1.
- Shah, R., Eldridge, D., Palombo, E. and Harding, I. (2014), "Optimisation and stability assessment of solid lipid nanoparticles using particle size and zeta potential", *Journal of Physical Science*, vol. 25, no. 1, pp. 59.
- Shao, Z., Shao, J., Tan, B., Guan, S., Liu, Z., Zhao, Z., He, F. and Zhao, J. (2015), "Targeted lung cancer therapy: preparation and optimization of transferrin-decorated nanostructured lipid carriers as novel nanomedicine for co-delivery of anticancer drugs and DNA", *International journal of nanomedicine*, vol. 10, pp. 1223-1233.
- Sharma, A. and Kakkar, A. (2015), "Designing Dendrimer and Miktoarm Polymer Based Multi-Tasking Nanocarriers for Efficient Medical Therapy", *Molecules*, vol. 20, no. 9, pp. 16987-17015.
- Sharma, P., Dube, B. and Sawant, K. (2011), "Development and evaluation of nanostructured lipid carriers of cytarabine for treatment of meningeal leukemia", *Journal of nanoscience and nanotechnology*, vol. 11, no. 8, pp. 6676-6682.
- Shaw, S. Y., Westly, E. C., Pittet, M. J., Subramanian, A., Schreiber, S. L. and Weissleder, R. (2008), "Perturbational profiling of nanomaterial biologic

activity", *Proceedings of the National Academy of Sciences*, vol. 105, no. 21, pp. 7387-7392.

Shete, H., Chatterjee, S., De, A. and Patravale, V. (2013), "Long chain lipid based tamoxifen NLC. Part II: Pharmacokinetic, biodistribution and in vitro anticancer efficacy studies", *International journal of pharmaceutics*, vol. 454, no. 1, pp. 584-592.

Shinde, G., Rajesh, K., Prajapati, N. and Murthy, R. (2013), "Formulation, development, and characterization of nanostructured lipid carrier (NLC) loaded gel for psoriasis", *Pharm Lett*, vol. 5, pp. 13-25.

Shrestha, H., Bala, R. and Arora, S. (2014), "Lipid-based drug delivery systems", *Journal of pharmaceutics*, vol. 2014.

Silva, A., González-Mira, E., García, M., Egea, M., Fonseca, J., Silva, R., Santos, D., Souto, E. and Ferreira, D. (2011), "Preparation, characterization and biocompatibility studies on risperidone-loaded solid lipid nanoparticles (SLN): high pressure homogenization versus ultrasound", *Colloids and Surfaces B: Biointerfaces*, vol. 86, no. 1, pp. 158-165.

Silva, A., Santos, D., Ferreira, D. and Souto, E. (2009), "Minoxidil-loaded nanostructured lipid carriers (NLC): characterization and rheological behaviour of topical formulations", *Die Pharmazie-An International Journal of Pharmaceutical Sciences*, vol. 64, no. 3, pp. 177-182.

Silva, E. L., Carneiro, G., Caetano, P. A., Goulart, G., Ferreira Costa, D., de Souza-Fagundes, E. M., Gomes, D. A. and Ferreira, L. A. M. (2015), "Nanostructured lipid carriers loaded with tributyrin as an alternative to improve anticancer activity of all-trans retinoic acid", *Expert review of anticancer therapy*, vol. 15, no. 2, pp. 247-256.

Simovic, S., Ghouchi-Eskandar, N., Moom Sinn, A., Losic, D. and A Prestidge, C. (2011), "Silica materials in drug delivery applications", *Current Drug Discovery Technologies*, vol. 8, no. 3, pp. 250-268.

Singhal, G. B., Patel, R. P., Prajapati, B. and Patel, N. A. (2011), "Solid lipid nanoparticles and nano lipid carriers: as novel solid lipid based drug carrier", *Int Res J Pharm*, vol. 2, no. 2, pp. 20-52.

Sinha, N. N. and Munichandraiah, N. (2009), "Synthesis and characterization of carbon-coated $\text{LiNi}_{1/3}\text{Co}_{1/3}\text{Mn}_{1/3}\text{O}_2$ in a single step by an inverse microemulsion route", *ACS applied materials & interfaces*, vol. 1, no. 6, pp. 1241-1249.

Smith, A. (1986), "Evaluation of poly (lactic acid) as a biodegradable drug delivery system for parenteral administration", *International journal of pharmaceutics*, vol. 30, no. 2-3, pp. 215-220.

- Soengas, M. S. and Lowe, S. W. (2003), "Apoptosis and melanoma chemoresistance", *Oncogene*, vol. 22, no. 20, pp. 3138-3151.
- Sonam, Chaudhary, H., Arora, V., Kholi, K. and Kumar, V. (2013), "Effect of physicochemical properties of biodegradable polymers on nano drug delivery", *Polymer Reviews*, vol. 53, no. 4, pp. 546-567.
- Song, C. and Liu, S. (2005), "A new healthy sunscreen system for human: Solid lipid nanoparticles as carrier for 3, 4, 5-trimethoxybenzoylchitin and the improvement by adding Vitamin E", *International journal of biological macromolecules*, vol. 36, no. 1, pp. 116-119.
- Song, S. H., Lee, K. M., Kang, J. B., Lee, S. G., Kang, M. J. and Choi, Y. W. (2014), "Improved skin delivery of voriconazole with a nanostructured lipid carrier-based hydrogel formulation", *Chemical and Pharmaceutical Bulletin*, vol. 62, no. 8, pp. 793-798.
- Souza, L., Silva, E., Martins, A., Mota, M., Braga, R., Lima, E., Valadares, M., Taveira, S. and Marreto, R. (2011), "Development of topotecan loaded lipid nanoparticles for chemical stabilization and prolonged release", *European Journal of Pharmaceutics and Biopharmaceutics*, vol. 79, no. 1, pp. 189-196.
- Stewart, B. and Wild, C. P. (2015), "World cancer report 2014", *World*, .
- Suh, H. and Jun, H. (1996), "Effectiveness and mode of action of isopropyl myristate as a permeation enhancer for naproxen through shed snake skin", *Journal of pharmacy and pharmacology*, vol. 48, no. 8, pp. 812-816.
- Sütő, B., Berkó, S., Kozma, G., Kukovecz, Á., Budai-Szűcs, M., Erős, G., Kemény, L., Sztojkov-Ivanov, A., Gáspár, R. and Csányi, E. (2016), "Development of ibuprofen-loaded nanostructured lipid carrier-based gels: characterization and investigation of in vitro and in vivo penetration through the skin", *International journal of nanomedicine*, vol. 11, pp. 1201.
- Tamjidi, F., Shahedi, M., Varshosaz, J. and Nasirpour, A. (2013), "Nanostructured lipid carriers (NLC): A potential delivery system for bioactive food molecules", *Innovative Food Science & Emerging Technologies*, vol. 19, pp. 29-43.
- Tang, C., Zhu, J., Zhou, Q., Wei, J., Zhu, R. and He, H. (2014), "Surface heterogeneity of SiO₂ polymorphs: an XPS investigation of α -quartz and α -cristobalite", *The Journal of Physical Chemistry C*, vol. 118, no. 45, pp. 26249-26257.
- Taratula, O., Kuzmov, A., Shah, M., Garbuzenko, O. B. and Minko, T. (2013), "Nanostructured lipid carriers as multifunctional nanomedicine platform for pulmonary co-delivery of anticancer drugs and siRNA", *Journal of Controlled Release*, vol. 171, no. 3, pp. 349-357.
- Tas, F. (2012), "Metastatic behavior in melanoma: timing, pattern, survival, and influencing factors", *Journal of oncology*, vol. 2012.

- Teeranachaideekul, V., Müller, R. H. and Junyaprasert, V. B. (2007), "Encapsulation of ascorbyl palmitate in nanostructured lipid carriers (NLC)—effects of formulation parameters on physicochemical stability", *International journal of pharmaceuticals*, vol. 340, no. 1, pp. 198-206.
- Thakkar, H. P., Desai, J. L. and Parmar, M. P. (2014), "Application of Box-Behnken design for optimization of formulation parameters for nanostructured lipid carriers of candesartan cilexetil", *Asian Journal of Pharmaceutics (AJP): Free full text articles from Asian J Pharm*, vol. 8, no. 2.
- Thatipamula, R., Palem, C., Gannu, R., Mudragada, S. and Yamsani, M. (2011), "Formulation and in vitro characterization of domperidone loaded solid lipid nanoparticles and nanostructured lipid carriers", *Daru*, vol. 19, no. 1, pp. 23-32.
- Tofani, R. P., Sumirtapura, Y. C. and Darijanto, S. T. (2016), "Formulation, Characterisation, and in Vitro Skin Diffusion of Nanostructured Lipid Carriers for Deoxyarbutin Compared to a Nanoemulsion and Conventional Cream", *Scientia pharmaceutica*, vol. 84, no. 4, pp. 634-645.
- Trotta, M., Debernardi, F. and Caputo, O. (2003), "Preparation of solid lipid nanoparticles by a solvent emulsification–diffusion technique", *International journal of pharmaceuticals*, vol. 257, no. 1, pp. 153-160.
- Tsao, H., Atkins, M. B. and Sober, A. J. (2004), "Management of cutaneous melanoma", *New England Journal of Medicine*, vol. 351, no. 10, pp. 998-1012.
- Türeli, A. E. (2015), *Nanoparticle preparation process using novel microjet reactor technology for enhancing dissolution rates of poorly water soluble drugs*, .
- Üner, M. and Yener, G. (2007), "Importance of solid lipid nanoparticles (SLN) in various administration routes and future perspectives", *International journal of nanomedicine*, vol. 2, no. 3, pp. 289-300.
- Velmurugan, R. and Selvamuthukumar, S. (2016), "Development and optimization of ifosfamide nanostructured lipid carriers for oral delivery using response surface methodology", *Applied Nanoscience*, vol. 6, no. 2, pp. 159-173.
- Vitorino, C., Carvalho, F. A., Almeida, A. J., Sousa, J. J. and Pais, A. A. (2011), "The size of solid lipid nanoparticles: an interpretation from experimental design", *Colloids and Surfaces B: Biointerfaces*, vol. 84, no. 1, pp. 117-130.
- Wa Kasongo, K., Shegokar, R., Müller, R. H. and Walker, R. B. (2011), "Formulation development and in vitro evaluation of didanosine-loaded nanostructured lipid carriers for the potential treatment of AIDS dementia complex", *Drug development and industrial pharmacy*, vol. 37, no. 4, pp. 396-407.
- Wagner, V., Dullaart, A., Bock, A. and Zweck, A. (2006), "The emerging nanomedicine landscape", *Nature biotechnology*, vol. 24, no. 10, pp. 1211-1218.

- Wang, B., Feng, W., Zhao, Y., Xing, G., Chai, Z., Wang, H. and Jia, G. (2005), "Status of study on biological and toxicological effects of nanoscale materials", *Science in China Series B: Chemistry*, vol. 48, no. 5, pp. 385-394.
- Wang, Z. (2004), "Roles of K channels in regulating tumour cell proliferation and apoptosis", *Pflügers Archiv*, vol. 448, no. 3, pp. 274-286.
- Wang, Z., Wu, J., Chen, T., Zhou, Q. and Wang, Y. (2015), "In vitro and in vivo antitumor efficacy of berberine-nanostructured lipid carriers against H22 tumor", *SPIE BiOS*, International Society for Optics and Photonics, pp. 93240Y.
- Warren, B. E. (1969), *X-ray Diffraction*, Courier Corporation.
- Wiechers, J. W. and Souto, E. B. (2010), "Delivering actives via solid lipid nanoparticles and nanostructured lipid carriers: Part I", *Cosmetics and Toiletries*, vol. 125, no. 10.
- Williams, A. C. and Barry, B. W. (2012), "Penetration enhancers", *Advanced Drug Delivery Reviews*, .
- Williams, D. B. and Carter, C. B. (1996), "The transmission electron microscope", in *Transmission electron microscopy*, Springer, , pp. 3-17.
- Wonderlin, W. and Strobl, J. (1996), "Potassium channels, proliferation and G1 progression", *Journal of Membrane Biology*, vol. 154, no. 2, pp. 91-107.
- Woodward, R. M., Wallace, V. P., Pye, R. J., Cole, B. E., Arnone, D. D., Linfield, E. H. and Pepper, M. (2003), "Terahertz pulse imaging of ex vivo basal cell carcinoma", *Journal of Investigative Dermatology*, vol. 120, no. 1, pp. 72-78.
- Xia, Q. and Wu, J. Y. (2011), "Preparation and Characterization of Coenzyme Q10-Loaded Nanostructured Lipid Carriers", *Materials Science Forum*, Vol. 694, Trans Tech Publ, pp. 170.
- Xie, S., Zhu, L., Dong, Z., Wang, X., Wang, Y., Li, X. and Zhou, W. (2011), "Preparation, characterization and pharmacokinetics of enrofloxacin-loaded solid lipid nanoparticles: influences of fatty acids", *Colloids and Surfaces B: Biointerfaces*, vol. 83, no. 2, pp. 382-387.
- Yakobson, B. I. and Smalley, R. E. (1997), "Fullerene nanotubes: C 1,000,000 and beyond: Some unusual new molecules—long, hollow fibers with tantalizing electronic and mechanical properties—have joined diamonds and graphite in the carbon family", *American Scientist*, vol. 85, no. 4, pp. 324-337.
- Yang, Y., Corona, A., Schubert, B., Reeder, R. and Henson, M. A. (2014), "The effect of oil type on the aggregation stability of nanostructured lipid carriers", *Journal of colloid and interface science*, vol. 418, pp. 261-272.

- Yang, Z., Liu, Z., Allaker, R., Reip, P., Oxford, J., Ahmad, Z. and Reng, G. (2013), "A review of nanoparticle functionality and toxicity on the central nervous system", in *Nanotechnology, the Brain, and the Future*, Springer, , pp. 313-332.
- Yassin, A. E. B., Anwer, M. K., Mowafy, H. A., El-Bagory, I. M., Bayomi, M. A. and Alsarra, I. A. (2010), "Optimization of 5-fluorouracil solid-lipid nanoparticles: a preliminary study to treat colon cancer", *International journal of medical sciences*, vol. 7, no. 6, pp. 398.
- Yue, X., Niu, M., Zhang, T., Wang, C., Wang, Z., Wu, W., Zhang, Q., Lai, C. and Zhou, L. (2016), "In vivo evaluation of a simvastatin-loaded nanostructured lipid carrier for bone tissue regeneration", *Nanotechnology*, vol. 27, no. 11, pp. 115708.
- Zhai, H. and Maibach, H. I. (2001), "Effects of skin occlusion on percutaneous absorption: an overview", *Skin Pharmacology and Physiology*, vol. 14, no. 1, pp. 1-10.
- Zhang, Y., Li, Y., Lv, Y. and Wang, J. (2015), "Effect of curcumin on the proliferation, apoptosis, migration, and invasion of human melanoma A375 cells", *Genet Mol Res*, vol. 14, no. 1, pp. 1056-1067.
- Zhou, J. and Zhou, D. (2015), "Improvement of oral bioavailability of lovastatin by using nanostructured lipid carriers", *Drug design, development and therapy*, vol. 9, pp. 5269.
- Zhu, H., Irfan, A., Sachse, S. and Njuguna, J. (2012), "Assessment of nanoparticle release and associated health effect of polymer-silicon composites", *IOP Conference Series: Materials Science and Engineering*, Vol. 40, IOP Publishing, pp. 012015.
- Zhu, Y., Li, J., Li, W., Zhang, Y., Yang, X., Chen, N., Sun, Y., Zhao, Y., Fan, C. and Huang, Q. (2012), "The biocompatibility of nanodiamonds and their application in drug delivery systems", *Theranostics*, vol. 2, no. 3, pp. 302.
- Zur Mühlen, A., Zur Mühlen, E., Niehus, H. and Mehnert, W. (1996), "Atomic force microscopy studies of solid lipid nanoparticles", *Pharmaceutical research*, vol. 13, no. 9, pp. 1411-1416.

APPENDICES

i. Appendix A

Characterization of silica nanoparticles

Introduction

In order to establish the methods of the characterization and cytotoxicity assessment, given size of silica nanoparticles SiNP20 and SiNP200, from Sigma Aldrich, were studied in chemophysical properties and their effects on A375 melanoma cells. The methods were involved particles size by Nanoparticles Tracking Analysis (NTA); particles size and polydispersity index (PDI) by Dynamic Light Scattering (DLS); zeta potential by Zetasizer; particles morphology by Transmission Electron Microscopy (TEM), and *in vitro* cytotoxicity study of SiNP20/SiNP200 by using MTT assay for cell viability and flowcytometry for cell apoptosis assessment. These methods were used later for NLC characterization and cell toxicity.

Characteristic of silica nanoparticles size, dispersity, stability and morphology

The Dynamic Light Scattering (DLS) was used to measure the silica particle size and the particles dispersity in colloidal system. The resultant hydrodynamic size of the silica particles (SiNP20 and SiNP200) in the colloidal system were compared with their given size (Table 1).

Table 1: Characteristics of colloidal silica (see Appendices C, for full Sigma Aldrich and Postnova Analytics specification sheets).

	SiNP20	SMP200
Manufacturer	Sigma-Aldrich	Postnova Analytics
Given size (nm)	20 nm	200 nm
Surface area (m²/g)	198-258	15

The measurements for SiNP20 and SiNP200 were applied by DLS (Malvern Nanosizer S) using distilled water and culture medium at three different concentrations (50, 100 and 200 µg/ml) after 24 hours incubation at 4 °C (Table 2).

Table 2: The particle size and polydispersity index (PDI) obtained from DLS measurements for colloidal silica in distilled water and culture medium at 50, 100 and 200 $\mu\text{g/ml}$ after 24 hours incubation at 4 $^{\circ}\text{C}$, mean \pm SD (n = 5).

Suspension	Distilled water		Culture medium		Concentrations $\mu\text{g/ml}$
	Particle size (nm)	PDI	Particle size (nm)	PDI	
SiNP20nm	21 \pm 5	0.21 \pm 0.04	119 \pm 2	0.35 \pm 0.07	50
	20 \pm 1	0.10 \pm 0.02	123 \pm 4	0.41 \pm 0.02	100
	21 \pm 8	0.10 \pm 0.03	127 \pm 5	0.38 \pm 0.01	200
SiNP200nm	237 \pm 5	0.08 \pm 0.02	184 \pm 5	0.10 \pm 0.04	50
	202 \pm 9	0.10 \pm 0.02	207 \pm 2	0.10 \pm 0.02	100
	198 \pm 2	0.10 \pm 0.04	213 \pm 8	0.10 \pm 0.06	200

The above results show the particles size have almost the given size except the SiNP20 in culture medium. In distilled water, they were no clear alteration in particles size for SiNP20 and the particles were in monodisperite (Figure 1).

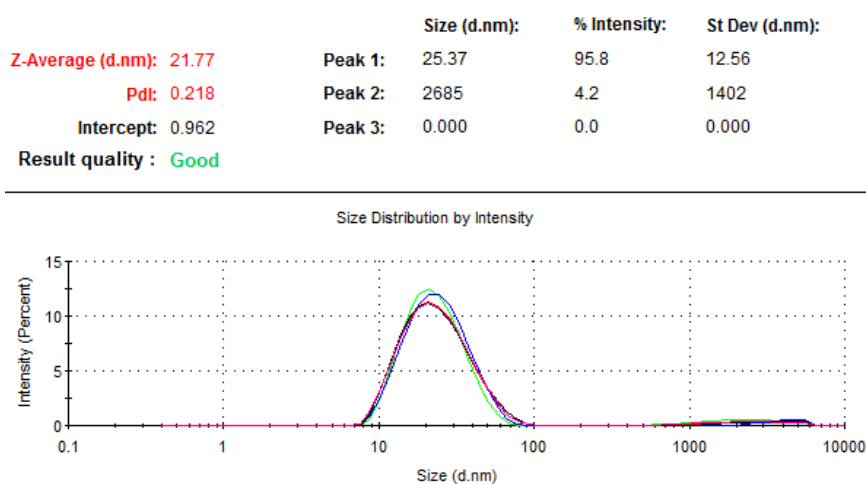


Figure 1: Data obtained from DLS for SiNP20 showed a typical size 21nm \pm 5 nanoparticles with PDI 0.21 \pm 0.04 in distilled water at 50 $\mu\text{g/ml}$ after 24 hours incubation at 4 $^{\circ}\text{C}$, each colour represents sample mean \pm SD (n=5).

Also, the results obtained from DLS for SiNP200 post distilled water incubation at 4 °C show, no different from given size at all concentrations. In addition, the particles were in monodisperite (Figure 2).

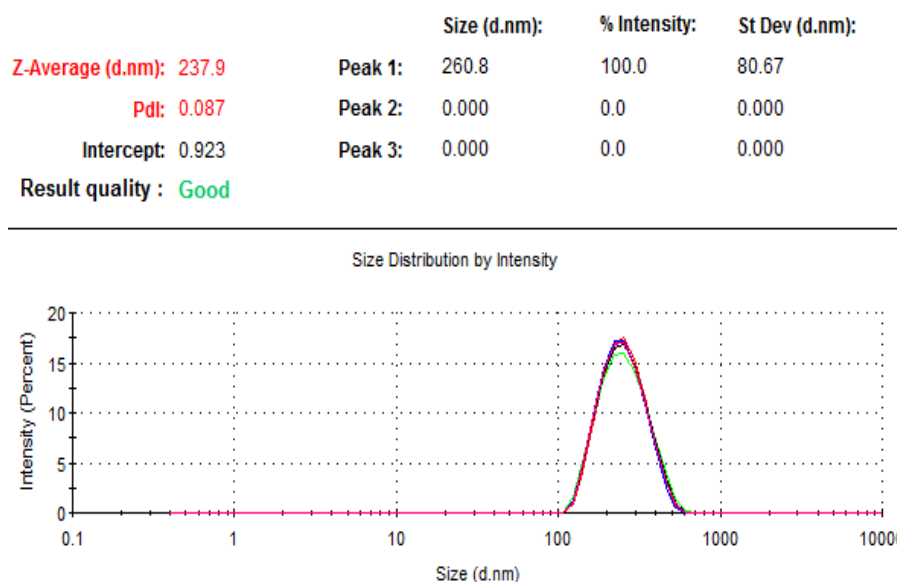


Figure 2: Data obtained from DLS for SiNP200 showed a typical size 237 nm±5 nanoparticles with PDI 0.08±0.02 in distilled water at 50µg/ml after 24 hours incubation at 4 °C, each colour represents sample mean ± SD (n=5).

For SiNP20, the results indicated an increasing in the particles size post 24 hours incubated at 4 °C in culture medium at all concentrations (50, 100 and 200 µg/ml) and the polydispersity index (PDI) indicated the particles have polydispersite in the medium (PDI ≥3). The increase in size suggested that SiNP20 might either form aggregates or adsorb proteins from the culture medium. For SiNP200, their size was smaller than their given one when measured at 50 µg/ml, whereas when measured at higher concentrations 200 µg/ml, it became slightly larger as compared with their given size. However, the PDI results show that the particles have polydispersite in culture medium at all concentrations (PDI=0.1).

Nanoparticle tracking analysis (NTA) was performed to complement the results obtained from DLS for SiNP20 particles in distilled water at 50 µg/ml after 24 hours

incubation at 4 °C. The NTA trace shows that the size distribution of particles was 21 nm and this result is compatible with DLS measurement (Figure 3).

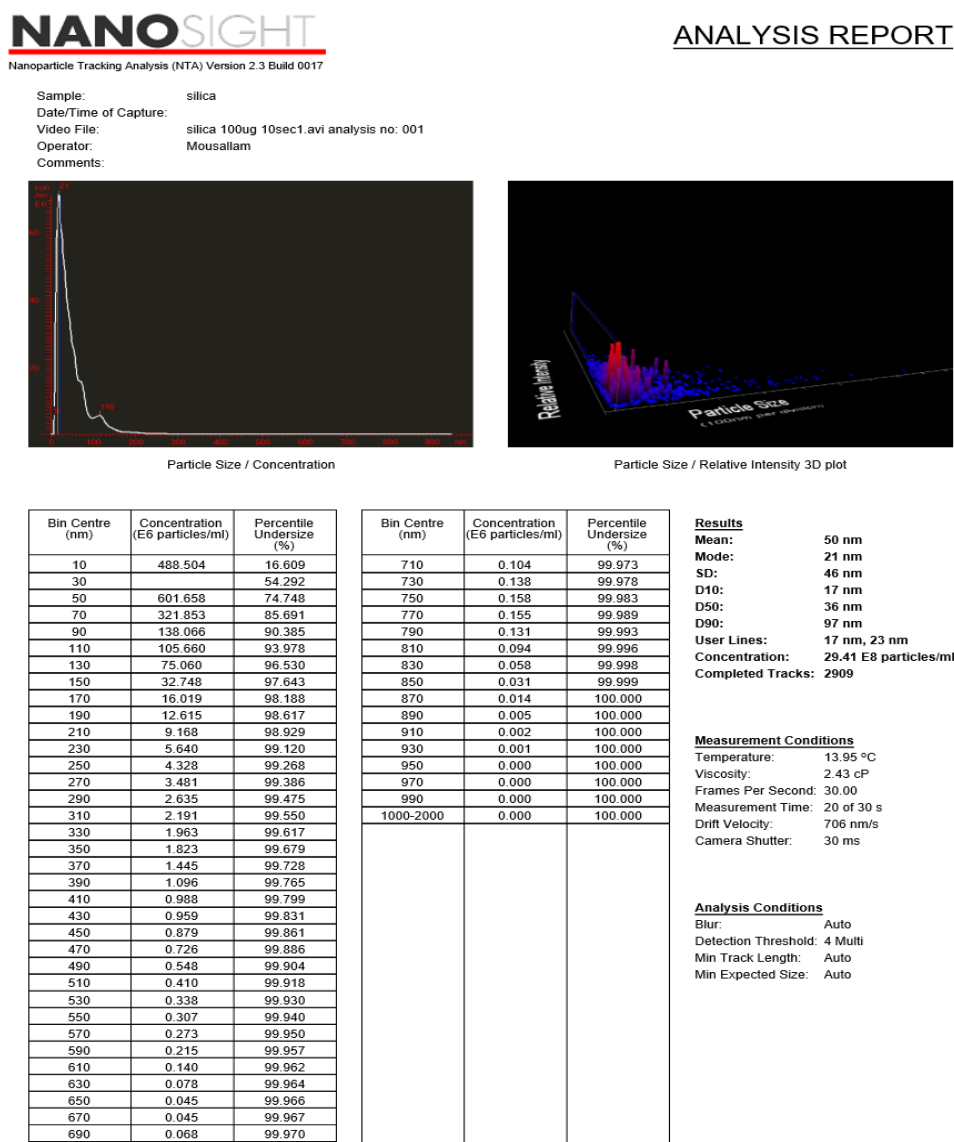


Figure 3: The relative intensity of SiNP20 by nanoparticles tracking analysis, red light represent intensity for particles, highest value at 21 ±46 nm, (mean ± SD n=2909).

The transmission electron microscope (TEM) were employed to obtain SiNP20 and SiNP200 information, on the shape of particles, and to confirm their size as measured by DLS. The particles were analysed post incubated in culture medium at 50µg/ml (Figure 4).

Figure 4, show images of silica particles in culture medium show difficult in determination of particle size, due to intrinsic problems during sample preparation linked to the sugars inside the media (data not shown).

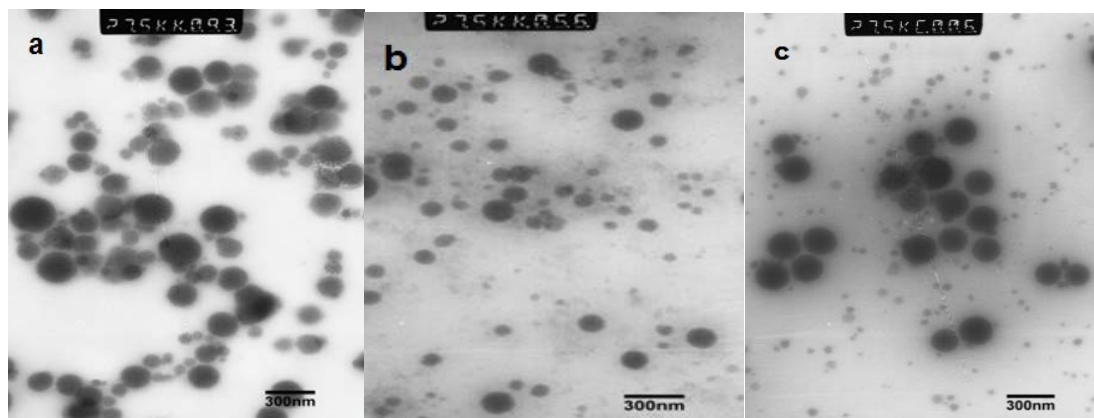


Figure 4: TEM images of SiNP20 and SiNP200 in culture medium at 50 μ g/ml, (a) culture medium (b) SiNP20nm (c) SiNP200nm, bar scale: 300 nm. Magnification: x 27000 using Philips CM20 TEM (Philips, Netherlands).

The final measurement applied for SiNP20 and SiNP200 was the zeta potential. The Zetasizer was used to measure the stability of particles in distilled water and cultural medium at 50, 100 and 200 μ g/ml (Table 3).

Table 3: The zeta potential obtained from Malvern 3000 HSa Zetasizer for colloidal silica in distilled water and culture medium at 50, 100 and 200 μ g/ml after 24 hours incubation at 4 °C, mean \pm SD (n = 5).

Suspension Conc.		Zeta potential (mV)	
		Distilled water	Culture medium
50 μ g/ml	SiNP20	-48.2 \pm 0.3	-22.3 \pm 0.9
	SiNP200	-42.7 \pm 0.1	-10.4 \pm 0.2
100 μ g/ml	SiNP20	-43.2 \pm 0.7	-22.4 \pm 0.1
	SiNP200	-31.2 \pm 0.8	-13.0 \pm 0.6
200 μ g/ml	SiNP20	-38.6 \pm 0.2	-24.7 \pm 0.6
	SiNP200	-34.4 \pm 0.1	-19.2 \pm 0.5

The above results show that all particles exhibited negative zeta potential, which present the negative charge of the surface of the silica nanoparticles. The surface charge of SiNP20 and SiNP200 in culture medium given a weak negative zeta potential rather than in distilled water solution. These results suggested that due to the weak zeta potential, these particles could be unstable in culture medium, which could have implications in the mechanism of their cytotoxicity. The zeta potential of SiNP200 indicated a weak negative charge on their surface comparing to SiNP20 in distilled water and culture medium.

In vitro cytotoxicity and apoptosis assessment on A375 melanoma cell line

The morphological features for A375 cells in culture medium (CM) and in culture medium with fetal bovine serum (CMFBS) after 24 hours treated with SiNP 20 nm were studied. The results obtained from light microscopy (Leica DM IL LED system) are shown in Figure 5.

A375 cells after seeding in CM without treatment (Figure 5A) were seen to be nearly confluent with each other and showed an adherent growth pattern and morphology with rounded at 24 hours. This feature of cell morphology was associated with active cell growth in present of fetal bovine serum culture medium (CMFBS), the cells had sharp ends in contact and at the same time showed preservation of their contact to each other without morphological change (Figure 5C). After 24 hours treatment with 50 $\mu\text{g/ml}$ with SiNP 20 nm, the A375 cells in CM appear to be shrinking and demonstrate what appear to be cytopathic changes (Figure 5B). while, the A375 cells in CMFBS showed change in medium suggesting forms of protein layer (corona). This change in A375 cells was due to forms on their surface once nanoparticles are in contact with biological fluids (Figure 5D).

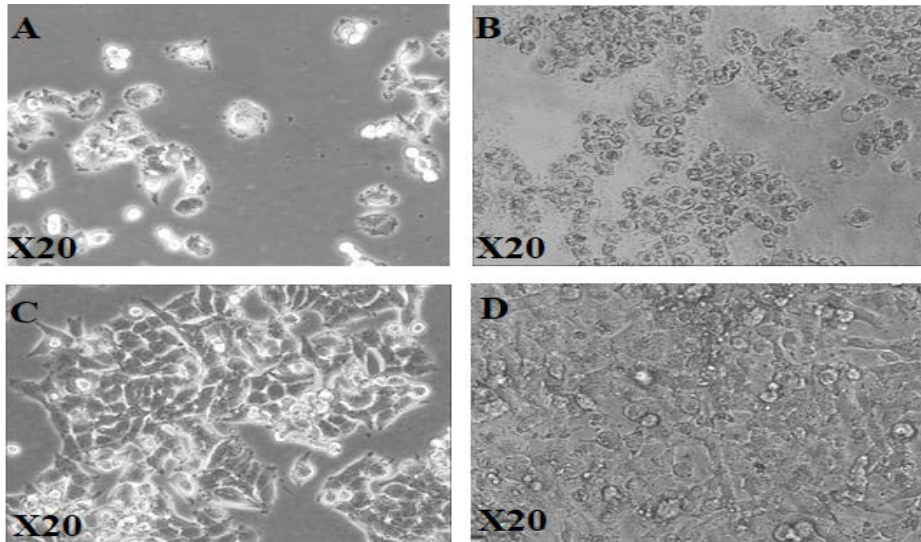


Figure 5: Morphology study for A375 cells (3×10^3 cells/ml) observed by light microscopy ($\times 20$) after 24 hours' incubation, A: cells without treatment in CM; B: cells in CM treated by $50 \mu\text{g/ml}$ of SiNP 20nm; C: cells without treatment in CMFBS; and D: cells in CMFBS treated by $50 \mu\text{g/ml}$ of SiNP 20nm.

MTT assay was used to evaluate the toxicity of SiNP (20 nm and 200 nm) on A375 cells. In A375 cells, SiNP 20 nm reduced cell viability at $50 \mu\text{g/ml}$ and above in the presence fetal bovine serum (FBS) in culture medium (CMFBS). SNPs 200 nm showed no effect on cell viability at 50, 100 and $200 \mu\text{g/ml}$ in the presence of FBS (Figure 6).

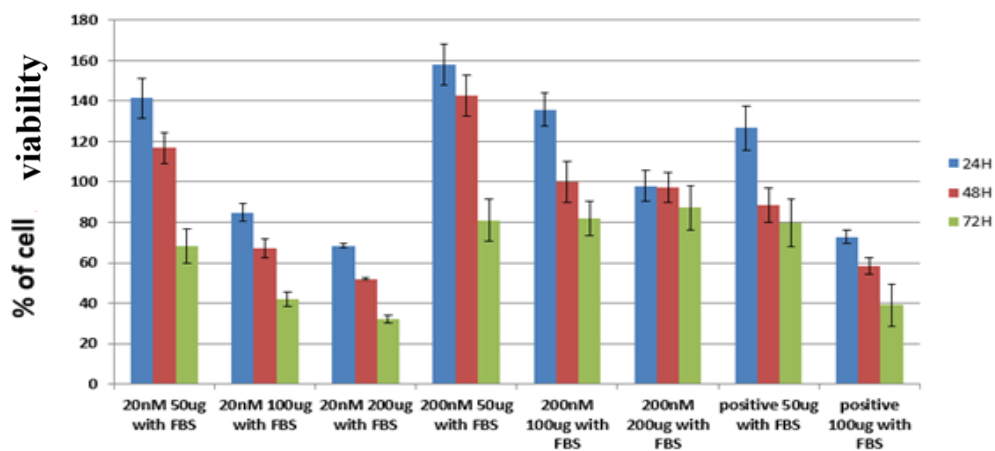


Figure 6: Viability of A375 Cells following treatment with SiNPs 20 nm and 200 nm (50, 100 and 200 $\mu\text{g/ml}$) at 24, 48 and 72 hours each value represents the mean S.D. (n=3).

The SiNP20 were also assessed by flow cytometry for induction of necrotic and apoptotic cell death. In A375 cells, SiNP20 at 50, 100 and 200 $\mu\text{g/ml}$ also induced a dose-dependent increase in apoptotic and necrotic cells with the effect more pronounced in the absence of FBS (Figure 7).

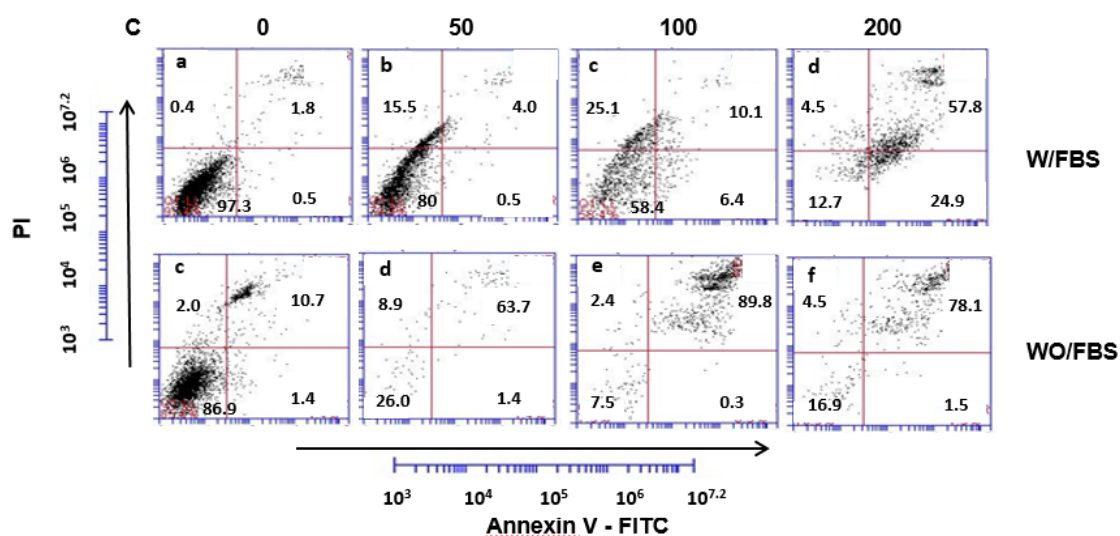


Figure 7: Flow cytometry graphs showing the effect of SiNP20 at 50, 100 and 200 $\mu\text{g/ml}$ in A375 cells, dose-dependent increase in apoptotic and necrotic cells b, c and d W/FBS (culture medium with FBS) & d, e and f WO/FBS (culture medium without FBS) with the effect more pronounced in the absence of FBS each value represents the mean (n=3).

In this study, the silica 20 nm and 200 nm materials were characterized in different cell culture media CM and CMFBS to gain information on average size, aggregation/agglomeration state, colloidal stability, shape, as well as the effect that serum and media composition had on particle stability. The selection of manufactured silica particles of different size allowed the differentiation of silica particles form- and size-dependent effects. When analysed by DLS, SiNP20 and SiNP200 showed aggregation in CM and their size and PDI increased compared to their given size. Such effect could be the result of protein corona formation, thus suggesting the role of FBS in improving colloidal stability for these particles. The morphology tested by

TEM and ZP for both silica, found that SiNP20 and SiNP200 dispersed well in culture medium, and they had the tendency to form aggregates very quickly. Zeta potential for larger particles (SiNP200) was reduced in CM, suggesting the occurrence of electrostatic interaction between the particles and biomolecules.

In the last few years, protein corona formation has gained so much importance that in the future it may be used for nanoparticles classification. Despite the increasing interest, only very recent contributions have addressed the question of how nanoparticles-protein coronas form, evolve with time and affect colloidal stability. Until recently, the main reason for colloidal instability of nanoparticles has been assumed to be cell culture medium, its high ionic strength, capable of reducing particles' surface potentials. On the other hand, proteins had been generally assumed to enhance the dispersion of nanoparticles in culture medium.

It is important to study the effects of nanomaterial exposure to the human body. Studies using *in vitro* models to define size-dependent effects of silica particles have been documented. This study assessed the potential toxicity of SiNP20 and SiNP200 using MTT assay. A375 cells were used as a model to assess the effect of these silica particles previously characterized in culture medium to analyze the correlation of cytotoxicity to their size and concentrations at the presence of fetal bovine serum (FBS). The study clearly demonstrated size-dependent and dose-dependent toxicity of silica nanoparticles in the order SiNP20 > SMP200 respectively. In this study, cell viability found that cytotoxicity generated by silica particles strongly depended on particle size and administered dose, with smaller silica particle producing higher toxic effect. Moreover, they found that silica nanoparticles were also cytotoxic in a dose- and time-dependent manner. Both SiNP20 and SMP200 tested in this study also appeared to cause cytotoxicity through induction of apoptosis.

The cytotoxicity of silica nanoparticles could ultimately lead to the loss of cell viability. It is the outcome of cell death via necrosis and apoptosis mechanisms. Necrosis is a form of shocking cell death that results from acute cellular injury. Apoptosis, also known as 'programmed cell death', on the other hand, consists of a series of biochemical events that lead to characteristic morphology and intracellular changes, followed by cell death. Such changes include cell shrinkage, nuclear and DNA fragmentation, chromatin condensation and global mRNA decay. While

apoptosis is highly regulated and controlled process during an organism's lifecycle., necrosis is caused by factors external to the cell or tissue, such as infection, toxins, or trauma, which result in the unregulated digestion of cell components. Both pathways can be triggered by the interaction between cells and nanomaterials. In this study, the mechanism silica nanoparticles cytotoxicity was measured by detection of necrosis and apoptosis. Using the optical microscopy technique of phase contrast imaging to assess morphology changes of cells following silica treatment proved useful in obtaining real time information on cellular response to the treatment. The size- and dose-dependent cellular effect of silica in CM detected by phase contrast imaging was very much comparable with the cytotoxicity detected by the MTT. The effects observed on cells treated with SiNP20, such as cell shrinkage and becoming rounded, were associated with apoptosis. To validate the induction of apoptosis as detected by phase contrast imaging, double staining with Annexin V and Propidium Iodide for flow cytometry was performed by using A375 cells. Annexin V has high affinity to phosphatidylserine, which translocate from the inner layer to the outer layer of cell membrane during apoptosis, while Propidium iodide (PI) is a DNA intercalating agent that penetrates cells only with a damaged cell membrane, normally associated with necrosis. In late apoptosis, cells become positive for both Annexin and PI staining due to the plasma membrane becoming permeabilized as a direct consequence of phosphatidylserine on the cell surface. In this study, a dose-dependent toxicity was demonstrated for SiNP20 in present and absence of fetal bovine serum (FBS) in culture medium. The results showed dose-dependent increase in apoptotic and necrotic cells with the effect more pronounced in the absence of FBS. Also, the occurrence of late apoptosis, as indicated by double positive Annexin V/PI-stained, was more emphasized in CM without FBS and thus providing further evidence of the role of serum in attenuating toxicity.

This study used manufactured SiNPs measurements to design methods to study properties and toxicity of nanoparticles and from the trials here the study prepared the work experiments for the NLC evaluation as well as collaboration with SiNPs project team*

*See the publication in appendix iii A

ii. Appendix B1 HSD specification sheet

T 25 digital ULTRA-TURRAX® Dispenser by IKA

The [T 25 digital ULTRA-TURRAX Dispenser](#) performs high circumferential speeds even when used with small (8 mm) rotor diameters. Designed to emulsify, homogenize and suspend a range of miscible materials, this high-quality lab homogenizer features a unique rotor-stator with a very powerful shear force that quickly macerates tissues and other materials into a homogenous substance.



High-performance digital dispenser for coarse and fine preparations

- Volume range: 1 to 2000 ml
- Speed range: 3000 - 25000 rpm
- Rotating knob for speed adjustment
- Accepts stainless steel, saw tooth and plastic disposable [dispersing elements](#) (sold separately)
- Digital speed display ensures accurate protocol adherence
- Electronic overload protection and electronic speed control
- Digital error code display for easy troubleshooting
- Enables high circumferential speeds
- Emulsifies, homogenizes, or suspends virtually any sample
- Scalable unit allows usage of identical processes from formulation to production
- **Includes:** T 25 digital ULTRA-TURRAX, extension arm, hexagon socket screw, flat key, shaft key, screwdriver DIN 911 and operating instructions
- Two-year manufacturer warranty, plus additional one-year warranty after registration

Ordering Information

IKA Part #	Description	Cat. #	Price
3725001	T 25 digital ULTRA-TURRAX®, 120V	6925-00	\$ 1,542

See [Stainless steel and plastic, disposable dispersing elements](#)
Plate stand and dispersing elements sold separately

Additional Features:

- Creates coarse to fine emulsions and suspensions
- Mixes and disperses products with a wide range of miscibility
- Stainless steel and disposable dispersing elements for fine, and coarse preparation
- Saw tooth dispersing elements for fibrous materials
- Dispersing elements feature a **quick-connect** coupling for fast and easy tool change
- Infinitely variable speed control
- High performance drive for speed stability and quiet operation
- Small sample dispersing system for analytical research
- Ergonomic, lightweight unit ideal for manual operation
- For use in labs, pharmacies and educational institutions
- Design award winner 2012
- Handheld or plate stand mounted operation

▪

T 25 digital ULTRA-TURRAX Dispersing Elements

Processing different materials requires a wide variety of dispersing units to satisfy your lab's application requirements. The T 25 accepts stainless steel, saw tooth and plastic dispersing elements that achieve the desired sample consistency from coarse to fine sample reductions.

Dispersing Elements for Fine Preparation



**S 25 N – 25 F Dispersing Element
(Shown)**

IKA Part #	Description	Cat. #	Price
1713800	S 25 KV - 25 G Dispersing element	6925-07	\$ 1,509

Specifications:

- Volume range: 25-2000 ml
- Stator diameter: 25 mm
- Shaft length: 194 mm
- For secondary processing of samples to a greater fineness



IKA Part #	Description	Cat. #	Price
2404000	S 25 KV - 25 F Dispersing element	6925-08	\$ 1,814

Specifications:

- Volume range: 25-2000 ml
- Stator diameter: 25 mm
- Shaft length: 270 mm
- Suitable for vacuum and pressurized applications
- For secondary processing of samples to a greater fineness

Appendix B2 materials specification sheet

For nanostructured lipid preparations:

The screenshot shows the Sigma-Aldrich website interface for the product Glycerol dibehenate. The header includes the company logo (SIGMA-ALDRICH is now MERCK), navigation menus for PRODUCTS, SERVICES, and INDUSTRIES, and user account options. The main content area features the product name, its USP reference standard status, and tabs for Purchase and Safety & Documentation. The Properties section lists related categories. The Price and Availability section shows a price of 314.50 GBP and a quantity of 0. The Description section provides general information and other notes. The Personalized Product Recommendations section suggests related products like Glycerin and Glycerol tripalmitate.

SIGMA-ALDRICH is now **MERCK**

United Kingdom

200,000+ PRODUCTS | 500+ SERVICES | Featured INDUSTRIES

Hello, Sign in. ACCOUNT | 24/7 SUPPORT | 0 Items ORDER

United Kingdom Home > 1295709 - Glycerol dibehenate

1295709 USP
Glycerol dibehenate
United States Pharmacopoeia (USP) Reference Standard

SDS

Purchase | Safety & Documentation

Properties

Related Categories
Analytical Standards, Analytical/Chromatography, Pharmacopoeia & Metrological Institutes Standards, USP Standards, USP Standards G - H More...

Price and Availability

SKU-Pack Size	Availability	Price (GBP)	Quantity
1295709-200MG	Only 2 left in stock (more on the way) - FROM	314.50	0

BULK ORDER? | ADD TO CART

Description

General description
This product is provided as delivered and specified by the issuing Pharmacopoeia. All information provided in support of this product, including SDS and any product information leaflets have been developed and issued under the Authority of the issuing Pharmacopoeia. For further information and support please go to the website of the issuing Pharmacopoeia.

Other Notes
Sales restrictions may apply.
USP issued SDS can be found [here](#).

Personalized Product Recommendations

<chem>OCC(O)CO</chem> 1295607 Glycerin United States Pharmacopoeia (USP) Reference Standard	<chem>CCCCCCCCC(=O)OCC(O)COC(=O)CCCCCCCC</chem> T8127 Glycerol tripalmitate ≥85%
--	---

United Kingdom Home > 305391 - Octadecylamine

305391 ALDRICH

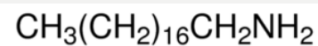
Octadecylamine

97%

Synonym: 1-Aminooctadecane, Stearylamine

[SDS](#)
[SIMILAR PRODUCTS](#)

CAS Number [124-30-1](#) | Linear Formula $\text{CH}_3(\text{CH}_2)_{17}\text{NH}_2$ | Molecular Weight 269.51
 Beilstein Registry Number [636111](#) | EC Number [204-695-3](#) | MDL number [MFCD00008159](#)
 PubChem Substance ID [24858428](#)
 POPULAR DOCUMENTS: [FTNMR \(PDF\)](#)


[Purchase](#)
[Safety & Documentation](#)
[Protocols & Articles](#) **1**
[Peer-Reviewed Papers](#) **76**

Properties

Related Categories	Amines, Building Blocks, C15 to C19, Chemical Synthesis, Nitrogen Compounds, More...
vapor pressure	10 mmHg (72 °C)
InChI Key	REYJJPVUYRZGE-UHFFFAOYSA-N
assay	97%
bp	232 °C/32 mmHg(lit.)
mp	50-52 °C(lit.)

Description

Packaging
25, 100 g in glass bottle

Application

Modified octadecylamine (ODA) based Langmuir-Blodgett (LB) films were investigated. These films may find uses as ion exchange systems.^[1] ODA may be used to functionalize carbon nanomaterials. Thermal decomposition of metal nitrates in the presence of ODA may be used to obtain metal oxide nano crystals of controlled size and shape.^[2] ODA based LB films was used to realise enzymatic field effect transistor (ENFET) biosensors.^[3]

Price and Availability

SKU-Pack Size	Availability	Price (GBP)	Quantity
305391-25G	Only 4 left in stock (more on the way) - FROM	109.50	<input type="text" value="0"/> + - i
305391-100G	Only 2 left in stock (more on the way) - FROM	328.50	<input type="text" value="0"/> + - i

[BULK ORDERS?](#)[ADD TO CART](#)

Suggested Laboratory Gloves



This substance has been tested against several types of hand protection for CE compliance. Click below to find the recommended gloves for handling this product.

[FOR SPLASH & IMMERSION PROTECTION](#)

Personalized Product Recommendations

 $\text{CH}_3(\text{CH}_2)_{16}\text{CH}_2\text{NH}_2$ $\text{CH}_3(\text{CH}_2)_{16}\text{CH}_2\text{NH}_2$

United Kingdom Home > 57668 - D-α-Tocopherol polyethylene glycol 1000 succinate

57668 SIGMA

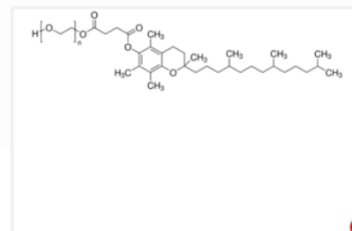
D-α-Tocopherol polyethylene glycol 1000 succinate

BioXtra, water soluble vitamin E conjugate

Synonym: D-α-Tocopherol polyethylene glycol succinate, TPGS, Vitamin E polyethylene glycol succinate, Vitamin E-TPGS

SDS | SIMILAR PRODUCTS

CAS Number 9002-96-4 | MDL number MFCD00146616 | eCI@ss 34058007



Purchase | Safety & Documentation | Peer-Reviewed Papers 37 | Related Products 1

Properties

product line	BioXtra
composition	α-tocopherol, ≥25%
mp	>36 °C
solubility	H ₂ O: 1 g/10 mL clear to faintly turbid, colorless to faintly yellow
cation traces	Al: ≤5 mg/kg
	Ba: ≤5 mg/kg
	Bi: ≤5 mg/kg
	Ca: ≤5 mg/kg
Show More (24)	

Description

Biochem/physiol Actions

Tocopherols (TCP) (vitamin E) are a series (α, β, γ and δ) of chiral organic molecules that vary in their degree of methylation of the phenol moiety of the chromanol ring. Tocopherols are lipid soluble anti-oxidants that protect cell membranes from oxidative damage. α-Tocopherol is the form of tocopherol preferentially absorbed by homo sapiens. Tocopherol polyethylene glycol 1000 succinate (TPGS) may be used to create biodegradable polymers and antioxidant surfactants.

Price and Availability

SKU-Pack Size	Availability	Price (GBP)	Quantity
57668-5G	Available to ship on 30.11.17 - FROM	46.40	0
57668-25G	Available to ship on 30.11.17 - FROM	124.00	0

BULK ORDERS?

ADD TO CART

Personalized Product Recommendations



763896
DL-α-Tocopherol
methoxypolyethylene glycol succinate

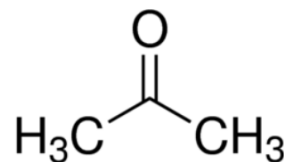


95255
D-α-Tocopherol succinate
BioXtra, ≥98.0% (HPLC)

522627 ALDRICH

Acetone

for HPLC, ≥99.9%

[SDS](#) [SIMILAR PRODUCTS](#)CAS Number [67-64-1](#) | Linear Formula [CH₃COCH₃](#) | Molecular Weight [58.08](#) | Beilstein Registry Number [635680](#)EC Number [200-662-2](#) | MDL number [MFCD00008765](#) POPULAR DOCUMENTS: [FTNMR \(PDF\)](#)**Purchase** Safety & Documentation**Properties**

grade	for HPLC
vapor density	2 (vs air)
vapor pressure	184 mmHg (20 °C)
InChI Key	CSCPPACGZOOOGX-UHFFFAOYSA-N
assay	≥99.9%
expl. lim.	13.2 %
impurities	<0.500% water
evapn. residue	<0.0002%
Show More (17) ▾	

Description**Application**

Acetone's luminescence intensity is dependent upon the solution components . The absorption of UV light by acetone, results in its photolysis and the production of radicals .

General description

Acetone is a high purity polar organic solvent that may be used as a mobile phase in high-performance liquid chromatography.

Price and Availability**Pricing & availability is not currently available.**Questions? [Contact Technical Service](#)**Personalized Product Recommendations** 

57668
D-α-Tocopherol polyethylene glycol
1000 succinate
BioXtra, water soluble vitamin E
conjugate



305391
Octadecylamine
97%

United Kingdom Home > 459836 - Ethyl alcohol, Pure

459836 SIGMA-ALDRICH

Ethyl alcohol, Pure

200 proof, anhydrous, ≥99.5%

Synonym: Ethanol, absolute alcohol, non-denatured ethanol

SDS SIMILAR PRODUCTS

CAS Number 64-17-5 Linear Formula CH₃CH₂OH Molecular Weight 46.07 EC Number 200-578-6

MDL number MFCD00003568 PubChem Substance ID 576506452

POPULAR DOCUMENTS: SPECIFICATION SHEET (PDF)



Purchase

Safety & Documentation

Protocols & Articles 12

Peer-Reviewed Papers 6342

Related Products 11

Properties

Related Categories	Allium cepa (Onion), Anhydrous Solvents, Cell Biology, Citrus aurantium (Seville orange), Ephedra sinica, More...
grade	anhydrous
InChI Key	LFQSCWFLJHTTHZ-UHFFFAOYSA-N
assay	≥99.5%
availability	not available in (Sales restrictions may apply)
concentration	200 proof
impurities	<0.005% water
evapn. residue	<0.0005%

Price and Availability

SKU-Pack Size	Availability	Price (GBP)	Quantity
459836-100ML	✓ Available to ship on 30.11.17 - FROM	19.10	0 <input type="text"/> <input type="button" value="+"/> <input type="button" value="i"/>
459836-500ML	✓ Available to ship on 30.11.17 - FROM	68.70	0 <input type="text"/> <input type="button" value="+"/> <input type="button" value="i"/>
459836-1L	✓ Available to ship on 30.11.17 - FROM	73.60	0 <input type="text"/> <input type="button" value="+"/> <input type="button" value="i"/>
459836-2L	✓ Available to ship on 30.11.17 - FROM	127.00	0 <input type="text"/> <input type="button" value="+"/> <input type="button" value="i"/>

BULK ORDERS?

ADD TO CART

K4894 SIGMA

Kolliphor® P 188

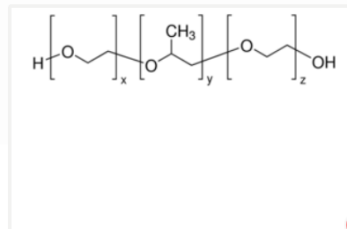
solid

Synonym: Lutrol® F68, Poloxamer 188, Poly(ethylene glycol)-*block*-poly(propylene glycol)-*block*-poly(ethylene glycol)

SDS

CAS Number 9003-11-6 | MDL number MFCD00082049

POPULAR DOCUMENTS: SPECIFICATION SHEET (PDF)



Purchase Safety & Documentation Peer-Reviewed Papers 27

Properties

form	solid
pH	5.0-7.5(2.5% solution)

Price and Availability

SKU-Pack Size	Availability	Price (GBP)	Quantity
K4894-500G	Available to ship on 30.11.17 - FROM	88.10	0

BULK ORDERS?

ADD TO CART

Description

Packaging
500 g in poly bottle

Application

Kolliphor® P 188 has been used as a supplement in F17 medium for the culture of HEK293-6E cells.^[1] It has also been used as a component of flow cytometry (FACS) buffer.^[2]

Legal Information

Kolliphor is a registered trademark of BASF
Lutrol is a registered trademark of BASF SE

Personalized Product Recommendations

15759
Kolliphor® P 188



78973
Kolliphor® P 188 micro

PRECIROL® ATO 5

GLYCERYL DISTEARATE / PALMITOSTEARATE

GATTEFOSSÉ

A high melting point lipid for use in modified release oral solid dosage forms (lipid matrix for sustained release, delayed release).

Glycerol distearate (type I) EP

Glyceryl distearate NF

Glyceryl palmitostearate (USA FDA IIG)

Key Features

- Fine white powder of well-controlled particle size distribution with an indicative particle size of 50µm
- A high melting point lipid for use in modified release oral solid dosage forms (lipid matrix for sustained release, delayed release).
- Use in coating techniques to provide taste masking.
- In coating techniques the physicochemical properties and plasticity of the lipid film provides high resistance to fracture, useful for flash melt and chewable tablets.
- Effective lubricant for capsule filling.
- Chemically inert and compatible with other ingredients.

Safety of use is supported by toxicological data, GRAS status and precedence of use in approved pharmaceutical products.

Physical Form

Powder

Hydrophilic-Lipophilic Balance (HLB)

2

Field of use

Human pharmaceutical products, veterinary products excluding food producing animals (EU)

LABRAFAC™ LIPOPHILE WL1349

TRIGLYCERIDES MEDIUM-CHAIN

GATTEFOSSÉ

Oily vehicle or oily phase for use in self-emulsifying lipid formulations to obtain a coarse dispersion ie. emulsion (SEDDS) or a fine dispersion ie. microemulsion (SMEDDS).

Key Features

Oral

- Oily vehicle or oily phase for use in self-emulsifying lipid formulations to obtain a coarse dispersion ie. emulsion (SEDDS) or a fine dispersion ie. microemulsion (SMEDDS).

Topical

- Good solvent for lipophilic active pharmaceutical ingredients, associated with enhanced drug penetration

Parenteral

- Conforms to relevant pharmacopoeia specifications for parenteral use.

Safety of use is supported by substantial toxicological data and precedence of use in approved pharmaceutical products.

Physical Form

liquid

Hydrophilic-Lipophilic Balance (HLB)

1

Field of use

Human pharmaceutical products, veterinary products including food producing animals

Soybean lecithin (E322)

Culinary data

Soybean lecithin is an emulsifier.

It enables:

- to aerate the preparations by giving them a foamy aspect,
- to stabilize hot or cold emulsions.



Technological data

Dissolution

It's advised to disperse the soybean lecithin in a hot or cold preparation by mixing.

The amount usually used ranges from 0.2 to 1g for 100g of final preparation.

Sensory properties

Don't give any taste to the culinary preparations at low quantity.

Storage

Store in a closed hermetic packaging, in a cool and dry place.

Toxicological data

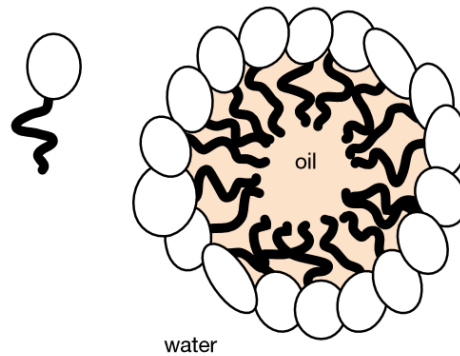
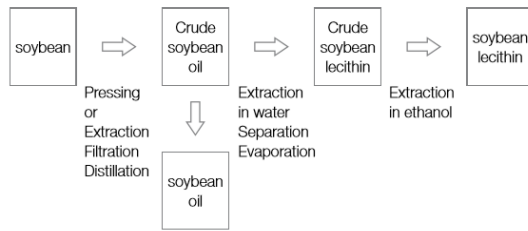
- The used quantity shouldn't exceed the concentrations used to obtain the desired effect
- Can not be consumed by person with soya allergies.
- No acceptable daily intake level.
- Lecithin, being a natural constituent of the cells, is used by the body as such or after metabolisation.

Scientific data

Origin

Lecithin is a constituent of the cell membranes of living organisms. It stabilises and softens the lipid bilayers the membranes are constituted of. Alimentary grade lecithin is obtained during the production of soybean oil.

It is separated into two fractions by an extraction in ethanol. The ethanol insoluble fraction stabilises water in oil emulsion, whereas the ethanol soluble fraction stabilises oil in water emulsion. It is this later that is sold.

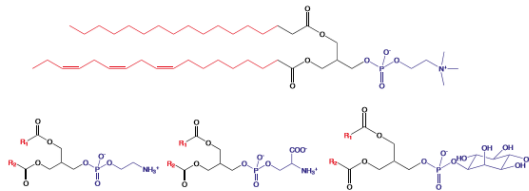


Positioning of the soybean lecithin between water and fat

Informations from Beltz H.-D., Grosch W., Schieberle P., *Food Chemistry*, 3rd Edition, Springer, 2004, 177-181.

Chemical composition

Under the name of lecithin is covered a large range of surface active molecules, also called phosphatidylcholines. They vary by the nature of the fatty acid they are constituted of. These fatty acids can be from various lengths, present or not insaturations varying in number and in positions.



Examples of molecules form the lecithin's family

The surface active properties from the soybean lecithin come from its being constituted of two parts: one is attracted to water (hydrophilic) and the other is repelled by water (lipophilic or hydrophobic). In the culinary preparations, the soybean lecithin's molecules will sit in the following manner: the hydrophilic part in water, and the lipophilic part out of water (either in oil or fat in the case of an emulsion, or in air in the case of a foam).

For the study drug Dacarbazine

United Kingdom Home > 1162308 - Dacarbazine

1162308 USP

Dacarbazine

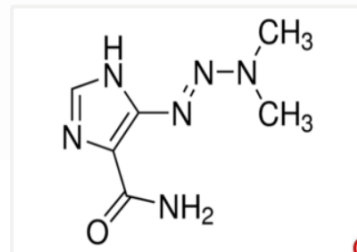
United States Pharmacopeia (USP) Reference Standard

Synonym: 5-(3,3-Dimethyl-1-triazenyl)imidazole-4-carboxamide, DTIC

SDS SIMILAR PRODUCTS

CAS Number 4342-03-4 Empirical Formula (Hill Notation) C₆H₁₀N₆O Molecular Weight 182.18

MDL number MFCD00057167 PubChem Substance ID 329749505



Purchase Safety & Documentation

Properties

Related Categories	Analytical Standards, Analytical/Chromatography, Pharmacopeia & Metrological Institutes Standards, USP Standards, USP Standards C - D More...
InChI Key	FDKXTQMXEQVLR-FZACJKMWSA-N

Description

General description

This product is provided as delivered and specified by the issuing Pharmacopeia. All information provided in support of this product, including SDS and any product information leaflets have been developed and issued under the Authority of the issuing Pharmacopeia.

For further information and support please go to the website of the issuing Pharmacopeia.

Other Notes

Sales restrictions may apply.

USP issued SDS can be found [here](#).

Price and Availability

SKU-Pack Size	Availability	Price (GBP)	Quantity
1162308-125MG	Estimated to ship on 08.02.18	219.60	<input type="text" value="0"/> <input type="button" value="+"/> <input type="button" value="i"/>

BULK ORDERS?

ADD TO CART

Personalized Product Recommendations



Y0000733
Dacarbazine
European Pharmacopeia (EP)
Reference Standard



D2390
Dacarbazine
antineoplastic purine analog

iii. Appendix C publications and Awards

A. Publications

Moia C., Huijun Zhu H., Almousallam M., Cell type- and size-dependent *in vitro* toxicity of silica particles in human skin cells, Scientific Tracks Abstracts: J Clin Toxicol, DOI: 10.4172/2161-0495.S1.012 (2014).



Claudia Moia et al., J Clin Toxicol 2014, 4:4
<http://dx.doi.org/10.4172/2161-0495.S1.012>

3rd International Summit on Toxicology & Applied Pharmacology

October 20-22, 2014 DoubleTree by Hilton Hotel Chicago-North Shore, USA

Cell type- and size-dependent *in vitro* toxicity of silica particles in human skin cells

Claudia Moia, Huijun Zhu and Meusallam Almousallam
Cranfield University, UK

Silica nanoparticles (SiNP) have been increasingly applied in biomedical areas including imaging and drug delivery. Although their bulk counter parts are generally regarded safe, the safety of SiNP and submicron silica particles (SMP) is yet to be established. This study aimed to investigate the size relevance of silica particles (SiP) in toxicity using two human skin cells *in vitro*. Since fetal bovine serum (FBS) is commonly used in cell culture to mimic *in vivo* environment, SiP toxicity is also investigated in the presence and absence of FBS to model the consequences of exposure via systemic and topical routes. SiPs of different size were assessed at 10-200 µg/ml for their effect on cell growth, viability, and ability to induce apoptosis. SiNP20 nm induced toxicity in keratinocyte HaCaT and melanoma A375 cells in the presence and absence of FBS, whilst SiNP 70 nm, SMP200 nm and SMP500 nm were toxic only in HaCaT cells in the absence of FBS. The toxicity in both types of cells was associated with the reduction of cell viability and induction of apoptosis. This study demonstrated size-dependent toxicity of SiP in both cell lines, with HaCaT being more sensitive. SiP showed higher toxicity in the absence of FBS than in the presence of FBS, suggesting that they could be more toxic via topical route than systemic route. As no blood supply can reach epidermis where keratinocytes and melanocytes are located, SiP can interact directly with these cells, leading to toxicity.

Biography

Claudia Moia obtained her Graduate Degree in 2009 and her Master's Degree in October 2011 in Biotechnology at the University of Pavia (Italy). As of May 2012 she is working as an Early Stage Researcher in Cranfield University (UK) as part of EU-funded Marie Curie ITN (initial training programme) network called NANODRUG, aiming to complete her PhD in Toxicology in May 2015.

c.moia@cranfield.ac.uk

Almoussallam, M., Moia, C. and Zhu, H. (2015), "Development of nanostructured lipid carrier for dacarbazine delivery", *International Nano Letters*, vol. 5, no. 4, pp. 241-248.

Int Nano Lett (2015) 5:241–248
DOI 10.1007/s40089-015-0161-8



ORIGINAL ARTICLE

Development of nanostructured lipid carrier for dacarbazine delivery

Musallam Almoussallam¹ · Claudia Moia¹ · Huijun Zhu¹

Received: 7 April 2015 / Accepted: 21 August 2015 / Published online: 21 September 2015
© The Author(s) 2015. This article is published with open access at Springerlink.com

Abstract Dacarbazine (Dac) is one of the most commonly used chemotherapy drugs for treating various cancers. However, its poor water solubility, short half-life in blood circulation, low response rate and high side effect limit its application. This study aimed to improve the drug solubility and prolong drug release by developing nanostructured lipid carriers (NLCs) for Dac delivery. The NLC and Dac-encapsulated NLC were synthesized with precinol ATO 5 and isopropyl myristate as lipids, tocopheryl polyethylene glycol succinate, soybean lecithin and Kolliphor P 188 as co-surfactants. The NLCs with controlled size were achieved using high shear dispersion following solidification of oil-in-water emulsion. For Dac encapsulation, the smallest NLC with 155 ± 10 nm in size, 0.2 ± 0.01 polydispersion index and -43.4 ± 2 mV zeta potential was selected. The resultant DLC-Dac possessed size, polydispersion index and zeta potential of 190 ± 10 , 0.2 ± 0.01 , and -43.5 ± 1.2 , respectively. The drug encapsulation efficiency and drug loading were 98.5 % and 14 %, respectively. In vitro drug release study showed a biphasic pattern, with 50 % released in the first 2 h, and the remaining released sustainably for up to 30 h. This is the first report on the development of NLC for Dac delivery, implying that NLC could be a new potential candidate as drug carrier to improve the therapeutic profile of Dac.

Keywords Nanostructured lipid carrier · Dacarbazine · High shear dispersion · Drug delivery

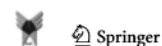
✉ Huijun Zhu
h.zhu@cranfield.ac.uk

¹ Institute of Environment, Health, Risks and Futures,
Cranfield University, Building 42, Bedfordshire MK43 0AL,
UK

Introduction

Dacarbazine (Dac), a highly lipid-soluble and light-sensitive agent chemically known as 5-(3,3-dimethyl-1-triazolyl)imidazole-4-carboxamide, is an antineoplastic drug that has been used to treat various cancers [1]. It is the only US Food and Drug Administration (FDA)-approved chemotherapeutic agent for treating wild-type melanoma, a skin cancer that accounts for the vast majority of skin cancer deaths [2, 3]. It is the most active single agent currently used for treating metastatic melanoma [4]. Over the last decades, the death rate has been increasing faster than most other types of cancer [5, 6]. At least a third of the patients with early-stage melanoma will develop metastases, for which the prognosis is dismal. Presently, no treatment can prolong the overall survival of the disease.

The oral adsorption of Dac is very low [7]. It is metabolized in the liver to an alkylating agent (diazomethane) that destroys cancer cells [8, 9], although different mechanism of Dac-toxicity was also suggested [10]. The only available formulation for clinical use is delivered through intravenous injection. After injection at 2.6–6.8 mg/body weight, the plasma concentration of the drug reached 6 $\mu\text{g/mL}$ with half-life around 41 min [11]. A single-dose of 850–1000 mg/m² [2] administered once every 3 weeks was referenced as standard therapy with response rate of 13–20 % of patients [12–14]. The effect could only last for 3–6 months as the melanoma cells develop resistance to drug-induced apoptosis and aberrant survival pathways during progression [15]. Like other chemotherapeutic agents, Dac also causes side effect by killing normal dividing cells. There is an imperative need for new Dac formulations that could extend the drug half-life in vivo while also achieving higher tolerable dose.



Previous studies have demonstrated that encapsulation of therapeutic agents in nanoparticles can improve their stability, bioavailability, pharmacokinetics and safety. It has been demonstrated that nanoformulation of Dac such as nanoemulsion, cubosomes and methoxy poly nanoparticles can prolong the shelf-life, enhance therapeutic efficiency and reduce side effect [16–19]. However, these formulations showed relatively low drug encapsulation efficiency and drug loading.

To this end, nanostructured lipid carrier (NLC) has emerged as a promising alternative. Being the second generation of solid lipid nanoparticles and made of a mixture of solid and liquid lipids, NLC contains highly ordered structures that increase the capacity for drug loading while significantly reducing the water content in the final formulation [20]. NLC remains solid at room and body temperature [21]. The production of NLC is of low cost with ease for scaling up [22]. Accordingly, NLCs have been investigated for drug delivery through different routes including oral, pulmonary intravenous injection, nose-to-brain, and dermal and ocular applications [23–26]. However, there has been no report on application of NLCs for Dac delivery. This study aimed to improve the drug solubility and prolong drug release by developing nanostructured lipid carriers (NLCs) for Dac delivery. NLCs were synthesized and studied for Dac encapsulation efficiency, drug loading, *in vitro* drug release, and stability during storage. This study suggests that the NLC developed in this study is a potential candidate for developing new formulation of Dac for improving the therapeutic profile of the drug.

Materials and methods

Materials

Dacarbazine (Dac), stearylamine (SA), D- α -tocopheryl polyethylene glycol succinate (TPGS), isopropyl myristate (IPM), Kolliphor[®] P 188, acetone and ethanol were purchased from Sigma Aldrich (Gillingham, Dorset, UK). Precirol ATO-5 and medium-chain triglycerides (MCT) were obtained from Gattefossé (Saint Priest Cédex, France). Glycerylbehenate (GB) was supplied by Fisher Scientific (Loughborough, UK). Soybean lecithin (SL) was obtained from Cuisine Innovation (Dijon, France). Double-distilled water was collected in the laboratory from Millipore-Q Gradient A10[™] ultra-pure water system (Millipore, France).

Formulation and preparation of NLCs and NLC-Dac

Three solid lipid and liquid lipid matrices were chosen to prepare NLCs (as shown in Table 1). The preparation

involved oil-in-water emulsion, evaporation and solidification followed by high shear dispersion (HSD). The solid lipid, liquid lipid and emulsifiers were mixed with 12.5 mL of organic solvents (equal volume of acetone and ethanol) at temperature 5 °C above their melting point. The emulsion was made by adding the oil phase drop-wise to an equal volume of aqueous phase, which contained nonionic surfactant kolliphor[®] P 188 (1–3 %) and was heated at the same temperature. The mixture was stirred for 4 h at 400 rpm using a magnetic stirrer, and then solidified at 0 °C overnight. Finally, the solution was subjected to HSD with a homogenizer (T25 digital Ultra-Turrax, IKA, UK) at 10,000–15,000 rpm for up to 40 min. The same procedure was used to achieve NLC-Dac, where 35 mg of Dac was added to the oil phase.

Dynamic light scattering (DLS) assay

DLS is concerned with the measurement of particles size and dispersity in a suspension. NLCs and NLC-Dac preparations were measured with a Malvern Zetasizer (Zetasizer Nanosizer S; Malvern Instruments Ltd, Worcestershire, UK) at 25 °C under a fixed angle of 90° as described previously [27]. The measurements were obtained at 633 nm with a 4-m He-Ne laser. To give an average value and standard deviation for the particle size and polydisperse index (PDI), three different batches for each formula were analyzed five times (run). Prior to the measurement, all the samples were diluted with double-distilled water to a suitable scattering intensity.

Zeta potential (ZP) assay

The electro-kinetic potential for particles in colloidal system is referred to zeta potential, indicating the level of repulsion between adjacent particles in solution. The potential difference between the dispersion medium fluid and the surface of the dispersed particle is a reflection of the stability of colloidal dispersions. The samples were diluted with double-distilled water and injected into a Zetasizer (Malvern Instruments Ltd, Worcestershire, UK). Five cycles of measurements were taken to derive an average zeta potential for each sample.

Transmission electron microscopy (TEM)

The structure and morphology of the NLCs were studied by TEM. NLC preparations were diluted with double-distilled water. A droplet of each sample was applied to a copper grid coated with carbon film and air-dried. The grid was then stained with 2 % (w/v) phosphotungstic acid (PTA) solution and dried under room temperature. The particles were examined using TEM (CM20, Philips) at an operating voltage of 200 kV.

Table 1 Components of the NLC preparations

Formulation	Solid lipid (mg)			Liquid lipid (mg)		Emulsifier (mg)		Surfactant (%)
	SA	GB	Precirol ATO5	IPM	MCT	SL	TPGS	Kolliphor® P 188
NLC/SI	180			60		30	30	1–3
NLC/GM		180			60	30	30	1–3
NLC/PI			180	60		30	30	1–3

NLC/SI NLC made of lipids stearylamine (SA) and isopropyl myristate, *NLC/GM* NLC made of lipids glyceryl behenate (GB) and medium-chain triglycerides (MCT), *NLC/PI* NLC made of lipids precirol ATO-5 and isopropyl myristate (IPM), *SL* soybean lecithin, *TPGS* D- α -tocopheryl polyethylene glycol succinate

Assessment of Dac encapsulation efficiency and loading capacity

According to previous study, Dac can be detected with UV spectrometer at the wavelength of 330 nm [16]. Using this method, a standard curve for Dac detection was established. Dac was dissolved in acetone 10–100 μ g/mL and analyzed by UV spectrometry (Double Beam UV-VIS, UV-2100 Shimadzu, Japan). The standard curve had a regression equation of $y = 0.2338x - 0.1896$ with $R^2 = 0.9605$. The preparation of NLC-Dac was centrifuged at 12,500 rpm, 4 °C for 45 min (Fresco17 Microcentrifuges, Thermo scientific, UK). The free drug in the supernatant was detected using UV spectrometer and the concentration was calculated according to the regression equation for the Dac standard curve. The encapsulation efficiency (EF) and drug loading (DL) percentage were derived from the following equations [28]:

$$EE \% = W_1 - W_2 / W_1 \times 100$$

$$DL \% = W_1 - W_2 / W_3 \times 100,$$

where W_1 amount of drug added in the NLC, W_2 amount of un-entrapped drug, W_3 amount of the lipids added.

In vitro drug release study

The preparation of NLC-Dac was diluted at 10 % with PBS (pH = 7.4) and incubated at 37 °C in a capped centrifugation tube. At intervals of 0–30 h, the solution was centrifuged at 12,500 rpm, 4 °C for 45 min (Fresco17 Microcentrifuges, Thermo scientific, UK). The supernatant was then taken for analysis of free drug using UV spectrometer. The concentration of Dac in the supernatant was calculated according to the regression equation of the Dac standard curve. The drug released from NLC was expressed as the percentage of total amount of drug in the solution.

Powder X-ray diffraction (PXRD) assay

PXRD was used to determine the crystalline structure in the NLC samples. The NLC and NLC-Dac preparations

were freeze-dried to obtain dried product and then subjected to PXRD analysis. The samples were fast frozen under -45 °C in a deep-freezer overnight. Next day, they were moved into an Edwards Modulyo K4 Freeze Dryer (Thermo Electron Corporation, UK). After 48 h, the NLC and NLC-Dac powders were collected and analyzed using an X-ray Diffractometer (D5005, Siemens, UK). The samples were pressed to a slit at 2, 2 and 1 mm and scanned at 40 kV, 40 mA, 0.02°/sec at diffraction angle of 2θ for 1 h 6 min under 10–90 °C.

Statistical analysis

All experiments were performed at least three times and one of the representative experiment data was presented in each figure. The mean values of three replicates were expressed with standard deviation (mean \pm SD). One-way ANOVA was performed using Minitab 16 software to determine significance of comparisons. Significant difference (P value \leq 0.05) was indicated by asterisk.

Results and discussion

Optimization of NLC synthesis

In order to achieve NLCs with desirable characteristics, the components of lipids and the synthesis parameters were optimized. A total of 24 preparations were designed to allow optimizing the lipid matrix, surfactant concentration and the HSD time and speed. As judged by PS and PDI of the NLCs, the best results were achieved with 1 % of surfactant and a sheer speed of 15,000 rpm for 30 min for synthesis of all the NLCs. The smallest NLC of 155 nm was achieved with the formulation NLC/PI (Fig. 1a, bluebars), whilst the size of the formulation NLC/SI and NLC-GM was significantly larger (compare red and green bars with blue bars). Therefore, only NLC/PI was taken for further analysis. The increase of surfactant concentration from 1 to 3 % was associated with a significant increase in PS (Fig. 1a, compare blue bars). The increase of HSD time to 30 min resulted in a decrease in the PS and PDI of

NLCs, whilst when the time exceeded 30 min, a reverse effect in PS and PDI occurred (Fig. 1b, c). The same was true when the speed exceeded 15000 rpm (data not shown).

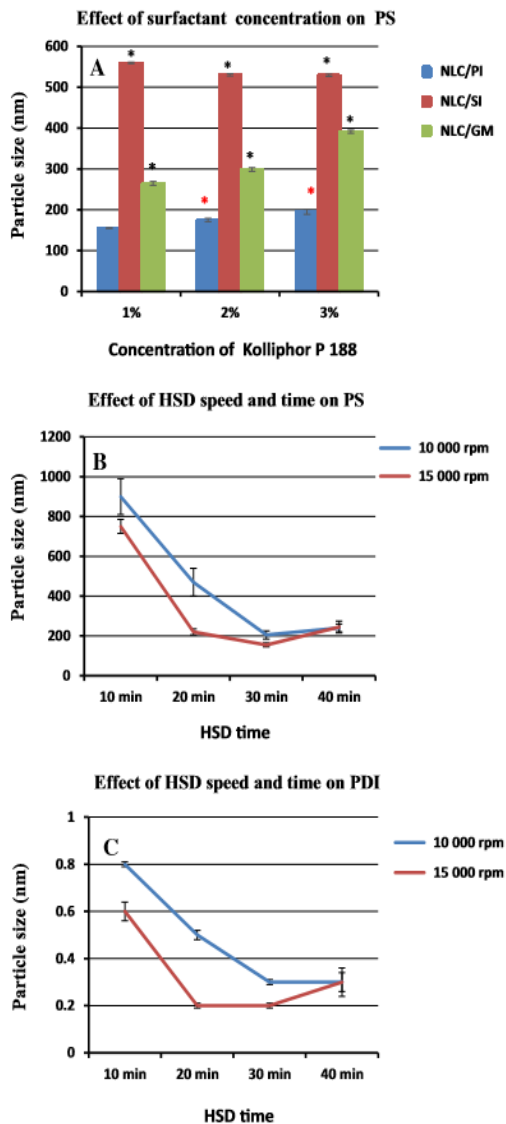


Fig. 1 Optimization of parameters used in NLC preparations. The optimal surfactant concentration and the speed and time of HSD were adjusted according to their effect on PS and PDI. **a** Effect of surfactant concentration on PS (black asterisks indicate significant difference as compared with blue bar at the same surfactant concentration; red asterisks indicate significant difference as compared with blue bar at 1% of surfactant). **b** Effect of HSD speed and time on PS of NLC/PI. **c** Effect of HSD speed and time on PDI of NLC/PI

Therefore, to prepare NLC/PI for further study, these optimal parameters were used.

The commonly used method for NLC synthesis involves oil-in-water emulsion, homogenization and solidification, which allows NLCs to disperse in an aqueous phase and the inner oil phase to solidify [24, 29, 30]. For different purposes modification(s) may be needed to achieve optimum preparations.

A modification has been made in this study to perform HSD after solidification. It was evident that the particle size can be controlled by the speed and time of the HSD. The failure of achieving any particles before solidification suggests that particles were formed during solidification. The application of HSD will disrupt the agglomerates of the particles, which formed possibly due to hydrophobic interaction, and also stabilize the particles by thoroughly remixing them with surfactant. The lowest particle size and PDI achieved after optimization of HSD speed and time indicated that sufficient dispersion energy was achieved and was well distributed within the solution for disruption of particle aggregates. Further increase of the HSD speed and time could result in a further reduction of PS, and consequently an increase in re-aggregation due to high inter-particle interaction force between small particles.

Characteristics of NLC/PI and NLC/PI-Dac

The NLCs were diluted with distilled water and characterized for PS, PDI and ZP. As shown in Table 2, NLC/PI exhibited a PS, PDI and ZP of 155 ± 10 nm, 0.2 ± 0.1 , and -43.4 ± 2.0 , respectively. As comparison, NLC/PI-Dac was larger with no change in PDI and little change in ZP.

Both NLC/PI and NLC/PI-Dac showed a spherical shape as observed under TEM, with NLC/PI being smaller than NLC/PI-Dac (Fig. 2, compare a with b), consistent with the results obtained by DLS measurement as shown in Table 2. Each NLC was covered by a dark layer (Fig. 2, indicated by black arrows outside NLCs), indicative of the presence of surfactant and external solution on the surface. The internal structures of the NLC/PI and NLC/PI-Dac were very different. For NLC/PI, a large grey area (Fig. 2a, indicated by white arrow) with several white rounded core structures (Fig. 2a, indicated by black arrow inside NLC/PI) were observed, indicative of the crystallization of solid

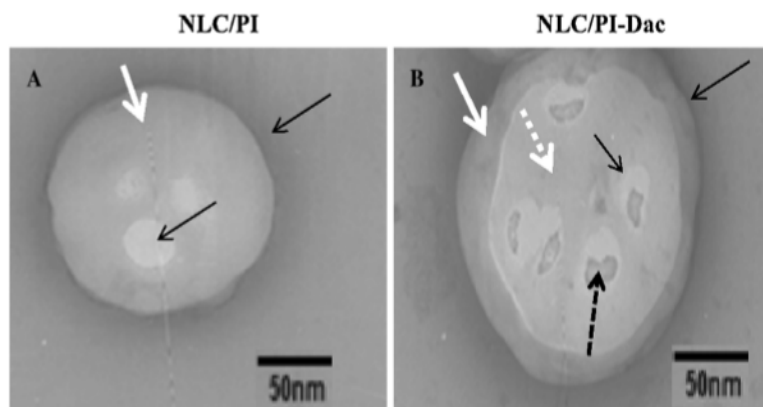
Table 2 Physical properties of NLC/PI and NLC/PI-Dac

Samples	PS (nm)	PDI	ZP (mV)
aNLC	155 ± 10	0.2 ± 0.01	-43.4 ± 2.0
aNLC-Dac	190 ± 10	0.2 ± 0.01	-43.5 ± 1.2

Each value represents the mean \pm SD ($n = 5$)

PS particle size, PDI polydispersion index, ZP zeta potential

Fig. 2 TEM images of NLC/PI (a) and NLC/PI-Dac (b). The black arrows outside the NLCs indicate surfactant layer; the white arrows indicate liquid lipid matrix; the black arrows inside the NLCs indicate crystallised solid lipid; the dotted white arrow in b indicates non-crystallized solid lipid structure; the dotted black arrow in b indicates encapsulated Dac. Bar scale 50 nm, magnification: $\times 55,000$



lipid within the matrix of liquid lipid. For NLC/PI-Dac, a well-defined white area (Fig. 2b, indicated by dotted white arrow) with several irregularly shaped core structures (Fig. 2b, indicated by black arrow inside NLC) was observed under a shell (Fig. 2b, indicated by white arrow). Within each core structure was a dark area (Fig. 2b, indicated by dotted black arrow), indicating the encapsulation of Dac.

The NLC/PI-Dac preparation achieved an encapsulation efficiency of 98.5 % of the drug as determined using the UV detection method on day 1 after synthesis (Table 3), which was equivalent to drug loading capacity of 14 %. When stored in sealed amber colored glass vials in the dark at 4 °C, the physical properties of the NLCs with respect to PS, PDI and EE % were stable for up to 3 months. As seen in Table 3, little change was detected over the time of storage.

ZP is found to be important in the colloidal stability of NPs in solution [31]. To achieve a good physical stability, ZP greater than 30 mV is required, whilst for excellent stability, ZP greater than 60 mV is required [31]. The NLC/PI and NLC/PI-Dac both presented ZP greater than 40 mV, indicating a good stability of the preparations. To achieve a good dispersion of lipid nanoparticles in aqueous phase and good stability during storage, surfactants of low toxicity and high stabilizing function have been commonly

used [32, 33]. The surfactants selected in the current study are among the most commonly used surfactants in lipid nanoparticle preparation and appeared compatible with lipid components used in the preparation of the NLC/PI. For preparation of NLC/SI and NLC/GM, further optimizations are required to achieve desired PS and PDI.

PXRD assay was performed to characterize the crystallinity of NLC/PI and NLC/PI-Dac with Dac as a reference (Fig. 3). As reported previously, the PXRD profile of Dac presented a number of distinctive sharp peaks. Such characteristic pattern was absent in the diffraction profile of NLC/PI-Dac, indicating that Dac was no longer present as crystalline form in the NLC/PI. Some sharp distinctive peaks were also present in the PXRD profile of the NLC/PI, but their intensity was much lower in the profile of NLC/PI-Dac, indicating that Dac loading prevented the formation of solid lipid crystals to certain extent.

Several previous attempts have been made to develop drug delivery vehicles for Dac to improve the therapeutic profile of the drug [16, 18, 19, 34]. However, the low drug encapsulation and loading efficiency present critical limitations for these new formulations to achieve a real benefit. For example, a drug encapsulation of 70 % and drug loading of 15 $\mu\text{g}/\text{mg}$ (1.5 %) were reported for methoxy poly (ethylene glycol)-poly (lactide) nanoparticles [18]. In comparison, the present study achieved a drug encapsulation greater than 98 % and drug loading 14 %, which could be due to the combination of the hydrophobic nature of Precirol ATO 5 and the oily component. The high level of drug incorporation was evidenced by DLS, TEM and PXRD assays. NLC/PI-Dac was much larger than NLC/PI, indicating a substantial level of drug loading. The difference in the lipid core structures and PXRD profiles between NLC/PI and NLC/PI-Dac suggested that Dac partially prevented the crystallization of the solid lipid, leading to increased drug–lipid binding capacity.

Table 3 Stability assessment of NLC/PI-Dac storage at 4 °C

Time (days)	PS	PDI	EE (%)
1	190 \pm 10	0.2 \pm 0.01	98.50
7	190 \pm 10	0.2 \pm 0	98.50
30	190 \pm 10	0.2 \pm 0.01	95.30
90	190 \pm 10	0.2 \pm 0.02	95.1

PS particle size, PDI polydispersion index, EE % encapsulation efficiency

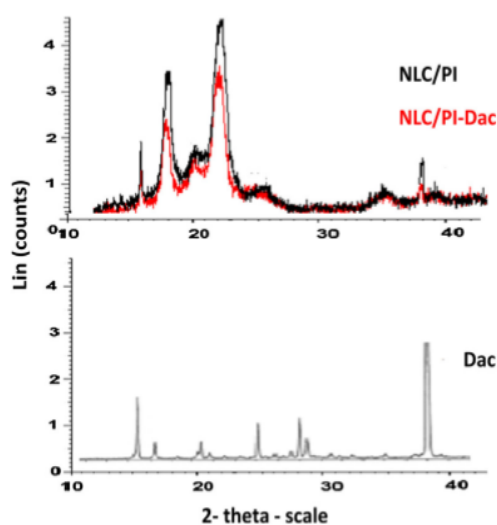


Fig. 3 PXRD pattern of Dac, NLC/PI-Dac and NLC/PI, respectively (from *bottom* to *top*). Dac exhibits a characteristic peak at 38° , while NLC/PI exhibits characteristic peaks at 23° and 19° and the intensity of the peaks reduced in NLC/PI-Dac. The x-axis represents the scattering angle and the y-axis represents the peak intensity expressed as lin counts

The release of Dac from NLC/PI *in vitro* appeared to follow a biphasic pattern. Nearly 50 % of the drug was released from the formulation in the first 2 h, followed by a sustainable release of the remaining drug for up to 30 h. It has been suggested that the presence of drug on the surface and outer shell of NLC contributes to the initial burst release, whilst drug incorporated in deeper lipid phase contributes to sustained release [29]. The present study appeared to agree with this suggestion. In the first phase, Dac could be released from the outer layer of the NLC through a short diffusion path, whilst in the second phase Dac could be released in a sustained manner from the deeper liquid lipid phase and solid lipid cores through diffusion and erosion mechanisms. A similar *in vitro* profile for drug release from NLC containing Precirol ATO 5 was also reported previously [29, 35] (Fig. 4).

The release pattern of a drug from NLCs is determined by the nature of lipid matrix, the ability of drug to partition into both aqueous and lipid phases, temperature and surfactant concentration used to prepare the NLCs. The use of surfactant and high temperature to melt the lipid will increase the drug solubility in the aqueous phase. Upon cooling, the drug will repartition into the lipid phase and the solid lipid recrystallizes to form a solid lipid core. TPGS has been often used as an emulsifier in preparation of polymer nanoparticles [36]. It has also been recently used in combination with SL in NLC preparation, resulting

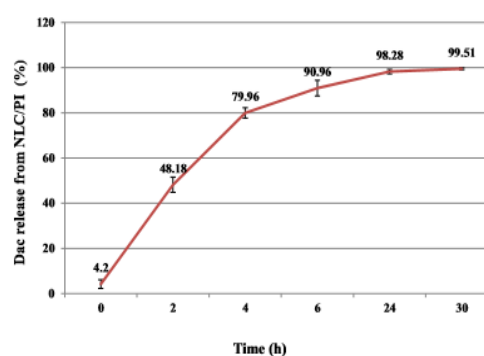


Fig. 4 *In vitro* drug release profile of Dac from NLC/PI in PBS (pH = 7.4). The NLC/PI-Dac preparation was diluted at 10 % in PBS and incubated at 37°C . At predetermined intervals, the release of Dac was determined by UV detection and expressed as percentage of total loaded amount of the drug

in a smaller size and higher drug EE as compared with their separate use [36, 37]. TPGS could protect the diffusion or partition of hydrophobic drug from NLC to external phase due to its big lipophilic alkyl tail (polyethylene glycol) and hydrophilic polar head portion (tocopherol succinate) [37].

Potential of NLC/PI for Dac delivery

The only formulation of Dac in clinical use is given by intravenous infusion with drug half-life less than 1 h [11]. A new formulation of Dac should prolong the drug half-life in the blood circulation, allowing enough drug to accumulate in target organ/tissue. Encapsulation of drug in NLC could provide a solution. Although NLC/PI-Dac developed in this study showed a relative earlier drug release as compared with the formulation reported by Ding et al. [15, 16], it has been demonstrated that a drug encapsulated in NLC with a similar *in vitro* release profile as NLC/PI-Dac developed in this study could reach the brain 2 h after intravenous injection [29]. For NLC/PI-Dac, although the drug in the outer layer of the NLCs could diffuse into the blood circulation, the drug incorporated inside NLC could be carried over to the side of action, therefore improving the Dac therapeutic profile. Moreover, it was suggested that lipid nanoparticles <200 nm could form a monolayer on the skin and prevent the evaporation of water from the skin. By forming a transcutaneous hydration gradient, lipid nanoparticles could facilitate drug to penetrate into the deeper layers of the skin [38]. Lipid-based vehicles have been proposed for treating cutaneous melanoma and epidermoid carcinoma through topical drug delivery [19, 39], indicating that the NLC/PI-Dac developed could also be beneficial via topical route for which early drug release would not potentially lead to severe

systemic toxicity. This study implicates that NLC could have the potential for drug delivery via multiple routes.

Conclusion

This is the first report on the development of NLCs for Dac delivery. The commonly used method for NLC synthesis has been modified as such that it involved oil-in-water emulsion, evaporation and solidification followed by HSD to achieve NLCs with desirable size. As compared with some existing approaches for Dac encapsulation with different materials, using NLC proved beneficial in improving the drug encapsulation and loading efficiency, prolonging drug release, storage stability, and simplified synthesis. This research suggests that NLC/PI is a new potential candidate for Dac delivery to overcome the limitations of short half-life, and low tolerant dose of the drug. Further study will be required to assess the profile of NLC/PI-Dac drug release and toxicity in vitro and in vivo.

Acknowledgments The authors acknowledge the Saudi Arabia-funded scholarship (1821) and the European commission framework 7-funded project NANODRUG (289454) for making the research possible. The authors are grateful to Kimpton Christine for technical guidance on PXRD assay and Dr. Xianwei Liu for expert support in TEM analysis at Cranfield University.

Open Access This article is distributed under the terms of the Creative Commons Attribution 4.0 International License (<http://creativecommons.org/licenses/by/4.0/>), which permits unrestricted use, distribution, and reproduction in any medium, provided you give appropriate credit to the original author(s) and the source, provide a link to the Creative Commons license, and indicate if changes were made.

References

- Sun, M., Nie, S., Pan, X., Zhang, R., Fan, Z., Wang, S.: Quercetin-nanostructured lipid carriers: characteristics and anti-breast cancer activities in vitro. *Colloid Surf. B Biointerface* **113**, 15–24 (2014)
- Eigentler, T.K., Caroli, U.M., Radny, P., Garbe, C.: Palliative therapy of disseminated malignant melanoma: a systematic review of 41 randomised clinical trials. *Lancet Oncol.* **4**(12), 748–759 (2003)
- Jerant, A.F., Johnson, J.T., Sheridan, C.D., Caffrey, T.J.: Early detection and treatment of skin cancer. *Am. Fam. Phys.* **62**(2), 357–368 (2000)
- Quirin, C., Mainka, A., Hesse, A., Nettelbeck, D.M.: Combining adenoviral oncolysis with temozolomide improves cell killing of melanoma cells. *Int. J. Cancer* **121**(12), 2801–2807 (2007)
- Lens, M.B., Dawes, M.: Global perspectives of contemporary epidemiological trends of cutaneous malignant melanoma. *Br. J. Dermatol.* **150**(2), 179–185 (2004)
- Chen, J., Shao, R., Zhang, X.D., Chen, C.: Applications of nanotechnology for melanoma treatment, diagnosis, and theranostics. *Int. J. Nanomedicine* **8**, 2677–2688 (2013)
- Ohshio, G., Hosotani, R., Imamura, M., Sakahara, H., Ochi, J., Kubota, N.: Gastrinoma with multiple liver metastases: effectiveness of dacarbazine (DTIC) therapy. *J. Hepatobiliary Pancreat.* **5**(3), 339–343 (1998)
- Loo, T.L., Housholder, G.E., Gerulath, A.H., Saunders, P.H., Farquhar, D.: Mechanism of action and pharmacology studies with DTIC (NSC 45388). *Cancer Treat. Rep.* **60**(2), 149–152 (1976)
- Gerulath, A.H., Loo, T.L.: Mechanism of action of 5-(3,3-dimethyl-1-triazeno)imidazole-4-carboxamide in mammalian cells in culture. *Biochem. Pharmacol.* **21**(17), 2335–2343 (1972)
- Bedia, C., Casas, J., Andrieu-Abadie, N., Fabriàs, G., Levade, T.: Acid ceramidase expression modulates the sensitivity of A375 melanoma cells to dacarbazine. *J. Biol. Chem.* **286**(32), 28200–28209 (2011)
- Breithaupt, H., Dammann, A., Aigner, K.: Pharmacokinetics of dacarbazine (DTIC) and its metabolite 5-aminoimidazole-4-carboxamide (AIC) following different dose schedules. *Cancer Chemother. Pharmacol.* **9**(2), 103–109 (1982)
- Chapman, P.B., Einhorn, L.H., Meyers, M.L., Saxman, S., Destro, A.N., Panageas, K.S., Begg, C.B., Agarwala, S.S., Schuchter, L.M., Ernstoff, M.S., Houghton, A.N., Kirkwood, J.M.: Phase III multicenter randomized trial of the dartmouth regimen versus dacarbazine in patients with metastatic melanoma. *J. Clin. Oncol.* **17**(9), 2745–2751 (1999)
- Luikart, S.D., Kennealey, G.T., Kirkwood, J.M.: Randomized phase III trial of vinblastine, bleomycin, and cis-dichlorodiammine-platinum versus dacarbazine in malignant melanoma. *J. Clin. Oncol.* **2**(3), 164–168 (1984)
- Eggermont, A.M.M., Kirkwood, J.M.: Re-evaluating the role of dacarbazine in metastatic melanoma: what have we learned in 30 years? *Eur. J. Cancer* **40**(12), 1825–1836 (2004)
- Soengas, M.S., Lowe, S.W.: Apoptosis and melanoma chemoresistance. *Oncogene* **22**(20), 3138–3151 (2003)
- Bei, D., Zhang, T., Murowchick, J.B., Youan, B.C.: Formulation of dacarbazine-loaded cubosomes. Part III. Physicochemical characterization. *AAPS PharmSciTech.* **11**(3), 1243–1249 (2010)
- Ding, B., Wu, X., Fan, W., Wu, Z., Gao, J., Zhang, W., Ma, L., Xiang, W., Zhu, Q., Liu, J., Ding, X., Gao, S.: Anti-DR5 monoclonal antibody-mediated DTIC-loaded nanoparticles combining chemotherapy and immunotherapy for malignant melanoma: target formulation development and in vitro anticancer activity. *Int. J. Nanomedicine* **6**, 1991–2005 (2011)
- Ding, B., Zhang, W., Wu, X., Wang, X., Fan, W., Gao, S., Gao, J., Ma, L., Ding, X., Hao, Q.: Biodegradable methoxy poly (ethylene glycol)-poly (lactide) nanoparticles for controlled delivery of dacarbazine: preparation, characterization and anticancer activity evaluation. *Afr. J. Pharm. Pharmacol.* **5**(11), 1369–1377 (2011)
- Kakumanu, S., Tagne, J.B., Wilson, T.A., Nicolosi, R.J.: A nanoemulsion formulation of dacarbazine reduces tumor size in a xenograft mouse epidermoid carcinoma model compared to dacarbazine suspension. *Nanomedicine Nanotechnol. Biol. Med.* **7**(3), 277–283 (2011). doi:10.1016/j.nano.2010.12.002
- Taratula, O., Kuzmov, A., Shah, M., Garbuzenko, O.B., Minko, T.: Nanostructured lipid carriers as multifunctional nanomedicine platform for pulmonary co-delivery of anticancer drugs and siRNA. *J. Control. Release* **171**(3), 349–357 (2013)
- Müller, R.H., Radtke, M., Wissing, S.A.: Nanostructured lipid matrices for improved microencapsulation of drugs. *Int. J. Pharm.* **242**(1–2), 121–128 (2002)
- Patidar, A., Thakur, D.S., Kumar, P., Verma, J.: A review on novel lipid based nanocarriers. *Int. J. Pharm. Pharm. Sci.* **2**(4), 30–35 (2010)
- Alam, M.I., Baboota, S., Ahuja, A., Ali, M., Ali, J., Sahni, J.K., Bhatnagar, A.: Pharmacoscintigraphic evaluation of potential of

- lipid nanocarriers for nose-to-brain delivery of antidepressant drug. *Int. J. Pharm.* **470**(1–2), 99–106 (2014)
24. Gonzalez-Mira, E., Egea, M.A., Souto, E.B., Calpena, A.C., Garcia, M.L.: Optimizing flurbiprofen-loaded NLC by central composite factorial design for ocular delivery. *Nanotechnology* **22**(4), 45101–45115 (2011)
 25. Pardeike, J., Hommoss, A., Müller, R.H.: Lipid nanoparticles (SLN, NLC) in cosmetic and pharmaceutical dermal products. *Int. J. Pharm.* **366**(1–2), 170–184 (2009)
 26. Pardeike, J., Weber, S., Haber, T., Wagner, J., Zarfl, H.P., Plank, H., Zimmer, A.: Development of an Itraconazole-loaded nanostructured lipid carrier (NLC) formulation for pulmonary application. *Int. J. Pharm.* **419**(1–2), 329–338 (2011). doi:[10.1016/j.ijpharm.2011.07.040](https://doi.org/10.1016/j.ijpharm.2011.07.040)
 27. Irfan, A., Cauchi, M., Edmands, W., Gooderham, N.J., Njuguna, J., Zhu, H.: Assessment of temporal dose-toxicity relationship of fumed silica nanoparticle in human lung A549 cells by conventional cytotoxicity and IH-NMR-based extracellular metabolic assays. *Toxicol. Sci.* **138**(2), 354–364 (2014)
 28. Neupane, Y.R., Srivastava, M., Ahmad, N., Kumar, N., Bhatnagar, A., Kohli, K.: Lipid based nanocarrier system for the potential oral delivery of decitabine: formulation design, characterization, ex vivo, and in vivo assessment. *Int. J. Pharm.* **477**(1–2), 601–612 (2014)
 29. Lim, W.M., Rajinikanth, P.S., Mallikarjun, C., Kang, Y.B.: Formulation and delivery of itraconazole to the brain using a nanolipid carrier system. *Int. J. Nanomedicine* **9**(1), 2117–2126 (2014)
 30. Puglia, C., Damiani, E., Offerta, A., Rizza, L., Tirendi, G.G., Tarico, M.S., Curreri, S., Bonina, F., Perrotta, R.E.: Evaluation of nanostructured lipid carriers (NLC) and nanoemulsions as carriers for UV-filters: characterization, in vitro penetration and photostability studies. *Eur. J. Pharm. Sci.* **51**(1), 211–217 (2014)
 31. Riddick, T.: *Zeta-Meter Manual*. Zeta-Meter Inc., New York (1968)
 32. Kullavadee, K.O., Uracha, R., Smith, S.M.: Effect of surfactant on characteristics of solid lipid nanoparticles (SLN). *Adv. Mater. Res.* **364**, 313–316 (2012)
 33. Leonardi, A., Bucolo, C., Romano, G.L., Platania, C.B.M., Drago, F., Puglisi, G., Pignatello, R.: Influence of different surfactants on the technological properties and in vivo ocular tolerability of lipid nanoparticles. *Int. J. Pharm.* **470**(1), 133–140 (2014)
 34. Bei, D., Marszalek, J., Youan, B.C.: Formulation of dacarbazine-loaded cubosomes—part I: influence of formulation variables. *AAPS PharmSciTech.* **10**(3), 1032–1039 (2009)
 35. Song, S.H., Lee, K.M., Kang, J.B., Lee, S.G., Kang, M.J., Choi, Y.W.: Improved skin delivery of voriconazole with a nanostructured lipid carrier-based hydrogel formulation. *Chem. Pharm. Bull.* **62**(8), 793–798 (2014)
 36. Mu, L., Feng, S.: Vitamin E TPGS used as emulsifier in the solvent evaporation/extraction technique for fabrication of polymeric nanospheres for controlled release of paclitaxel. *J. Control. Release* **80**(1), 129–144 (2002)
 37. Zhou, L., Chen, Y., Zhang, Z., He, J., Du, M., Wu, Q.: Preparation of tripterine nanostructured lipid carriers and their absorption in rat intestine. *Die Pharmazie Int. J. Pharm. Sci.* **67**(4), 304–310 (2012)
 38. Wissing, S.A., Müller, R.H.: Cosmetic applications for solid lipid nanoparticles (SLN). *Int. J. Pharm.* **254**(1), 65–68 (2003). doi:[10.1016/S0378-5173\(02\)00684-1](https://doi.org/10.1016/S0378-5173(02)00684-1)
 39. Lei, M., Wang, J., Ma, M., Yu, M., Tan, F., Li, N.: Dual drug encapsulation in a novel nano-vesicular carrier for the treatment of cutaneous melanoma: characterization and in vitro/in vivo evaluation. *RSC Adv.* **5**(26), 20467–20478 (2015). doi:[10.1039/C4RA16306K](https://doi.org/10.1039/C4RA16306K)



Almoussalam, M. and Zhu, H. (2016), "Encapsulation of cancer therapeutic agent dacarbazine using nanostructured lipid carrier", *JoVE (Journal of Visualized Experiments)*, no. 110, pp. e53760-e53760.



TITLE: Encapsulation of cancer therapeutic agent dacarbazine using nanostructured lipid carrier

AUTHORS: Almoussalam, Musallam Institute of Environment, Health, Risks and Futures Cranfield University Bedfordshire, United Kingdom m.m.almoussalam@cranfield.ac.uk

Zhu, Huijun Institute of Environment, Health, Risks and Futures Cranfield University Bedfordshire, United Kingdom h.zhu@cranfield.ac.uk

CORRESPONDING AUTHOR: Zhu, Huijun

KEYWORDS: Nanostructured lipid carrier (NLC), dacarbazine (Dac), high shear dispersion (HSD), drug delivery

SHORT ABSTRACT: The most commonly used method for nanostructured lipid carrier (NLC) synthesis involves oil-in-water emulsion, homogenization and solidification. This was modified here by applying high shear dispersion after solidification to achieve a NLC with desirable size, improved drug encapsulation and drug loading efficiency as a potential carrier for dacarbazine delivery .

LONG ABSTRACT: The only formula of dacarbazine (Dac) in clinical use is intravenous infusion, presenting a poor therapeutic profile due to the low dispersity of the drug in aqueous solution. To overcome this, a nanostructured lipid carrier (NLC) consisting of glyceryl palmitostearate and isopropyl myristate was developed to encapsulate Dac. NLCs with controlled size were achieved using high shear dispersion (HSD) following solidification of oil-in-water emulsion. The synthesis parameters, including surfactant concentration, the speed and time of HSD were optimized to achieve the smallest NLC with size, polydispersion index and zeta potential of 155 ± 10 nm, 0.2 ± 0.01 , and -43.4 ± 2 mV, respectively. The optimal parameters were also employed for Dac-loaded NLC preparation. The resultant NLC loaded with Dac possessed size, polydispersion index and zeta potential of 190 ± 10 nm, 0.2 ± 0.01 , and -43.5 ± 1.2 mV, respectively. The drug encapsulation efficiency and drug loading reached 98% and 14%,

respectively. This is the first report on encapsulation of Dac using NLC, implying that NLC could be a new potential candidate as drug carrier to improve the therapeutic profile of Dac .

INTRODUCTION :

Dacarbazine (Dac) is an alkylating agent that exerts anti-tumor activity through nucleic acids methylation or direct DNA damage, leading to cell cycle arrest and cell death 1 .

As a first line chemotherapeutic agent, Dac has been used alone or in combination with other chemotherapy drugs for treating various cancers 2-6. It is the most active agent so far used in treating cutaneous and metastatic melanoma, which is the most aggressive form of skin cancer 3, 7, 8. The response rate, however, is only 20% at best, and the therapeutic effects are often accompanied with severe systemic side effects .

In its natural form, Dac is hydrophilic and is unstable due to its photosensitivity 9. The only available formula for clinical use currently is a sterile powder to be used in suspension for intravenous infusion 7, 8. The low response rate and high systemic toxicity rate of the drug is largely attributable to its poor water solubility, therefore low availability at target site, and high distribution at non-target sites, which limits the maximum dose of the drug 10. The rapid degradation and metabolism after intravenous admission together with the development of drug resistance limit the clinical application and therapeutic effect of the drug 11. Therefore, there is an urgent need to develop alternative Dac formulations for treating malignant melanoma .

Colloidal systems containing liposomes, micelles or nanostructured particles have been intensively investigated for their use in drug delivery as reviewed by Marilene et al. 12. Nanostructured particles as potential drug carriers have been attracting increasing attention in the last decade due to their ability to increase drug loading efficiency, control drug release, improve drug pharmacokinetics and biodistribution, and therefore reduce drug systemic toxicity 13. Only a few nanoformulations, however, have been investigated so far for Dac delivery, showing protection of the drug from photo degeneration, increased drug solubility, and improved therapeutic effect 10, 14, , 15. However these formulations suffered from low encapsulating efficiency while some also using synthetic polymer nanoparticles that are not cost effective .

Nanostructured lipid carriers (NLC), made of a mixture of solid and liquid lipids, have been developed for drug delivery 16, 17. The drugs to be encapsulated are often soluble in both the liquid lipids and solid lipids phases 18, resulting in a high loading and controlled release 19. This study aims to develop a new Dac formulation based on NLC-encapsulation using glyceryl palmitostearate and isopropyl myristate as lipids. The preparation involved oil-in-water emulsion, evaporation, solidification, and homogenization. The preparations have been characterized for NLC size, shape, ultrastructure, and dispersity, drug encapsulation efficiency and drug loading 20.

PROTOCOL :

1 .Preparation of oil-in-water emulsion

1.1 (Weigh glyceryl palmitostearate (120 mg), isopropyl myristate (60 mg), d- α -tocopheryl polyethylene glycol succinate (30 mg) and soybean lecithin (30 mg), and add them to 12.5 mL of organic solvents (6.25 mL acetone and 6.25 mL ethanol). Quickly dissolve the mixture at the temperature 70 oC (5 oC above the melting point of the solid lipid) in water bath .

1.2 (Add either 125, 250 or 375 mg of Poloxamer188 in 12.5 mL of ddH₂O to achieve 1-3% (respectively) of Poloxamer 188 solution, which is subject to heating at the same temperature as above .

1.3 (Add the aqueous phase solution from step 1.2 to the oil phase solution from step 1.1 dropwise to form emulsions under magnetic stirring at 400 rpm . Stir the emulsion at 400 rpm for another 4 h to allow evaporation of the organic solvents .

2 .Solidification and homogenization

2.1 (Leave the emulsion in a cold room (4 oC) for 2 h to solidify/crystallize .

2.2 (To obtain NLC, subject the emulsion to high sheer dispersion (HSD) with a homogenizer at 10000-15000 rpm for 10- 40 min .

3 Optimization of the NLC preparation

3.1 (Take samples from step 2.2 with a surfactant concentration of 1, 2 and 3% undergoing HSD at speeds of 10000, 15000 and 20000 rpm, respectively, and time intervals of 10, 20, 30 and 40 min, respectively .

3.2 (Examine the samples for particle size (PS), poly dispersion index (PDI), morphology and ultrastructure 20 .

Note: The parameters that produce particles with the smallest size (155 nm) and PDI (0.2) value are determined as optimal .

4 .Preparation of Dac-loaded NLC (NLC-Dac)

4.1 (Prepare oil phase solution as described in step 1.1 with the addition of Dac (70 mg) before dissolving the mixture at 70 oC in water bath .

4.2 (Prepare an aqueous phase solution as described in step 1.2 with 1% surfactant, and add this solution to that prepared in step 4.1 dropwise to form an emulsion under magnetic stirring at 400 rpm. Stir the emulsion for further 4 h to evaporate the organic solvents .

4.3 (Leave the emulsion in a cold room (4 oC) for 2 h to solidify/crystallize as described in step 2, and finally, subject the emulsion to high sheer dispersion (HSD) using the optimal parameters determined in step 3 .

REPRESENTATIVE RESULTS: The preparations of the NLC and NLC-Dac using glyceryl palmitostearate and isopropyl myristate with different parameters were characterized for PS, PDI, morphology and ultrastructure 20. The PS and PDI of the NLCs were surfactant concentration, HSD speed and duration dependent. As judged by PS and PDI of the NLCs, the best results were achieved with 1% of surfactant and a sheer dispersion speed of 15000 rpm for 30 min (Figure 1 A, B and C), which therefore were selected as the optimal parameters for NLC preparation in this study .

]place Figure 1 here [

The optimal parameters were used for NLC-Dac preparation. The smallest size achieved was 150 ± 10 nm for NLC (Figure 2 A) and 190 ± 10 nm for NLC-Dac (Figure 2 B), both with PDI of 0.2 ± 0.001 , indicating a good uniformity .

] place Figure 2 here [

Both NLC and NLC-Dac showed a spherical shape as observed under TEM (Figure 3) .

]place Figure 3 here [

The uploading and encapsulation of Dac in NLC is indicated by the size and structure changes as seen in Figures 2 and 3 where NLC-Dac shows a larger size and altered internal structures as compared with NLC. The basic structure of NLC comprises a surfactant layer, a liquid lipid matrix and solid lipid crystals (Figure 3 A). NLC-Dac also exhibited the basic structure as a NLC but with expanded surfactant layer, liquid lipid matrix and solid lipid crystals, together with an extra substructure inside the solid lipid crystals (Figure 3 B), indicative of drug loading and encapsulation. The solid lipid crystals seen in NLC appeared denser than that in NLC-Dac, indicating that the solid lipid is less crystallized in NLC-Dac .

The drug encapsulation efficiency (EF) and drug loading (DL) percentage were derived from the following equations: $EE\% = \frac{W1 - W2}{W1} \times 100 = 98.5\%$ $DL\% = \frac{W1 - W2}{W3} \times 100 = 14\%$ where W1 amount of Dac added in the NLC, W2 amount of un-entrapped Dac, W3 amount of the lipids added 20 .



Figure 1: Optimization of parameters used in NLC preparation. The optimal surfactant concentration and the speed and time of HSD were determined according to their effect on PS and PDI. A. Effect of surfactant concentration on PS; B. Effect of HSD speed and time on PS; C. Effect of HSD speed and time on PDI. This Figure has been modified from 20 . The data are presented as mean value of 3 replicates \pm standard deviation (mean \pm SD) .

Figure 2: DLS measurement of NLC. A. The optimal size distribution of plain NLC; B. the optimal size distribution of NLC-Dac .

Figure 3: TEM imaging of NLC and NLC-Dac. Both NLC and NLC-Dac showed a spherical shape. A. Basic NLC structure comprises a surfactant layer (solid black arrow), liquid lipid matrix (white solid arrow), and solid lipid crystals (dotted white arrows); B. NLC-Dac also exhibited the basic structure as seen in NLC but the surfactant layer, liquid lipid matrix and solid lipid crystals appeared expanded; an extra substructure could be seen inside the solid lipid crystals (indicated by dotted black arrows), indicative of drug loading. Bar scale: 50 nm, Magnification: x 55000. This Figure has been modified from 20 .

DISCUSSION:

Lipid-based nanostructured particles have been utilized to provide a highly lipophilic carrier for delivery of hydrophobic drugs. A NLC is the second generation of solid lipid nanostructured carrier, which are solid at room and body temperature. The incorporation of a solid lipid into a liquid lipid in a NLC results in a less perfect crystallization, thus increasing the drug loading efficiency and also reducing the expulsion of encapsulated drugs during storage .

For NLC synthesis, the most commonly used method involves oil-in-water emulsion, homogenization and solidification/crystallization 21, 22. The homogenization allows NLCs to disperse thoroughly in an aqueous phase, whilst the solidification at low temperature allows the inner oil phase to crystallize. Different homogenization methods have been reported including magnetic stirring, ultrasonication, and HSD that are used before and/or during solidification 23 24 .

In this study, the commonly used method was initially followed for NLC preparation. As the result was unsatisfactory, the method was modified such that HSD was applied after solidification. This modification proved highly effective in particle generation, PS and PDI control, while also making the NLC synthesis simpler, compared with previous reports on NLC preparation using the same lipids 23 25. It was worth noting that the length of the evaporation (protocol 1.3) and solidification (protocol 2.1) is very critical as too long or too short a time would have negative effects on the generation of NLC .

This study suggests that NLC particles and their aggregation were formed during solidification. The HSD could disrupt the aggregation, which was possibly due to hydrophobic interaction between NLCs, and also stabilize the particles by thoroughly remixing them with surfactant. The synthesis procedure was optimized such that the NLC and NLC-Dac were produced with a size 155 ± 10 nm and 190 ± 10 nm, respectively, and a PDI of 0.2 ± 0.01 . The high level of uniformity with particle sizes and the small PDI values indicates that a sufficient dispersion energy was achieved and is well distributed within the solution for disruption of particle aggregates. It has been suggested that particles of 100–200 nm are not prone to uptake by non-targeted cells, including mononuclear phagocytic system, thus having a long blood circulation time in vivo 26 27, whilst a PDI of more than 0.5 is an indication of particle aggregation 28; the lower the PDI value, the higher the size homogeneity between the particles 29. Further increase of the HSD speed and time above the optimal point could result in further PS reduction, and consequently an increase in interactions between small particles as well as re-aggregation. The difference in size

and structure between NLC and NLC-Dac suggests that the Dac loading and encapsulation was successful. The drug binding to the outer layer of the NLC and encapsulation inside lipid matrices provide the potential for prolonged drug release, that could involve drug release

firstly from the outer layer, followed by the release from the liquid lipid matrix and then from the solid lipid crystals of the NLC 30 .

Currently four nanoformulations have been attempted for delivery of Dac as a single agent. The latest formulation reported was designed for dual encapsulation of Dac and vitamin A 32. However, these formulations suffered from a low encapsulation efficiency and/or relatively complex synthesis procedures. This is the first report for encapsulation of Dac with a NLC, proving advantageous over other encapsulations reported previously. NLC-Dac is easy to make and presents higher drug encapsulation and drug loading efficiency 20. The NLC-Dac showed nearly 50% of drug released within the first 2 h whilst the remaining released slowly for up to 30 h 20. The early release could be due to the binding of the drug with surfactant layer on the surface of the NLC, indicating that this formulation may not be ideal to replace the formulation currently in clinical use. However, the drug in NLC-Dac appeared more stable compared with the nanoemulsion reported previously 10. In addition, lipid based vehicles have been proposed for treating cutaneous melanoma and epidermoid carcinoma through topical drug delivery 32 10, indicating that the NLC-Dac developed in this study could also be potentially beneficial for topical application where early drug release would not potentially lead to severe systemic toxicity .

Due to the collective limitations with the available drug delivery carriers developed so far, further research is needed to develop more advanced nanomaterials for Dac delivery for targeted cancer treatment .

ACKNOWLEDGMENTS: The authors acknowledge the Saudi Arabia-funded scholarship (I821) for making the research possible. The authors are grateful to Dr Xianwei Liu for expert support in TEM analysis at Cranfield University .

DISCLOSURES: The authors have nothing to disclose .

REFERENCES

1. Loo, T.L., Housholder, G.E., Gerulath, A.H., Saunders, P.H., Farquhar, D., Mechanism of action and pharmacology studies with DTIC (NSC 45388). *Cancer Treat Rep.* 60 (2), 149-152 (1976).
2. Behringer, K., et al., Omission of dacarbazine or bleomycin, or both, from the ABVD regimen in treatment of early-stage favourable Hodgkin's lymphoma (GHSG HD13): An open-label, randomised, non-inferiority trial. *The Lancet.* 385 (9976), 1418-1427, doi:10.1016/S01406736(14)61469-0 (2014).
3. Carvajal, R.D., et al., A phase 2 randomised study of ramucirumab (IMC-1121B) with or without dacarbazine in patients with metastatic melanoma. *Eur J Cancer.* 50 (12), 2099-2107, <http://dx.doi.org/10.1016/j.ejca.2014.03.289> (2014)
4. Jiang, G., Li, R., Sun, C., Liu, Y.-., Zheng, J., Dacarbazine combined targeted therapy versus dacarbazine alone in patients with malignant melanoma: A meta-analysis. *PLoS ONE.* 9 (12), doi: 10.1371/journal.pone.0111920 (2014).
5. Lazar, V., et al., Sorafenib plus dacarbazine in solid tumors: A phase I study with dynamic contrast-enhanced ultrasonography and genomic analysis of sequential tumor biopsy samples. *Invest New Drugs.* 32 (2), 312-322, doi:10.1007/s10637-013-9993-0 (2014).
6. Niemeijer, N.D., Alblas, G., Van Hulsteijn, L.T., Dekkers, O.M., Corssmit, E.P.M., Chemotherapy with cyclophosphamide, vincristine and dacarbazine for malignant paraganglioma and pheochromocytoma: Systematic review and meta-analysis. *Clin Endocrinol (Oxf).* 81 (5), 642-651, doi:10.1111/cen.12542 (2014).
7. Bedikian, A.Y., Garbe, C., Conry, R., Lebbe, C., Grob, J.J., Dacarbazine with or without oblimersen (a Bcl-2 antisense oligonucleotide) in chemotherapy-naïve patients with advanced melanoma and low-normal serum lactate dehydrogenase: 'The AGENDA trial'. *Melanoma Res.* 24 (3), 237-243, doi:10.1097/CMR.000000000000056 (2014).
8. Daponte, A., et al., Phase III randomized study of fotemustine and dacarbazine versus dacarbazine with or without interferon- α in advanced malignant melanoma. *J Trans Med.* 11 (1) (2013).
9. Jiao, J., Rhodes, D.G., Burgess, D.J., Multiple Emulsion Stability: Pressure Balance and Interfacial Film Strength. *J Colloid Interface Sci.* 250 (2), 444-450, doi: 10.1006/jcis.2002.8365 (2002).
10. Kakumanu, S., Tagne, J.B., Wilson, T.A., Nicolosi, R.J., A nanoemulsion formulation of dacarbazine reduces tumor size in a xenograft mouse epidermoid carcinoma model compared to dacarbazine suspension. *Nanomedicine* 7 (3), 277-283, doi:10.1016/j.nano.2010.12.002 (2011).
11. Xie, T., Nguyen, T., Hupe, M., Wei, M.L., Multidrug resistance decreases with mutations of melanosomal regulatory genes. *Cancer Res.* 69 (3), 992-999, doi:10.1158/0008-5472.CAN-080506 (2009).
12. Estanqueiro, M., Amaral, M.H., Conceição, J., Lobo, J.M.S., Nanotechnological carriers for cancer chemotherapy: the state of the art. *Colloids Surf., B.* 126, 631-648, doi:10.1016/j.colsurfb.2014.12.041 (2015).
13. Koziara, J.M., Whisman, T.R., Tseng, M.T., Mumper, R.J., In-vivo efficacy of novel paclitaxel nanoparticles in paclitaxel-resistant human colorectal tumors. *J Controlled Release.* 112 (3), 312-319, doi:10.1016/j.jconrel.2006.03.001 (2006).
14. Ding, B.-., et al., Biodegradable methoxy poly (ethylene glycol)-poly (lactide) nanoparticles for controlled delivery of dacarbazine: Preparation, characterization and anticancer activity evaluation. *Afr J Pharm Pharmacol.* 5 (11), 1369-1377, doi: 10.5897/AJPP11.236 (2011).

15. Ding, B., et al., Anti-DR5 monoclonal antibody-mediated DTIC-loaded nanoparticles combining chemotherapy and immunotherapy for malignant melanoma: target formulation development and in vitro anticancer activity. *Int J Nanomedicine*. 6 , 1991-2005, 10.2147/IJN.S24094 (2011).
16. Jennings, V., Thünemann, A.F., Gohla, S.H., Characterisation of a novel solid lipid nanoparticle carrier system based on binary mixtures of liquid and solid lipids. *Int J Pharm*. 199 (2), 167-177, doi:10.1016/S0378-5173(00)00378-1 (2000).
17. Müller, R.H., Radtke, M., Wissing, S.A., Nanostructured lipid matrices for improved microencapsulation of drugs. *Int J Pharm*. 242 (1-2), 121-128, doi:10.1016/S03785173(02)00180-1 (2002).
18. Pouton, C.W. Lipid formulations for oral administration of drugs: Non-emulsifying, selfemulsifying and 'self-microemulsifying' drug delivery systems. *Eur. J. Pharm. Sci.* 11 (SUPPL. 2), S93-S98, doi:10.1016/S0928-0987(00)00167-6 (2000).
19. Jores, K., Mehnert, W., Drechsler, M., Bunjes, H., Johann, C., Mäder, K., Investigations on the structure of solid lipid nanoparticles (SLN) and oil-loaded solid lipid nanoparticles by photon correlation spectroscopy, field-flow fractionation and transmission electron microscopy. *J Controlled Release*. 95 (2), 217-227, doi:10.1016/j.jconrel.2003.11.012 (2004).
20. Almousallam, M., Zhu, H., Encapsulation of cancer therapeutic agent dacarbazine using nanostructured lipid carrier. *Int nano lett*. In press, DOI 10.1007/s40089-015-0161-8 (2015).
21. Ng, W.K., et al. Thymoquinone-loaded nanostructured lipid carrier exhibited cytotoxicity towards breast cancer cell lines (MDA-MB-231 and MCF-7) and cervical cancer cell lines (HeLa and SiHa). *BioMed Research International*. 2015, <http://dx.doi.org/10.1155/2015/263131> (2015).
22. Sun, M., et al. Quercetin-nanostructured lipid carriers: Characteristics and anti-breast cancer activities in vitro. *Colloids Surf., B*. 113 , 15-24, doi:10.1016/j.colsurfb.2013.08.032 (2014).
23. Savla, R., Garbuzenko, O.B., Chen, S., Rodriguez-Rodriguez, L., Minko, T., Tumor-Targeted Responsive Nanoparticle-Based Systems for Magnetic Resonance Imaging and Therapy. *Pharm Res*. 31 (12), 3487-3502, doi:10.1007/s11095-014-1436-x (2014).
24. Chen, Y., et al., Formulation, characterization, and evaluation of in vitro skin permeation and in vivo pharmacodynamics of surface-charged tripterine-loaded nanostructured lipid carriers. *Int J Nanomedicine*. 7, 3023, doi:10.2147/IJN.S32476. Epub 2012 Jun 19 (2012).
25. Sanna, V., Caria, G., Mariani, A., Effect of lipid nanoparticles containing fatty alcohols having different chain length on the ex vivo skin permeability of Econazole nitrate. *Powder Technol*. 201 (1), 32-36, doi:10.1016/j.powtec.2010.02.035 (2010).
26. Brigger, I., Dubernet, C., Couvreur, P., Nanoparticles in cancer therapy and diagnosis. *Adv Drug Deliv Rev*. 54 (5), 631-651, doi: 10.1016/S0169-409X(02)00044-3, (2002).
27. Visaria, R.K., et al., Enhancement of tumor thermal therapy using gold nanoparticle-assisted tumor necrosis factor- α delivery. *Mol Cancer Ther*. 5 (4), 1014-1020, doi: 10.1158/15357163.MCT-05-0381, (2006).
28. Tripathi, A., Gupta, R., Saraf, S.A., PLGA nanoparticles of anti tubercular drug: Drug loading and release studies of a water in-soluble drug. *Int J PharmTech Res*. 2 (3), 2116-2123 (2010).
29. Joshi, M., Patravale, V., Nanostructured lipid carrier (NLC) based gel of celecoxib. *Int J Pharm*. 346 (1-2), 124-132, doi:10.1016/j.ijpharm.2007.05.060 (2008).
30. Lim, W.M., Rajinikanth, P.S., Mallikarjun, C., Kang, Y.B., Formulation and delivery of itraconazole to the brain using a nanolipid carrier system. *Int J Nanomedicine*. 9 (1), 2117-2126, doi:10.2147/IJN.S57565 (2014).

31. Bei, D., Zhang, T., Murowchick, J.B., Youan, B.-C., Formulation of dacarbazine-loaded cubosomes. Part III. physicochemical characterization. *AAPS PharmSciTech.* 11 (3), 1243-1249, doi:10.1208/s12249-010-9496-7 (2010).

32. Lei, M., et al., Dual drug encapsulation in a novel nano-vesicular carrier for the treatment of cutaneous melanoma: Characterization and in vitro/in vivo evaluation. *RSC Advances.* 5 (26)

doi: 20467-20478, 10.1039/C4RA16306K (2015).

Preparation and *in vitro* assessment of nanostructured lipid carrier for dacarbazine delivery



Mousallam Almoussalam & Huijun Zhu*
School Of Energy, Environment and Agrifood

*corresponding author
Email: h.zhu@cranfield.ac.uk

Introduction

Dacarbazine (DTIC) is one of the most commonly used chemotherapy drugs for treating various cancers. However, its poor solubility, short half-life in blood circulation, low response rate and high side effect limits its application. This study aimed to improve the therapeutic efficiency of the drug by developing nanostructured lipid carrier (NLC) for DTIC delivery.

Materials

ATO-5, isopropyl myristate, tocopheryl polyethylene glycol succinate, soybean lecithin and Kolliphor P 188.

Methods

NLC and NLC-DTIC were synthesised using oil-in-water emulsion-solidification-high shear dispersion and . Characterized with transmission electron microscopy (TEM), dynamic light scattering (DLS), UV spectrophotometry and *in vitro* cytotoxicity (MTT assay)

Results

Fig 1. Size distribution of NLC and NLC-DTIC as measured by DLS

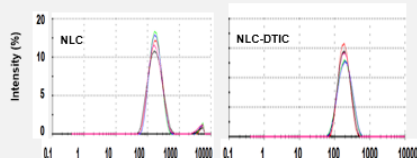


Fig 1. The average size of NLC and NLC-DTIC was 167 nm \pm 10 and 185 nm \pm 10, respectively, suggesting a good homogeneity of the NLCs produced.

Fig 2. Zeta potential of NLC and NLC-DTIC

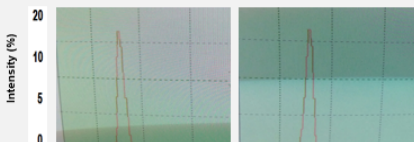


Fig 2. The zeta potential of NLC and NLC-DTIC was - 42 \pm 0.7 and -43 \pm 0.4, respectively, suggesting a good stability of the NLCs in solution.

Fig 3. TEM for NLC and NLC-DTIC

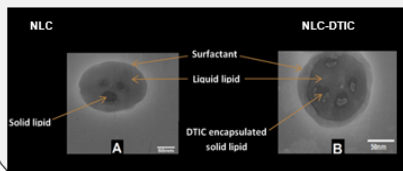


Fig 3. The differences in the structure between NLC and NLC-DTIC suggest the success of drug encapsulation.

Fig 4. Drug release profile of NLC-DTIC

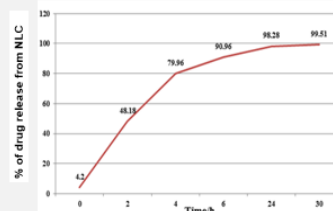


Fig 4. Drug released 50% in the first 2 h, and the remaining released within 30 h, suggesting a biphasic drug release pattern.

Fig 5. Cytotoxicity of NLC and DLG-DTIC in a 375 cells

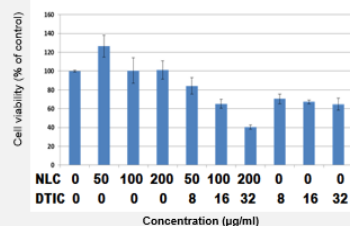


Fig 5. A375 cells were treated for 72 melanoma cells showed an Fig by NCL-DTIC as compared with free DTIC

Conclusion:

This study demonstrated that NLC is a good candidate as carrier for intracellular delivery of DTIC. This is the first report on the development of NLC for DTIC delivery.

B. Awards

Certificate of Excellence for Students Scholarships from the Embassy of the Kingdom of Saudi Arabia in the United Kingdom

